TECHNICAL REPORT STANDARD TITLE PAGE

1. Report No.	2. Government Accession No.	3. Recipient's Catalog No.
CFHR 3-5-72-176-1		

4. Title and Subtitle	5. Report Date
"The Behavior of Axially Loaded Drilled Shafts in Sand"	December 1972
	6. Performing Organization Code

7. Author(s)	8. Performing Organization Report No.
Fadlo T. Touma and Lymon C. Reese	Research Report 176-1

9. Performing Organization Name and Address	10. Work Unit No.
Center for Highway Research The University of Texas at Austin Austin, Texas 78712	11. Contract or Grant No. Research Study 3-5-72-176
	13. Type of Report and Period Covered Interim Sept. 1971 - Oct. 1972
12. Sponsoring Agency Name and Address Texas Highway Department 11th & Brazos Austin, Texas 78701	14. Sponsoring Agency Code

15. Supplementary Notes

Research performed in cooperation with Department of Transportation, Federal Highway Administration.
Research Study Title: "The Behavior of Drilled Shafts"

16. Abstract

Study is mainly concerned with analysis of behavior of five full-scale instrumented drilled shafts cast in soil profiles containing sand and test loaded to failure. Two shafts were cast by the dry method and three by the slurry displacement method.

From field observations and measurements taken during construction and load tests, important findings were made concerning the construction and the design of drilled shafts. With respect to construction, the slurry displacement method was found to possess a great potential for future use, but this method must be used with care, to prevent the entrapment of mud and sediments at the tip and sides of the shaft and in the concrete.

With respect to design, the measured load transfer was correlated with the properties of the sand measured by dynamic penetrometers. Pressure-settlement curves were obtained for the tips of shafts in very dense sand and sand of medium density. The total side load transfer was correlated with the integral over the periphery of the shaft of the product $\overline{p} \tan \overline{\phi}$, where $\overline{p}$ = effective overburden pressure and $\overline{\phi}$ = effective friction angle .

The coefficient of correlation was found to be about 0.7 for shafts with penetrations in sand not exceeding 25 ft. There were indications that this coefficient decreases with depth and, therefore, care must be exercised when the results are extrapolated to deeper shafts.

17. Key Words	18. Distribution Statement
bored piles, design, drilled shafts, sand, slurry, standard penetration test	

19. Security Classif. (of this report)	20. Security Classif. (of this page)	21. No. of Pages	22. Price
Unclassified	Unclassified	275	

Form DOT F 1700.7 (8-69)

THE BEHAVIOR OF AXIALLY LOADED DRILLED SHAFTS IN SAND

by

Fadlo T. Touma
Lymon C. Reese

Research Report Number 176-1

The Behavior of Drilled Shafts
Research Project 3-5-72-176

conducted for

The Texas Highway Department

in cooperation with the
U. S. Department of Transportation
Federal Highway Administration

by the

CENTER FOR HIGHWAY RESEARCH
THE UNIVERSITY OF TEXAS AT AUSTIN

December 1972

PREFACE

This report is the first report on the findings of Research Project 3-5-72-176, "The Behavior of Drilled Shafts."

This report presents the results of an investigation of the behavior of drilled shafts in sand. The study is based on the results of load tests on five full-scale instrumented drilled shafts cast in soil profiles containing sand. Two test shafts were constructed by the dry procedure and the other three shafts were cast by slurry displacement. The report includes an evaluation of these construction procedures.

The authors would like to acknowledge the work of a number of people who contributed to this report. The field work was completed with the technical assistance of Mr. Harold Dalrymple, Mr. James Anagnos, Mr. Fred Koch, and Dr. Michael O'Neill. The planning and execution of the work were done with the cooperation of Messrs. H. D. Butler, Horace Hoy, Tom Bell, and Gaston Berthelot of the Texas Highway Department.

The authors would like also to gratefully acknowledge the support of the Federal Highway Administration.

Fadlo Touma
Lymon C. Reese

December 1972

This page replaces an intentionally blank page in the original.
-- CTR Library Digitization Team

ABSTRACT

This study is mainly concerned with the analysis of the behavior of five full-scale instrumented drilled shafts cast in soil profiles containing sand and test loaded to failure. Two shafts were cast by the dry method and the other three shafts were cast by the slurry displacement method.

From field observations and measurements taken during construction and load tests, important findings were made concerning the construction and the design of drilled shafts. With respect to the construction, the slurry displacement method was found to possess a great potential for future use. This method, however, must be used with care, to prevent the entrapment of mud and sediments at the tip and sides of the shaft and in the concrete.

With respect to the design, the measured load transfer was correlated with the properties of the sand measured by dynamic penetrometers. Pressure-settlement curves were obtained for the tips of shafts in very dense sand and sand of medium density. The total side load transfer was correlated with the integral over the periphery of the shaft of the product $\bar{p}$ and $\bar{\phi}$, where

$\bar{p}$ = effective overburden pressure

$\bar{\phi}$ = effective friction angle

The coefficient of correlation was found to be about 0.7 for shafts with penetrations in sand not exceeding 25 ft. There were indications that this coefficient decreases with depth and, therefore, care must be exercised when the results are extrapolated to deeper shafts.

KEY WORDS: bored piles, design, drilled shafts, sand, slurry, SPT.

This page replaces an intentionally blank page in the original.
-- CTR Library Digitization Team

SUMMARY

This study can be divided into three major sections:

1. An evaluation of the slurry displacement technique
2. An analysis of the factors controlling the behavior of drilled shafts
3. An analysis of the tests on five full scale instrumented drilled shafts constructed in sand

The slurry displacement technique was found to hold great potential for the construction of drilled shafts. However, great care must be observed in using this method to prevent the caving of holes in expansive clays and to prevent the entrapment of mud and soft sediments at the tip and at the sides of the shaft.

There are many factors that control the behavior of drilled shafts and this study did not evaluate the influence of each of these variables. The test results were used to obtain empirical evaluations of the tip and side resistance of shafts in sand. Large displacements were found required to mobilize significant tip resistance. An expression for evaluating an allowable tip pressure was derived as a function of the tip diameter and the degree of compactness of the sand. It was also found that the side resistance of shafts penetrating less than 25 ft. in sand can be evaluated as 0.7 of the integral over the periphery of the shaft of the product $\bar{p} \tan \bar{\phi}$. There are indications that a smaller fraction of this integral could be developed in shafts of greater penetration in sands.

Based on the findings of this study a design procedure was developed for shafts penetrating in sand up to 25 ft.

This page replaces an intentionally blank page in the original.
-- CTR Library Digitization Team

IMPLEMENTATION STATEMENT

This study presents a method for the design of drilled shafts in sand. The method is based on full scale field tests and is recommended for immediate implementation. This method is believed to be safer and more economical than existing methods.

However, the proposed design procedure is limited to shafts penetrating no more than 25 ft. into sand; therefore, it is recommended that further field studies be carried out on the behavior of long drilled shafts in sand. Further, additional load tests of short to moderate-length drilled shafts, perhaps uninstrumented, should be carried out in order to refine and improve the proposed design procedure.

The study also presents an evaluation of the slurry displacement technique. It was found that this technique can be used successfully in the construction of drilled shafts in caving soils.

This page replaces an intentionally blank page in the original.
-- CTR Library Digitization Team

TABLE OF CONTENTS

LIST OF TABLES

This page replaces an intentionally blank page in the original.
-- CTR Library Digitization Team

LIST OF FIGURES

This page replaces an intentionally blank page in the original.
-- CTR Library Digitization Team

NOMENCLATURE

Symbol	Typical Units	Definition
A	sq ft	Cross-sectional area of shaft
A_t	sq ft	Cross-sectional area of tip of shaft
A_1, A_2	sq ft	Constants used in solving differential equations
B	ft	Diameter of shaft
C	ft	Circumference of shaft
C_t	--	Function related to critical height of a column of concrete
C_w	--	Coefficient of settlement
c	psi	Apparent cohesion of soil
D	ft	Diameter of the borehole
D_r	--	Relative density of sand
D_{number}	mm	Diameter such that the aggregate weight of all smaller grains is (number) per cent of the total weight of the sample
d	ft	Diameter of the tremie
d_w	ft	Height of the water table above the tip of the shaft
E	lbs/sq ft	Young's modulus of elasticity (general)
e	--	Void ratio of soil
e	--	Base for Neperian logarithm
F_{cone}, F_{spoon}	lbs	Force driving the cone or spoon penetrometers
F_1, F_2	psi	Functions used in analyzing the flow of concrete

Symbol	Typical Units	Definition
f_o	psi	Average vertical shear stress at the outerface of the tremie
f_r	psi	Average vertical shear stress at any distance r in the borehole
H	ft	Height (general)
H_c	ft	Height of concrete column above the tip of the tremie
H_m	ft	Critical height beyond which the concrete pressure does not increase
h_c	ft	Height of column of concrete in a hole
h_m	ft	Height of column of mud in a hole
h_1, h_2	ft	Hydraulic head loss in the tremie and in the borehole respectively due to the flow of concrete in a section $\Delta\ell$ of the hole
Δh	ft	Total head loss due to concrete flow in a section $\Delta\ell$ of the hole
I_r	--	Stiffness index
I_w	--	Settlement index
i	--	Hydraulic gradient
K	ft	Constant used in the analysis of the flow of the concrete in a borehole
K_o	--	Coefficient of earth pressure at rest
K_s	--	Coefficient of earth pressure (general)
k	--	Constant (general)
k_1, k_2	sec	Constants function of the viscosity of concrete and roughness of the tremie and the borehole respectively

Symbol	Typical Units	Definition
L, ℓ	ft	Length (general)
ℓ_n	ft	Length of shaft where soil does not resist deformation
$\Delta\ell$	ft	Length of a section
N	--	Penetration test blow count (general)
N_γ	--	Bearing capacity factor (friction)
N_c	--	Bearing capacity factor (cohesion)
N_q	--	Bearing capacity factor (overburden)
N'_q	--	Bearing capacity factor (general for deep foundations)
n	--	Ratio of the diameter of the hole to the diameter of the tremie
P_1	psi	Hydrostatic pressure at the bottom of the tremie
P_2	psi	Hydrostatic pressure at the surface of the concrete column
P_h	psi	Horizontal pressure
P_{max}	psi	Peak stress in the penetrometer
P_v	psi	Vertical pressure
$\bar{p}$	psi	Effective normal pressure on the failure plane
$\bar{p}_h$	psi	Effective horizontal pressure
$\bar{p}_v$	psi	Effective vertical pressure
Q	lbs	Total load on top of shaft
Q_s	lbs	Load carried by periphery of shaft

Symbol	Typical Units	Definition
Q_t	lbs	Load carried by tip of shaft
Q_z	lbs	Total load in shaft at a point located a distance z from top of shaft
q	psi	Confining pressure
q_c	ft^3/sec	Rate of flow of concrete in borehole
$\bar{q}_o$	psi	Effective pressure in the soil at the level of the tip of the shaft
q_s	psi	Unit shear stress developed at the periphery of the shaft (general)
q_{sz}	psi	Unit shear stress developed at the periphery of the shaft and at a depth z
q_t	psi	Ultimate tip resistance
q_u	psi	Unconfined compressive strength
R	in	Radius of borehole
R_c	ft/hr	Rate of placement of concrete in borehole
r	in	Radius at any point in the borehole
r_o	in	External radius of tremie
SPT	--	Blow count of Standard Penetration Test
s	psi	Shear strength of soil
T	°F	Temperature of concrete
T_c	psi/in	Stiffness of cushion
V_1, V_2	ft/sec	Average velocity of flow of concrete in the tremie and in the borehole
V_h	ft/sec	Velocity of hammer at impact
v	ft/sec	Velocity of sound in drilling rods

Symbol	Typical Units	Definitions
W	psi	Pressure due to the weight of a concrete column
W_p	lb	Weight of drilling rod
W_h	lb	Weight of hammer
w_s	ft	Compression in shaft due to load
w_z	ft	Vertical movement of shaft at point z
w_t	ft	Vertical movement at bottom of shaft
w_T	ft	Total vertical movement of top of shaft
z	ft	Vertical coordinate from top of shaft to a point in the shaft
α_{avg}	--	Correlation factor between the shear strength of a stratum to the side shear resistance developed in the stratum
β	lb/cu ft	Shear modulus of soil
γ	lb/cu ft	Unit weight of material (general)
$\overline{\gamma}$	lb/cu ft	Effective unit weight of soil
γ_c	lb/cu ft	Unit weight of concrete
γ_m	lb/cu ft	Unit weight of mud
γ_w	lb/cu ft	Unit weight of water
δ	degrees	Angle of shear resistance between the soil and the shaft
ϕ	degrees	Apparent angle of internal friction of soil
$\overline{\phi}$	degrees	Effective angle of internal friction of soil
$\hbar$	--	Constant used in the relation between the friction angle and the void ratio of sand

Symbol	Typical Units	Definitions
λ	--	Coefficient of volumetric strain of the concrete
η	ft/lb	$\frac{C}{EA}$
ν	--	Poisson's ratio
σ	psi	Normal stress
$\bar{\sigma}$	psi	Effective normal stress
σ_r	psi	Radial stress
σ_1, σ_2	psi	Major and minor principal stresses
τ	psi	Shear stress

CHAPTER I. INTRODUCTION

GENERAL

Engineering is the "art and science by which the properties of matter and the sources of power in nature are made useful to man in structures, machines, and manufactured products" (Webster). While an "art" is a skill acquired by observation and intuition, a "science" is a skill acquired by a systemized knowledge, and a logical analysis of the cause and the effect.

The application of engineering skills can only be perfected if these skills are based on scientific foundations. In its development, engineering has followed various courses. Many of the engineering techniques started as a pure art and were later supported by a scientific analysis while several others were developed from pure abstract logic. Engineering cannot progress as an art, for if the scientific explanations of applied skills are not explored, those skills may result in the misuse of material either by the production of an unsafe structure or by the waste of material due to unnecessary conservatism.

The art and the practice of deep foundation engineering have constantly progressed at large paces leaving the slow paced supporting scientific theories a considerable distance behind. Old methods of construction are continuously improved and new methods are continuously created while few theories are being advanced on the behavior of deep foundations constructed by the new methods.

Drilled shafts, interchangeably called "drilled piers," "drilled caissons," or "bored piles," are only one manifestation of this phenomenon. In this case, the application of modern drilling equipment to the construction of drilled shafts has not only revolutionized the methods of construction of these shafts but has also made them successfully competitive with other types of foundations. Situations where drilled shafts are advantageously replacing driven piles and shallow foundations are becoming more common. The adaptation of drilled shafts to most types of soils will bring them into more widespread use in the coming years because of their evident advantages. However, as the new methods of construction are applied, a better understanding of the behavior of drilled shafts constructed by these methods is needed to make a better use of these shafts and bring more confidence in their design.

EVOLUTION OF DRILLED SHAFTS AND RELATED RESEARCH

The multitude of the existing methods of construction of drilled shafts is the product of a long process of evolution of construction techniques. A detailed historical account of the development of drilled shafts has been reported by various authors (Greer, D. M., 1969; O'Neill and Reese, 1970). To include the work of these authors here seems repetitious and unnecessary. However, an evaluation of the research needed on drilled shafts at this stage requires a brief recapitulation of the major steps in the evolution of modern drilled shafts.

The first drilled deep foundations were hand drilled. The "Chicago Caissons" or "Chicago Wells" used to found the first skyscrapers on the "hardpan" layer of the city of Chicago are the best known examples of hand-dug piers. These caissons used wood lagging to protect the walls of the hole and the lagging was left in the hole after concreting. The "Gow Caissons" that followed later in the first decades of this century were also hand drilled but used steel casings of various diameters to form a step tapered hole. The casings were extracted one section at a time during the concreting process.

Mechanized drilling reported to be first initiated in Texas used a horse driven helical auger to drill piers past the depth of soil affected by seasonal variations. It was not until about the time of the second World War that steam and fuel powered engines were used to drill large diameter shafts for the foundations of buildings and power poles. The effectiveness of mechanically drilled shafts resulted in their widespread use in various parts of the world and particularly in areas where the soil permitted the drilling of free-standing holes, such as in Texas, California, Colorado, Illinois, and some parts of Canada and England, where stiff clays prevail to a considerable depth below the surface. These same areas contributed most of the research done to date on the behavior of drilled shafts in clays (Meyerhof and Murdock, 1953; Dubose, 1955; Whitaker and Cooke, 1966; O'Neill and Reese, 1970). A comprehensive survey of the research done on drilled shafts in stiff clays is presented by O'Neill and Reese, 1970.

Free-standing holes can be drilled in sandy soils above the water table if the sand is cemented or is moist enough to develop shear strength from capillary water pressures. However, few drilled shafts have been built in such soils and there is little information available on the behavior of drilled shafts cast in such soils.

The use of drilled shafts in free-standing soils offers evident economical advantages over other types of foundations. However, the cost of construction of drilled shafts can increase excessively when penetration of water bearing sand and gravel layers is required. Until recently, unstable layers were avoided and were only penetrated when bearing of the shaft on an underlying competent layer was desired. The slurry displacement method of construction has been employed recently in drilled shaft construction. The layers of soil which formerly caved are maintained in place by the slurry and these layers can be counted on for transfer of load by side friction. This recent practice resulted primarily from individual efforts of the drilling contractors who innovated several procedures to construct drilled shafts in such soils. The drilling firms I.C.O.S. and Soletanche developed and patented drilling equipment for the new procedures. Most of the new methods of construction are still an art and considerable research is needed to analyze and improve those methods. On the other hand, the emergence of the new techniques brought forward new variables in the behavior of drilled shafts and a comprehensive study is needed to assess the effects of these variables.

Drilled shafts are also constructed in shales and weathered rock for the purpose of developing a desired bearing capacity. The side friction and tip resistance that can be developed in those soils has not yet been evaluated.

Drilled shafts seated or anchored in rock penetrate very often layers of expansive clays and there has not yet been proposed a comprehensive analysis of shafts subjected to expansive pressures. Research on drilled shafts is needed in the following areas:

1. The study of behavior of drilled shafts in granular soils,
2. The analysis and improvement of methods of construction,
3. The analysis of variables introduced by the different methods of construction,
4. The study of behavior of drilled shafts in expansive clay layers, and
5. The study of load transfer in very stiff shales and soft or weathered rock.

Research in the areas listed above is considered of immediate importance. As the state of the art concerning drilled shafts advances, new areas of research will be exposed in both the areas of construction and analysis of behavior. Examples of such future possibilities are a study of shafts belled at more than one level and the chemical interaction of concrete with clays of various mineralogical composition.

In the following section, some of the procedures used to construct drilled shafts are described with a particular emphasis on the procedures used in caving soils. This description covers only the general principles of construction, and many details are left out. There are as many minor modifications to these procedures as the existing number of drilled shafts contractors.

METHODS OF CONSTRUCTION OF DRILLED SHAFTS

Before any of the methods of construction is described, a clarification of the definition of "drilled shafts" is needed. The terms "drilled shafts" or "drilled caissons" are applied to the type of deep foundation formed by casting concrete in a hole drilled in the ground. A "belled shaft" is a drilled shaft that has an enlargement formed at its bottom. When steel reinforcement is used in the concrete of the shaft it may consist of a cage of steel bars, a rolled steel section, or an outer steel casing (shell).

The construction of drilled shafts, as known today, may be considered to be the product of evolution of two types of deep foundations: caissons and cast-in-situ piles. While the construction of drilled shafts has kept some of the features of the construction of large caissons, several types of cast-in-situ piles may be claimed to belong to the drilled shaft category defined above. Nondisplacement, cast-in-situ piles constructed by driving an open-end pipe pile, drilling the inner soil plug out, and filling the hole with concrete deserve, in the opinion of the authors, the

appelation of "drilled shafts" whether the steel casing is withdrawn from the ground or not. The construction of certain types of cast-in-situ piles, such as the Franki piles, requires the displacement of a volume of soil equal to the volume of the pile. These piles, being basically displacement piles, are eliminated from the drilled shaft designation. Some of the literature classifies separately nondisplacement cast-in-situ piles and drilled shafts. This separate classification is based on the idea that more than one pile and a pile cap are employed to support one column load while a drilled shaft is usually built coaxially with the loading column. However, this difference in the terminology is not of any practical engineering significance, and in this study no distinction shall be made between the nondisplacement, cast-in-situ pile and the drilled shaft as defined above.

Because the methods of construction have a primary influence on the behavior of a drilled shaft, it seems appropriate to classify drilled shafts by their various methods of construction. In this study, drilled shafts shall be classified under two categories:

a. Shafts built by the dry process, where the drilling and the concreting phases are executed in a dry hole,
b. Shafts built by the wet process, where either one or both of the drilling or concreting phases are executed in a hole containing a drilling fluid.

Different construction techniques are included in each of these categories, and, therefore, a unique behavior of all the shafts under one category cannot be expected.

Shafts Built by the Dry Process

Drilled shafts under this category are constructed without the use of drilling fluid. The walls of the hole may be either free-standing or may be supported by a steel casing.

1. Free standing holes: (Fig. 1.1). These holes may be drilled in naturally stable soils such as stiff clays, cemented sands and silts, moist sands above the water table, or in artificially stabilized soils. Stabilization of caving sands may be achieved by a lowering of the water table or by grouting. Bentonite grouts and chemical grouts are reported to have been used successfully in stabilizing large masses of sand before drilling and belling was achieved (Glossop and Greeves, 1946; Polivka, et al., 1957). Grouting usually reduces the permeability enough to allow a completely dry operation.

In some particular situations, a technique similar to that used in installing sand drains is used in drilled shaft installation. A hollow-stem, continuous flight auger is advanced in the ground to the full depth of the drilled shaft and, as the auger is removed, cement grout is injected through the stem to replace the removed soil.

2. Cased holes: (Fig. 1.2). When an unstable sand layer is underlain by a layer of clay, a casing may be driven by impact hammer or by a vibrator through the sand layer and sealed in the impervious clay layer.

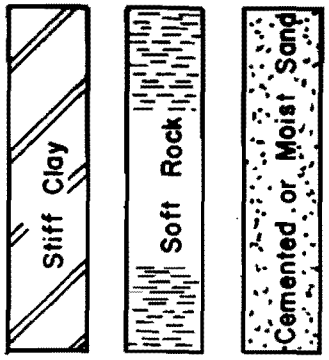

a. Naturally Stable Soils

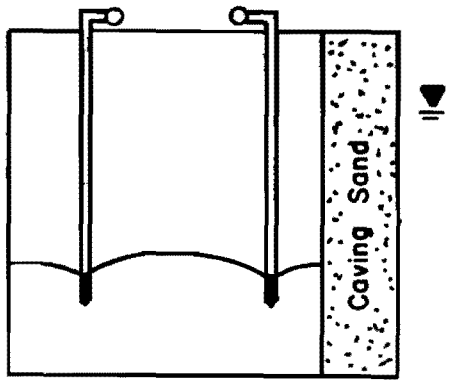

b. Stabilization of Water-Bearing Caving Sand by Well Points

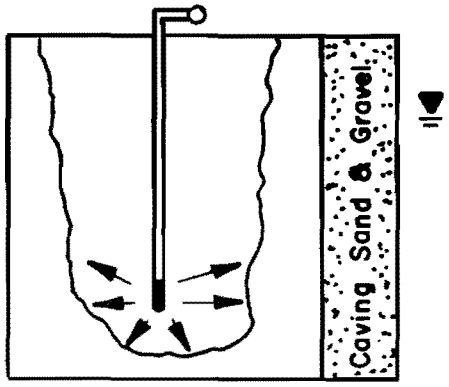

c. Stabilization of Caving Sand by Grouting

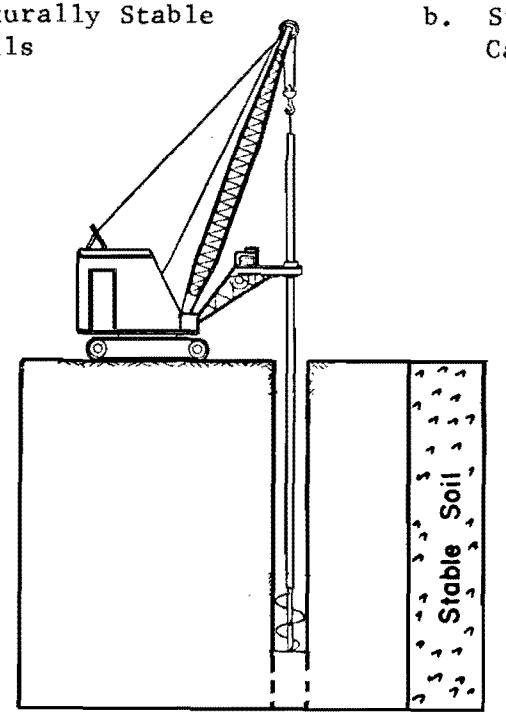

d. Drilling in the Dry

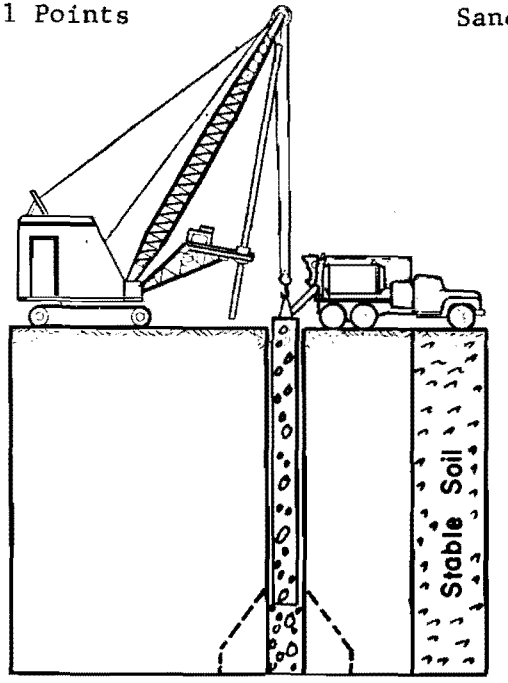

e. Concreting in the Dry

Fig. 1.1 Dry Drilling and Concreting, Without Casing

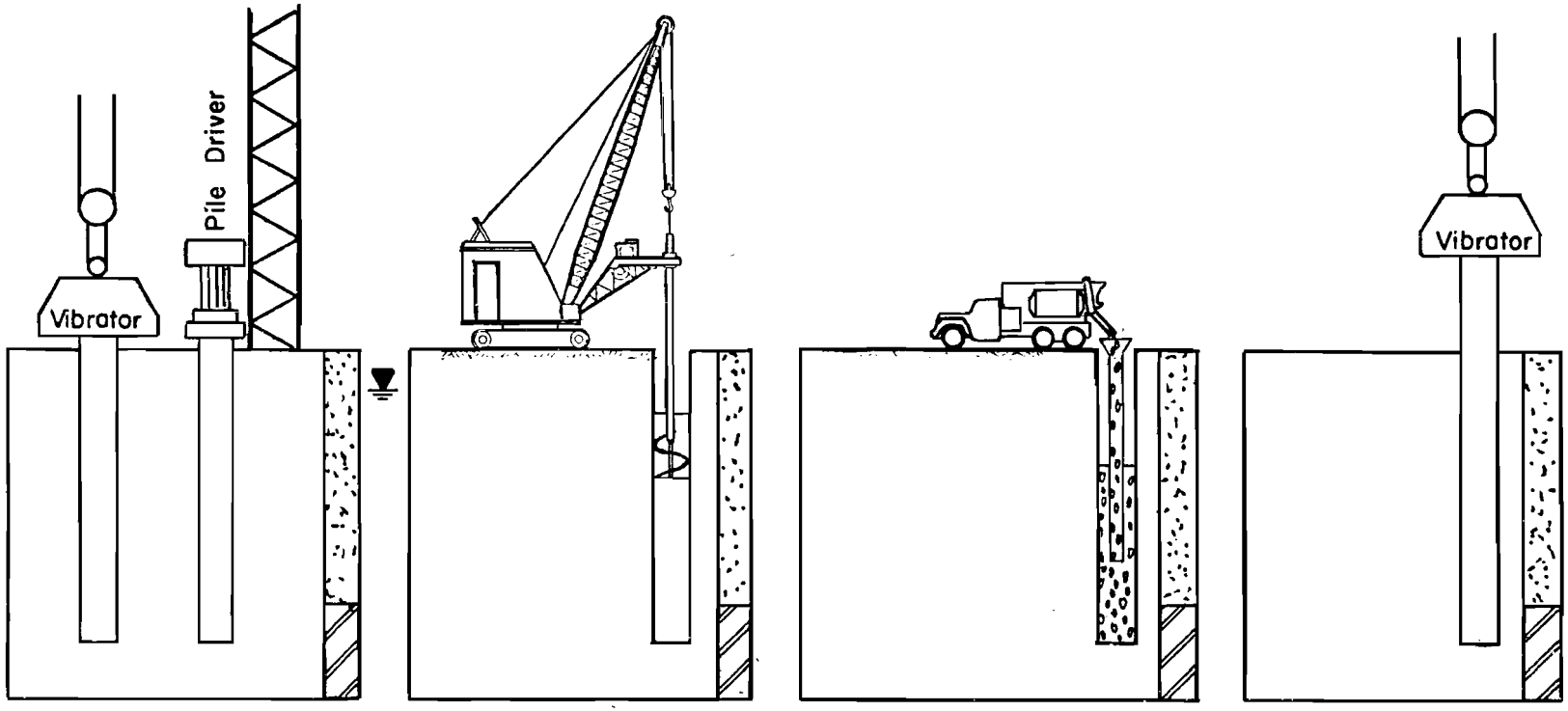

a. Driving of Casing and Sealing in the Clay

b. Drilling and Cleaning of Casing

c. Concreting in the Dry

d. Extraction of Casing

NOTES: 1. The extraction of the casing is optional
2. Concreting in the dry may be possible without sealing of the casing in the clay whenever the water table is below the tip of the shaft

Fig. 1.2 Dry Drilling and Concreting with Preinstalled Casing

The soil plug may then be drilled out by a drilling bucket, a helical auger or a hammer grab. In certain situations the soil may be removed by jetting and any accumulated water removed by a bailing bucket. Concrete is then cast in the hole. The casing may or may not be withdrawn.

Dry construction is preferable whenever possible to wet construction because the bottom of the hole may be cleared and inspected, and because the danger of soil or concrete contamination by the drilling fluid is eliminated.

Shafts Built by the Wet Process

This procedure uses essentially water or a drilling mud (slurry) to protect the walls of the drilled hole. In certain situations the slurry may serve the purpose of carrying soil cuttings out when jetting, rotary, or percussion drilling is used. In such instances, the mud is then circulated through settling pits to free it from its suspended solids. Steel casing may be used in conjunction with this process either to overcome difficult drilling situations or to permit concreting in the dry.

1. Uncased holes: (Fig. 1.3). This method consists of drilling the hole with the use of a drilling fluid, which is usually a bentonite mud, and then casting tremie concrete to displace the mud. This method shall be referred to in this study as the slurry displacement method and shall receive a special treatment in the following chapter.

2. Cased holes: Situations where excessive groundwater pressure exists which cannot be balanced by the mud pressure require the use of a casing to protect the walls of the hole. The casing may then be driven,

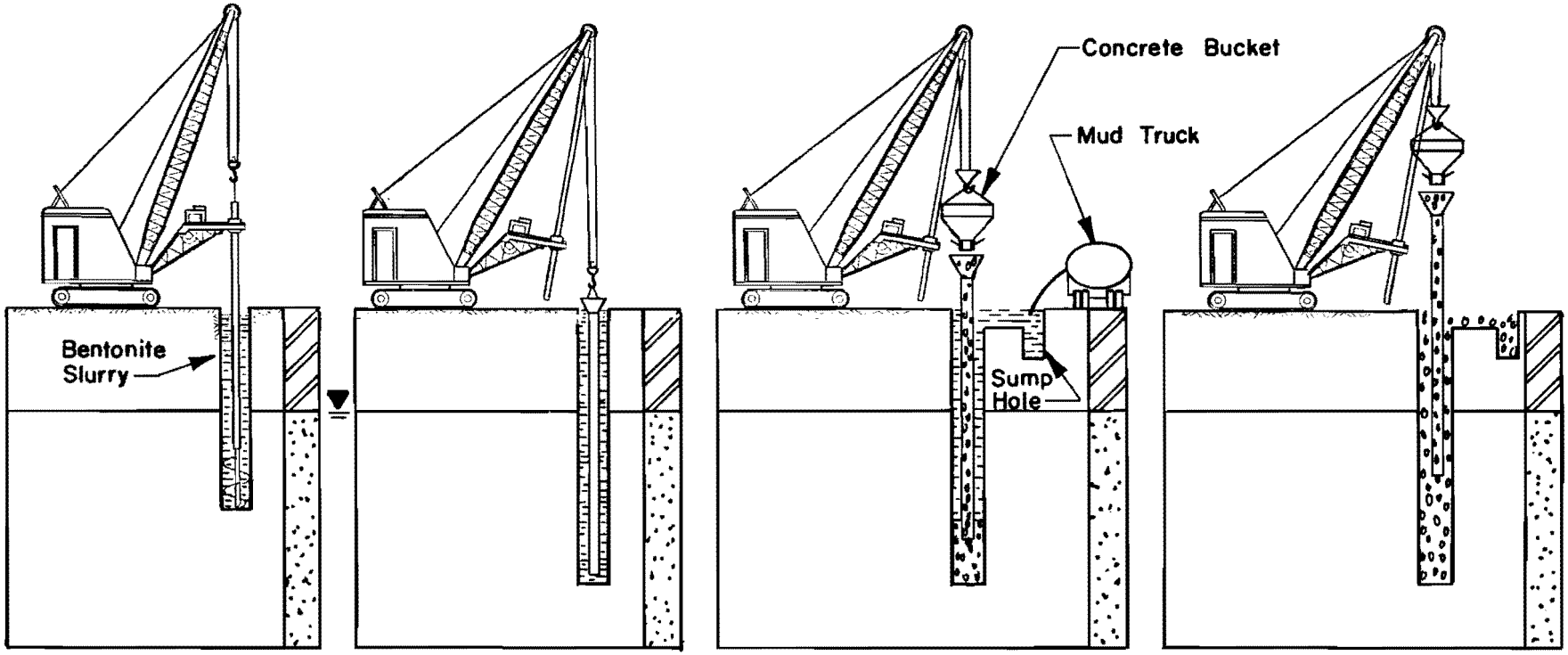

a. Drilling under Slurry

b. Setting Sealed Tremie after Cleaning of the Bottom of Hole

c. Placing Concrete and Unplugging the Tremie

d. Finishing Concreting

Fig. 1.3 Wet Drilling and Concreting, Without Casing (Slurry Displacement Method)

vibrated, or sunk by jetting in the soil. If the casing cannot be sealed in a watertight formation, drilling mud or soil-water slurry may be used to prevent "blowing" of the bottom of the hole. Tremie concrete is then cast to displace the mud, while the casing is being withdrawn (Fig. 1.4). In certain exceptional cases of large underground water flows, the casing may be left in the ground to prevent intrusion of ground water or soil into the concrete. The penetration of layers of gravel and large boulders may be very difficult. The "Benoto" drilling procedure, designed to penetrate such layers, makes use of horizontal oscillations and vertical jacking to drive a thick walled casing while a hammer grab excavates the soil. When large boulders are encountered, chisels or chopping buckets may be used to open a way for the casing. The casing used in this process is very expensive, and in the case of excessive groundwater flow, a thin metallic skirt is inserted inside the casing, which is pulled out during concreting.

In certain cases where waterbearing, loose sand is encountered, bentonite mud can be worked with a helical auger in the sand to form a column of mud and sand through which the casing is inserted and the soil augered thereafter. This procedure is commonly called the "mudding-in" procedure.

Casings are also used in combination with the wet process where a concreting operation in the dry is desired. In this process, a steel casing is inserted in a hole stabilized by a drilling fluid and sealed in an impervious clay layer. The fluid is then bailed out and drilling continued in the dry if desired. After inspection of the bottom of the

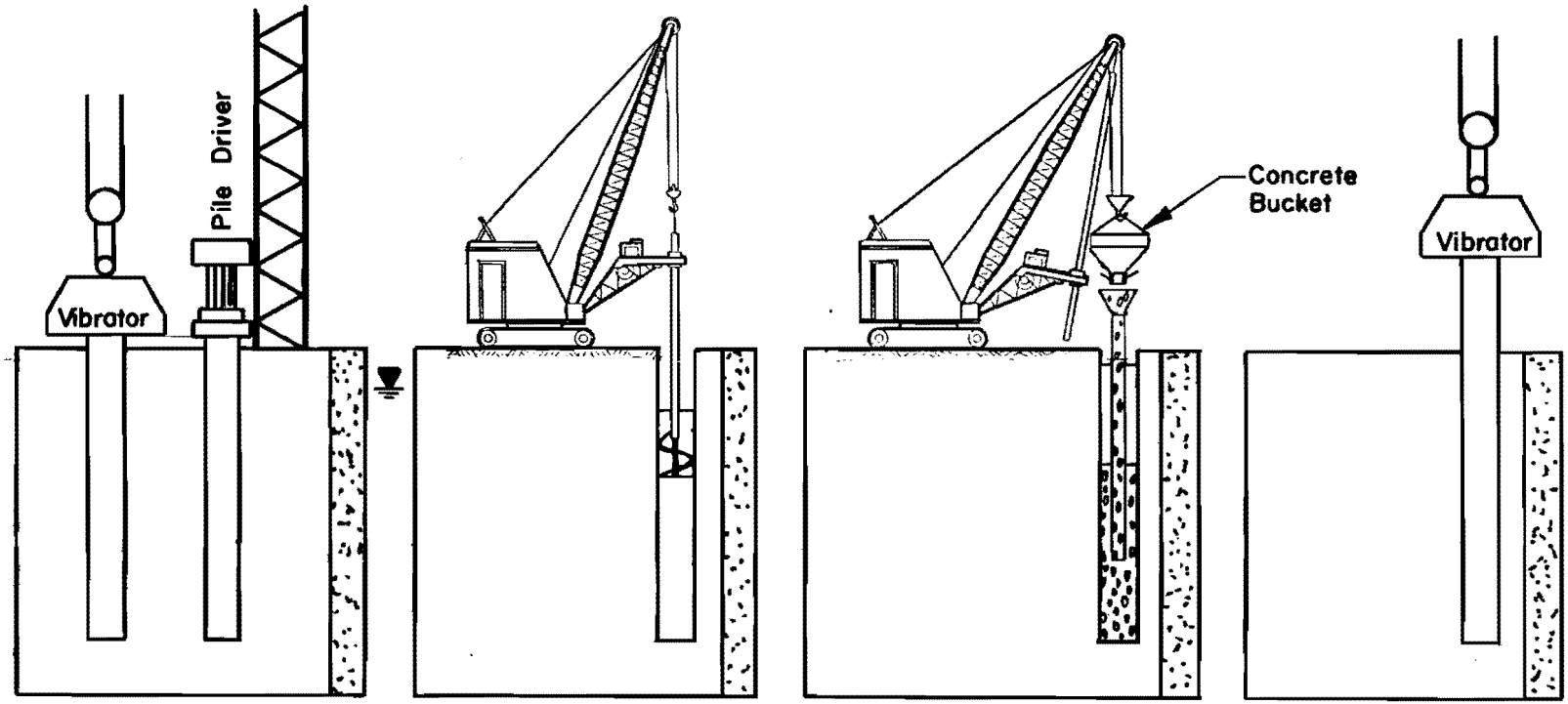

a. Impact or Vibratory Driving of Casing

b. Drilling under Water

c. Tremie Concreting

d. Extraction of the Casing

Fig. 1.4 Wet Drilling and Concreting, with Preinstalled Casing

hole, concrete may be cast in the dry. The casing is removed (Fig. 1.5) when the concrete has reached an appropriate level in the hole. This method of construction is commonly used by drilling contractors in Texas. A complete description of this method and a comprehensive analysis of the behavior of shafts built by this method have been reported by O'Neill and Reese, 1970; Barker and Reese, 1970; and Welch and Reese, 1972. In the absence of an impervious layer, chemicals may be injected to stabilize the bottom of the hole and allow the sealing of the casing.

SCOPE OF THIS STUDY

This study is primarily concerned with the analysis of the behavior of drilled shafts cast in sandy soils by the wet and the dry procedures and without the use of a casing. The study is based on the analysis of the results of axial load tests on five drilled shafts constructed in soil profiles containing sandy soils. All the test shafts were instrumented at different levels with "Mustran" load cells developed at the Center for Highway Research of The University of Texas at Austin (Barker and Reese, 1970).

In Live Oak County, Texas, two drilled shafts were cast using the dry process in slightly cemented sands above the water table. In the Houston area three other shafts were cast using the slurry displacement method in sands below the water table. Several axial load tests to failure were performed on each shaft. The instruments were read with a high speed

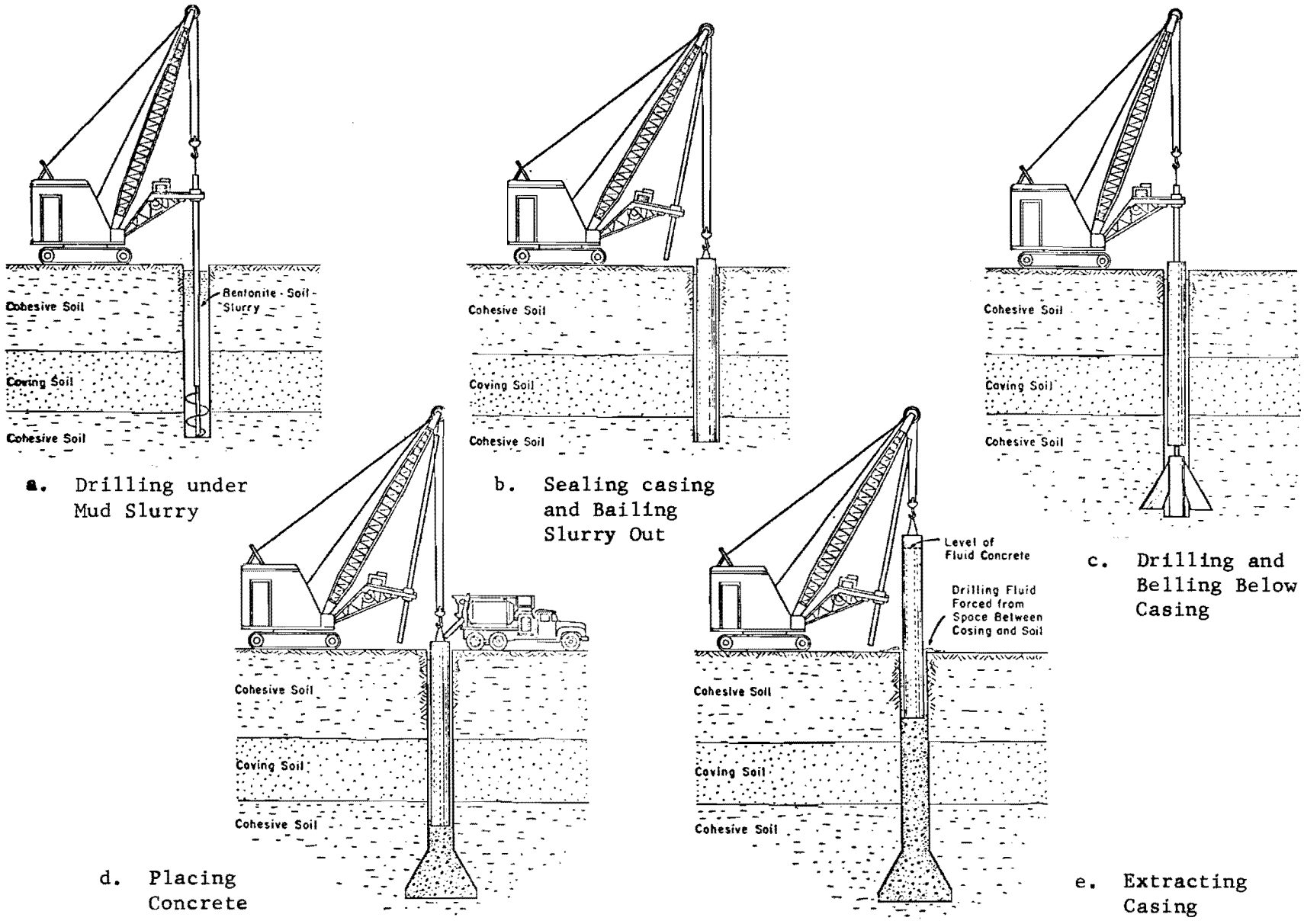

Fig. 1.5 Wet Drilling and Dry Concreting, with Casing
(After O'Neill and Reese, 1970)

digital recording system at each increment of load. The data were then analyzed and interpreted to determine design factors related to the behavior of shafts built by these procedures.

The study based on these tests will cover the following:

1. A review and an analysis of the slurry displacement construction method, based on available literature, field observations, and laboratory tests.
2. An analysis of the behavior of drilled shafts constructed in cohesionless soils.
3. A description of the soil investigations, including *in situ* soil tests and laboratory tests.
4. A description of the instrumentation, installation and testing of the drilled shafts.
5. A presentation of the results expressed in terms of load settlement curves, load distribution curves, load transfer curves, and correlations between the load transfer and the measured properties of the soil.
6. Application of the results to future designs, and recommendations for improvements in construction procedures.

This page replaces an intentionally blank page in the original.
-- CTR Library Digitization Team

CHAPTER II. THE SLURRY DISPLACEMENT METHOD

HISTORICAL

The first use of water-based mud for drilling purposes is attributed to the oil industry. Some of its first applications in civil engineering were in the drilling of boreholes for soil exploration and as a lubricant in the sinking of large caissons. The use of drilling muds in the construction of bored piles did not start until the second quarter of this century, when the development of mechanized drilling necessitated the use of a fluid to support the walls of the hole during drilling. Previously, this support was provided by a casing or by strutting in hand-drilled holes.

The construction by the slurry displacement method of bored piles was first reported by the Italians (Veder, 1953). Piles constructed by this method were not considered to constitute good bearing elements. It was believed that debris at the bottom of the hole eliminated the tip resistance and that the bentonite mud acted as a lubricant between the shaft and the soil and destroyed the side friction. Furthermore, the quality of the tremie concrete and of the bond between the reinforcing steel and the concrete were not considered structurally dependable. However, this first application of the slurry displacement method was the start of the rapid development of techniques for the construction of concrete diaphragms for cut-off walls that took place in the 1950's. During that period, several special drilling machines, used in the drilling of continuous slurry trenches, were designed and patented and in

less than a decade a large number of concrete diaphragms were constructed in Europe (Chadeisson, 1961a). Much of this work was reported in several papers at the International Conference on Soil Mechanics and Foundation Engineering in Paris (Chadeisson, 1961a; Barbedette and Beria, 1961; Edison Group, et al., 1961).

The slurry displacement method continued to be used in the construction of drilled shafts, but engineers remained very skeptical as to the bearing capacity of such shafts. During the last decade, a number of axial load tests on drilled shafts constructed by slurry displacement have been reported (Chadeisson, 1961b; Burland, 1963; Fernandez-Renau, 1965; Komornik and Wiseman, 1967; Hager, 1970; Farmer, et al., 1970). The reported performance of these shafts was comparable and sometimes considerably better than that of shafts constructed by conventional procedures. However, the behavior of shafts constructed by the slurry displacement technique has received up to the present little systemized analysis. The lack of such an analysis and the complex nature of these deep foundations left civil engineers puzzled as to the degree of confidence to be allotted to shafts constructed by slurry displacement. It is one of the aims of this research to analyze various aspects of the slurry displacement method.

THE DRILLING MUD

In the oil industry, drilling mud is the subject of a very specialized study, and the problems encountered in deep well drilling are intricate.

Some of these problems deal with the effects of high pressure, high temperature, and prolonged periods of drilling on drilling mud and hole stability. Such problems are practically nonexistent in the "surface" drilling required for slurry trenches and bored piles. This fact has led engineers to believe that no special care should be taken with drilling muds used for civil engineering purposes. Schneebeli (1971) reports the words of an Italian engineer talking about mud: "This is not a drilling mud; this is dirty water." However, the collapse of boreholes and the poor execution of drilled shafts remain common but unfortunate events on drilling sites. Many such failures can be prevented by a minimal knowledge of the basic principles of drilling muds. A brief and elementary report on the behavior of drilling muds is, therefore, presented in the following paragraphs.

The drilling mud used in the construction of bored piles is a water-base mud that consists of three phases:

1. The liquid phase or water,
2. The colloidal fraction which is the reactive portion, and
3. The inert fraction which consists of sands, weighting material, and other inert solids (API, 1969).

The colloidal fraction of clay consists of sub-microscopic particles that, due to a charge deficiency in their molecular structure, generally carry negative charges over most of their surface area (Fig. 2.1a). This property of clays and their ability to hydrate allow them, when added to

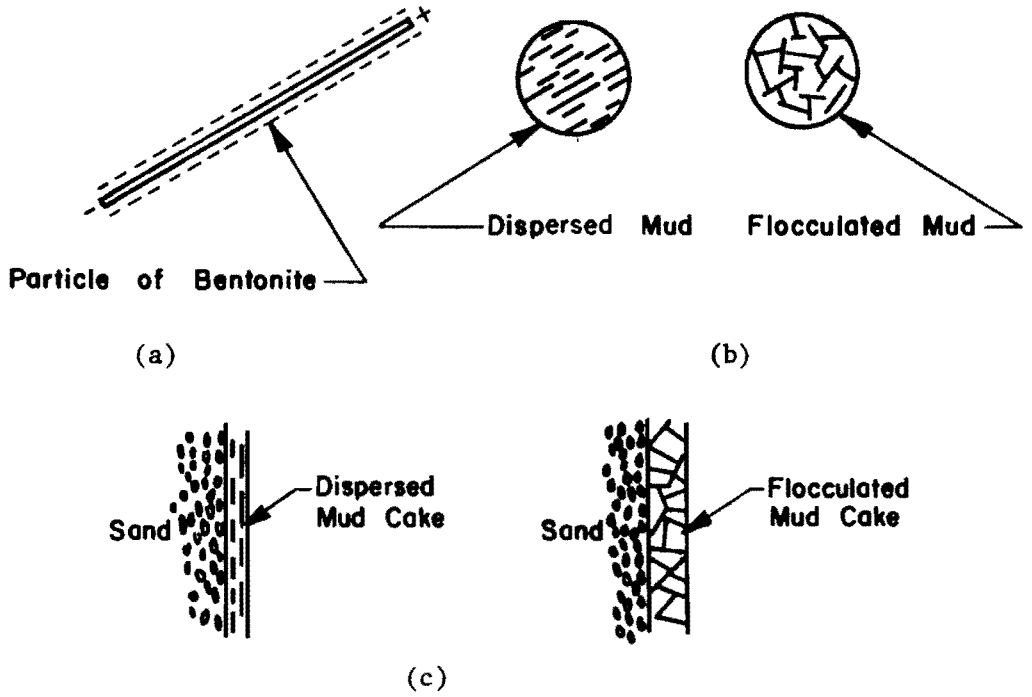

Fig. 2.1 Dispersed and Flocculated Muds

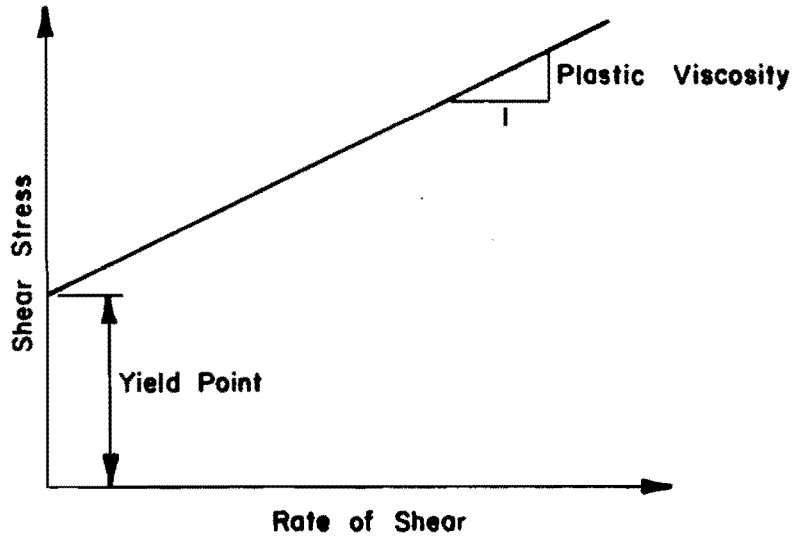

Fig. 2.2 Binghamian Behavior of Drilling Muds

fresh water, to increase the viscosity of water and to suspend inert solids such as sands and silts. Bentonite, which is mainly composed of sodium montmorillonite, is the principal source of drilling clays. Clays and clay shales, encountered during drilling, are also used when they can be conveniently mixed and dispersed.

In the construction of drilled shafts, the drilling mud serves the main function of supporting the walls of the hole. In connection with this function, the following properties of the drilling mud are of interest.

Wall Building and Filtration Control

Where a pervious unstable soil layer is penetrated and the pressure of the drilling mud is higher than the pore pressure of the soil formation, water tends to flow into the formation. This flow filters the mud and causes the formation of an impervious mud "cake" on the surface of the hole. The cake prevents further flow of the mud and provides a sealing membrane that allows the application of the mud pressure on the pervious formation (Fig. 2.1c). A well dispersed clay allows the formation of a thinner and a more impervious cake than that formed by a flocculated clay (Fig. 2.1c). A cake does not usually form on clay layers because of their low permeability and the small hydraulic gradient of the mud. This hydraulic gradient may be greatly increased by an osmotic pressure created when clay shales of a high salt concentration are penetrated. However, the hydration of the shale causes its softening and sloughing before the mud cake is formed.

Viscosity

Viscosity may be termed as the resistance of a fluid to flow. Water-base drilling muds usually exhibit the characteristics of a Binghamian fluid (Fig. 2.2) having a threshold resistance (yield point) and a plastic viscosity. The yield point is equivalent to the static shear strength of the mud, a strength that develops from attractional forces between the clay particles. While these forces are partially destroyed by stirring, the thixotropic properties of clays allow the forces to build up again when the mud is given time to rest. The plastic viscosity depends mainly on the viscosity of the water and on the friction between the solid particles in suspension. The two components of viscosity are practically independent. While the addition of water reduces the plastic viscosity by reducing the concentration of the solids, a chemical dispersing agent is required to reduce the yield point by reducing the attraction between particles. If the drilling fluid has no viscosity, cuttings would not be lifted nor would solids remain in suspension. Therefore, the viscosity is a very important property of drilling fluids.

Density

A 5% bentonite mud has a specific gravity of about 1.04 which may be too small to prevent the collapse of the hole. However, the density of mud can be greatly increased if silt, sand, and weighting material (Barite) are in suspension in the mud. In the construction of foundations the weighting of the mud for stability purposes is an extreme measure taken when unusual artesian pressures are encountered or when arching is not

effective such as in drilling large diameter holes. Such weighting procedures (density > 1.4) have been reported by DuGuid, et al. (1971) in connection with the construction of slurry trenches.

Of all the mud properties mentioned above, the wall-building capacity is the most important. This property is controlled by the following chemical characteristics of the mud.

pH

A suspension of bentonite in fresh water produces a satisfactorily dispersed alkaline solution having a pH of 8.0 or more. A lower pH usually results in mud flocculation and the formation of a bulky, pervious wall cake.

Hardness of Water

The presence of divalent magnesium and calcium ions in hard waters reduces the dispersability of the mud. Excessive hardness is treated by soda ash and, in the case where a calcium mud system is used, other chemicals such as chrome lignosulfonate are added to disperse the mud. Unlike other dispersive agents that disperse the mud by creating repulsive charges, the chrome lignosulfonates improves the dispersion by physically separating the clay particles (API, 1969).

Salt Concentration

Salt water is a very effective flocculent of bentonite muds. Attapulgite clays are very successfully used in salt waters. However, in certain cases, a bentonite mud premixed in fresh water may be used when salt contamination is not excessive.

Contamination

Contamination and flocculation of the mud can result from the penetration of formations containing gypsum or lime, the use of contaminated water, and the reuse of cement-contaminated mud from a previous construction. Regeneration of the mud or the use of a calcium mud system are two of the measures to take when such contamination problems are encountered.

STABILITY OF THE HOLE

The sizes of drilled shafts range from a few inches to over ten feet in diameter and from a few feet to over 100 feet in depth. The stability of such holes depends greatly on the size of the hole, the formations penetrated, the mud, and the drilling technique used.

Size of the Hole

The pressure required to keep a hole open is dependent on the diameter of the shaft. In an infinitely large hole, the horizontal pressure required to stabilize the walls of the hole is equal to the sum of the active earth pressure and the hydrostatic pore pressure. As the diameter of the hole decreases, this pressure is reduced by the ring-arching action. Approximate solutions to this problem indicate that only a small fraction of the hydrostatic water pressure is required to stabilize the hole (Terzaghi, 1943). As an example, a ten-foot-diameter hole in dry sand exerts at a depth of 100 feet a pressure of about 345 psf on the protecting casing. The pressures in an average size hole (two to five feet) are considerably smaller.

Soil Formation

A hole in clay with a small diameter cannot fail if the clay has a finite shear strength (Terzaghi, 1943) and if the clay does not have "quick" properties. A hole in perfectly cohesionless sand cannot possibly stand open because an element of sand at the surface of the hole does not possess any shear strength. However, the presence even of weak, cementing calcareous and siliceous bonds in natural sands and the existence of a thin mud cake when drilling under mud reduce the earth pressure and make the stability of the hole mainly dependent on the balancing of the hydrostatic pressure of the ground water.

The collapse of holes in clay is usually due to a softening of the clay by absorption of the water. In a dry hole, the water may be provided by the ground water flowing into the hole, and in a wet hole, the water is readily accessible from the mud. This softening process is greatly accelerated in both cases by the existence of fissures.

Drilling Mud

The stabilizing effect of mud in the construction of slurry trenches has been the subject of continuous, polemic debates since 1963 (Nash and Jones, 1963; discussions by Veder, Jones, Morgenstern, 1963; Morgenstern and Amir-Tahmasseb, 1965; Duguid, et al., 1971; Schneebeli, 1971). A discussion of these debates is not relevant to the stability of drilled holes where the stresses have been proved to be very small and can be balanced by a slightly weighted mud. The stability of holes drilled under mud in expansive clays deserves, however, special attention. The

softening of the clay by imbibition of water from the driling mud is known to cause the collapse of a hole by a progressive action of softening and sloughing that may be greatly accelerated by the existence of fissures. This water imbibition is due to an osmotic pressure gradient resulting from a different salt concentration between the mud and the pore fluid. On the other hand the dispersibility and erodibility of a clay are a function of the ratio of the exchangeable sodium ions to the total exchangeable ions in the pore fluid (Sherard, 1972) and a function of the dispersive power and, therefore, the alkalinity of the mud. When an erodible formation is penetrated, a calcium mud is recommended. When a sodium mud is used, the addition of lime and deflocculating agents is reported to result in a successful performance (API, 1969). In certain situations a successful operation may be achieved if the mud is kept at a minimum pH and the drilling is done rapidly.

Drilling Techniques

The collapse of a hole may be triggered by poor drilling techniques. Typical examples of this problem are:

a. The erosion of the soil in the hole at the level of the surface of the mud due to the fluctuation of that surface. This problem can be solved by use of a short, surface casing that contains the fluctuating surface.

b. The suction of the hole resulting from a rapid extraction of the drilling tool.

c. The mechanical erosion resulting from the wobbling of the drilling tool in a non-plumb hole or from careless, erratic drilling.

CONCRETING

An analytical, rigorous solution for the flow of concrete in the slurry displacement method is quite complicated. In this section, the factors affecting the flow are discussed for a better understanding of the concreting procedure.

Size of the Tremie

Ideally, when using the tremie in placing concrete, the tremie is held in place while the concrete is poured and the mud is displaced continuously. Figure 2.3 shows a scheme of this concreting procedure at an intermediate phase.

For this type of flow, the size of the tremie can be optimized to obtain the most efficient flow conditions. In analyzing this problem it shall be assumed that the flow is laminar and, therefore, that the head losses are a linear function of the velocity of flow. In a section $\Delta\ell$ of the hole (Fig. 2.3), the head losses can be divided into:

a. Head losses in the tremie:

$$h_1 = k_1 \frac{\Delta\ell}{d} V_1$$

$$V_1 = \frac{4q_c}{\pi d^2}$$

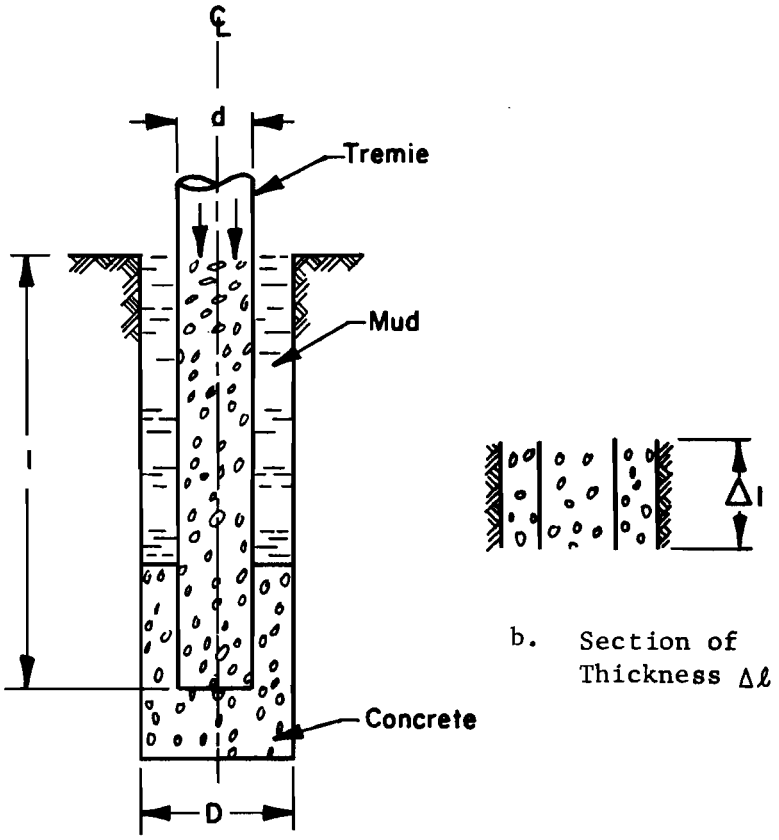

b. Section of Thickness $\Delta \ell$

a. Section Through the Hole

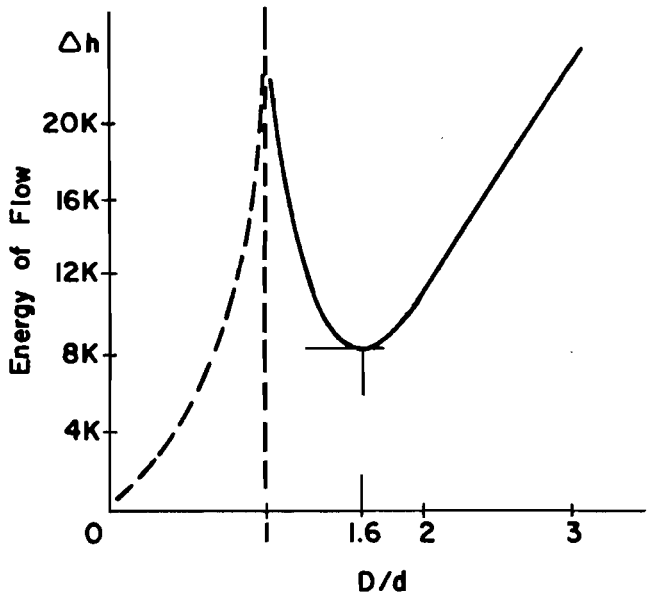

c. Energy of Flow Vs. Diameter Ratio

Fig. 2.3 Optimization of the Size of the Tremie

where

k_1 = a constant which is a function of the roughness of the tremie and the viscosity of the concrete,

V_1 = average velocity of flow in the tremie,

q_c = rate of flow of the concrete.

b. Head losses in the borehole:

$$h_2 = k_2 \frac{\Delta \ell}{D-d} V_2$$

$$V_2 = \frac{4q_c}{\pi(D^2-d^2)}$$

where

k_2 = a constant which is a function of the roughness of the tremie, the roughness of the walls of the borehole, and the viscosity of the concrete,

V_2 = average velocity of the flow in the borehole.

If the roughness of the walls of the borehole is considered equivalent to that of the tremie, the total head loss can be expressed as

$$\Delta h = \frac{4q_c}{\pi} \frac{k_1 \Delta \ell}{D^3} \left[\left(\frac{D}{d} \right)^3 + \frac{D^3}{(D-d)^2 (D+d)} \right]$$

Let $n = \frac{D}{d}$ and rewrite this expression as

$$\Delta h = K \left[n^3 + \frac{n^3}{n^3-n^2-n+1} \right]$$

where

$$K = \frac{4q_c}{\pi} \frac{k_1 \Delta \ell}{D^3}$$

For a hole having a certain diameter and a certain length the value of n can be optimized for the minimum head loss. Figure 2.3b shows a plot of Δh versus n which indicates that optimum flow conditions take place for a diameter ratio D/d of 1.6. Due to oversimplifications in the analysis, the true optimum ratio can fall anywhere between 1.4 and 1.8. Furthermore, the effective diameter of the borehole is significantly reduced by the existence of the steel reinforcement and the thickness of the walls of the tremie. As an example, a 12 to 14-in. tremie performs best in a 30-inch hole if the effective diameter of the hole is considered to be about 22 in.

However, difficulties in sinking a large sealed tremie provide an upper limit to the size of the tremie, and the drilling contractor does not normally use tremies larger than 14 in. These difficulties may be overcome by the weighting of the tremie, and in certain concreting procedures the tremie may be sunk unsealed, in which case a plastic plug (Palmer and Holland, 1966) is pushed down the tremie by the first charge of concrete to prevent mixing of concrete and mud.

Characteristics of the Flow of the Concrete

An easy and vigorous flow of the concrete is desired in the slurry displacement method to insure the scouring of the walls of the hole and to prevent mud entrapment. The best concrete is, therefore, the most fluid concrete that would satisfy the structural requirements. Such a concrete should preferably have the following constituents and properties:

Cement:	7 to 8 bags per cubic yard of concrete
Aggregates:	round natural aggregates (<0.75 in.)
Slump:	greater than 6 inches yet the concrete should not be easily segregated
Entrained air:	4 to 5%

Plasticizers and retarders may be added but should not impair the structural integrity of the concrete.

The ideal flow described above is inhibited when concrete is placed in a small hole, with a poorly cleaned tremie, when a heavy mud is used, and when the concrete is stiff. The concrete may not be able to flow under normal hydraulic gradients and flow may have to be induced by partial extraction of the tremie. The analysis of these non-ideal flow conditions depends greatly on the value of the yield strength of the fluid concrete (Binghamian yield), which has to be overcome before any flow takes place. In the following section an approximate analysis of non-ideal flow is suggested.

Figures 2.4a and 2.4b show schematically free body diagrams of a column of concrete during concreting. In these diagrams the following notation is employed.

r_o = external radius of the tremie, in.;

r = radius to any point in the borehole, in.;

R = radius of the borehole, in.;

H_c = height of concrete column from the bottom of the tremie to the interface with the mud, in.;

P_1 = hydrostatic pressure at the bottom of the tremie, psi;

P_2 = hydrostatic pressure at the surface of the concrete column, psi;

W = pressure due to the weight of a concrete column, psi;

f_o = average vertical shear stress at the outerface of the tremie, psi;

f_r = average vertical shear stress at any distance r in the borehole, psi.

In this analysis it shall be assumed that the effects of arching in the concrete are not significant and that, therefore, the hydraulic gradient is constant throughout the concrete column. Figure 2.4c shows the free-body diagram of a sectorial section of a unit height. The summation of vertical forces on this section yields:

$$f_r = f_o \frac{r_o}{r} + \frac{i(r^2 - r_o^2)}{2r} \gamma_c$$

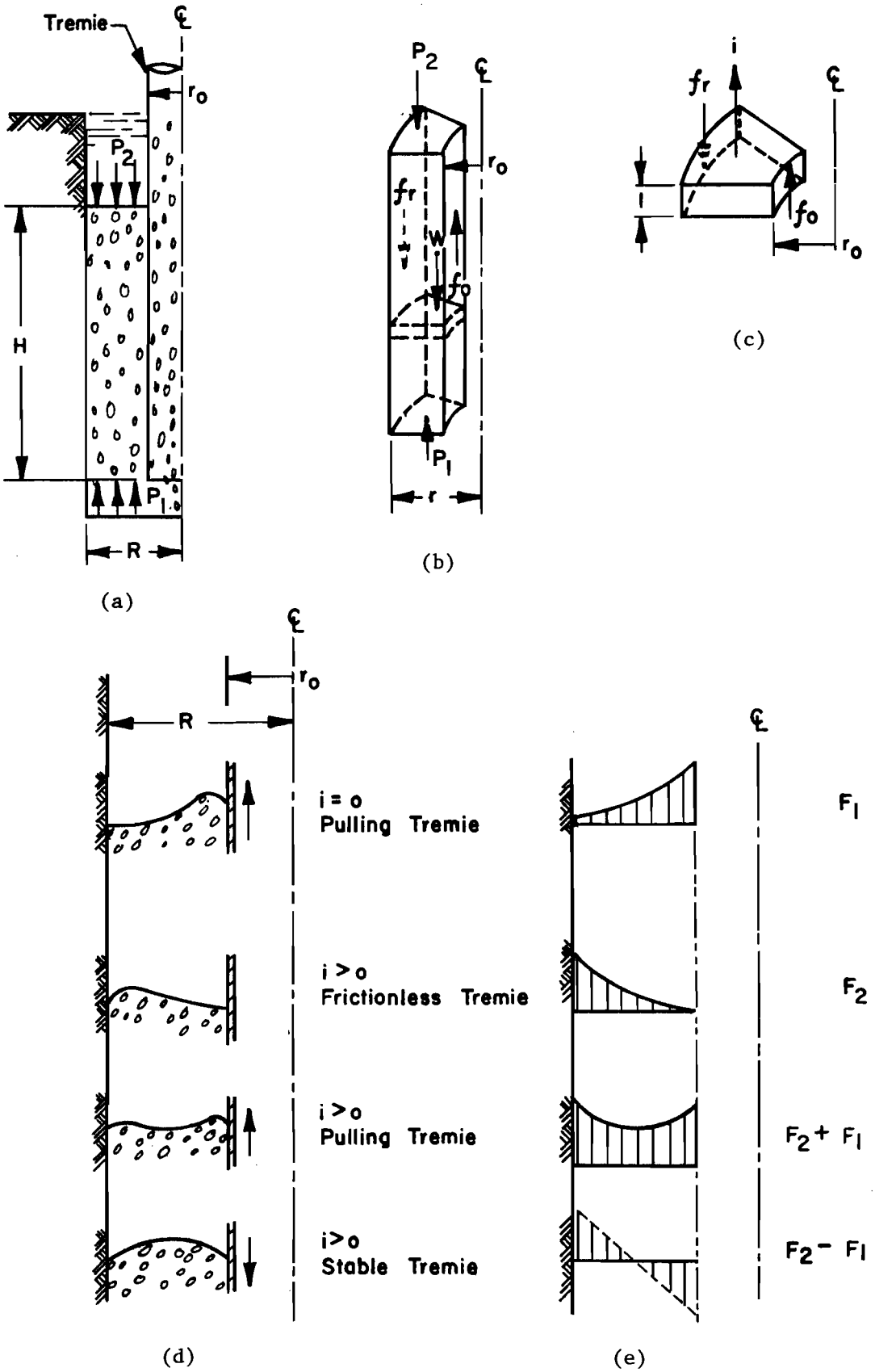

Fig. 2.4 Schematical Description of the Flow of Concrete

where

i = hydraulic gradient,

γ_c = unit weight of concrete, lb/in^3.

Let $F_1 = f_o \frac{r_o}{r}$

and $F_2 = \frac{i(r^2 - r_o^2)}{2r} \gamma_c$

Figure 2.4e shows the independent plots of these functions. When the shear stress f_r exceeds the yield strength of the fluid concrete, a flow of the concrete takes place. The plot of the function F_1 shows that flow takes place at the periphery of the tremie when the tremie is pulled upward. Under these flow conditions, the concrete flows outward and away from the tremie preventing any scour of the walls. In the case of an ideally frictionless tremie, no force can develop at the walls of the tremie and the shear stress in the concrete column is given only by the function F_2. This case provides a better scour of the walls of the hole where the shear stresses in the concrete are largest. When a significant hydraulic gradient is used in conjunction with a rough surface tremie, the flow tends to scour the walls of the tremie and of the borehole. However, when "pumping" of the tremie is practiced the continuous motion of the tremie reduces the thixotropic strength of the concrete around it and forces the concrete to flow into paths in the immediate vicinity of the tremie (Schneebeli, 1971), thus preventing the scour of the walls of the hole.

Quality of the Tremie Concreting

Good quality concrete can be obtained when the tremie-concreting operation is performed properly. The essentials of good concreting techniques have been presented by Palmer and Holland (1966) and by Barker and Reese (1970). Some of the factors impairing the quality of tremie concrete are discussed in this section.

The excellent curing conditions for concrete in soils below the water table have been shown to give better concrete properties than common curing procedures (Veder, 1969). However, tremie concreting presents the danger of contamination of the concrete by the drilling mud if improper techniques are used. Mud entrapment in the concrete has been observed to take place in the following circumstances:

1. When a steel reinforcing cage is used which unduly restricts the upward flow of the concrete (the excessive horizontal reinforcement can be particularly detrimental to the flow).
2. When a flocculated or poorly mixed, heavy mud is used.

Furthermore, chances for the entrapment of mud are increased when the concrete flow is assisted by the "pumping" of the tremie. As the cement-coated tremie comes out of the concrete, mud flocculates on contact with cement and coats the surface of the tremie. This coat of mud is easily trapped in the concrete when the tremie is lowered again. Such contamination has not been observed to impair significantly the quality of the concrete; however, serious contamination due to the "pumping" of the tremie takes

place when the tip of the tremie gets close to the surface of the concrete. A significantly increased velocity of flow of the concrete could then occur, causing considerable turbulence at the concrete-mud interface and resulting in the entrapment of mud and sediments in the "whirl." Recommended minimum values for the embedment of the tip of the tremie have ranged from 5m (Komornik and Wiseman, 1967) to 0.5m (Jezequel, 1971). It is believed that the embedment of the tremie should be a function of the diameter of the tremie, the diameter of the hole, and the pressure in the concrete at the end of the tremie. Assessment of the optimum embedment by means of analysis is not possible at present. It is believed that a value of about 1.5m (5 ft) is a reasonable value for average size shafts (30-in hole and 12-in tremie).

The collapse of the walls of the hole and the falling of surface debris may cause contamination of the concrete, and as mentioned previously the construction techniques which are employed should be selected to minimize the amount of extra soil in the hole.

The quality of the bond between the concrete and the steel reinforcement is a matter of concern (Sadlier and Dominioni, 1963; Cole, 1963). Recently, pull-out tests were conducted by personnel of the Texas Highway Department (H. D. Butler, 1972) on the steel of an extracted shaft, which had been constructed by slurry displacement, and on laboratory specimens cast under mud to simulate tremie concreting. The results of these tests indicated a significant drop in the bond resistance of smooth steel bars and a negligible drop in the bond resistance of deformed bars. These results

are in agreement with the results of tests reported by Cole (1963). The influence of a thin coating of bentonite is minimal because the bond resistance of a deformed bar is mainly mechanical. It should, however, be emphasized that the bond may be greatly reduced when flocculated lumps of mud are entrapped on the steel, and every measure should be taken to prevent such mud entrapment. The horizontal reinforcement, consisting usually of mild steel (spirals) and being the most liable to mud entrapment, constitutes a vulnerable place for a bond failure.

BEARING CAPACITY CONSIDERATIONS

Conditions at the Tip of the Shaft

When the drilling of the hole is completed, a drilling bucket is usually used to remove loose debris and to form a flat bottom to the hole. The steel reinforcement is then introduced. When reinforcement is used over the full length of the shaft, concrete chairs are attached at the bottom of the cage to prevent the sinking of the cage. A temporarily sealed tremie is then introduced. During these operations, sediments suspended in the mud and debris falling from the surface collect and mix at the bottom of the hole. The natural soil at the bottom of the hole is disturbed by the placing of the steel and of the tremie. After the first charge of concrete, the tremie is lifted and the seal is broken. Fig. 2.5a describes these steps and shows the tip conditions which are obtained when the tremie is sealed by a wood block and a plastic sheet. The entrapment at the bottom of sediments may result in the formation of a pointed tip of the shaft. The

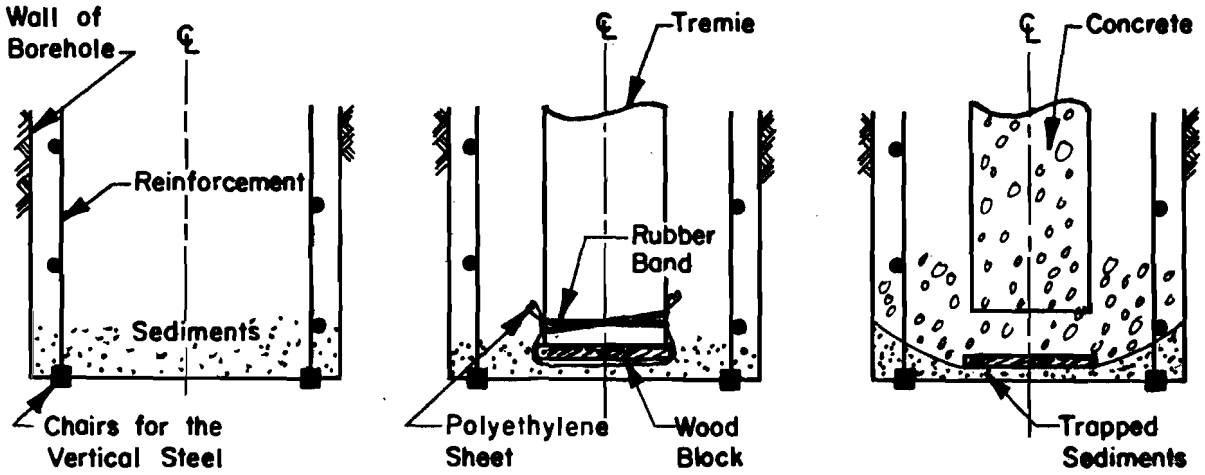

a. Wood Block and Polyethylene Sheet

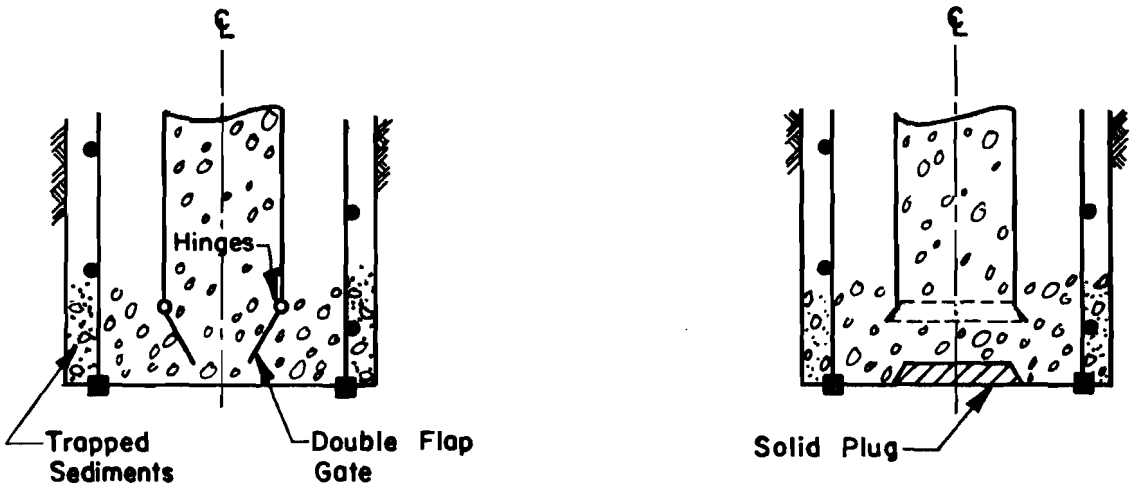

b. Proposed Alternatives for the Seal

Fig. 2.5 Effects of the Tremie Seal on the Conditions at the Tip of the Shaft

use of the type of seal shown in Fig. 2.5a is not recommended in shafts greatly depending for their bearing capacity on the tip resistance. For such shafts a better seal should be devised. Possible improved seals are a water tight flap gate hinged at two points or a tapered solid seal (Fig. 2.5b). These two types of seals take advantage of the fact that the first charge of concrete flows under the highest gradient and its initial surge can be used advantageously to remove the bottom sediments (Jezequel, 1971). Also, for better washing action the tremie size should be optimum as suggested by the analysis in a previous section.

Soil-Concrete Interface

The nature and the characteristics of the interface between the concrete and the soil have a decisive influence on the load transfer of drilled shafts. In shafts constructed by slurry displacement the phenomena described in the following paragraphs are postulated to take place during the formation of the interface over the total depth of the shaft.

Figure 2.5 shows what are believed to be the conditions of the interface near the tip of the shaft. The heavy sediments at the bottom of the shaft, if given the chance to be lifted by the first turbulent flow of the concrete, may be trapped on the walls of the shaft, at a distance extending probably to one diameter from the tip of the shaft.

The filtration of the mud into granular layers causes the formation of a mud cake on the surface of those layers. The thickness of the cake depends on the rate of loss of water, which in turn depends on the grain size distribution of the soil, on the mud head applied, and on the

characteristics of the mud in use. When a well-dispersed mud is used in drilling through fine sands, the thickness of the cake may be in the order of 1/16 inch. When a flocculated mud loaded with sand is used in drilling through a course granular formation, a cake in the order of 1 inch thick or more may build up. Veder (1963) also showed that the thickness of the cake is a function of an electrical current which occurs between the mud and the native soil. The magnitude of this current and, therefore, the thickness of the cake are dependent on the chemistry of both the mud and the soil formation.

The vertical travel of the auger in the hole is coupled with a horizontal wobbling which has the effect of mechanically eroding the soil formation at certain places, scraping the cake at others, and probably depositing a coating of mud and soil at yet other places. Furthermore, if the mud is heavily charged with sand, during the concreting process, sediments from the mud collect on the surface of the concrete. When the concrete is forced by the upward motion of the tremie to flow outward from the tremie (Fig. 2.4d), the sediments are trapped between the concrete and the walls of the hole (Fig. 2.6a). The sediments, usually consisting of sand, squeeze into the mud-soil cake already existing on the walls of the hole. This coating is usually softer than the cement paste and the concrete aggregates in turn squeeze into the coating and may also engage the soil formation, resulting in a rough concrete surface (Fig. 2.6b). When the mud cake is absent, and the concrete is cast against a relatively stiff soil formation, the surface of the concrete has been observed to be as smooth as when cast against a rigid formwork (Fig. 2.6c).

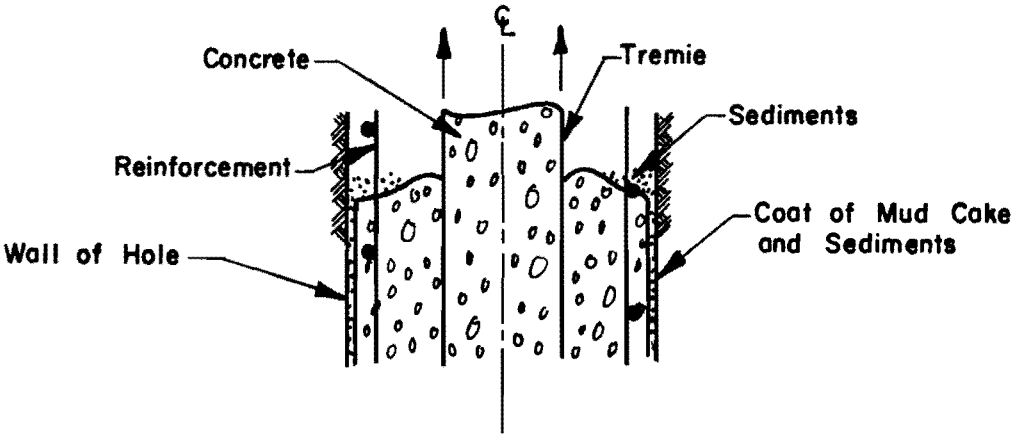

a. Formation of Coating

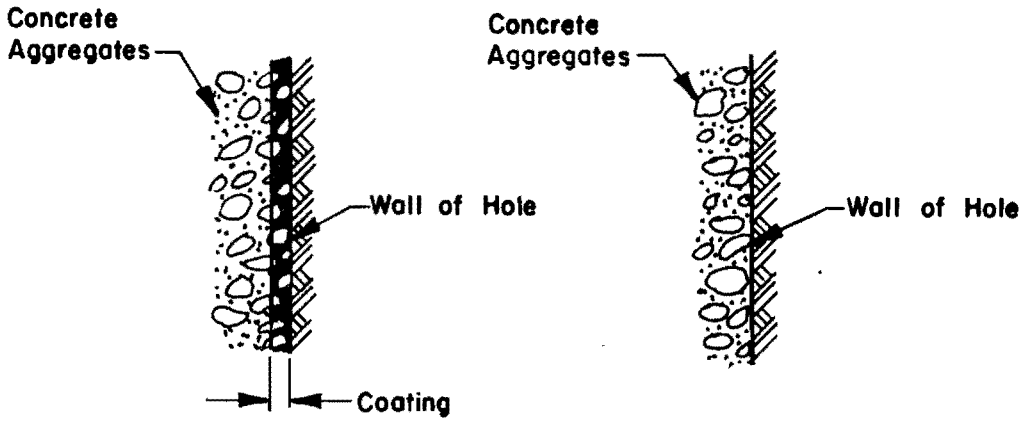

b. With Mud Cake

c. Without Mud Cake

Fig. 2.6 Concrete Soil Interface

Penetration of the Mud in the Soil

Various studies on the drilling of bored piles attribute the stability of the hole to the penetration of the thixotropic mud into the granular soil formation (Veder, 1953; McKinney and Gray, 1963; Elson, reported by Florentin, 1969). While drilling muds may penetrate several feet into layers of gravels and pebbles, their penetration into fine sand is insignificant. Laboratory tests conducted by the author to study the penetration of a 5% bentonite into Ottawa sands of different sizes and having uniformity coefficients of one are reported in Fig. 2.7. Similar tests, conducted on a fine sand having uniformity coefficients of 1.5 to 2.0, showed no measurable penetration even at high pressures. Studies of the grouting of granular materials (King and Bush, 1961) suggested, based on field results, two criteria limiting the gradation of grouts with respect to that of soils:

a. $$\frac{D_{15} \text{ of grouted soil}}{D_{85} \text{ of grout}} > 15$$

b. $$\frac{D_{10} \text{ of grouted soil}}{D_{90} \text{ of grout}} > 8$$

Certain authors even recommend for the first criterion a ratio as high as 20 to 30 to obtain a grout which will flow into the soil formation. Considering the fine sand used in the laboratory penetration tests, which had a D_{15} of 0.1 mm, the first criterion would require a D_{85} of the grout smaller than about 5 microns. This criterion is not usually satisfied in

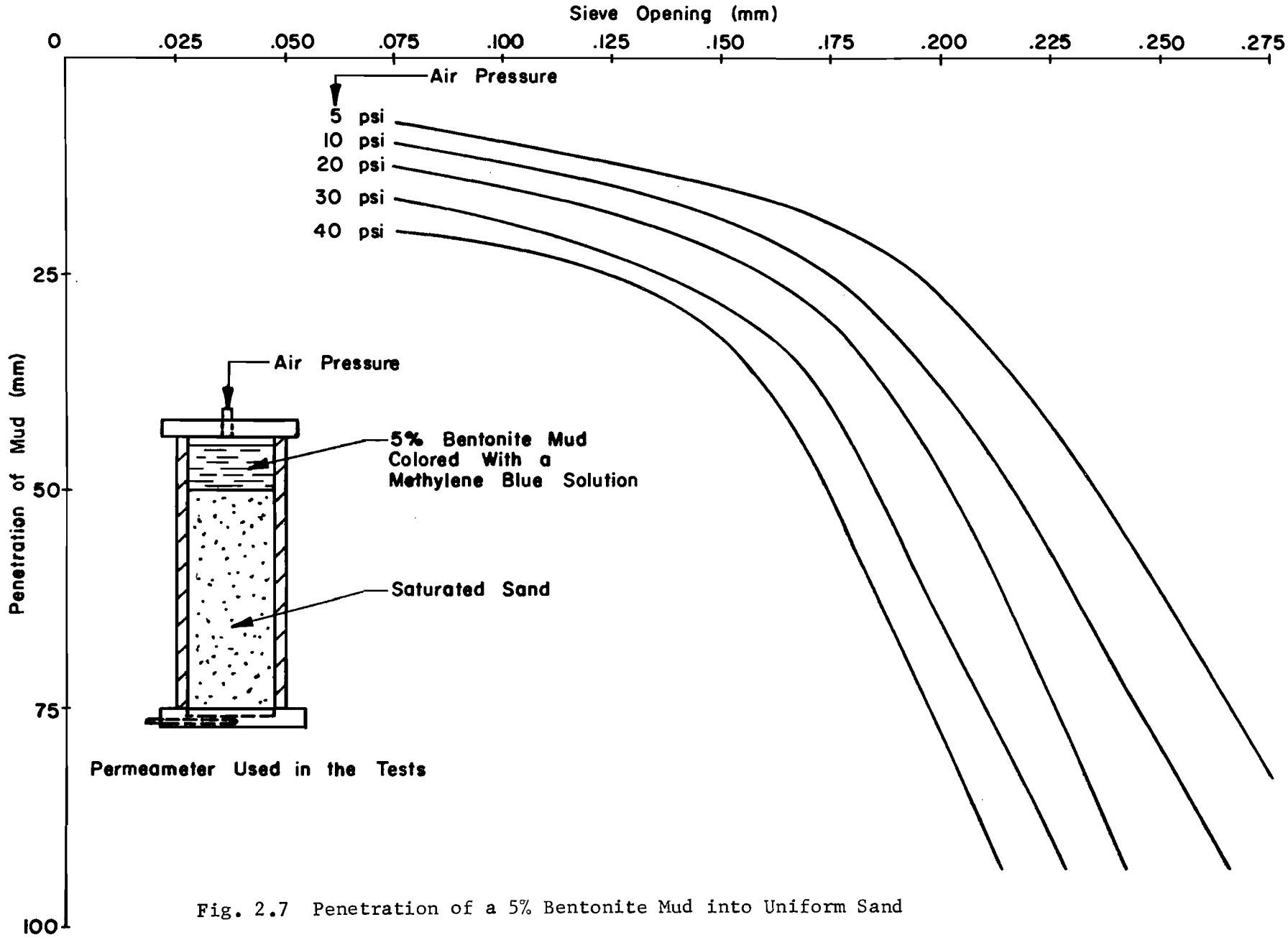

Fig. 2.7 Penetration of a 5% Bentonite Mud into Uniform Sand

commercial bentonite. In the drilling of a borehole, the mud is usually charged with silts and sands and its penetration into layers finer than a medium sand is almost impossible. The effects of mud penetration into coarse grained soils are not yet well understood.

STRESSES IN THE SOIL

The opening of a hole in the ground results in a relief of horizontal stresses near the hole. Overconsolidated soils have a coefficient of earth pressure at rest that is significantly greater than 0.5 (Hendron, 1963). To restore the original horizontal stresses in such soils by the imposition of hydrostatic stresses from mud or concrete is impossible. This relief of horizontal stress is usually coupled with a strain in the soil that may result in the opening of fissures in clay and in the destruction of cementing bonds in sand. Therefore, the magnitude of the stress relief can influence significantly changes in the properties of the soil. The stress relief in the slurry displacement method is considerably smaller than that which occurs in most conventional drilling methods.

Lateral pressures between the concrete and the soil have a decisive influence on the load transfer of the shaft. Studies on the pressure developed on the formwork of a concrete column indicate that this pressure reaches an ultimate value for heights of concrete greater than a certain critical value (Peurifoy, 1965). The existence of an upper limit to this pressure has been attributed to the setting and the arching of the concrete.

In concreting under mud, the pressures in the concrete are at least equal to the pressure of the column of mud above it. Furthermore, when the concrete is allowed to flow in large diameter holes without the "pumping" of the tremie, and when the tip of the tremie is close to the bottom of the shaft, the pressure in the concrete may be larger than the hydrostatic pressure of a column of concrete. In Fig. 2.8 the pressure at a point A at the bottom of the shaft is given by the following expressions:

a. Wet concreting:

$$P_v = h_c \gamma_c + h_m \gamma_m + \frac{Cq_s h_c}{A}$$

$$P_h = P_v - 2q_s$$

b. Dry concreting:

$$P_v = h_c \gamma_c - \frac{Cq_s h_c}{A}$$

$$P_h = P_v - 2q_s$$

where

P_v = vertical pressure at point A, psi;

P_h = horizontal pressure at point A, psi;

γ_c = unit weight of concrete, lb/in^3;

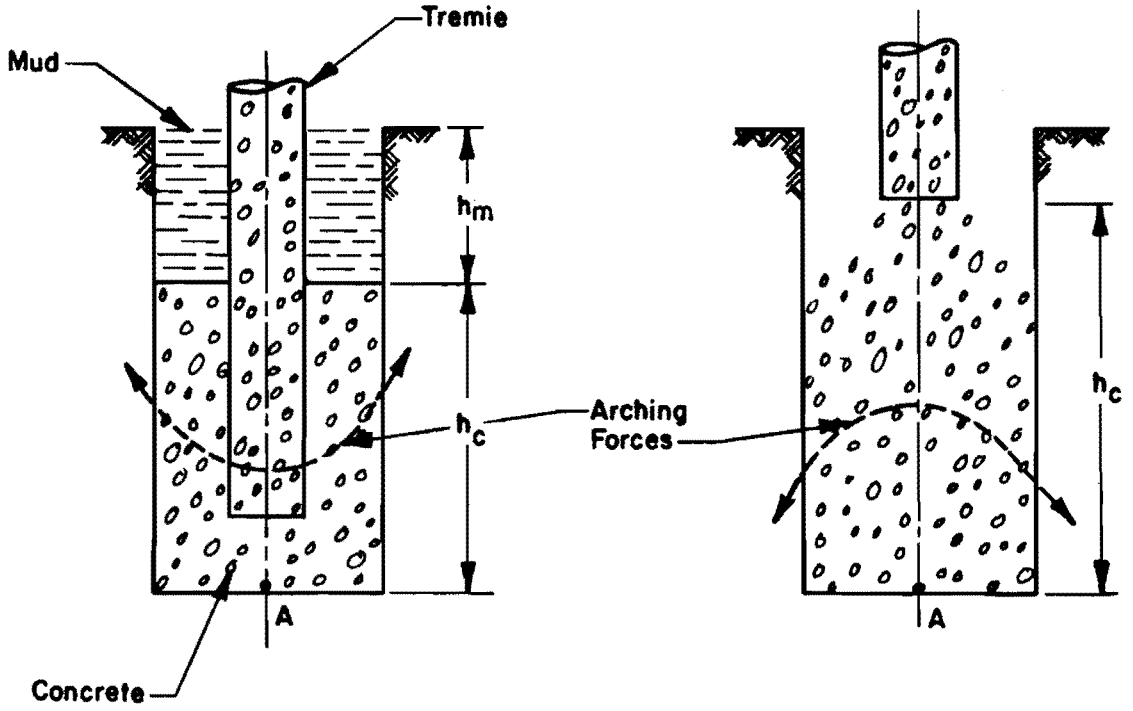

a. Concreting by Slurry Displacement

b. Concreting in the Dry

Fig. 2.8 Effect of Concreting Procedure on the Pressure in the Concrete

h_c = height of column of concrete, in;

h_m = height of column of mud, in;

γ_m = unit weight of mud, lb/in^3;

C = circumference of the shaft, in;

q_s = shear stress developed on the periphery of the shaft;

= shear strength of the plastic concrete, psi

A = cross sectional area of the shaft, in^2.

The side shear forces developed on the periphery of the concrete column may be locked in the concrete when concreting is completed due to a combined action of setting and arching. These forces result in a pressure in excess of the hydrostatic pressure when concreting is completed under mud.

This page replaces an intentionally blank page in the original.
-- CTR Library Digitization Team

CHAPTER III. THE ANALYSIS OF DRILLED SHAFTS

BEARING CAPACITY THEORIES

The ultimate bearing capacity Q of a deep foundation is conventionally considered as the sum of the resistances to penetration Q_s and Q_t developed respectively by the sides and the tip of the foundation element, Fig. 3.1. The following sections offer a brief discussion of each one of these components.

Tip Resistance

The theories proposed for the evaluation of the tip resistance of a deep foundation are based on two main approaches. The first approach considers the soil at the tip of the foundation as a rigid plastic incompressible material and evaluates the force required to bring the soil inside a logarithmic spiral failure surface into a plastic state, using an extension of the solution originally derived for shallow footings (Terzaghi, 1943; Meyerhof, 1951; Vesić, 1963), Fig. 3.1a. The principal difficulty encountered in the use of the logarithmic spiral to compute bearing capacity is the selection of the shape and dimensions of the failure surface. The computations of various investigators are based on failure surfaces of different dimensions and, hence, the results obtained have been greatly different (Vesić, 1965).

The second approach to the evaluation of the tip resistance of a deep foundation equates the problem of the penetration of the tip of the foundation to that of the expansion of a spherical cavity inside a semi-infinite, elasto-plastic medium (Skempton, et al., 1953, after Vesić, 1965; Ladanyi,

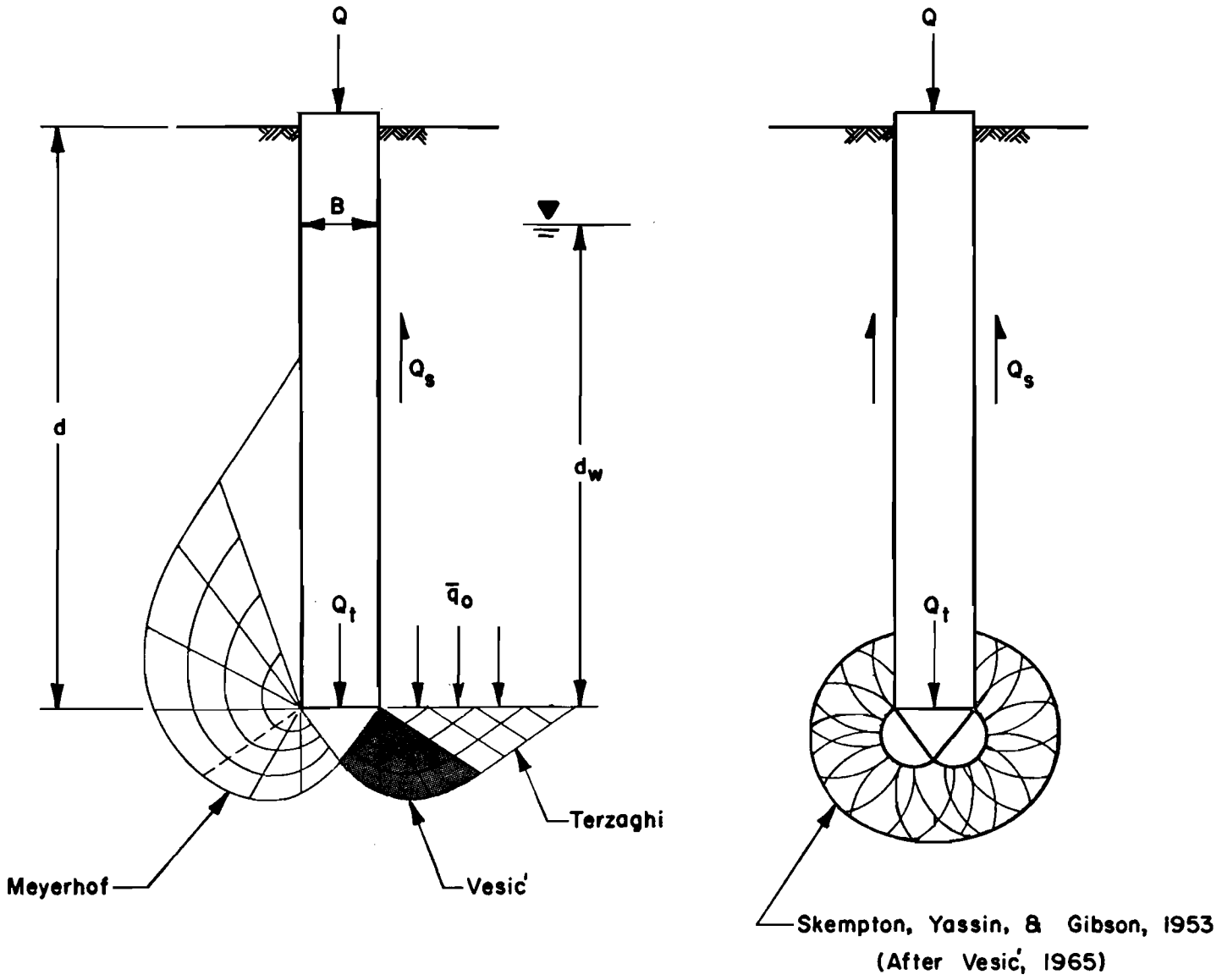

Fig. 3.1 Diagrams of Failure Surfaces at the Tip

1961; Vesić, 1972). In this approach the elastic properties of the soil (Young's modulus and Poisson's ratio) are introduced as variables in the expression for the ultimate tip resistance.

The ultimate bearing capacity of a circular deep foundation on cohesionless soil is expressed by theories from the first approach as

$$q_t = \frac{Q_t}{A_t} = \frac{1}{2}\,\bar{\gamma} \cdot B \cdot N_\gamma + \bar{q}_o \cdot N_q + \gamma_w \cdot d_w \quad \ldots\ldots\ldots \quad (3.1)$$

where

q_t = ultimate average tip pressure,

A_t = cross-sectional area of the tip,

$\bar{\gamma}$ = average effective unit weight of the soil around the tip,

B = diameter of the tip,

$\bar{q}_o$ = effective pressure in the soil at the level of the tip,

γ_w = unit weight of ground water,

d_w = height of the water level above the tip,

N_γ, N_q = bearing capacity coefficients related respectively to the weight of the soil inside the failure zone and the effective pressure $\bar{q}_o$.

It has been found convenient in the analysis of deep foundations to express Equation 3.1 in the following form:

$$q_t = N'_q \cdot \bar{q}_o \quad \ldots\ldots\ldots\ldots\ldots\ldots\ldots\ldots \quad (3.2)$$

where

N'_q = a factor combining the effects of N_q and N_γ

The values of N'_q given for deep foundations by the different theories differ extremely (Vesić, 1967). Experimental studies of bearing capacity have met only with partial success mainly due to the scale effects in laboratory model tests and due to the heterogeneity of natural deposits in full-scale field tests. It is not the purpose of this study to discuss the merits and the drawbacks of the different theories, yet in the following sections the factors influencing the values of N'_q shall be discussed in the light of the findings of research conducted during the last decade.

Angle of Shearing Resistance. The extent of the failure surface and therefore, the magnitude of N'_q depend on the friction angle ϕ of the sand. The Mohr envelope for a given sand is curved for low and moderately high pressures (< 50 kg/cm^2) but at higher pressures tends to become a straight line that is only a function of the composition of the sand. At stresses less than those which cause crushing (about 10 kg/cm^2) the value of ϕ is a function of the relative density of the sand and has been expressed by various authors (Caquot and Kérisel, 1949; Vesić, 1963) as

$$\phi = \tan^{-1} \frac{k}{e} \quad \ldots\ldots\ldots\ldots\ldots\ldots\ldots\ldots \quad (3.3)$$

where

k = constant of the particular sand and includes the effects of factors other than the density and the stress level,

e = initial void ratio of the sand.

Compressibility of the Sand. The influence of the compressibility of sand on the ultimate bearing capacity of the tip of deep foundations may be as important or more important than the friction angle of the soil. This conclusion can be made from the analysis of the expansion of a sphere in a semi-infinite medium. The analysis shows that the limit pressure that can be applied to the sphere is a function of the modulus of elasticity of the soil and of the Poisson's ratio (Kérisel, 1964; Vesić, 1965, 1972). Vesić (1965) showed that the tip resistance depends strongly on the stiffness index I_r which he defined as

$$I_r = \frac{E}{(1+\nu)(c+q \tan \phi)} \quad \ldots\ldots\ldots\ldots\ldots\ldots \quad (3.4)$$

where

E = the initial tangent modulus,

ν = Poisson's ratio,

c = cohesion of the soil,

q = confining pressure.

Recent studies on the compressibility of sand (Seed and Lee, 1967; Vesić and Clough, 1968) have shown that

1. Significant crushing of the sand grains and consequently significant compression takes place at confining pressures larger than 10 kg/cm^2. The magnitude of the compression is a function of the original density of the sand.
2. Dilation of sand takes place only when the sand is sheared at pressures below a certain critical value which ranges between 10 and 100 kg/cm^2.
3. The modulus of deformation E increases approximately as the 1/2 power of the mean normal stress in the low pressure range (0 - 10 kg/cm^2) and approximately as the 1/3 power in the elevated pressure range (10 - 100 kg/cm^2). Finally, beyond a certain critical mean pressure the sand behaves as a linearly deformable solid with the modulus of deformation E being proportional to the mean normal stress.

The influence of other factors on the compressibility of sand has not yet received much attention. The mineralogical composition of the sand exerts a considerable influence on its compressibility. The most common minerals in sand deposits are quartz, feldspar, and hornblend. These minerals have a hardness ranging between 5 and 7 on the Moh's scale. However, the existence of large deposits of sands composed of carbonate minerals is also common (Libyan sand, Lambe and Whitman, 1969). The carbonate sands result commonly from the accumulation under water of marine life shells or from the deposition of carbonates dissolved in

acidic rain water. The deposition of these carbonates in loose sediments causes a cementation of the sand grains and may prevent further consolidation under later deposition of sediments.

The angularity, texture, and size of the individual grains also influence the compressibility of sand. Sand grains that are large and angular and with a rough surface tend to crush and, therefore, compress more than grains that are small, round, and smooth.

Method of Installation of the Foundation. The method of installation of the pile influences the ultimate tip resistance because the method of installation affects the relative density of the sand and also affects the stresses in the sand. In a driven pile a zone of highly densified sand is formed in the immediate vicinity of the tip (Berezantzev, et al., 1957, 1961; Robinsky and Morrison, 1964), while loosening of the sand at the bottom of the hole may take place when installing a bored pile. The loosening of the sand at the bottom of a drilled hole can result from the release of stress and from possible seepage into the hole. Furthermore, when poor construction techniques are used in drilling the hole for a drilled shaft, loose soils may be left at the bottom of the hole as a result of the careless cleaning of the hole, the sloughing of the walls of the hole, the deposition of sediments suspended in the drilling mud, and the entrainment in the hole of surface debris (Reese and Touma, 1972). The existence of very compressible material at the bottom of a drilled hole usually results in a smaller tip resistance for drilled shafts than for driven piles.

The Dimensions of the Foundation. The influence of the dimensions of the pile on the ultimate tip resistance is a complex function of the two factors emphasized above, namely, the friction angle and the compressibility of the sand. At shallow depths, sand of medium to high density can be treated as an incompressible material and the general shear failure theorized by Terzaghi and Meyerhof can take place. For a general shear failure the bearing capacity factor N'_q increases with the depth and with the diameter of the foundation. This increase is linear to a certain depth, beyond which the effects of a reduced friction angle (due to a curved Mohr envelope) and an increased compressibility (due to higher confining pressures) cause a reduction in the rate of increase of N'_q with depth (Kérisel, 1961; De Beer, 1963; Vesić, 1963). Furthermore, the contribution of the weight term N_γ is relatively reduced with depth and consequently the influence of the diameter on the ultimate unit tip bearing capacity becomes negligible. De Beer (1963) used Meyerhof's theory to prove that for a dense sand the value of N'_q decreases with depth beyond a critical depth of about twenty diameters.

Experimental data on model and full-scale piles (Kérisel, 1961; Vesić, 1963) indicate that the ultimate resistance of the tip increases with depth and tends asymptotically to a limiting value at a critical depth varying between ten diameters for loose sand and twenty diameters for dense sand. Figure 3.2 presents measured values of the ultimate tip resistance of piles jacked in sand as a function of the size and the depth of the piles, and the density of the sand. The tendency of the bearing capacity to become

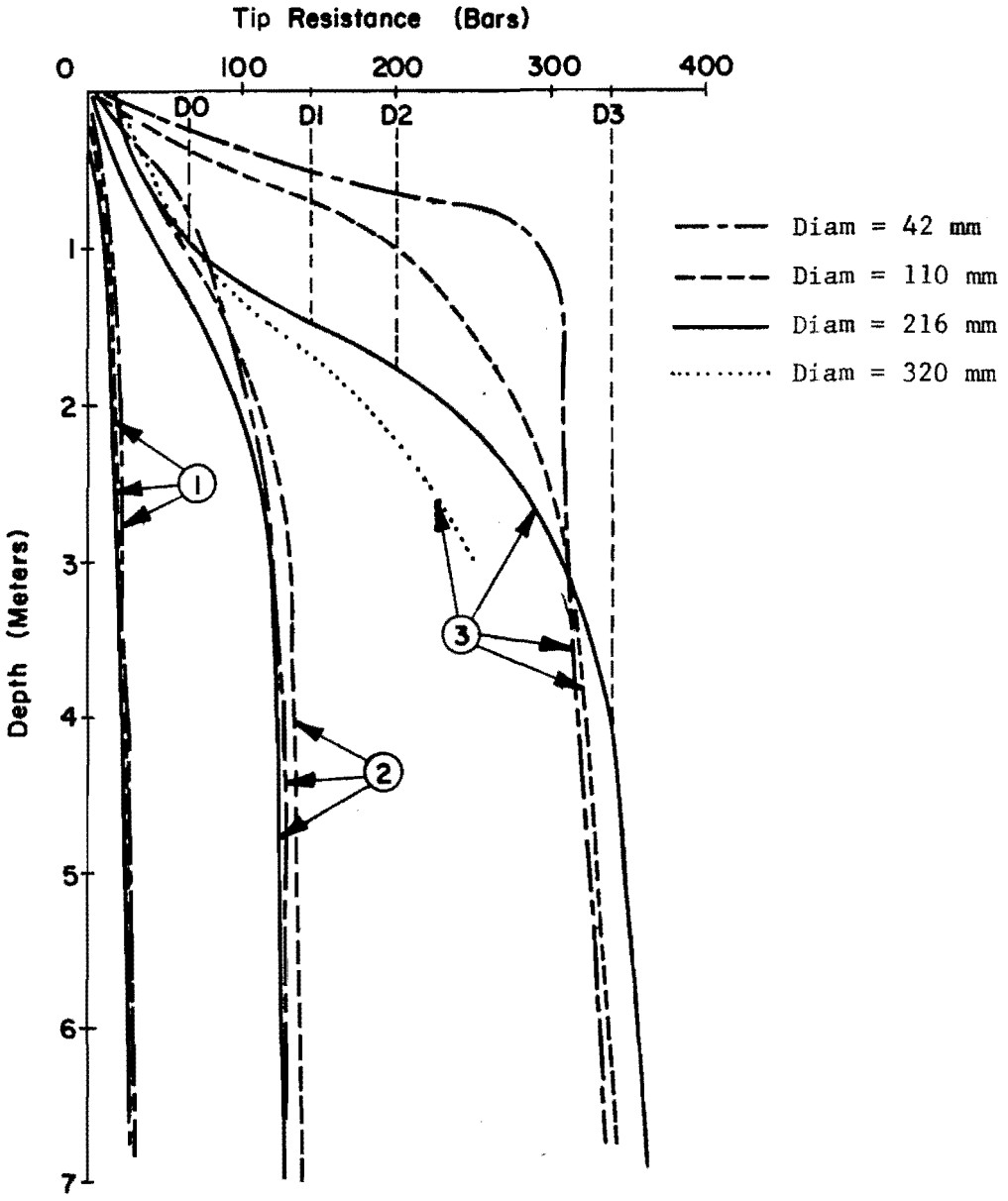

① Sedimentation	② Slight Compaction	③ Heavy Compaction
γ_d = 1.58	γ_d = 1.68	γ_d = 1.75
D_r = 72%	D_r = 86.5%	D_r = 94%
ϕ = 35°	ϕ = 38°	ϕ = 42°

Fig. 3.2 Point Resistance in Sand Vs. Depth
(After Kérisel, 1961)

a constant has been explained (Kérisel, 1961, 1964; Vesić, 1963) by the fact that only "punching failure" can take place at great depths as a result of the compressibility of the sand. The compression of the sand, followed by an arching of the sand around the tip of the foundation, has the effect of reducing the vertical pressure $\bar{q}_o$ at that level to a constant value which is independent of the depth of the foundation. The constant ultimate tip resistance q_t was given by Vesić (1971), as a function of the relative density D_r, in the following equations:

$$q_t = 4(10)^{2.4\ D_r^3} \qquad \text{(Driven Piles)} \quad . \quad . \quad . \quad . \quad . \quad . \quad . \quad . \quad . \quad . \quad (3.5)$$

$$q_t = 1.5(10)^{2.4\ D_r^3} \qquad \text{(Drilled Shafts)} \quad . \quad . \quad . \quad . \quad . \quad . \quad . \quad . \quad . \quad (3.6)$$

However, the practical application of these expressions, presented as an exponential function of the relative density, is limited by the capability to evaluate the relative density of natural sand deposits. A small change in the relative density influences significantly, at high densities, the values of the tip resistance evaluated from these expressions. It must further be mentioned that since compressibility is the major property of the soil controlling the tip resistance, q_t cannot be expressed as a function of the relative density only.

The Side Resistance

The side resistance of a pile in sand is conventionally expressed as

$$q_s = \bar{p}_v \cdot K_s \cdot \tan \delta$$

$$= \bar{p}_h \cdot \tan \delta \quad \ldots\ldots\ldots\ldots\ldots\ldots\ldots\ldots \quad (3.7)$$

where

q_s = unit peak load transfer at a point on the surface of the pile,

$\bar{p}_v$ = effective vertical pressure at a point on the surface of the pile,

$K_s = \dfrac{\bar{p}_h}{\bar{p}_v}$ = coefficient of earth pressure,

δ = angle of shear resistance between the soil and the pile material,

$\bar{p}_h$ = effective horizontal pressure at a point on the surface of the pile.

The terms of this expression are unknown functions of several variables, such as the type, density, and stress history of the soil; the dimensions, geometry, and method of installation of the pile; the strain in the soil; and the depth below the surface of the point in consideration. The following paragraphs present a discussion of these terms and the findings of recent work.

The Earth Pressure. The average value of the effective vertical pressure $\bar{p}_v$ at a point in a semi-infinite mass of soil is equal to the effective overburden pressure of the soil. The insertion of the pile changes the value of $\bar{p}_v$ in the vicinity of the pile in an unknown manner. In regard to stress changes, the expansion of a cylindrical cavity at great depth in an infinite medium (Ladanyi, 1963; Vesić, 1972) has been used to simulate the driving of a pile. There are a number of obvious differences between the process of driving a pile and that of expanding a cavity; however, the equations derived by Ladanyi and Vesić are useful in developing additional understanding of the effects of pile driving.

The changes of stresses generated by the construction of a drilled shaft are discussed in a subsequent section.

The Coefficient of Earth Pressure. In linearly elastic materials the coefficient of earth pressure at rest K_o is given by

$$K_o = \frac{\nu}{1-\nu} \quad \ldots\ldots\ldots\ldots\ldots\ldots\ldots\ldots \quad (3.8)$$

where

ν = Poisson's ratio

In sands the value of K_o is dependent on the type of sand, its relative density, and the overconsolidation ratio. Experimental studies have shown that for normally consolidated sands reasonable values of K_o are given by the following expression (Jaky, 1944, after Henkel, 1970):

$$K_o = 1 - \sin \bar{\phi}$$

Jaky's expression yields values of K_o between 0.4 and 0.5. The expression does not apply to overconsolidated sand; Hendron (1963) has shown that K_o can be as high as 2.5 for high overconsolidation ratios.

While the earth pressure at rest is an important parameter related to the earth pressure which will exist at the installed pile, the method of installation is also of critical importance. The installation of the pile causes highly complex strains and the coefficient of earth pressure K_s becomes an indeterminate function of the dimensions of the pile and the depth below the ground surface. Attempts to measure the horizontal pressures on bored piles (Kérisel, 1957; Reese, et al., 1968) and on driven piles (Reese and Seed, 1955; Koizumi, et al., 1971) have met with little success. The failure to obtain reliable data on horizontal pressures is due principally to the technical limitations of the pressure cells. Furthermore, there is the physical problem of installing the large number of cells required to reasonably portray an average pattern of stress distribution that may be greatly affected by localized stresses. Indirect measurements of K_s have been deduced from load tests on model and full-scale piles by measuring the side friction and by assuming a vertical pressure equal to the overburden pressure. The values of K_s reported from such measurements vary between 0.2 and 3.0 for driven piles (Meyerhof, 1956; Ireland, 1957; Mansur and Hunter, 1970) and between 0.3 and 0.5 for bored piles (Martins, 1963; De Beer, 1964). This large scatter in the results may be due to

errors in the theories of skin friction and in the experimental measurements, and to the complex nature of K_s.

Mazurkiewicz (1968) summarizes the values of K_s obtained from theoretical considerations. The scatter of the theoretical values is similar to that observed in the experimental ones. However, for bored piles there seems to be a general agreement that K_s will assume values limited between the coefficient of active earth pressure and the coefficient of earth pressure at rest.

The Angle of Shear Resistance δ. The angle of shear resistance δ between the concrete and the soil has been found to be, in the case of sand, practically equal to the friction angle ϕ of the sand (Potyondy, 1961). The value of the friction angle ϕ is, as discussed in previous paragraphs, mainly dependent on the relative density of the sand. The changes in the density of the sand surrounding the pile are a function of the method of installation of the pile. Robinsky and Morrison (1964) have shown for a driven pile that, although the displaced volume of sand increases the density of the sand surrounding the pile, the vertical motion of the pile forces the stretching and consequently the loosening of the sand at the periphery of the pile. In bored piles the relief of stresses resulting from the boring of the hole causes a loosening of the sand. The amount of loosening is a function of the drilling and concreting procedures which are used.

The difficulty of evaluating independently the terms of Eq. 3.9 led some researchers to investigate only the average skin friction developed

at the periphery of the pile. The average skin friction was found to increase almost linearly with depth and to tend beyond a certain critical depth to a constant value, which is a function only of the original relative density of the sand (Vesić, 1963, 1965, 1970; Kérisel, 1961, 1964). The critical depth varies from ten diameters in loose sand to twenty diameters in dense sand. The value of the constant average skin friction was found from empirical measurements to be given by

$$q_s = 0.08(10)^{1.5} D_r^4 \qquad \text{(Driven Piles)} \quad . \quad . \quad . \quad . \quad . \quad . \quad . \quad . \quad . \quad (3.9)$$

$$q_s = 0.025(10)^{1.5} D_r^4 \qquad \text{(Drilled Shafts) (Vesić, 1970)} \quad . \quad (3.10)$$

The limitations to the practical application of these expressions are the same as those discussed in a previous section for similar expressions for the tip resistance of piles.

THE LOAD-SETTLEMENT CURVE

The bearing capacity of drilled shafts is usually determined from either a static formula that relates the ultimate tip and side resistances of the shaft to the shear strength of the soil or from an experimental load-settlement curve, with the ultimate load being selected by one of a number of empirical graphical procedures (Chellis, 1961). In friction piles the ultimate load is attained at relatively small downward displacements of the pile; therefore, the amount of settlement at the ultimate

load is a matter of little concern. Experience with load tests on drilled shafts in sand that obtain their support principally in point bearing has indicated that the load-settlement relationship follows a long sweeping curve that tends asymptotically to an ultimate value at excessively large settlements as shown in Fig. 3.3 (Brezantzev, 1961; Vesić, 1963; Kérisel, 1964; Koizumi, et al., 1971). Some of the load-settlement curves reported in this study are similar to the lower curve shown in Fig. 3.3. For such piles the settlement can be a matter of great concern and the safe load can only be determined by taking into account the tolerance of the supported structure to total or differential settlement.

A pile normally constitutes an element in a complex two- or three-dimensional structure such as a bridge bent or a drilling platform. In some such structures there is continuity between the piles and the superstructure and the analysis to determine reactions and moments at the top of the piles requires the solution of simultaneous equations of compatibility and equilibrium (Reese, et al., 1970; Awoshika and Reese, 1971). Load-settlement curves are essential to such analyses. The development of load-settlement curves for bored piles is, therefore, very useful in the design of a pile-structure system. The cost of field load tests suggests the need for analytical procedures to allow the computation of load-settlement curves from a knowledge of the properties of the soil and of the pile. One procedure suggested by Reese (1964) uses a model (Fig. 3.4) in which the pile is divided into a number of deformable elements and the soil is replaced by mechanisms. When the load-deformation properties of

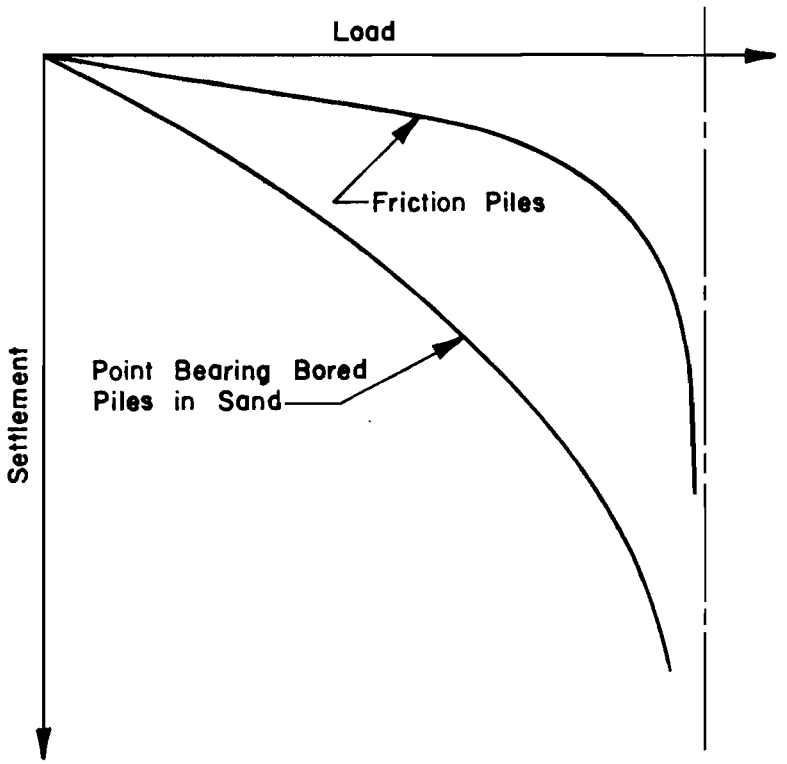

Fig. 3.3 Load Settlement Curves for Friction and Point Bearing Bored Piles

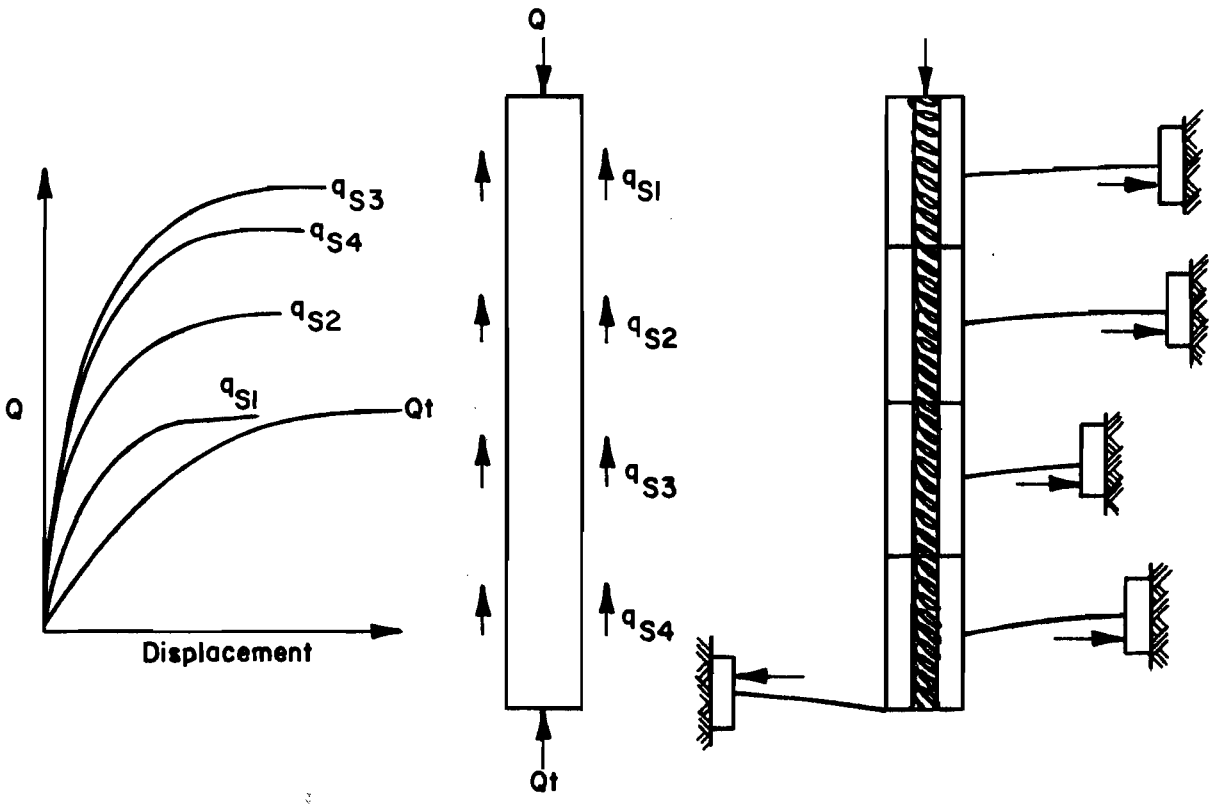

Fig. 3.4 Mechanical Model of Axially Loaded Pile (After Reese, 1964)

the mechanisms are known, the analysis of the model can be easily computerized to obtain the load-settlement curve (Coyle and Reese, 1968; Vijayvergiya and Reese, 1969).

Procedures to obtain the load-deformation properties of the mechanisms for piles in clay have been developed (Coyle and Reese, 1968; Barker and Reese, 1970; O'Neill and Reese, 1971). Coyle and Sulaiman (1969) recommended procedures, based on a field test and on laboratory model tests, for developing load transfer versus pile settlement curves for sands. Parker and Reese (1970) correlated the measured load transfer curves on buried model piles in sands with stress-strain curves obtained from triaxial tests.

The data presented by the above mentioned authors and by Vesić (1963) indicate that the values of displacement required to mobilize the side friction in buried and driven piles in sand vary between 0.02 and 0.5 in. The reasons for this wide scatter are not yet well known. It is believed that the load-deformation properties of a point on the periphery of a pile in sand are a complex function of the relative density of the sand, the overburden pressure, the relative depth of the point, the diameter of the pile, the arrangement of the soil layers, and the tip resistance.

The load-deformation curve for the mechanism at the tip of a pile is conventionally given by an expression similar to the one suggested by Mindlin (1936) for the settlement under a force in a semi-infinite elastic medium. This expression is typically written as

$$w_t = q_t \frac{(1-\nu^2)}{E} I_w B \quad \ldots\ldots\ldots\ldots\ldots\ldots\ldots\ldots \quad (3.11)$$

where

w_t = settlement of the tip of the pile, ft;

I_w = settlement factor;

B = diameter of the pile, ft;

q_t = tip pressure, tsf;

E = modulus of elasticity of the sand, tsf;

ν = Poisson's ratio of the sand.

Vesić (1970) defined empirically a similar expression:

$$w_t = \frac{C_w \cdot Q_t}{(1+D_r^2)\, Bq_t} \quad \ldots\ldots\ldots\ldots\ldots\ldots\ldots\ldots \quad (3.12)$$

where

Q_t = load at the tip, tons;

B = diameter of the pile, ft;

D_r = relative density of the sand;

q_t = ultimate tip pressure, tsf;

C_w = a coefficient of settlement that varies from 0.04 for driven piles to 0.18 for buried piles.

Expression 3.12 must be used in conjunction with the ultimate values of tip resistance q_t given by Vesić (1970). The coefficient of settlement C_w for

buried piles was obtained by Vesić from tests on model footings and its application to full sized bored piles is of questionable value.

ANALYSIS OF THE STRESS AROUND A DRILLED SHAFT

This section describes qualitatively the state of stress in the soil surrounding the shaft as influenced by the drilling of the hole, the placement and the curing of the concrete, and the loading of the shaft.

Drilling of the Hole

The analysis of the stresses generated in the vicinity of a hole drilled in sand is complicated and depends greatly on the method of construction. Approximate closed-form solutions of the problems of a lined hole in sand have been suggested by Westergaard (1940) and Terzaghi (1943). A general solution to take care of layered systems of variable densities and variable coefficients of earth pressure has not yet been proposed. It is believed that a solution by finite elements may offer some very useful insight into this problem if the constitutive relationships of the natural sand can be formulated properly.

A radial element of sand on the periphery of a hole is subjected to a radial stress σ_r, a tangential stress σ_θ, and a vertical stress σ_z, as shown in Fig. 3.5a. The shear stress τ_{rz} is of significant value only in large diameter holes (Westergaard, 1940), and if this stress is neglected in small diameter drilled shafts the radial stress becomes a major principal stress causing failure of the elements to take place along horizontal planes instead of along vertical planes as is the case in large diameter

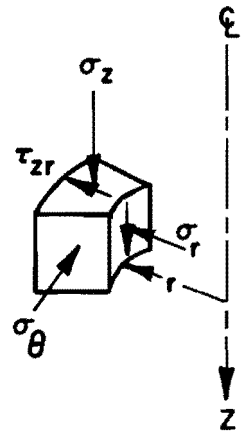

a. Stresses on a Radial Element

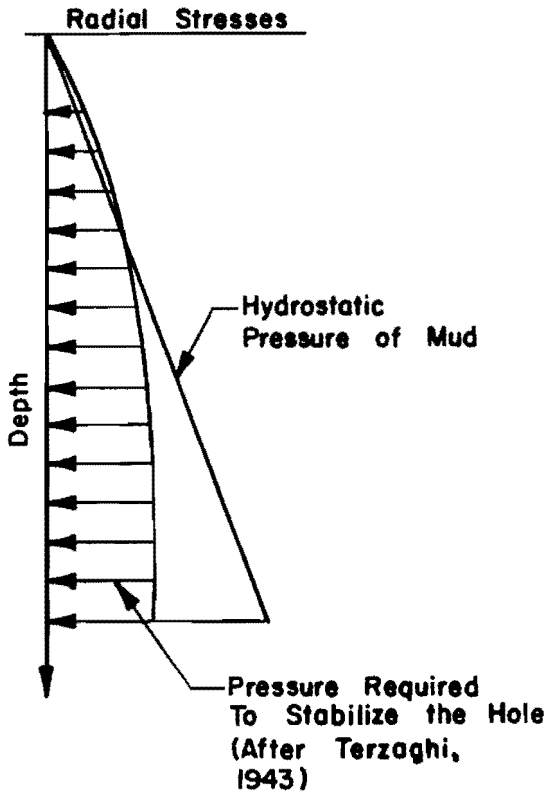

b. Profile of Radial Stresses

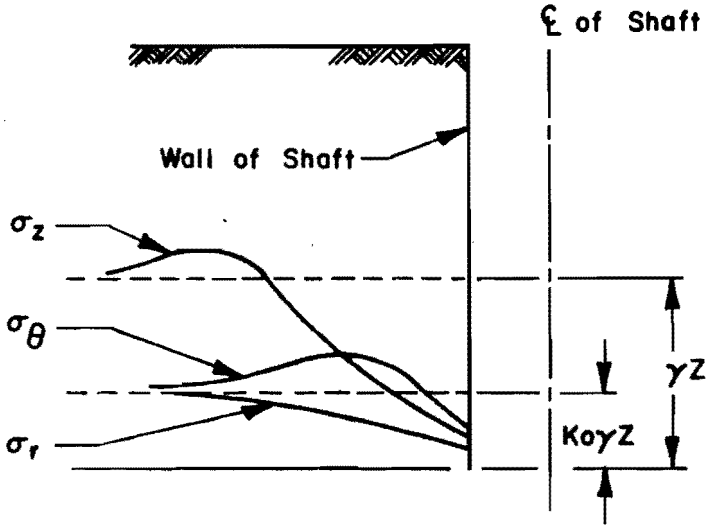

c. Stresses Around the Hole

Fig. 3.5 Stresses Generated by Drilling

holes. If the analysis is limited to small diameter holes, the radial and tangential stresses can be considered as the minor and major stresses, respectively. Figure 3.5c represents what is believed to be the pattern of variation of the principal stresses on the periphery of the shaft. When the hole is drilled under mud, the value of the radial stress drops from the horizontal pressure at rest ($K_o \sigma_z$) to the pressure provided by the drilling fluid. When the hole is opened without the use of slurry, the radial stress at the wall of the hole is reduced to zero, and the sand must possess an apparent cohesion to keep the sand from sloughing. A zone of soil at the plastic state develops on the periphery of the hole when drilling is done without slurry. In wet drilling the plastification of the soil is a function of the radial pressure of the mud and of the shear strength of the soil. The extent of this zone and its effects on the properties of the soil are not well understood. It is believed that the flow of the sand at the periphery of the open hole loosens the sand and may partially destroy any cementing bonds (carbonaceous or siliceous) between the grains. Figure 3.5b shows the effective radial pressure distribution required to stabilize the hole and the effective hydrostatic pressure of the mud. Near the ground surface the pressure of the mud may not be enough to prevent the sloughing of the soil, and a short casing may be required. At greater depths, the required stabilizing pressure becomes almost constant and the excess hydrostatic pressure of the mud reduces the extent of the plastified zone.

Concreting

The vertical and radial pressures at a point in the freshly poured concrete column depend on several factors. Some of these factors are the rate of placement, the temperature, and the consistency of the concrete; the size of the hole; the depth of the point under consideration; and the method of construction. The full effects of these factors are not known. The findings of Rodin in 1952 (After Courtois, 1966) and Peurifoy (1965) and the recommendations given in the ACI code on the pressure of concrete on formwork agree on the following points:

1. The maximum lateral pressure of the concrete on formwork may be computed fairly closely by the following expression:

$$P_h = 150 + 900 \frac{R_c}{T} \quad \text{(ACI)} \quad \ldots\ldots\ldots\ldots\ldots\ldots\ldots\ldots (3.13)$$

where

P_h = concrete pressure, psf;
R_c = rate of rise of concrete in the formwork, ft/hr;
T = temperature of the concrete, °F.

The value of P_h is limited by the smaller value of 3000 psf or 150 times the maximum height of fresh concrete in the forms.

2. The concrete pressure at a point increases with the rise of the column of concrete until a critical value H_m is reached and

remains constant or possibly drops for greater heights. The critical height H_m is given by Rodin as

$$H_m = C_t R_c^{1/3} \quad \ldots\ldots\ldots\ldots\ldots\ldots\ldots\ldots\ldots\ldots \quad (3.14)$$

where

C_t = a function related to the temperature of the concrete.

The above mentioned research has been limited to rates of placement smaller than 10 ft/hr. Such rates of placement are common in the construction of concrete walls. Much higher rates may be experienced in the construction of drilled shafts (30-40 ft/hr) and higher pressures than the upper limit specified above may be exerted. Higher concrete pressures are also expected to result from concreting under mud than from dry concreting as the pressure in the former case is at any time at least equal to the pressure of a column of mud. The size of the hole and the consistency of the fluid concrete control the arching of the concrete and, therefore, the pressure in the hole. Figures 3.6a and 3.6b show the probable stress profiles immediately after concreting for both dry and wet concreting. Figure 3.6c shows the forms of the patterns of stress distribution in the soil surrounding the hole.

Volumetric Strains in the Concrete

After casting, the concrete incurs volumetric strains as a result of curing and changes in its temperature. Concrete which is cured in a

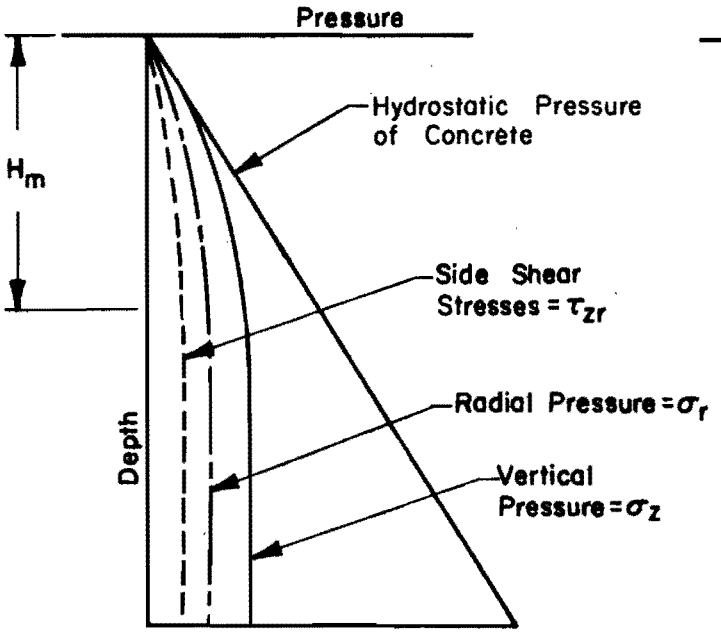

a. Stresses at the Surface of the Shaft in Dry Concreting

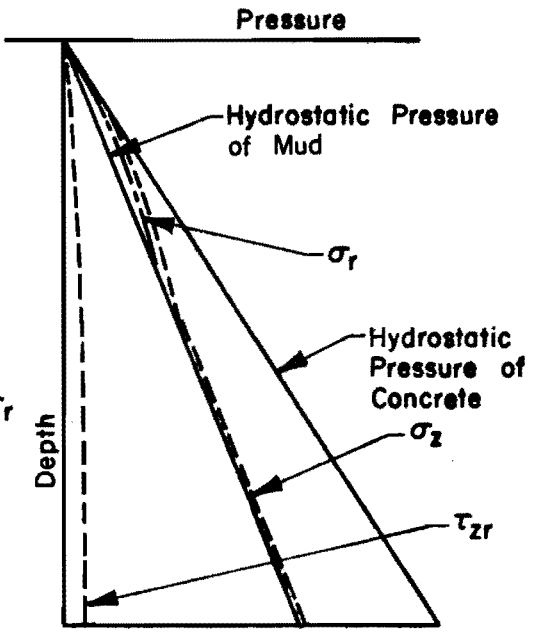

b. Stresses at the Surface of the Shaft when Concreting by Slurry Displacement

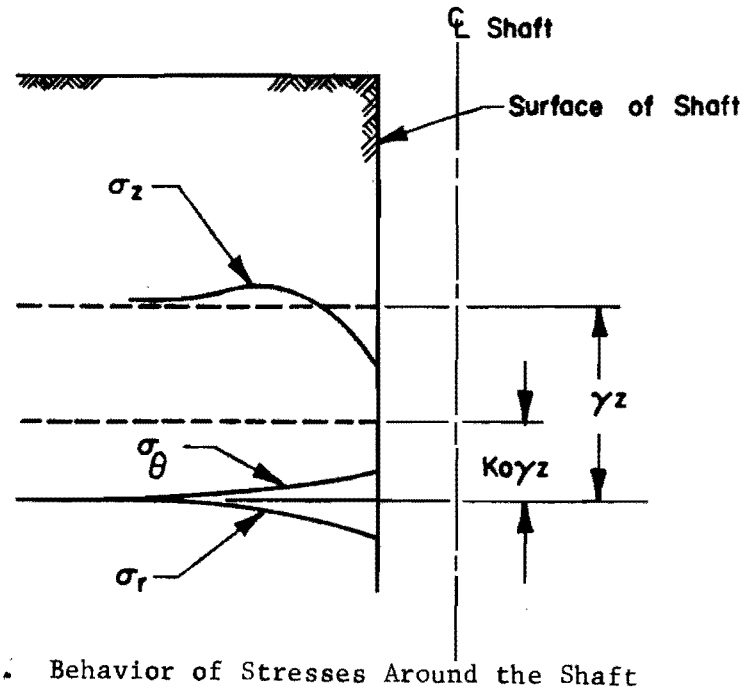

c. Behavior of Stresses Around the Shaft

Fig. 3.6 Stresses at the Periphery of the Shaft after Concreting

relatively dry medium has a tendency to shrink as a result of a loss of the water required to hydrate the cement grains. On the other hand, concrete which is cured in a wet medium with free access to water has the tendency to expand (Neville, 1963). However, due to the imperviousness of the concrete and of some soils, a long period of time (as long as a year, Neville, 1963) may be required to cause this expansion.

The thermal strains of the concrete depend on its temperature during casting. This temperature varies between 60°F and 90°F depending on the air temperature, the admixtures used, and the duration of mixing. The temperature during casting of plant-mixed cement in the summertime is about 90°F. During setting, the temperature (as measured in shafts tested in this study) rises to over 120°F and cools to about 75°F in a period of two days. The resulting volumetric strain in this instance is a contraction of about 100 μ in/in. The net volumetric strain between the end of construction and time of loading of a drilled shaft may be a contraction or an expansion. Contraction occurs in the general case and may reach values as high as 200 μ in/in, as discussed in later chapters. The effect of these strains may be negligible on the radial stresses but could be significant on the shear stresses on the surface of a long shaft. In the following section, a simplified analysis based on the assumption of a homogeneous linearly elastic soil is presented. Such an analysis can also be used when volumetric strains occur in the soil such as in expansive clays.

Figure 3.7a represents the shear stresses developed on the periphery of a pile incurring a uniform volumetric contraction. The tip resistance

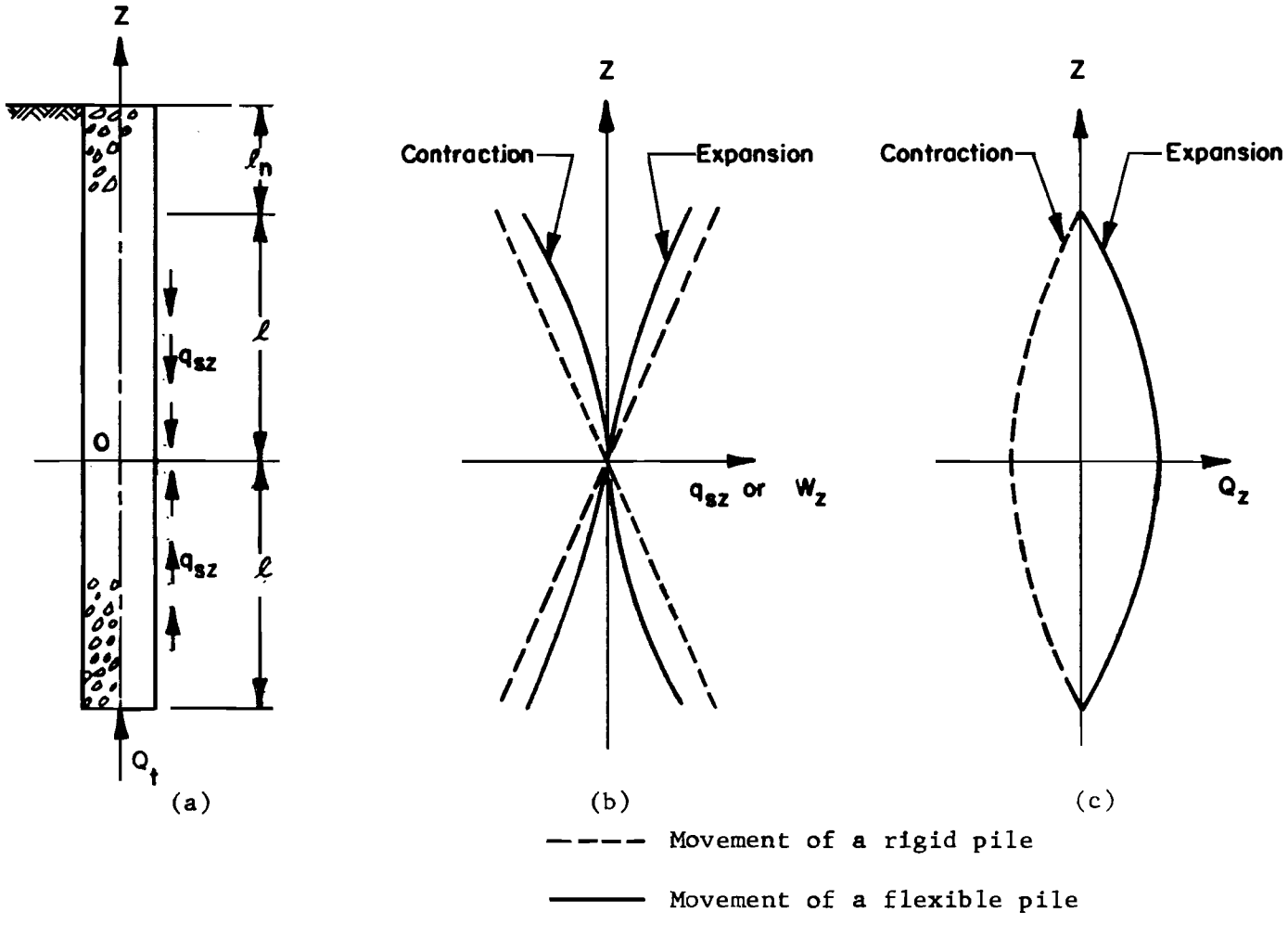

Fig. 3.7 Stresses Due to Volumetric Strain

q_t may be neglected for the envisaged displacements of the pile. If the resistance of the soil is neglected for a distance ℓ_n below the surface of the ground, and if the soil is assumed to have a uniform shear stiffness, the point of zero movement divides equally the length of the shaft below ℓ_n. In developing an expression for the shear stresses on the wall of the shaft as a function of volumetric strains from curing or from temperature variations, it is convenient to define the following terms.

w_z = displacement of a point on the pile,

λ = coefficient of volumetric strain taken positive for an expansion,

ℓ = half of the length the pile offering resistance to deformation,

C = circumference of the pile,

A = cross-sectional area of the pile,

E = modulus of elasticity of concrete,

β = shear modulus of the soil = $\frac{q_{sz}}{w_z}$,

q_{sz} = unit shear stress developed at the periphery of the shaft and at a depth z,

Q = load at any point in the pile, considered positive when it is a compression.

The following relation can be written at any point in the pile:

$$\frac{ds_z}{dz} = \pm \lambda \pm \frac{Q_z}{EA} \quad \ldots\ldots\ldots\ldots\ldots\ldots\ldots\ldots\ldots\ldots \quad (3.15)$$

Equation 3.15 becomes, for the case of an expansion of the shaft, the following:

$$\frac{dw_z}{dz} = \lambda - \frac{Q_z}{EA} \quad \ldots\ldots\ldots\ldots\ldots\ldots\ldots\ldots\ldots\ldots \quad (3.16)$$

Differentiating Equation 3.16 with respect to z gives the following:

$$\frac{d^2w_z}{dz^2} = - \frac{1}{EA} \frac{dQ_z}{dz} \quad \ldots\ldots\ldots\ldots\ldots\ldots\ldots\ldots\ldots\ldots \quad (3.17)$$

where

$$\frac{dQ_z}{dz} = q_{sz} \cdot C$$

$$= \beta w_z C \quad \ldots\ldots\ldots\ldots\ldots\ldots\ldots\ldots\ldots\ldots \quad (3.18)$$

Therefore

$$\frac{d^2w_z}{dz^2} = \frac{\beta w_z C}{EA} \quad \ldots\ldots\ldots\ldots\ldots\ldots\ldots\ldots\ldots\ldots \quad (3.19)$$

Equation 3.19 can be written as the following:

$$\frac{d^2 w_z}{dz^2} - k^2 w_z = 0 \quad \ldots\ldots\ldots\ldots\ldots\ldots\ldots\ldots \quad (3.20)$$

where

$$k = \sqrt{\frac{\beta C}{EA}}$$

Equation 3.20 has a closed form solution of the following form:

$$w_z = A_1 e^{kz} + A_2 e^{-kz} \quad \ldots\ldots\ldots\ldots\ldots\ldots\ldots\ldots \quad (3.21)$$

The constants A_1 and A_2 can be evaluated from the boundary conditions:

$$w_z = 0 \text{ at } z = 0, \text{ and } \frac{dw_z}{dz} = 0 \text{ at } z = \ell$$

Employing these boundary conditions, Equation 3.21 can be rewritten as

$$w_z = \frac{\lambda\,(e^{kz} - e^{-kz})}{k\,(e^{k\ell} + e^{k\ell})} \quad \ldots\ldots\ldots\ldots\ldots\ldots\ldots\ldots \quad (3.22)$$

Figures 3.7b and 3.7c represent schematical plots with respect to depth of the functions w_z, q_{sz}, and Q_z. If the pile is infinitely rigid, the functions w_z and q_{sz} become linear and the function Q_z becomes a parabola.

To give an idea of the order of magnitude of the stress involved, consider a drilled shaft 30 inches in diameter and 50 feet deep in dry

sand. The dimensions of such a shaft are consistent with shafts described in this study. If the resistance of the upper ten feet of soil is neglected, the displacement of the shaft at the bottom of the shaft and at ten feet below the surface for a contraction strain of 200 microinches/inch is about 0.05 in. As will be shown in subsequent chapters, a strain of this magnitude may develop when shafts are constructed in dry soils. In most soils the ultimate side shear is mobilized at a movement of the order of 0.1 to 0.2 inch and a movement of 0.05 inch may mobilize 25% to 50% of the shear strength of the soil.

Furthermore, because the stiffness of sand increases with depth, the point of zero movement is shifted to a lower position in the shaft than in the example presented above, resulting in a larger displacement than the value computed above, and resulting in the mobilization of a larger fraction of the shear strength of the upper layers of sand. When the net strain in the concrete is contraction, the shear stresses in the upper soil layers are in the same direction as those mobilized during an axial compression loading while the shear stresses in the lower layers are similar to those taking place in an axial tension loading. When the shaft is later loaded in compression, the upper layers of sand will offer a smaller resistance to downward movement than the lower layers.

Axial Loading of the Shaft

The stresses generated in the soil by the axial loading of the shaft are of a very complex nature. The loosening of the soil on the periphery of the shaft and the nonhomogeneity of natural deposits result in an indeterminate stress distribution. The computation of stresses in the

sand during axial loading of the pile is a very intricate and complex problem and requires the analysis of the complete pile-soil system. The stress at any point on the periphery of the pile is influenced by the load transfer at all levels in the pile. Furthermore, the compression of the soil under the high pressure at the tip is believed to cause arching of the sand around the tip in a manner similar to that described by Terzaghi (1936) for the yielding trap door and to influence the stresses in the sand to a considerable distance above the tip. Figure 3.8a presents schematically the radial and vertical shear stresses generated at level B as a result of the shear transfer q_{sa} developed at level A (Terzaghi, 1943). The figure also presents the shear stresses at level B due to the shear transfer q_{sb}. When these stresses are added to the stresses existing before loading, the stress distribution in the soil surrounding the shaft can assume the pattern presented in Figure 3.8b. Failure can, therefore, take place at any point around the shaft where the value of the shear τ_{rz} exceeds the value of the product $\sigma_r \tan \phi$. The failure at a distance from the surface of the shaft, however, requires that the sand be compressible or have room to displace, such as around the tip of the shaft.

The vertical force developed at the tip of the shaft compresses the soil in the immediate vicinity of the tip. In drilled shafts, a plastic zone develops at the tip at very large displacements (Vesić, 1963) and is much smaller than that developed in driven piles. There is little information, however, on the extent of this zone. The data reported by Koizumi, et al. (1971) on a pile loaded in a cased open hole show a noticeable

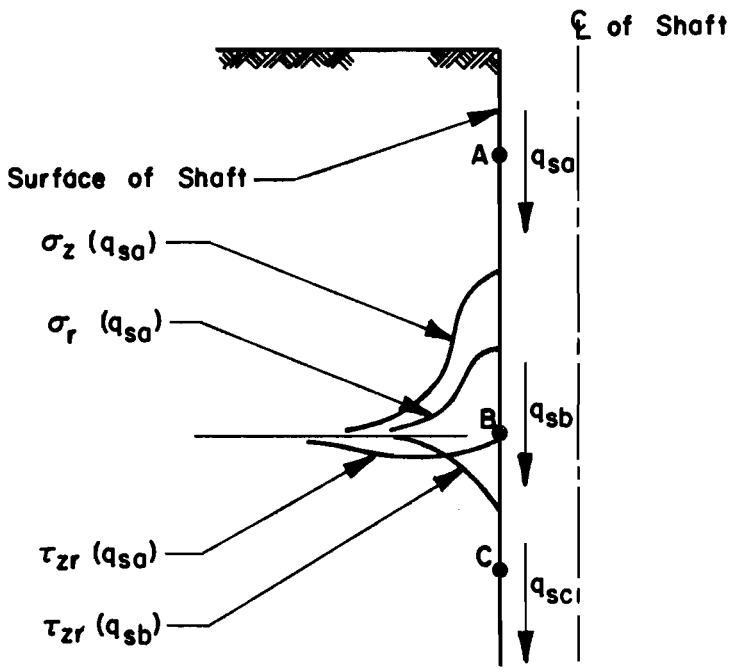

a. Influence of Load Transfer on the Stresses in the Soil

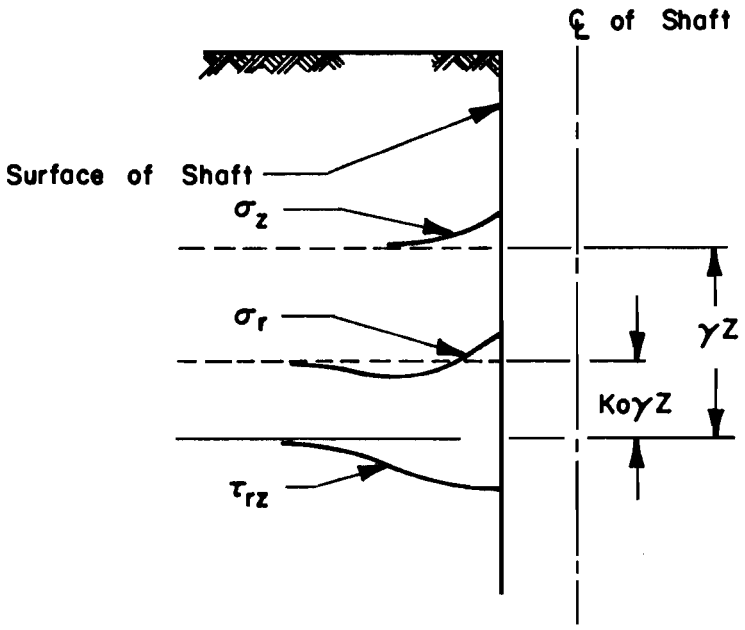

b. Superposition of the Stresses Around the Shaft

Fig. 3.8 Stresses from Axial Loading

densification of the sand at the tip of the pile to a distance of about one and one-half radii from the surface of the pile. It is, therefore, believed that the extent of the compacted zone is of the order of the size of the pile.

Two distinct zones develop around the tip of the pile as a result of the downward movement. These are the flow zone and the arching zone. The deformation patterns, due to downward movement, of a horizontal plane through the pile tip and at some distance above the tip, are shown in Fig. 3.9. For the downward movement of the pile indicated there would be slippage between the sides of the pile and the soil, as shown. The lack of compatibility between the deformation patterns at the pile tip and above the tip leads to arching. The arching phenomenon causes an increase in stresses in the non-yielding sand at some distance from the pile tip and a decrease in stresses in the yielding soil near the tip. There can be a flow of soil toward the pile near the tip to replace the subsiding soil in the region indicated in Fig. 3.9. It can be postulated that above the zone of flow there will be, also as a result of arching, an increase in the horizontal stresses at the pile wall (See Fig. 3.9). Failure in the sand above the pile tip could in these circumstances take place at a certain distance from the pile.

The dimensions of the two zones which are postulated are thought to be mainly a function of the relative density of the sand and of the displacement of the tip. In a very compressible loose sand, the tip resistance is small and the compression is limited to a small area under the tip, thus causing a reduced influence on the sides. In a very dense sand, significant

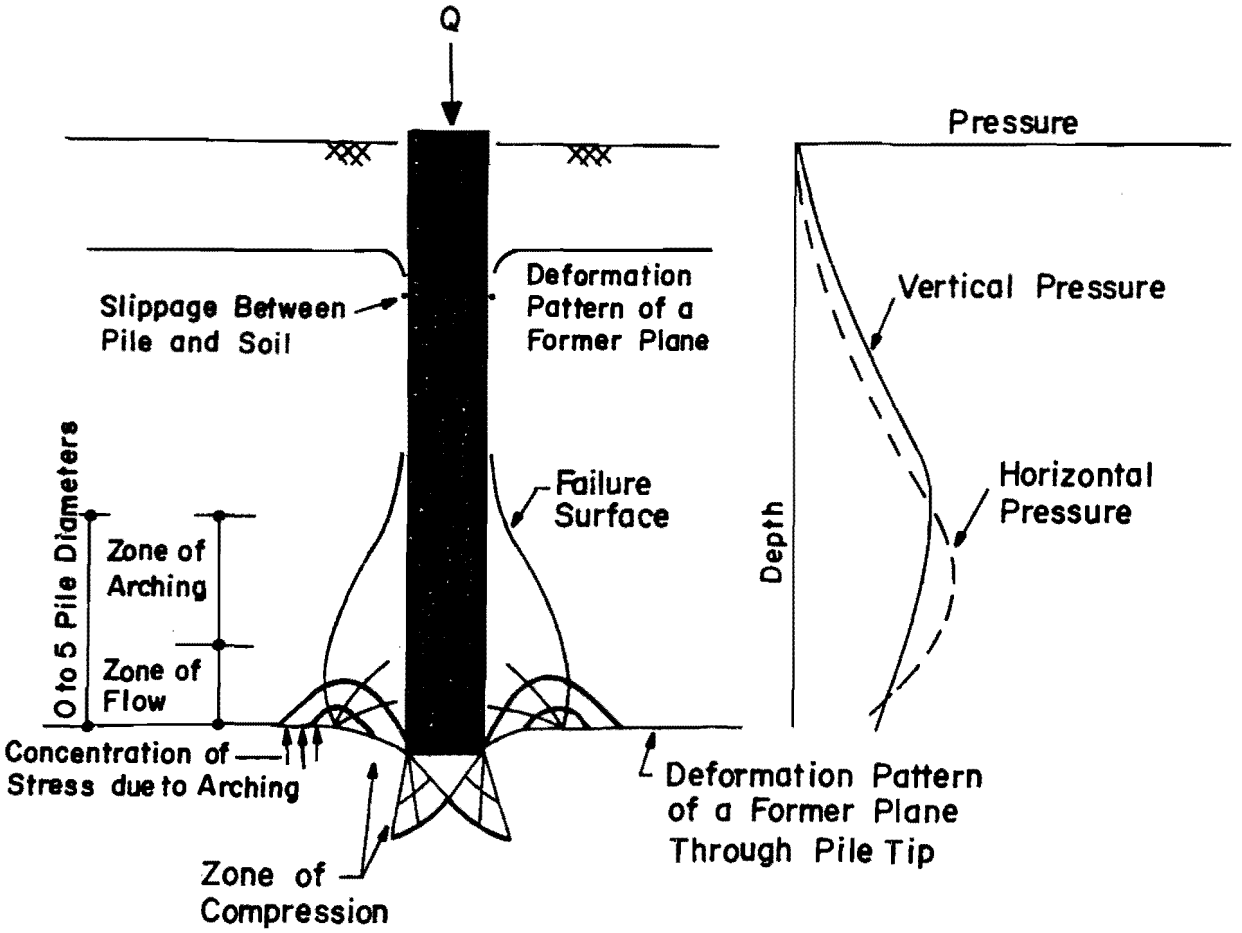

Fig. 3.9 Influence of the Tip on the Stresses Around the Pile

compression of the sand below the level of the tip takes place at high pressures and the zones of flow and arching may extend to a distance of a few pile diameters above the tip of the pile.

CHAPTER IV. INVESTIGATIONS OF TEST SITES

LOCATIONS OF TEST SITES

The Center for Highway Research (CFHR) at the University of Texas at Austin since 1965 has conducted a research program to investigate the behavior of drilled shafts installed in a variety of soils. To date, nine instrumented drilled shafts have been installed and tested at various locations in the state of Texas. Figures 4.1 and 4.2 indicate the location of the nine test sites. A prospective test site (X) is now being studied. Test sites I through IV have been the subject of previous research and have been reported by Reese and Hudson (1968), Vijayvergiya and Reese (1969), O'Neill and Reese (1970), Barker and Reese (1970), and Welch and Reese (1972). Test sites V through IX constitute the subject of this current study.

In this research program undertaken jointly by the Center for Highway Research and the Texas Highway Department, the test shafts are generally located in future bridge bents to allow the use of permanent shafts of the bents in providing the reaction for the test load and to allow a direct implementation of the results of the load tests in the design of the other shafts of the bridge.

Table 4.1 shows the location of the test shafts with respect to the bridge bent in which each test shaft is located.

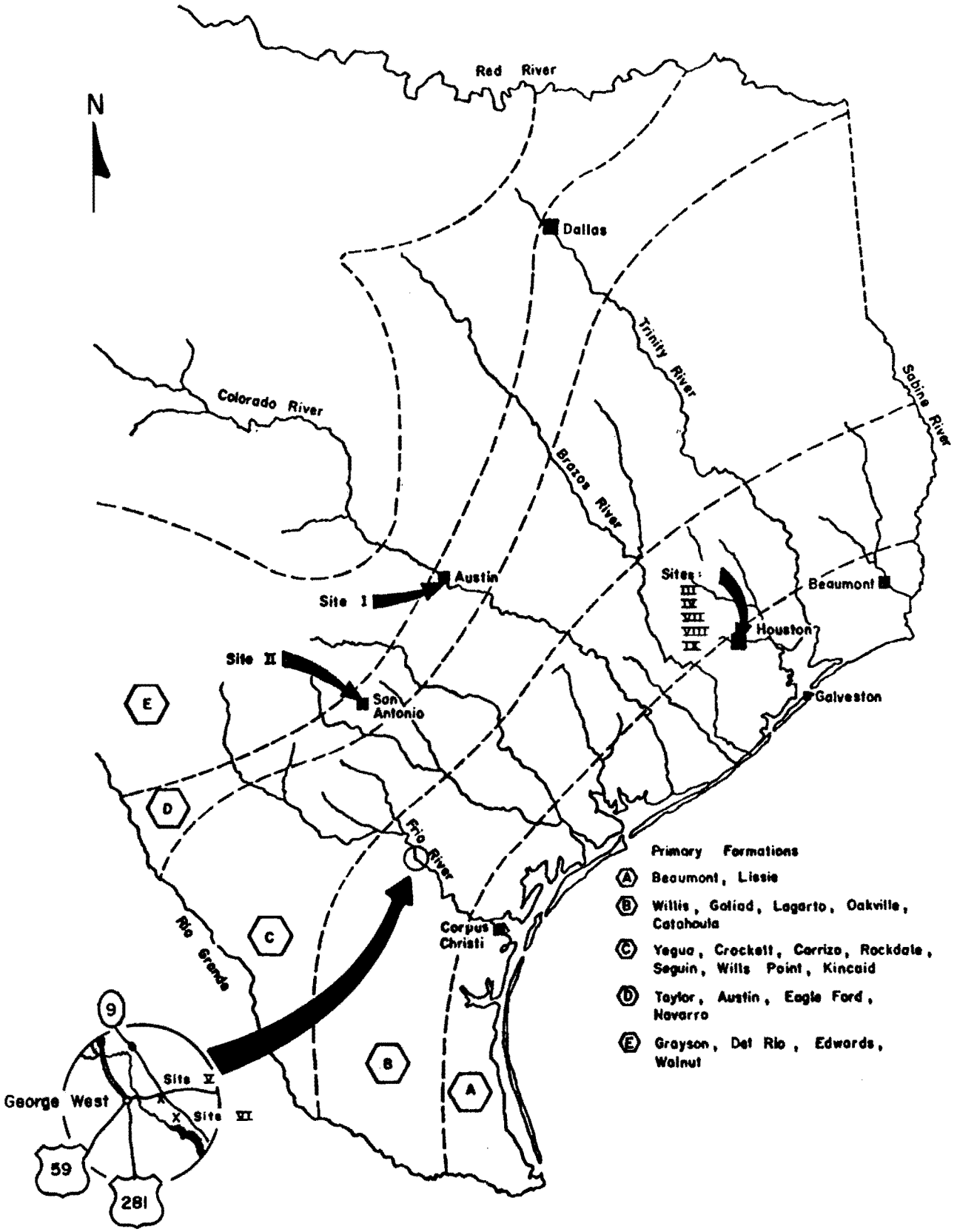

Fig. 4.1 Location of the Different Test Sites
(Adapted after Barker & Reese, 1970)

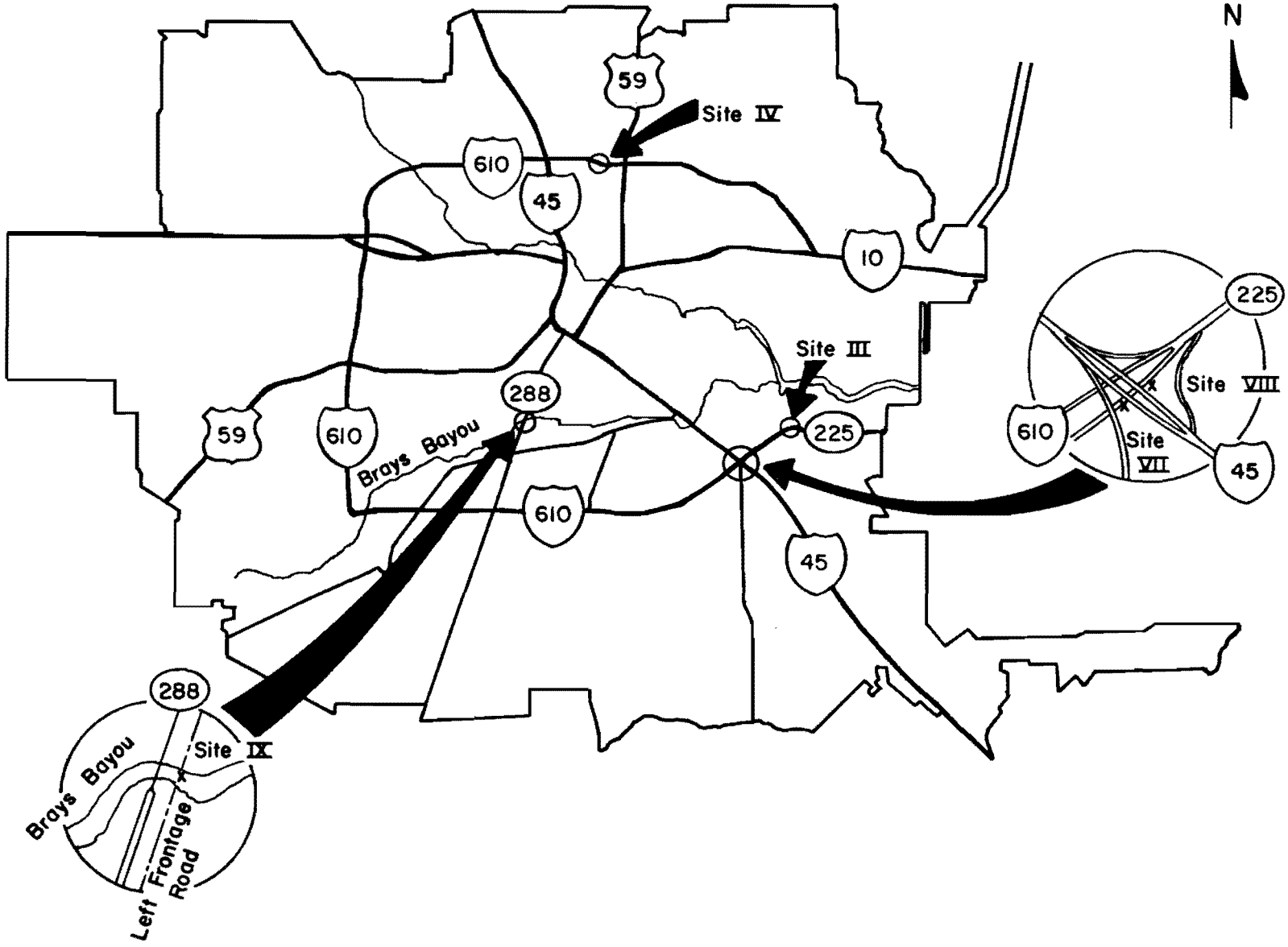

Fig. 4.2 Test Sites in Houston

Table 4.1 Location of Test Shafts and Type of Soil Tests

Site	Designation	Location	Soil Tests
V	US59	West bay of bent No. 3 of the left roadway of IH-37 and US59 structure	THDP, SPT, UT triaxial tests, granulometric analysis, Dutch cone, and A & M penetrometer
VI	HH	North bay of bent No. 2 of the left main lane of IH-37 and Hailey Hollow structure	THDP, SPT, UT triaxial tests, granulometric analysis
VII	G1	South middle bay of bent No. 12 of I610 (east bound) and I-45 interchange	THDP, SPT, transmatic triaxial tests, UT triaxial tests, granulometric analysis
VIII	G2	North bay of bent No. 27 of I610 (east bound) and I-45 interchange	THDP, SPT, transmatic triaxial tests, UT triaxial tests, granulometric analysis
IX	BB	West bay of bent No. 5 of left frontage street of IH 288 and Brays Bayou structure	THDP, SPT, transmatic triaxial tests, UT triaxial tests, granulometric analysis

SOIL INVESTIGATION PROGRAM

The soil investigation program at the test sites had two main objectives:

1. To evaluate the shear strength of the soil as the principal variable controlling the load transfer in a drilled shaft.
2. To evaluate properties of the soil, such as grain size distribution and Atterberg limits, that may influence the load transfer through a physical-chemical interaction with the drilling fluid or the concrete of the shaft.

Table 4.1 lists the soil test conducted at each site. Appendix A contains a brief description of the soil tests as well as the results of those tests.

The soil profiles at the test sites consist in general of an upper layer of overconsolidated clay overlaying a layer of sand. The evaluation of the properties of these soil layers is discussed in the following sections.

Clay

In this study, mainly concerned with the behavior of drilled shafts in sand, the properties of the clay layers were investigated to allow a comparison with the results of previous research and to evaluate the effect of variations in the construction procedure on the load transfer.

The evaluation of the shear strength of soils is in general a major problem. The sensitivity of soft clays and the fissured and heterogenous structure of stiff clays constitute the major difficulties in evaluating

the shear strength of clay. A comprehensive study of various shear strength tests, namely the Texas Highway Department cone penetrometer (THDP), the "transmatic triaxial," the "UT triaxial," the direct shear, and the pocket penetrometer tests, has been presented by O'Neill and Reese (1970). Their main findings were:

1. A statistical average of shear strength values obtained from the UT triaxial and from direct shear tests gives a good estimate of the undrained shear strength of fissured clays.
2. Values of shear strength from the transmatic triaxial test are very conservative. The principal reasons for underestimation of shear strength are the significant disturbance of the untrimmed samples and the incomplete failure of the specimen at any particular stage in the transmatic test.
3. The curve presently used to predict the unconfined compression strength of clay from the THDP test yields results which are very conservative (Appendix).
4. The pocket penetrometer values are the closest representative values of the unconfined compression strength of the unfissured clay.

The standard penetration test (SPT) may be used to evaluate the shear strength of clay. However, as in any penetration test, the resistance to penetration is not only a function of the shear strength of the clay but is also a function of other factors. Some of these other factors are

the sensitivity and the stress-strain properties of the clay and variables related to the procedure used in conducting the test. The difficulty in using SPT to obtain the unconfined compressive strength is illustrated in Fig. 4.3, where different authorities obtained a multitude of widely scattered curves. In the drilled shaft studies, correlations for local clays do not exist and, therefore, an accurate evaluation of the shear strength of clay from the SPT could not be made. It was, however, reasoned that, since most of the clay deposits encountered at the test sites fell in the range of medium to high plasticity and had a low sensitivity, the line labeled (A) in Fig. 4.3 may give a reasonable representation of the shear strength of clay. This line is very close to the line given by Terzaghi and Peck (1948). The equation of this line is given by the following expression.

$$q_u = \frac{N}{7.5} \quad \ldots\ldots\ldots\ldots\ldots\ldots\ldots\ldots \quad (4.1)$$

where

q_u = unconfined compressive strength,

N = SPT blow count.

Sand

The difficulties encountered in evaluating the shear strength of sand are discussed in the following paragraphs.

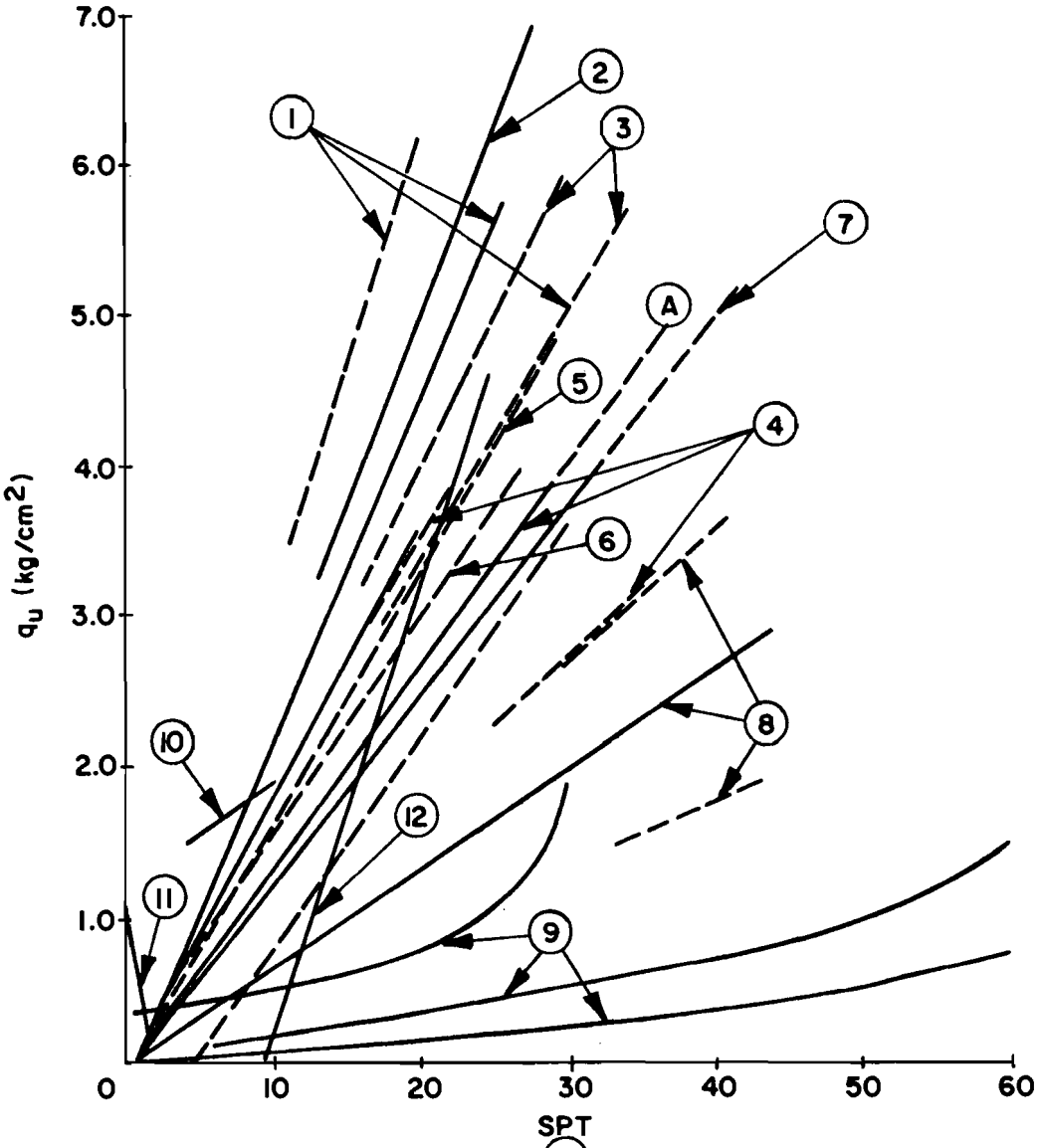

(1) Sowers - Very Plastic Clay
(2) Peck - Reed (Most Data)
(3) Ireland
(4) Sowers - Clays, Medium Plasticity
(5) Fletcher
(6) Golder
(7) Terzaghi - Peck
(8) Sowers - Clays, Very Low Plasticity
(9) Trow
(10) DeMello
(11) DeMello - Santos Clays
(12) DeMello - S Paulo Clays

Fig. 4.3 Attempted Correlations Between SPT and q_u (kg/cm^2) for Clays (After DeMello)

1. The shear strength of a granular material is usually defined with respect to a failure criterion and a strength test. However, refined theories of failure of sand are only of academic interest when a practical problem like the one under study is being discussed. The influence of a multitude of variables and unknowns such as the construction procedure and the initial state of stress is more significant than a change of a few degrees in the friction angle. It seems, therefore, that refinement beyond the simplest strength tests and the Mohr-Coulomb theory of failure is not justifiable.
2. In the Mohr-Coulomb theory of failure, the shear strength of soil can be expressed by the following equation.

$$s = c + \bar{p} \tan \bar{\phi} \quad \ldots\ldots\ldots\ldots\ldots\ldots\ldots \quad (4.2)$$

where

s = shear strength of the soil,

c = cohesion,

$\bar{p}$ = effective normal pressure on the failure plane,

$\bar{\phi}$ = effective friction angle.

In a natural soil deposit, the variables on the right hand side of Eq. 4.2 cannot now be measured. The cohesion is a function of the stress level because the Mohr envelope is only a straight line

for certain ranges of stress (Vesić, 1968). Furthermore, cementation of natural soil deposits by the deposition of calcium carbonates or by the formation of silica cements may affect the cohesion considerably (Denisov, et al., 1963). In sands above the water table, moisture creates an unmeasurable apparent cohesion.

The effective stress $\bar{p}$ in a sand deposit is a major unknown, mainly because the coefficient of earth pressure is unknown. This coefficient has been proven to vary with the overconsolidation ratio (Hendron, 1963). While the overconsolidation ratio can be reasonably estimated in clays, there does not seem to be a practical way of measuring this ratio in sand deposits. The angle of shear resistance $\bar{\phi}$ is mainly a function of the relative density of the sand. However, other factors such as the gradation of the sand, the mineralogy, the angularity, and the size of the grains may significantly influence the shear strength of the sand. It is, therefore, important when evaluating the friction angle by any test to have the sample represent as nearly as possible the field conditions of the sand in regard to density and to composition.

3. Sand deposits may be quite heterogeneous. The sand gradation may vary significantly within one layer. Furthermore, sand deposits may be interbedded with very thin layers of clay as a result of seasonal variations in deposition or may contain clay lumps that have been eroded and deposited before disintegrating.

In planning the soil investigation program employed in these studies, several approaches were evaluated in light of the indicated difficulties above. Vesić (1970) in his study of the Ogeechee River site mentions the use of the standard penetration test, the static cone test, and the nuclear probe for measurements of moisture contents and densities. He also used laboratory triaxial testing. Various other investigators have reported success in obtaining undisturbed samples of loose sand by special piston samplers (Bishop, 1948; Sarota and Jennings, 1957) and of dense or cemented sand by a double-core barrel (Denisson barrel, Taylor, 1948). In some instances, undisturbed sampling of sand was made possible by freezing the soil or by injection of chemicals. Other elaborate approaches consist of digging pits (combined with dewatering when water is present) and hand carving samples of sand (Wu, 1957).

After careful considerations, most of these approaches were rejected as not being feasible or as being irrelevant to this study. Driving of the tube of the nuclear probe (Vesić, 1970) was suspected to change the density of the sand in the space around the probe, and the installation of such a tube in a borehole was considered an impossible task. Furthermore, according to literature on the nuclear probe, the accuracy to be expected is ±2 pcf in density. Such errors would mean a considerable variation in the relative density of the sand.

An attempt to use the Dutch cone was unsuccessful because of the unavailability of the standard driving equipments and because of the limitations of this test in very dense sands. Attempts to extract undisturbed

samples of the sand with a piston sampler and with the Texas Highway Department double core barrel were also unsuccessful. The disturbance of the sample during sampling, transportation, and handling in the laboratory eliminates the benefits of such an approach. It was felt that the evaluation of the sand properties by the Dutch cone and by undisturbed sampling testing was only necessary for academic interest since these methods are not common on the American continent and attempts to use them were not pursued further.

The investigation of the sand layers of this study was then made using two dynamic penetration tests: the Texas Highway Department cone penetrometer and the standard penetration test. It was felt that the evaluation of the in situ properties of sand with tools commonly used by the practicing engineer will provide some valuable information to the profession.

The engineers of the Texas Highway Department use a single chart (Appendix) to evaluate the shear strength of both sand and clay from results of their penetrometer tests. One may question this approach if it is admitted that the penetration phenomenon is basically related to a bearing capacity failure and that the problem in sand is essentially a partially drained problem whereas it is a quick problem in clay. In this study results of the Texas Highway Department cone penetrometer were used in the following manner: a statistical correlation was made between the THDP and SPT by comparing blow counts in holes at the same site and using the results of all test sites; the results of the THDP at one site were then transformed to equivalent SPT blow count to verify the measured SPT results. This verification was felt necessary since only one borehole for SPT measurements was made at the Houston sites.

The standard penetration test has long been used to estimate the relative density or the friction angle of the sand. The first correlations between the SPT and the relative density were given by Terzaghi and Peck (1967) and later by Peck, Hanson, and Thornburn (1953) (Fig. 4.4). Research conducted at the US Bureau of Reclamation by Gibbs and Holtz (1957) led to a more rational correlation between the relative density of sand and the SPT by including the effect of the overburden pressure (Fig. 4.5). Results of similar research conducted by Schultz, et al. (1965) are summarized in Fig. 4.6. Bazaraa (1967) concluded from the analysis of 1300 penetration tests that the USBR Charts overestimated the relative density and he recommended the use of more conservative relationships (Fig. 4.6).

Recently, De Mello (1971) gave the standard penetration tests an evaluation by presenting a rational analysis of the penetration phenomenon and the results of a statistical analysis of a large volume of data. Using expressions from the theory of bearing capacity, and a statistical regression analysis of the USBR tests, De Mello derived the following relationship:

$$SPT = 4.0 + 0.015 \frac{2.4}{\tan\phi} \tan^2 \left(\frac{\pi}{4} + \frac{\phi}{2}\right) e^{\pi \tan\phi - 1}$$

$$+ \sigma \tan^2 \left(\frac{\pi}{4} + \frac{\phi}{2}\right) e^{\pi \tan\phi} \pm 8.7 \quad \ldots\ldots\ldots \quad (4.2)$$

where

σ = overburden pressure T/m^2.

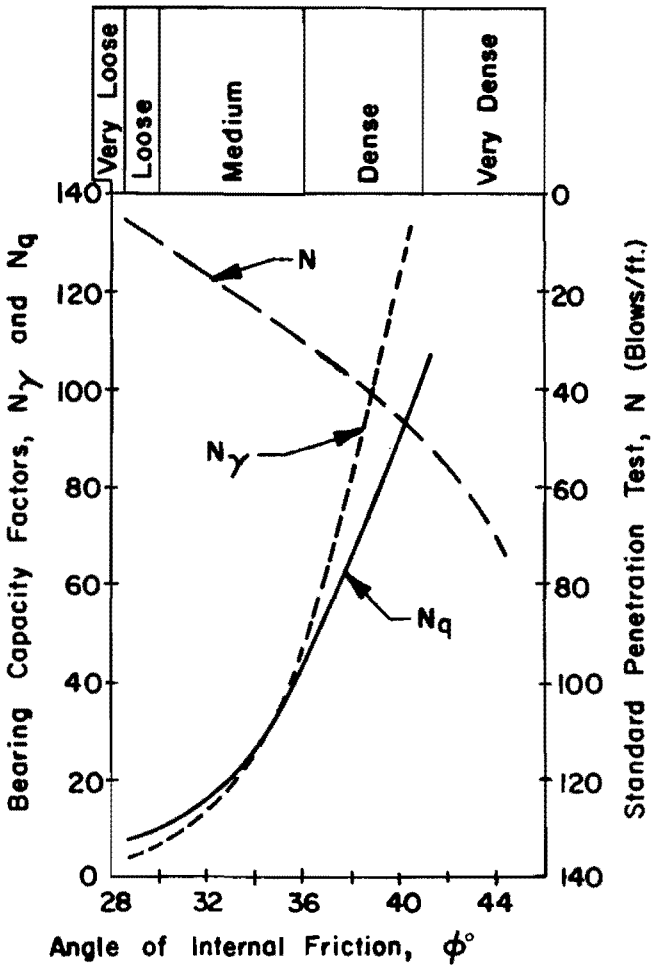

Fig. 4.4 Curves Showing the Relationship Between ϕ, Bearing Capacity Factors, and Values of N from the Standard Penetration Test

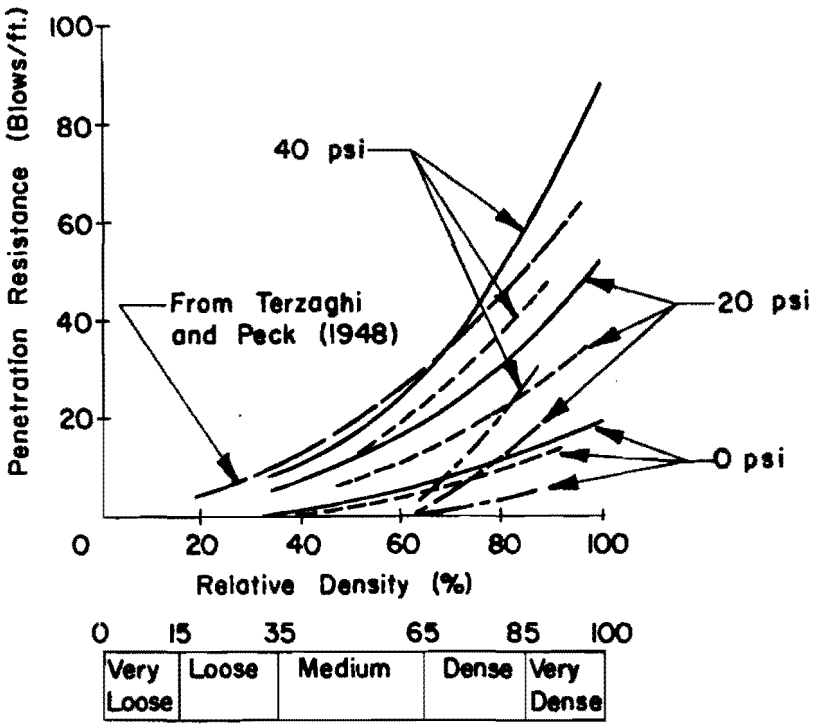

——— Results for air-dry and partially wetted cohesionless sand and considered conservatively reliable in all sands

– – – – Laboratory tank data for saturated coarse sand

—— — — Laboratory tank data for saturated fine sand

Fig. 4.5 Relationship Between Penetration Resistance and Relative Density for Cohesionless Sand (Gibbs and Holtz, 1957)

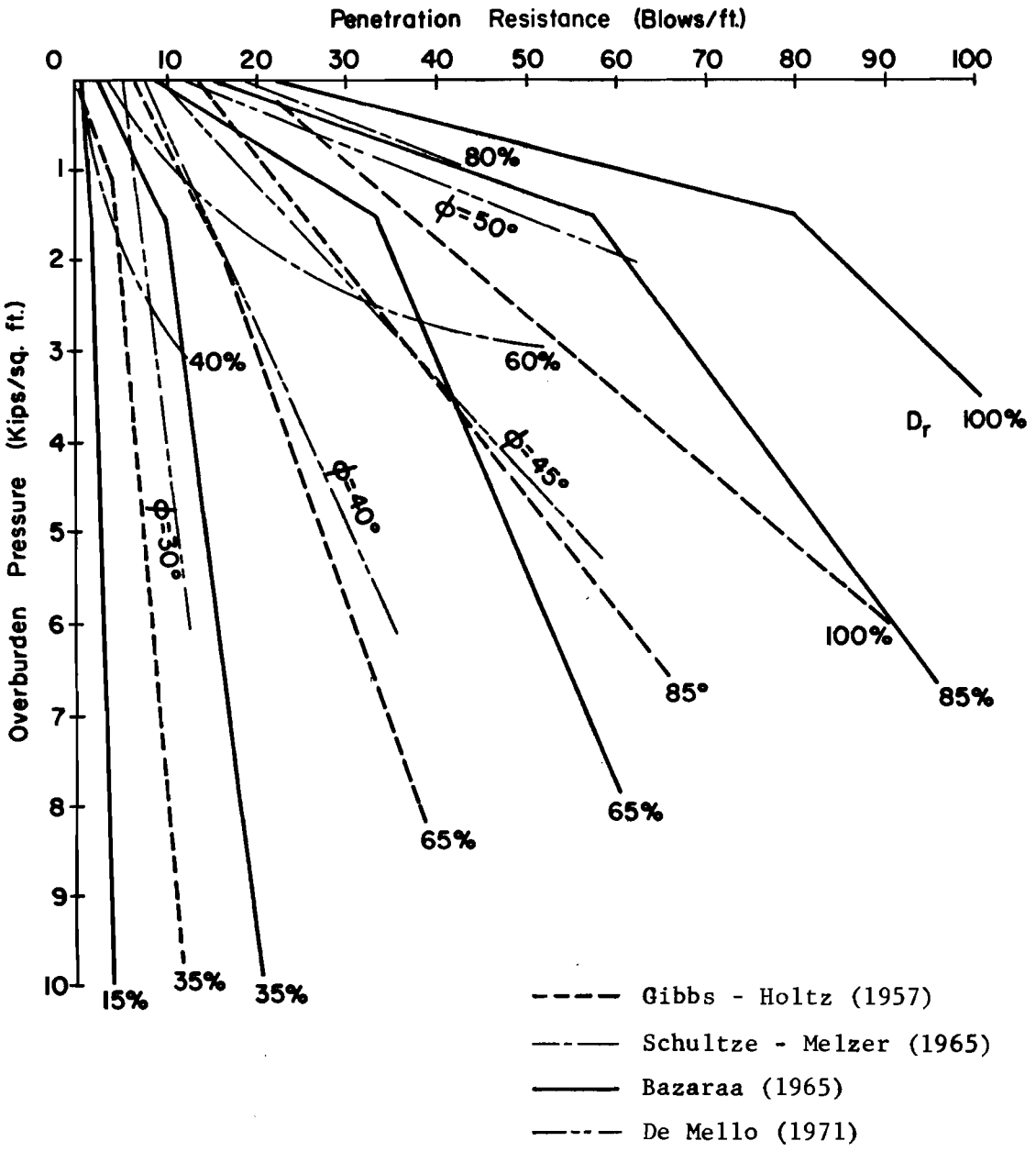

Fig. 4.6 Various Relationships Between Penetration Resistance and Relative Density for Cohesionless Sand (Adapted after Bazaraa, 1967)

De Mello contends that the "shear resistance is the principal parameter at play" in resisting penetration, and rejects the USBR approach of correlating the standard penetration test with the relative density. Figure 4.7 shows a comparison between the triaxial ϕ_{max} values and the ϕ values estimated from the above regression analysis.

For purposes of this study and with the views already explained in mind, the SPT data were interpreted in the light of reasoning presented in the following paragraphs.

The analysis of De Mello is, in the opinion of the authors, the best analysis that has been made of the penetration test. However, this analysis does not consider two aspects of the penetration resistance: the compressibility of the sand and the friction on the sides of the penetrometer. One can think of two sands having the same angle of shear resistance but having two different compressibilities (due to differences in gradation, angularity and mineralogy). The two sands would exhibit different penetration resistances. On the other hand, sands of perfectly similar physical characteristics may indicate different blow counts due to a difference in the overconsolidation ratio and consequently a difference in the coefficient of earth pressure and the side resistance.

Neglecting the effect of overconsolidation, cementation, and other variables related to the SPT test procedure, it seems reasonable to assume the penetration resistance to be a function both of the relative density and of the angle of shear resistance of the soil. With two variables and one output, the penetration test may not give accurate information on

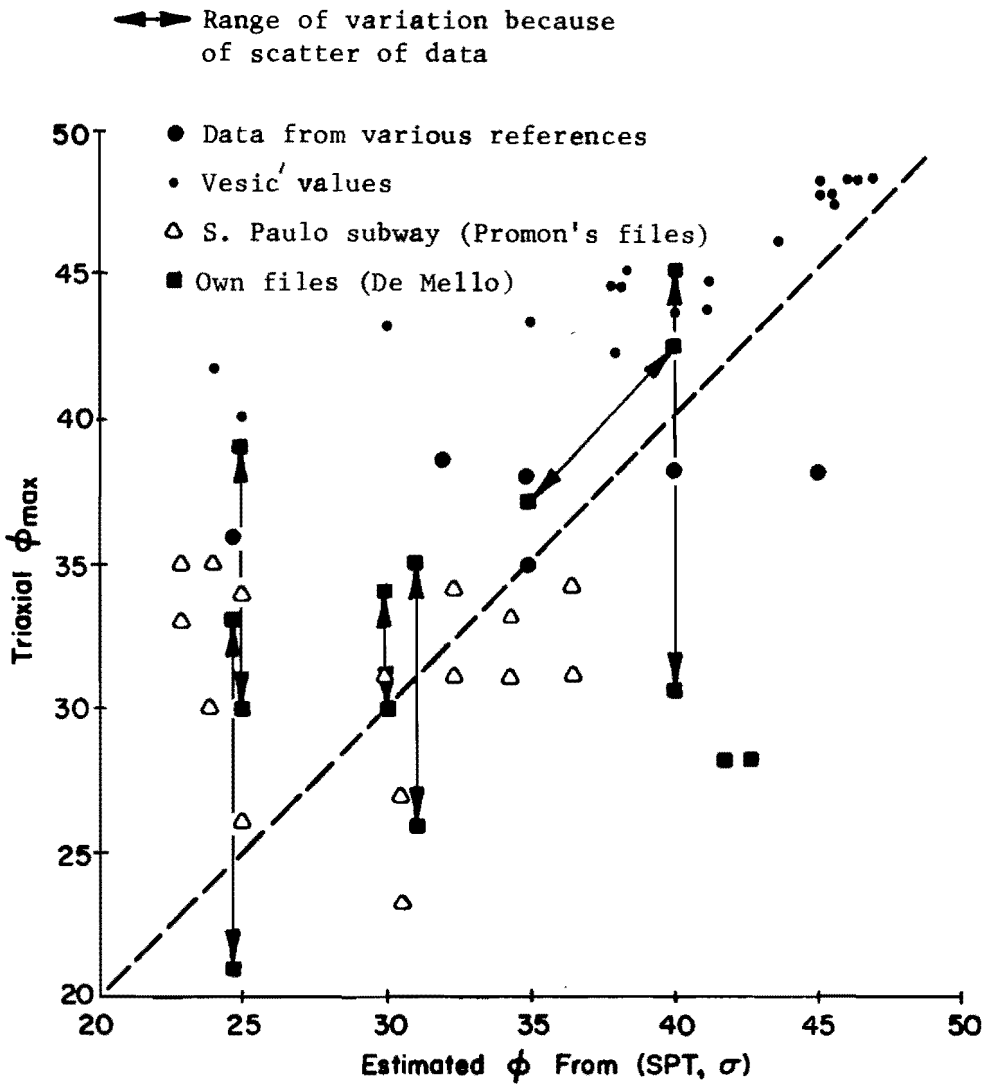

Fig. 4.7 Comparison of Triaxial ϕ_{max} Values with ϕ Estimated from Equation 4.2 (De Mello, 1971)

either one of the variables. If the SPT is combined with another field or laboratory test, it is possible that the influences of the variables can be separated.

The next rational step, along this line of thinking, is to treat the SPT blow count as an index property of the soil, directly related to the behavior of foundations. However, a friction angle means more than a number from a test that is not yet standardized (Ireland, et al., 1970). Furthermore, certain aspects in the behavior of foundations, e.g., the side shear on a pile, are mainly functions of the friction angle of the soil and must, therefore, be expressed in terms of the friction angle.

De Mello, Fig. 4.8, presents a statistical regression analysis of voluminous data in trying to relate the friction angle to the relative density of the sand. As could be expected, such a universal relationship does not seem to exist for all sands, but does seem to exist for "average" sands. The term "average" is not explicitly defined by De Mello, but he indicates that average sands are quartz sands of average uniformity of gradation that occur most frequently and are similar to the sands used in the USBR research.

If one accepts the existence of a relationship between the friction angle and relative density for average sands, then the penetration resistance can be expressed as a function of either variable.

In looking for such an expression among the large number which have been proposed, the relations given by the USBR are found to be most reasonable. While Bazaraa (1965) indicates that the SPT overestimates

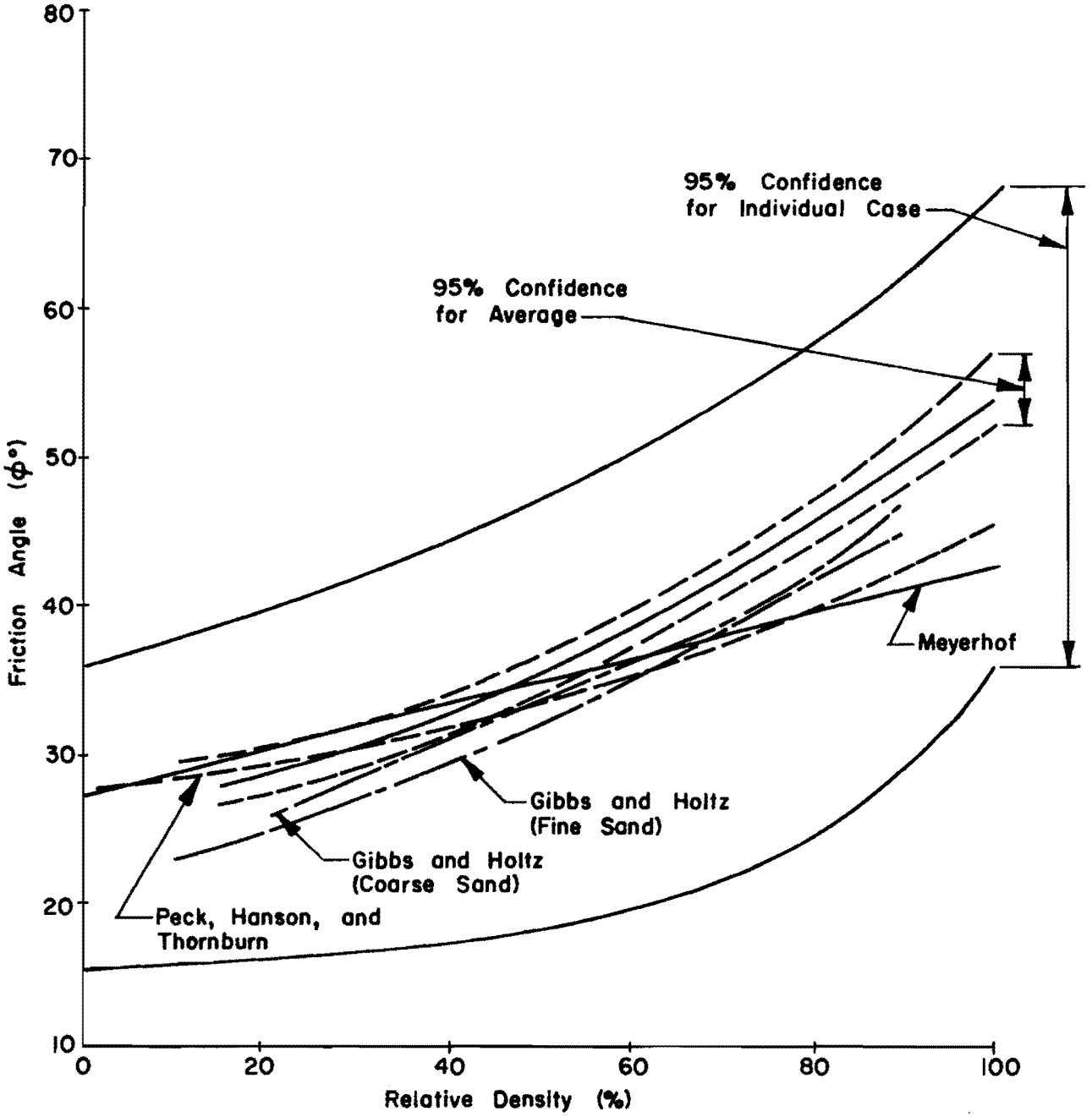

Fig. 4.8 Dispersion Around Universal Relation $\phi = f(Dr)$ (De Mello, 1971)

the relative density of the sand, De Mello (1971) suggests that the SPT underestimates it. The disagreement is apparently due to the several other factors that neither one of the authors included in his analysis. The criticism of Gibbs and Holtz for neglecting the effect of the weight of the drive rods seems unjustified for depths between 15 and 80 feet below the surface because the energy transmitted to the penetrometer in this range of depths does not vary significantly.

It was, therefore, decided in this study to obtain the relative density of the sand from the USBR charts. There does not seem, however, to be an obvious choice of the relation to be used in correlating the relative density to the friction angle of the sand. A relation proposed by Peck, et al. (1953) seemed reasonable and was very close to the curve given by De Mello for average sand, and was, therefore, adopted for this study.

With regard to possible errors in the friction angle from the use of the procedures outlined above, it can be argued that an error of a few degrees in estimating the friction angle cannot be very significant in the analysis of drilled shafts when the side resistance of the shaft is considered. Because the side resistance is a function of tan ϕ, one can write the following:

$$q_s \sim \tan \phi \quad \ldots\ldots\ldots\ldots\ldots\ldots\ldots\ldots\ldots \quad (4.3)$$

where

q_s = unit shear stress

and

$$dq_s \sim \frac{1}{\cos^2 \phi} d\phi \quad \ldots\ldots\ldots\ldots\ldots\ldots\ldots\ldots \quad (4.4)$$

The relative error in side friction can further be expressed as the following:

$$\frac{\Delta q_s}{q_s} = \Delta\phi \cdot \frac{1}{\cos^2 \phi \cdot \tan \phi} \quad \ldots\ldots\ldots\ldots\ldots\ldots \quad (4.5)$$

The relative error in q_s due to an error in ϕ of one degree varies between 3.5% and 4% for a range of angles between 30 and 50 degrees.

An error of 20 percent in evaluating the side resistance of a drilled shaft may not be very significant when the effects of other unknowns in evaluating the properties of the sand or in the construction procedure are considered.

On the other hand, many of the existing theories concerning the bearing capacity of deep foundations show that a slight change in the friction angle, particularly at higher densities, causes a significant change in the bearing capacity of the tip of the foundation. It is, however, an accepted fact that the bearing capacity failure of deep foundations is of the punching failure type (Vesić, 1963). The large bearing capacity predicted for large diameter deep foundations, by theories based on the plastic

equilibrium of the soil mass, is not realistic, because the stresses generated by such bearing pressures lead to the crushing of the soil grains (Vesić, 1968), and consequently to prohibitive settlements. It seems, then, that for deep foundations, the bearing capacity of the tip of the foundation is more sensitive to the compressibility of the soil than to the angle of shearing resistance.

CORRELATIONS BETWEEN SPT AND THDP

A correlation between the standard penetration test (SPT) and the Texas Highway Department cone penetrometer (THDP) is needed for the purposes of this study and for the purpose of making the results of this study useful to the users of the THDP. A correlation based strictly on analytical considerations is very complicated, and a statistical correlation is more rational. However, a discussion of the basic principles and variables involved in the penetration phenomenon is necessary before any correlation is attempted.

The penetration phenomenon is similar to that of pile driving that has been the subject of many investigations (Terzaghi, 1943). Figure 4.9 shows schematically the free body diagrams of the penetrometers and the compression wave generated in the drilling rod at the impact with the hammer. The wave is simplified in a sharp triangular shape that characterizes the steel to steel impact. When the wave reaches the soil, the shear strength of the soil is partly or fully mobilized to resist the displacement of the

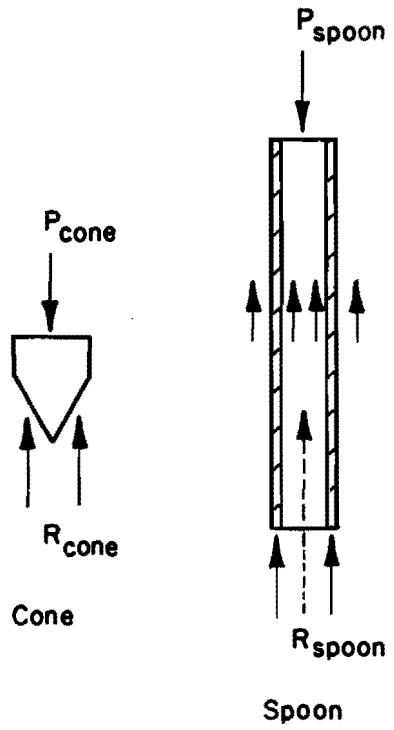

a. Free Body Diagram of Penetrometers

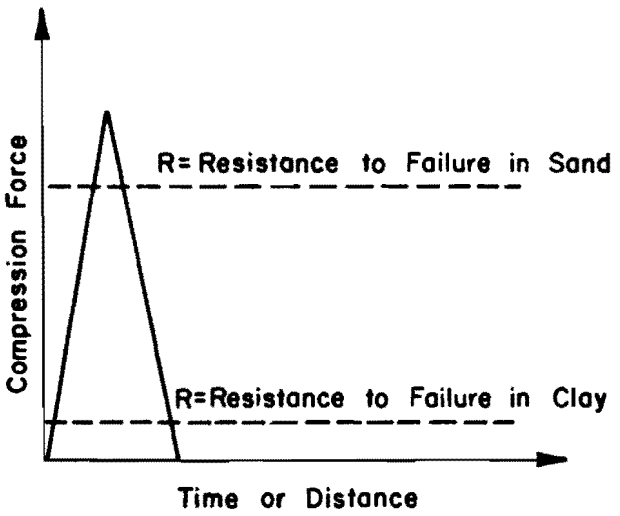

b. Compression Wave in Drilling Rods

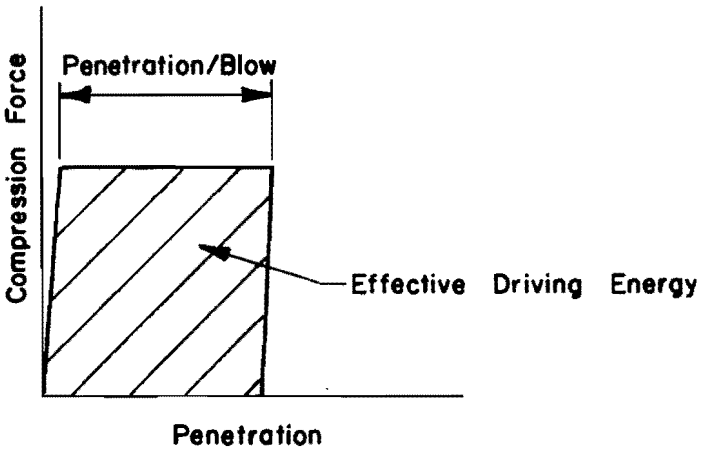

c. Energy Dissipation by Penetration

Fig. 4.9 Illustrations of Penetration Principles

penetrometer. If the soil resistance is smaller than the peak force applied, the soil fails and penetration takes place. The energy of the wave is then dissipated in plastic deformation of the soil (See Fig. 4.9c). If the soil resistance is larger than the peak force of the wave, the soil reflects the wave and the energy is dissipated in heating the system.

Most clayey soils (such as the clay soil tested in this study) exert a small resistance to both types of penetrometers, and the impact energy is usually readily dissipated by penetration, with similar small amounts of heat losses in both penetrometers. However, for the same penetrometers, the bearing resistance is significantly larger in sands than in clays (particularly sands of medium densities and above, as are the sands tested in this study). This fact results in greater heat losses when sandy soils are tested.

Furthermore, the peak stress of the compression wave can be roughly estimated by

$$P_{max} = E \frac{V_h}{v} \frac{W_h}{W_p \ (1+E/T_c \ L)} \qquad \text{(Terzaghi, 1943)}$$

where

E = elastic modulus of drilling rod,

W_p = weight of drilling rod,

W_h = weight of hammer,

L = length of rod,

T_c = stiffness of cushion,

V_h = velocity of hammer at impact,

v = velocity of sound in drilling rods.

For two penetrometers using comparable driving mechanisms and driving rods and differing only in the weights of the driving hammers, the ratio of the peak stresses of the compression waves can be expressed as the following.

$$\frac{(P_{max})_{cone}}{(P_{max})_{spoon}} = \sqrt{\frac{(\text{DRIVING ENERGY})_{cone}}{(\text{DRIVING ENERGY})_{spoon}}}$$

$$= \sqrt{\frac{170 \text{ X } 2.0}{140 \text{ X } 2.5}}$$

$$= 0.985$$

It can, therefore, be concluded that the peak stresses applied at the penetrometer level are fairly comparable in both types of penetrometers. Because the soil resistance is significantly larger for the larger cross-sectional area of the cone than that of the spoon, while the peak driving force is practically the same, it follows that the heat losses in the THDP are larger than in the SPT.

Figures 4.10 and 4.11 show the plots for clay and for sand of the penetration resistance of the two penetrometers. The comparisons were only made for tests taken at about equal depths to eliminate the error due to the weight of the rods (De Mello, 1971) and due to variations in the type of soil.

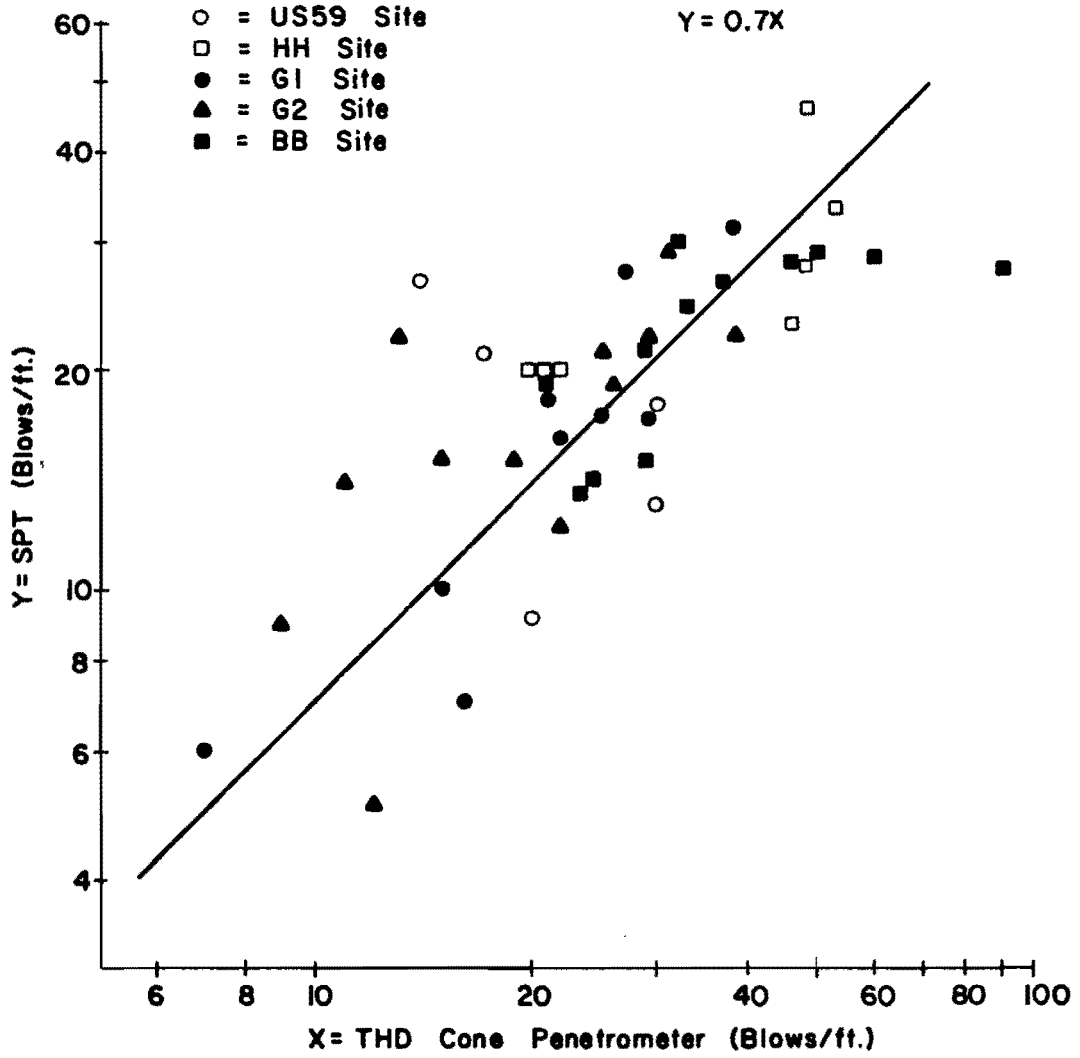

Fig. 4.10 Correlation Between SPT and THD Cone Penetrometer in Clay

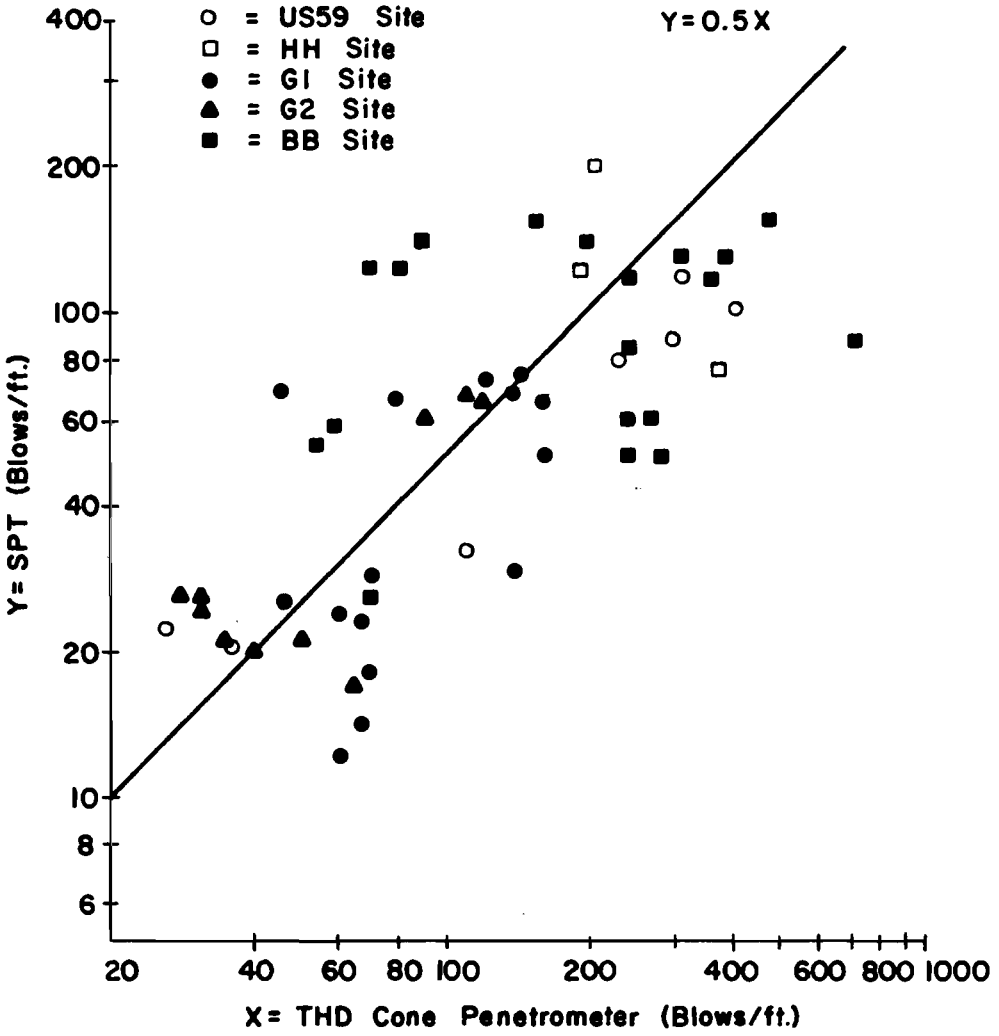

Fig. 4.11 Correlation Between SPT and THD Cone Penetrometer in Sand

A rigorous statistical analysis was not attempted due to the limited amount of data available. Furthermore, a linear correlation is proposed for both soils. A straight line relationship is rational for clays and soft driving soils because the heat losses are not enough to produce non-linear effects. There are larger heat losses in dense sand and in hard driving soil and the losses are not comparable in both tests. As a result a nonlinear correlation between the two tests may be anticipated. However, the large scatter of the data in sands did not seem to warrant a nonlinear correlation and a linear correlation as shown in Fig. 4.11 was adopted.

This page replaces an intentionally blank page in the original.
-- CTR Library Digitization Team

CHAPTER V. DESCRIPTION OF FIELD WORK

This chapter describes the various phases of the field testing program which were carried out. Personnel from the Texas Highway Department and from the Center for Highway Research at The University of Texas at Austin cooperated in performing the work.

DESIGN OF TEST SHAFTS

The test shafts located at the sites of future bridges were designed to satisfy the following requirements:

1. To carry, with a reasonable factor of safety, a load equal to the design load of the shaft.
2. To penetrate the maximum possible distance into the sand layers and to give information on the load transfer in these layers.
3. To have a maximum capacity within the limits of the loading system (1000 tons).

INSTRUMENTATION

The instrumentation of the test shafts consisted mainly of Mustran cells for the purposes of measuring the load at various sections in the shaft during the load test. Thermocouples were also installed in the test shafts to measure the temperature of concrete during curing.

The thermocouples were "Quick tip" iron-constantan thermocouples manufactured by the Leeds and Northrup Company and were installed at three

or four levels in each shaft, as shown in Fig. 5.1.

The Mustran cell is a strain-sensing cell developed at the Center for Highway Research specifically to meet the needs of the research on the behavior of drilled shafts. The construction and operation of the cell have been described in detail by Barker and Reese (1969, 1970) and by O'Neill and Reese (1970). In the following sections, a very brief description of the cell and of the recent modifications in its usage are presented.

The Mustran cell consists of a one-half inch square steel bar instrumented with two 90° foil strain gage rosettes to form a four-arm bridge circuit. Two steel caps are fastened at the ends of the bar after enclosing it in a 1-5/16 inch rubber hose to provide shock protection and waterproofing. Additional protection against the entry of water is provided by partially filling the cavity around the bar with anhydrous calcium chloride and by pressurizing the cell and lead wire with dry nitrogen.

Two types of Mustran cells are manufactured in the shops of The University of Texas. Type-1 cells are distinguished basically from type-2 cells by a reduction in the cross-sectional area of the bar at the location of the strain gages to provide a higher multiplication of the concrete strains. Also, the steel bar in type-1 cell has a length of four inches as compared to five and one-half inches in the type-2 cell. The sensitivity of the type-2 cells was estimated to be adequate for the test shafts of this study and was, therefore, used exclusively in all of the shafts described in this report. Various laboratory tests were conducted on the cells, prior to their shipping for field use, to check their

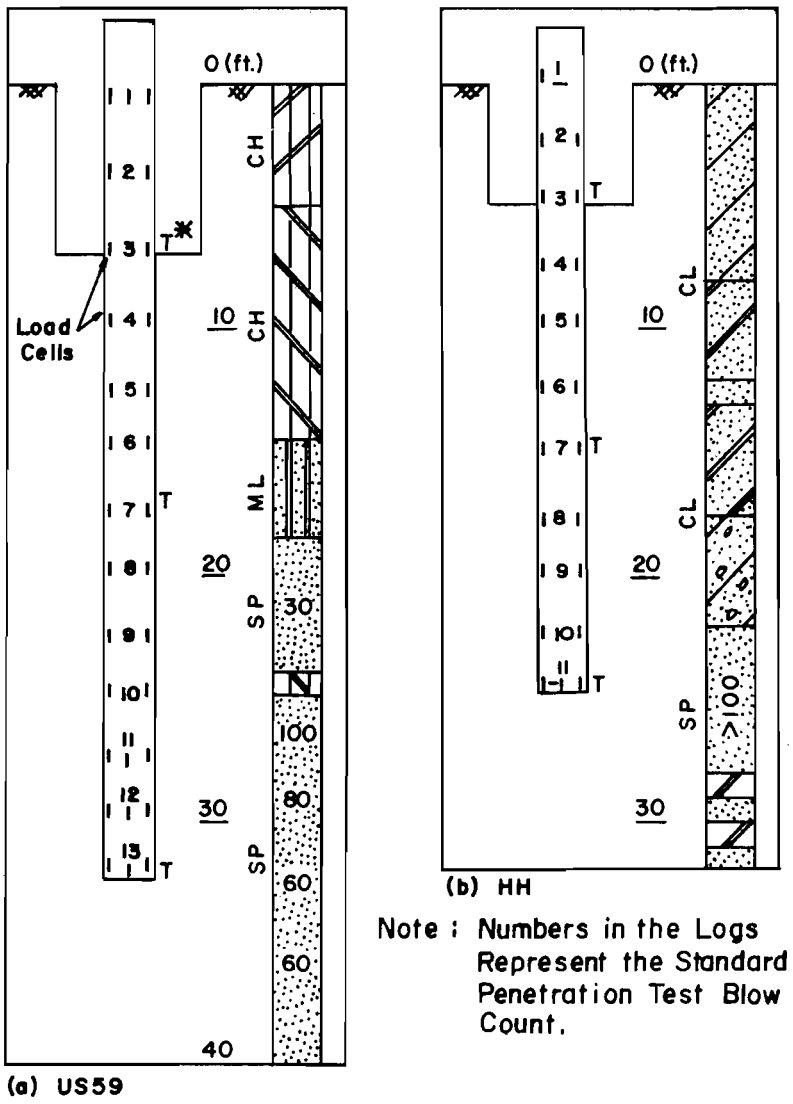

Fig. 5.1 Soil Profiles and Sketches of Pile Instrumentation (Continued)

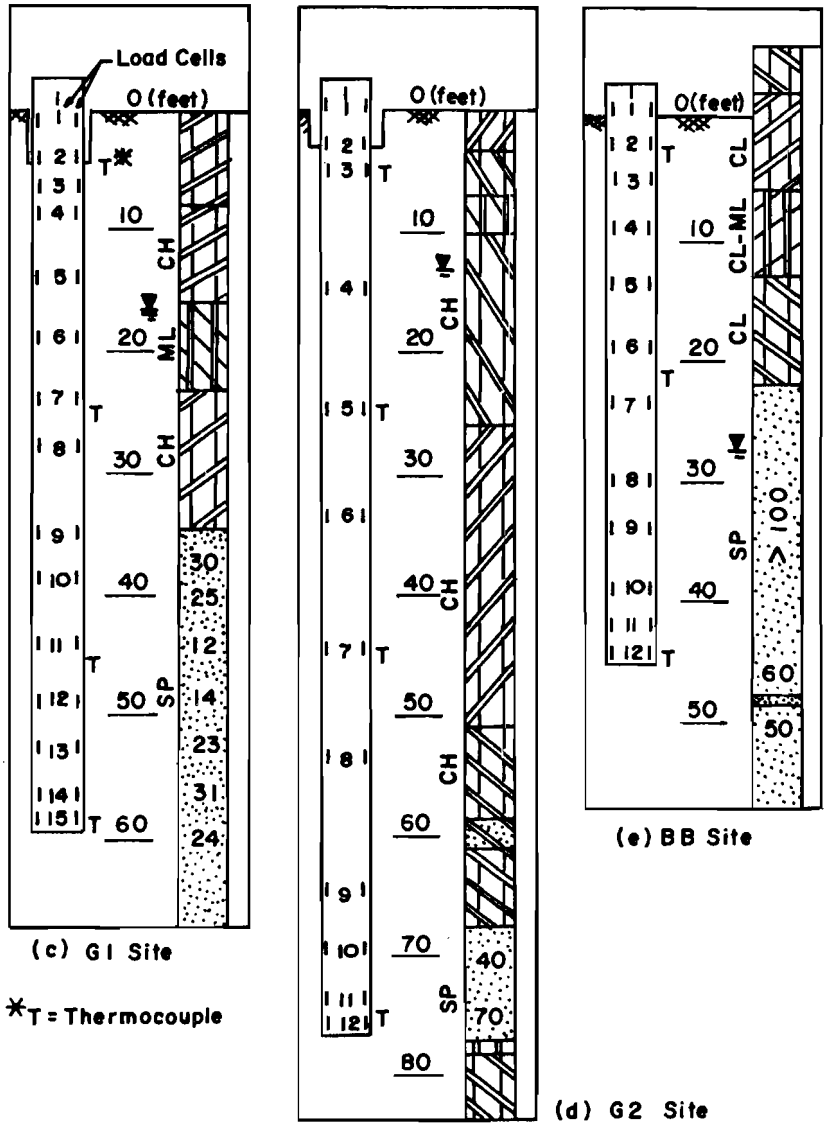

Fig. 5.1 (Continued)

electrical stability, their response to loading and their waterproofness. The resistance-to-ground of the strain gages and their indicated strain, as compared to a reference bridge of similar gages, were measured periodically for a few weeks following the construction of the cells. Gages exhibiting a resistance-to-ground smaller than 100 megohms or indicating a drift in the strain reading were reopened and treated till a satisfactory performance was obtained. The cells were exercised by subjecting them to a cyclic loading of one ton at a constant rate of strain. The applied load, measured by a calibrated load cell, and the response of the gages were plotted instantaneously by an x-y chart plotter. Cells exhibiting a nonlinear response or an abnormally different output than the average output of the other gages were opened and repaired. The output of most of the cells was, therefore, practically the same except for some cells that exhibited slightly different output (up to 10%). This difference was later accounted for in reducing the data. The Mustran system of each shaft, consisting of the Mustran cells, lead wires, and plugboard and the enclosing manifold, was pressurized with dry nitrogen and submerged in water to detect possible leaks.

In the field, the Mustran cells were installed in pairs on two diametrically opposite bars of the cage of reinforcing steel. Figure 5.1 shows the soil profile and sketches of the locations of the instruments in the test shaft. The cells in the exposed part of the shaft serve to develop a calibration curve relating the known applied load on the top of the shaft to the output of the cells. This calibration curve is later adjusted as necessary to reflect variations in pile diameter and is used

to compute the load in the shaft at the other levels of cells. The photographs in Fig. 5.2 show Mustran cells installed on the cage of reinforcing steel. Figure 5.2a shows two cells at about mid-height of the cage on diametrically opposite bars. Figure 5.2b is a view of the lower end of the cage and shows four Mustran cells. The extra cells were placed at the bottom of the shaft in order to measure more accurately the load in point bearing. Figure 5.2c shows the construction of the shaft at the G2 site. The lead wires from the instrumentation are collected in a manifold which is pressurized with dry nitrogen as a further protection against migration of moisture into the electrical system.

The distribution of the gages in the shafts was based on the following considerations:

1. To insure a good calibration level at the top of the shaft.
2. To obtain more information from sand layers because clay was the subject of previous research.
3. To obtain an accurate measurement of the tip resistance.

These considerations explain the higher intensity of gages at the top and bottom levels of the shaft as shown in Fig. 5.1.

The non-loading performance of the Mustran cells was monitored with a Budd strain indicator with the output of each cell being compared to that of a reference bridge. During test loading, readings from the Mustran cells were obtained with a digital data logging system (Honeywell, Model 620) and recorded on a paper tape at the approximate rate of one reading

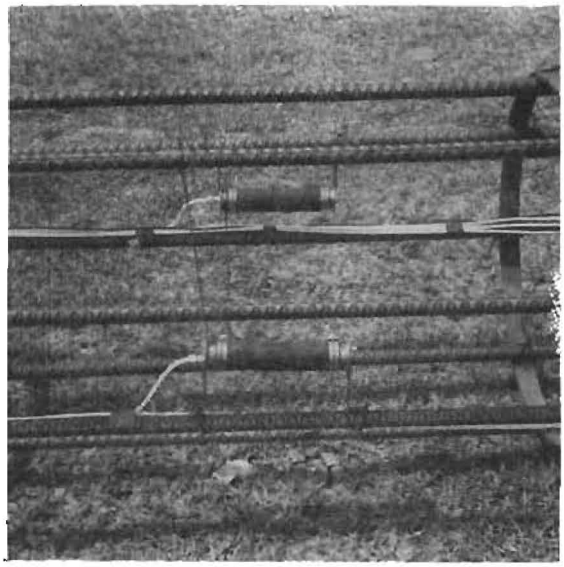

a. Detail of Installation of Mustran Cells

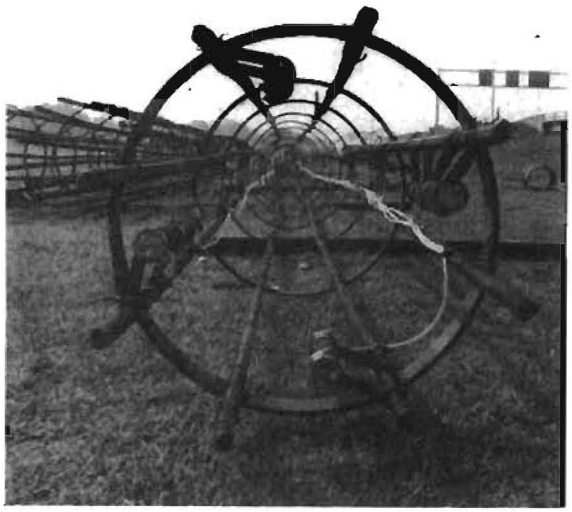

b. View from the Tip of the Instrumented Steel Cage

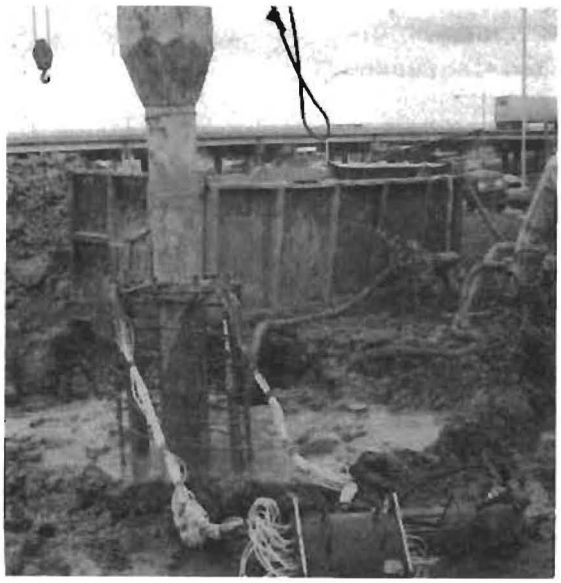

c. Lead Wires and Pressuring System During Construction

Fig. 5.2 Instrumentation

per second. The cells were continuously powered and monitored for at least one hour before the test to provide data on their possible electrical drift. No significant drift in the cells or in the system was detected. Failures in the cells which did occur were of a mechanical nature related mainly to the construction techniques of the test shafts.

CONSTRUCTION

Two methods of construction were used to install the test shafts: the dry method and the slurry displacement method. The dry method was used in installing the test shafts in Live Oak County (shafts US59 and HH) and the slurry displacement method was used in installing the test shafts in Harris County (shafts G1, G2, BB). The procedure which was followed in each method of construction, except for minor variations, was as follows:

Dry Method

1. Open a hole until the plan elevation is reached.
2. Lower a workman who manually cleans the bottom of the hole.
3. Set the instrumented cage of reinforcing steel in the hole.
4. Insert a tremie in the hole and suspend it from one of the lines of the crane. The tremie used was a 10-inch pipe about 25 ft. long and had staggered openings in the sides.
5. Apply a dry nitrogen pressure of about 20 psi on the Mustran system to prevent the migration of water from the concrete into the cells.

6. Pour the concrete in the hopper or into one of the side openings of the tremie.
7. Fill the hole to about 7 ft. from the surface of the ground by a continuous pouring of the concrete.
8. Retract carefully the tremie and continue filling the hole by using the chute of the concrete truck.
9. Form the last 7 to 9 ft. of the shaft with a sonotube to prevent the formation of a tapered shaft close to the surface of the ground. (It has been previously reported that the drilling process invariably results in a tapered hole due to the rapid entry of the auger in the hole [Barker and Reese, 1970].)
10. When the concrete is set, remove the soil from around the shaft to a distance slightly below the calibration levels of the Mustran cells.

Slurry Displacement Method

1. Open a hole without slurry until a water-bearing, caving layer is encountered.
2. Immediately introduce the premixed mud slurry and keep its level within three to five feet of the ground surface.
3. Continue drilling to plan elevation under slurry.
4. Clean the bottom of the hole with a bucket or an auger immediately before the cage of reinforcing steel is set in place.

5. Attach four concrete blocks at the bottom of the cage to avoid sinking of the cage in the sand, and then set the cage in the hole. (A bottle of nitrogen is tied to the steel cage to keep the Mustran system continuously pressurized, during the installation of the cage.)
6. Insert a temporarily sealed tremie, 10 inches in diameter, through guides welded to the reinforcing steel cage and set the tremie in the hole.
7. Fill the tremie with concrete and unplug it by lifting it a few inches.
8. Place concrete while keeping the tremie tip well embedded in the concrete. Flow of concrete through the tremie is assisted as necessary by carefully raising and lowering the tremie.
9. Waste the first portion of the concrete flow, because this concrete is usually contaminated with mud, and form the top five to seven feet of the shaft with a sonotube.
10. When the concrete is set, remove the soil from around the shaft to a distance slightly below the calibration levels of Mustran cells.

Figure 5.3 shows the different phases of the construction of the test shafts. Figure 5.3a shows the drilling process under mud. In Fig. 5.3b a man is being lowered in a dry hole to clean the bottom of the hole. Figure 5.3c shows the tool which is employed to clean the bottom of a hole drilled with slurry. Figure 5.3d shows a long, instrumented steel

a. Drilling Under Mud

b. Manual Cleaning of the Bottom of a Dry Hole

c. Bucket Cleaning of the Bottom of a Hole Drilled Under Mud

Fig. 5.3 Construction - Drilling and Cleaning

(Continued)

d. Lifting of Instrumented Steel Cage

e. Installation of Steel Cage in the Hole

f. Temporary Seal of Tremie

Fig. 5.3 (Continued)

(Continued)

g. Concreting of a Dry Hole

h. Concreting by Slurry Displacement

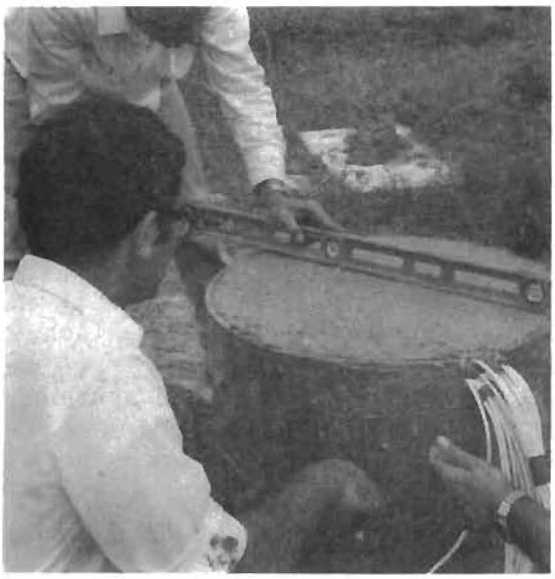

i. Forming of the Top Section of a Test Shaft

Fig. 5.3 (Continued)

cage, lifted with three points to avoid excessive bending of the cage; while Fig. 5.3e shows the installation of the same cage in the hole. Figure 5.3f shows the temporary seal of the tremie. Figures 5.3g and 5.3h illustrate the concreting procedure followed in concreting dry holes and in concreting by slurry displacement. Figure 5.3i shows the last phase of the construction, consisting of forming the top section of the shaft in a sonotube.

Table 5.1 presents data on the dimensions of the shaft and some of the field data related to the concreting phase of the construction. The time required to concrete the hole and the temperature of the concrete have a decisive influence on the lateral pressure developed by the concrete against the walls of the hole.

Comments Concerning the Construction of Shaft US59

There was sloughing of the walls of the hole during drilling in the sand at about 18 feet below the surface of the ground. The sloughing was limited to an area of about two square feet and extended about two inches into the walls of the hole. Difficult drilling was experienced in the very dense dry sand below a depth of 25 ft. The wobbling of the kelly bar beyond that depth created corrugations in the walls extending to the bottom of the hole. The depth of the corrugations was estimated at about one inch.

Due to some technical difficulties, pressurizing of the Mustran system was not possible till about two hours after concreting was completed. The resistance-to-ground of the cells was still excellent after that time and no moisture is believed to have reached the gages.

Table 5.1 Location and Geometric Descriptions of Test Shafts

Shaft	dn, in.	da, in.	De, ft.	Db, ft.	As	Conc. Slump, in.	No. of Conc. Trucks	Air Temp., °F	Time for Concreting
US59 Cast 8-25-70	30	--	9.5	25.4	8#9	2.5-3.0	2	89	≃½ hr.
HH Cast 8-31-70	24	--	7.2	19.8	8#7	5.0-6.0	1	92	≃½ hr.
G1 Cast 9-02-71	36	37.7	7.0	54.8	10#8	6.0-7.0	3	91	≃1 hr.
G2 Cast 8-19-71	30	31.4	5.5	73.5	8#8	5.5-6.5	3	90	≃1.5-2 hr.
BB Cast 9-03-71	30	31.4	3.0	45.0	8#8	6	2	83	≃½ hr.

De = exposed height of shaft

Db = buried height of shaft

dn = nominal diameter (or sonotube diameter)

As = steel reinforcement

da = averaged measured diameter

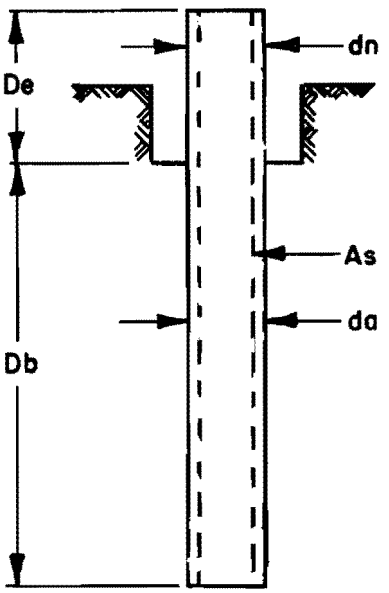

Generalized Elevation of Test Shafts

Comments Concerning the Construction of Shaft HH

The depth of the hole at this site was smaller than the length of the tremie and, as a result, the concrete was poured through one of the side openings of the tremie. This procedure forced the concrete into a sinuous chute and is believed to have caused a segregation of the concrete at the tip of the shaft.

Comments Concerning the Construction of Shaft G1

At this site, cleaning of the bottom of the hole with an auger was unsuccessful. Cuttings and loose soil were believed to have fallen back to the bottom. As the site was muddy and the top of the hole was not protected, the workmen caused soft mud to fall into the hole while walking around the shaft during and after the installation of the steel cage. The belief that soft material existed at the bottom of the hole was later sustained by the fact that the tremie sank about six inches when the first bucket of concrete was poured into the tremie.

Comments Concerning the Construction of Shaft G2

A first attempt to install the shaft in the south bay of the bent failed because the contractor did not keep the mud slurry at a high enough level in the hole. Keeping the mud slurry near the level of the caving soils accelerated the caving because of the scouring action caused by the fluctuation of the mud surface. The first hole was filled with concrete and abandoned.

The second attempt was successful because the mud slurry was kept near the ground surface. Also, premixed mud slurry was used, a procedure

which was found advantageous. In-hole mixing as used during the first attempt could have aided the scour and the caving which was observed.

The bottom of the hole was cleaned with a bucket just before the steel cage was introduced. Unusually nonhomogeneous soil conditions existed at the site and there was uncertainty about the character of the soil at the tip of the shaft.

Comments Concerning the Construction of Shaft BB

Two observations were made concerning the mud at this site:

a. The mud slurry was too thick because some water drained out of the hole leaving a thick bentonite gel.
b. Contaminated water from Brays Bayou was used in mixing the mud. This contaminated water caused flocculation of the bentonite and inhibited the formation of an impervious mud cake.

Soil borings at the site indicated that the sand formation contained occasional sandstone lenses. At the shaft location these lenses were not encountered; however, a 10-inch auger advanced in the sand below plan tip elevation indicated hard layers interpreted as sandstone 2.5 feet below the tip.

Data on the Concrete of the Test Shafts

Table 5.2 presents laboratory data on the compressive strength and the modulus of elasticity measured on concrete cylinders. Cylinders recovered from the construction of the shafts in Live Oak County were cured in a 100% moisture room and tested at the laboratories of The University of

Table 5.2 Data on the Concrete of the Test Shafts

Shaft	Specimen	Compressive Strength f'_c, psi	Modulus of Elasticity, psi	Manufacturer	Laboratories
US59	Cylinder 1	4700	6.0×10^6	South Texas	U. T.
	Cylinder 2	4050	6.0×10^6	Material Co.,	U. T.
	Beam 1	4820 (932)*		Beeville	THD
	Beam 2	4150 (725)*			THD
HH	Cylinder 1	5750	5.4×10^6	South Texas	U. T.
	Cylinder 2	6250	5.8×10^6	Material Co.,	U. T.
	Cylinder 3	6100	5.8×10^6	Beeville	U. T.
	Cylinder 4	6000	----		U. T.
	Cylinder 5	5100	5.2×10^6		U. T.
	Beam 1	4750 (750)*			THD
	Beam 2	4220 (670)*			THD
G1	Cylinder 1	5651	5.3×10^6	Gifford	THD
	Cylinder 2	5612	4.8×10^6	Hill,	THD
	Cylinder 3	5246	4.6×10^6	Houston	THD
	Cylinder 4	5088	5.0×10^6		THD
	Cylinder 5	5123	4.7×10^6		THD
	Cylinder 6	5105	4.8×10^6		THD
G2	Cylinder 1	4965	5.1×10^6	Gifford	THD
	Cylinder 2	5177	4.4×10^6	Hill,	THD
	Cylinder 3	4912	5.1×10^6	Houston	THD
	Cylinder 4	4735	4.8×10^6		THD
	Cylinder 5	4647	5.1×10^6		THD
	Cylinder 6	4735	4.9×10^6		THD

(Continued)

Table 5.2 (Continued)

Shaft	Specimen	Compressive Strength f'_c, psi	Modulus of Elasticity, psi	Manufacturer	Laboratories
BB	Cylinder 1	4843	5.2×10^6	Gifford	THD
	Cylinder 2	5035	5.0×10^6	Hill,	THD
	Cylinder 3	4718	4.3×10^6	Houston	THD
	Cylinder 4	4701	4.2×10^6		THD

* The tensile flexure strength F_t measured from the center point loading is related to the compressive strength f'_c by $F_t = 1.22 \times k \times f'_c$

where $k = 0.14$ for $f'_c = 5000$ psi

$= 0.13$ for $f'_c = 6000$ psi (Neville, 1971)

Table 5.3 Data on Drilling Mud

Shaft	Specific Gravity of Mud	pH of Mud
G1	1.30	7.5-7.7
G2	1.05	8.5-10.1
BB	1.40	6.6-7.6

Texas. Concrete beams were also cast at these sites and were cured in water and tested in flexure by the Texas Highway Department to obtain the modulus of rupture. The concrete cylinders recovered from the construction of the shafts in Harris County were tested by the Texas Highway Department. The scatter of the results of compressive strength and modulus of elasticity of the concrete is very remarkable. Some of the factors influencing this scatter are

1. The difference in the mixture of each batch represented by a concrete truck.
2. The different mixing time for each truck. The trucks are usually dispatched at one time to the construction site but have to unload at the rate imposed by the construction.
3. The problems inherent to sampling techniques. A large number of samples is needed to allow a statistical consideration of the quantities evaluated. This approach was not considered practical and the cylinders recovered averaged about 1 cylinder per 3 cubic yards of concrete.
4. Differences in the testing techniques. The concrete specimens were tested in different laboratories and by different personnel, a fact that results in inevitable differences in the results.

Of the above mentioned factors, only the first two affect the real strength and stiffness of the concrete in the shaft. The variation in the stiffness of concrete cast from different trucks results in an erratic scatter of the data obtained from the Mustran cells.

Table 5.3 presents the values of the density and the pH of the mud used in the construction of shafts in Harris County. It is believed that the low pH at G1 and BB sites caused the mud to flocculate and, therefore, increase in density by suspending solids.

LOAD TESTS

The test shafts were loaded to failure at periods of time varying, for the different shafts, between 16 and 60 days after the end of construction. The load tests at an early age were intended to detect significant effects of early loading on the capacity of drilled shafts.

Apparatus and Procedure

The loading system used in the tests is the same as that described by Barker and Reese (1969, 1970), and O'Neill and Reese (1970). The main features of this system are:

1. A reaction beam supported by two anchor shafts which are permanent elements in the bridge.
2. Two calibrated hydraulic jacks.
3. An air operated oil pump provided with a bourdon gage and an electrical pressure transducer to measure the pressure in the hydraulic system.

The beam used in the tests at Live Oak County is the same as that described by O'Neill and Reese (1970). A newly built reaction beam was

used in the tests at Harris County. Some of the features of the new beam were improved connections between the anchor shafts and the beam for easier erection of the reaction frame, and an improved design of the loading box which provides the bearing area between the beam and the jack. Both beams were designed to allow a load of 1000 tons to be applied to the test shaft. The anchor shafts were, therefore, designed for a pullout force of 500 tons. The spacing of the anchor shafts was in all cases more than seven times the diameter of the test shaft. The anchor shafts were believed to have a minimal influence on the behavior of the test shaft.

The capacity of each jack was limited to 500 tons, a load which corresponded to a pressure of 20000 psi in the hydraulic system. The jacks were calibrated periodically to provide a fixed relation between the hydraulic pressure and the applied load. Special provisions were taken during the installation of the jacks to minimize the eccentricity of the applied load. The top of the shaft was carefully leveled with a quick setting capping compound before a one-inch-thick steel plate and the jacks were placed. A one-inch-thick plywood board was inserted between the shaft and the steel plate in the tests at Harris County and rotary swivel heads were placed between the jacks and the beam in the tests at Live Oak County in a further attempt to reduce the eccentricity of the load.

The settlement of the test shaft was measured with two dial indicators mounted on diametrically opposite positions on the butt of the shaft. The dial indicators had a two-inch travel and a resolution of .001 inch.

The settlement was measured with reference to two 4-in. by 4-in. timber beams 20 feet long anchored at their ends in the ground.

The quick test procedure (QL) prescribed by the Texas Highway Department "Special Provisions to Specifications Item 405, 1965," and described by O'Neill and Reese (1970), was used in most tests. In this testing procedure each load increment was maintained for two and a half minutes before the next increment was applied. The magnitude of the load increment varied for the first test, between one-twentieth and one-thirtieth of the estimated ultimate load. The loading increments on subsequent tests and the unloading increments were arbitrarily chosen between two and five times the loading increment of the first test. A set of readings of the Mustran cells was started in all tests at one-half and at two minutes after the application of the load. The settlement gages were read at the same time as the load cells in the tests at Liveoak County and at five seconds and at two and a half minutes after the application of the load in the tests at Harris County. In the following chapters only the two-and-a-half-minute data is reduced and interpreted.

The following special tests were conducted at the different sites:

US59 Test-4. Four holes 6 and 12 inches in diameter were drilled at distances of three to four feet from the test shaft for a depth varying between 18 and 30 feet. The holes were later filled with gravel and a surface pit was dug around the shaft and was soaked for a period of three days. A total estimated volume of 10,000 gallons seeped into the soil surrounding the shaft. The change in moisture content of the soil

surrounding the shaft is shown in Fig. A26. Test 4 was conducted to study the effect of this change on the capacity of the shaft.

US59 Test-5 and HH Test-3. In these tests, the load increments were maintained between 2½ and 30 minutes to observe the speed of penetration of the shaft under constant loading.

G1 Test-3. This test was of the cyclic type described by Barker and Reese (1970) and was conducted to study the effect of cyclic loading on the behavior of drilled shafts in sand.

Table 5.4 summarizes the data from the load tests conducted at the various sites and Fig. 5.4 shows some phases and details of the load tests. Figure 5.4a shows the reaction system; Fig. 5.4b shows the jacks, the swivel heads and the hydraulic equipment; and Fig. 5.4c shows the read-out digital system.

EXTRACTION OF THE SHAFTS

The extraction of the shafts cast by slurry displacement was planned to ascertain the effects of the construction technique on the integrity of the concrete, the geometry of the shaft, and the concrete-soil interface. The three shafts were extracted after load testing was finished. The extraction was accomplished by drilling an annular opening around the shaft to the depth of the test shaft. The shaft was loosened using a large block-and-tackle frame and then extracted easily with the rig cable. The operation encountered difficulties at the G2 site where the annular opening kept sloughing and had to be protected by a large casing.

Table 5.4 Dates and General Information on Load Tests

Shaft	Test	Type	Date of Test	Load Incr.	Unloading Incr.	Maximum Load Applied
US59	1	QL	9-17-70	20T	100T	600T
	2	QL	9-17-70	50T	100T	500T**
Cast 8-25-70	3	QL	9-17-70	100-50T	100T	700T
	4	QL (Soaked)	10-08-70	25T	100T	700T
	5	ML* (Soaked)	10-08-70	100T	one Incr.	750T
HH	1	QL	10-20-70	20T	---+	400T**
Cast 8-31-70	2	QL	10-20-70	100-20T	100T	580T
	3	ML*	10-20-70	100T	one Incr.	500T**
G1	1	QL	10-19-71	25T	50T	480T
Cast 8-19-71	2	QL	10-19-71	50T	100T	450T
Extracted 11-5-71	3	QL (Cyclic)	10-19-71	75T	one Incr.	450T
G2	1	QL	10-12-71	25T	50T	700T
Cast 9-3-71	2	QL	10-12-71	50T	100T	680T
Extracted 10-26-71						
BB	1	QL	10-07-71	25T	---+	750T
Cast 9-21-71	2	QL	10-08-71	50T	75T	750T
Extracted 10-13-71	3	QL	10-08-71	100T	300T	600T**

+ Hydraulic system broke and an unloading curve could not be obtained
* Loads maintained up to 25 minutes to study the speed of penetration of the shaft under constant load
** Load not taken to failure

a. Reaction System

b. Loading Jacks and Swivel Heads

c. Data Logging System

Fig. 5.4 Load Testing

When a shaft was removed from the soil, measurements were made of its length and of the perimeter at the location of each of the Mustran cells. The soil-concrete interface was carefully examined by studying original soil still adhering to the shaft surface. Some Mustran cells were exposed by use of a jack hammer to observe their seating conditions in the concrete. In removing the cells, concrete was examined for possible contamination from slurry. Table 5.5 presents the measured dimensions of the extracted shafts. Figure 5.5 presents photographs taken during the extraction phase; Figure 5.5a shows the extraction of the G1 shaft; Figure 5.5b shows the measuring of the shaft diameter; Figure 5.5c shows an uncovered Mustran cell; and Figs. 5.5d, 5.5e, and 5.5f show the tips of the extracted shafts.

Table 5.5 Depths and Diameters of Shafts at Cells Locations

Level	Shaft G1		Shaft G2		Shaft BB	
	Depth*, ft.	Diameter, in.	Depth*, ft.	Diameter, in.	Depth*, ft.	Diameter, in.
1	3.7	36.0	2.5	30.0	2.7	30.0
2	6.7	38.0	5.5	32.0	5.2	31.2
3	9.2	37.6	7.5	31.7	8.6	31.1
4	11.7	37.6	17.5	31.4	12.0	31.3
5	16.7	37.6	27.5	31.3	17.0	--
6	21.7	37.7	36.3	31.6	22.2	31.5
7	26.8	37.4	47.4	31.3	27.0	32.0
8	30.7	37.4	56.4	31.6	33.2	31.6
9	37.9	37.5	67.5	31.4	37.1	--
10	41.6	37.4	72.4	31.6	42.2	31.3
11	46.7	38.0	76.5	31.3	45.0	31.0
12	51.7	38.6	78.8	31.1	47.4	25.2
13	55.9	38.6				
14	59.5	37.6				
15	61.5	36.8				
Average		37.7		31.4		31.4

* Depths are measured from the top of the shaft

a. Extraction of the Shaft at G1 Site

b. Measurement of the Diameter of the Shaft

c. Extraction of Mustran Cells

Fig. 5.5 Extraction of the Shafts

(Continued)

d. The Tip of Shaft G1

e. The Tip of Shaft BB

f. The Tip of Shaft G2

Fig. 5.5 (Continued)

CHAPTER VI. ANALYSIS OF THE DATA

GENERAL PERFORMANCE OF THE MUSTRAN CELLS

To date, over 300 Mustran cells have been used in the testing of drilled shafts and their general performance in short-term testing has proven to be satisfactory. The Mustran cells are rugged and electrically stable, and their resolution is competitive with if not superior to other commercially available strain-measuring gages. Poor performance of some Mustran cells has, however, been observed, and it is important to understand the reasons for the failure of the cells and to recognize a faulty output when it occurs.

Electrical Failures

Shorting to ground of the cells may be the result of defective construction such that one of the lead wires gets in direct contact with the metal of the cell or with the unprotected ground line. Although great care is observed in the laboratory to check the continuity of the cell circuit, rough field handling may precipitate the shorting of a defective connection.

Moisture may also penetrate the cell through a defective fitting and migrate through the waterproofing coat of the strain gages. Cells suffering from the presence of moisture may exhibit an acceptable resistance to ground but show a continuous drift in output with time.

Mechanical Failure

Mechanical failures of the Mustran cells result from accidental impact of the cells during construction or from other phenomena related to the

casting and the curing of the concrete. Mustran cells at lower levels of the shaft incur a greater risk of being completely disconnected and destroyed by the vertical traveling of the tremie in the case of shafts cast by slurry displacement, and by the impact of the free falling concrete in the case of shafts cast in the dry. Segregation and the existence of voids in the concrete can result in a reduced section of the shaft or in a poor embedment of the Mustran cells.

It has also been observed that the cells located in the top three feet of the shaft exhibit a smaller response to load than the lower cells. Freshly placed concrete tends to settle as a result of the plastic shrinkage and the bleeding of the cement mortar (Neville, 1971). However, the reinforcing steel tends to resist this settlement and, consequently, there may be vertical cracking of the concrete at the top of the shaft. The settlement of the concrete may also result in a gap below the bottom cap of the top level of cells with bleeding water moving in and filling the gap. Later, the water may be used for the hydration of the concrete leaving a permanent void under the cell. This phenomenon is similar to that causing the lower bond resistance of the upper layers of steel in a concrete beam (Neville, 1971). Furthermore, the severe curing conditions of the exposed part of the shaft may result in the warping and the cracking of the concrete and, consequently, in an erroneous output of the cells.

Special embedment problems with the cells were encountered in the shafts cast by slurry displacement as a result of the entrapment of mud at the end caps of the cells. This phenomenon was particularly evident

in the upper sections of the shaft where the energy of flow of the concrete is greatly reduced and where the mud may have severely gelled due to its continuous contact with the concrete. This fact was later sustained by the inspection of the embedment of cells in extracted shafts.

It is generally possible to detect erroneous output of cells from plots of the non-loading output of the cells versus time and plots of the loading output of the cells versus the applied load. The following observations can be made concerning such plots:

1. A typical plot of the nonloading output of Mustran cells is presented in Fig. 6.1. The sharp rise and drop of the curve immediately after the casting of the concrete is associated with the rise in temperature of the setting concrete. It has been a common observation that for most well-behaved cells the curve levels off in a few days after the end of construction. Unstable cells show a continuous drift (Fig. 6.1) which may be caused by a moisture migration into the gages.
2. A typical plot of the average output of good calibration cells versus the pressure in the hydraulic system is shown in the solid line of Fig. 6.2. The hysteresis of the plot is due to the friction in the jacks, which reverses directions during loading and unloading (Barker and Reese, 1970; O'Neill and Reese, 1970). When the cells are well behaved and no permanent plastic strain occurs in the concrete, the curve returns to the origin on unloading. If, however, plastic strains are locked in the concrete,

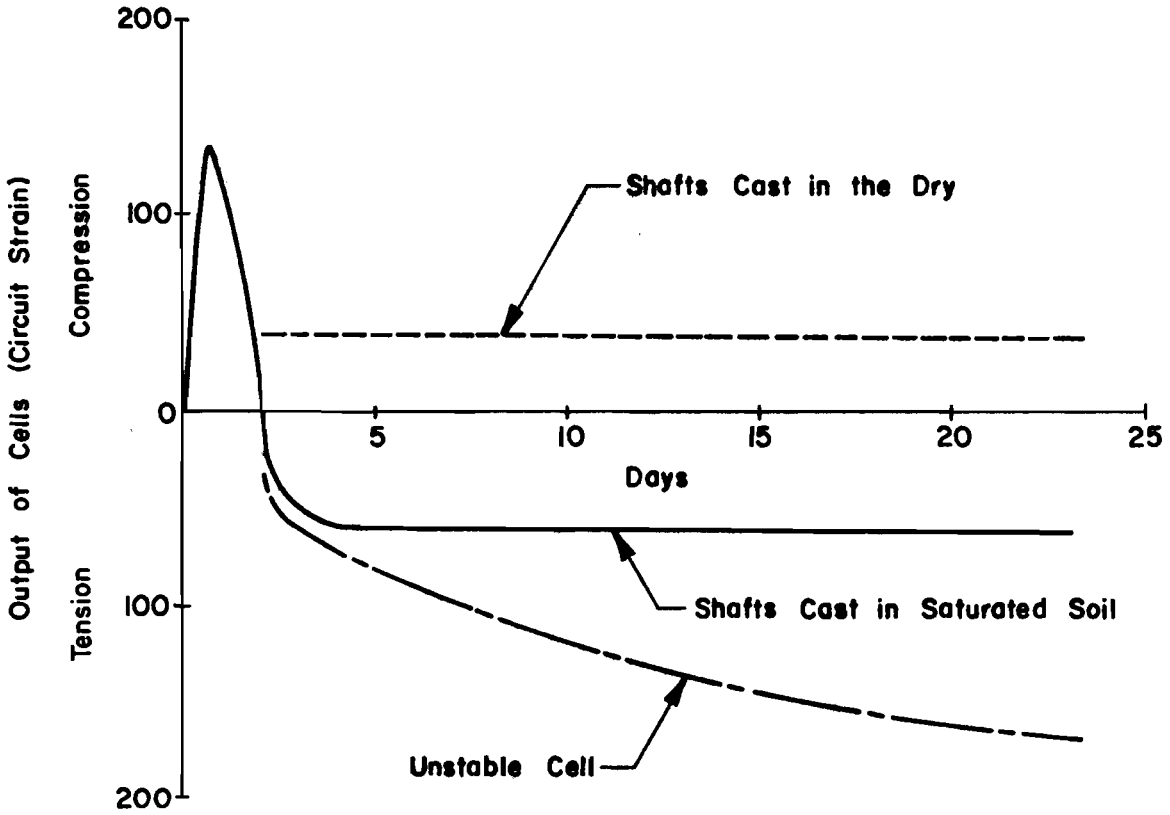

Fig. 6.1 Non-Loading Output of Mustran Cells

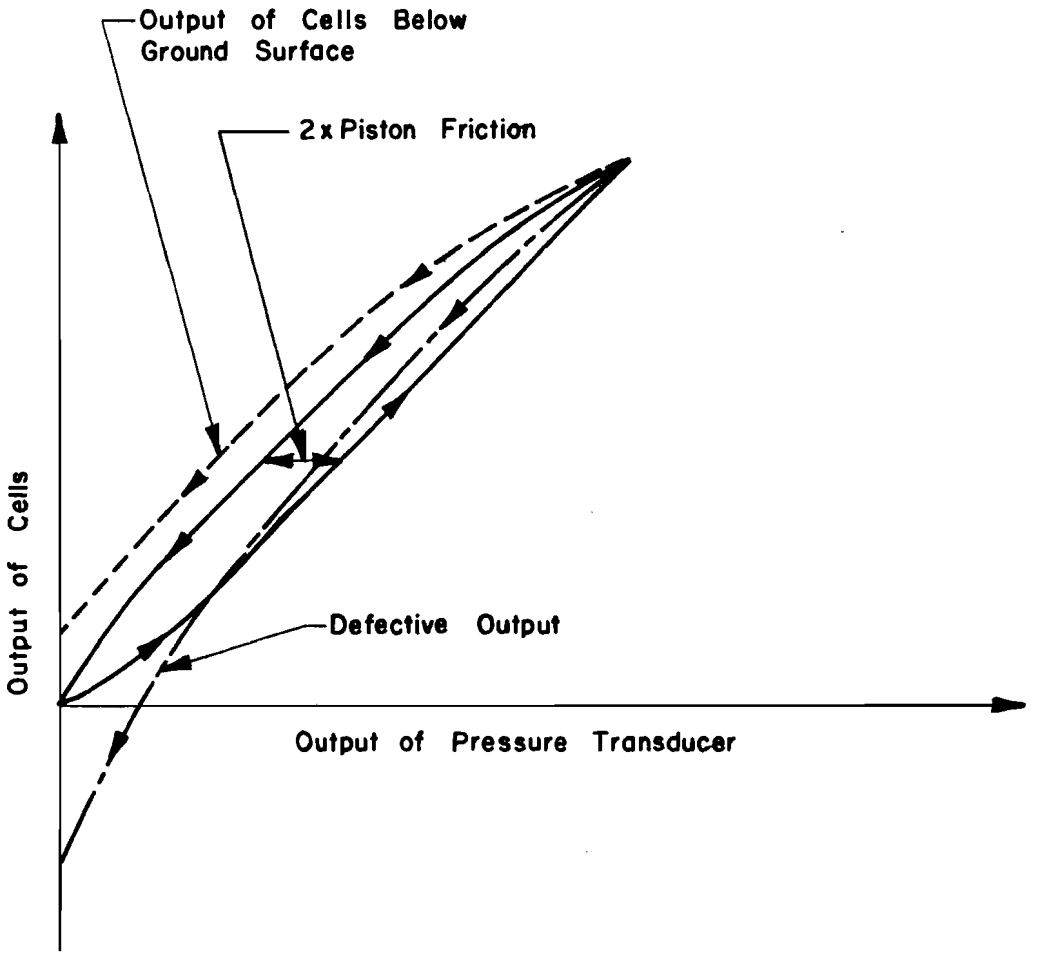

Fig. 6.2 Raw Loading Output from Calibration Cells

the cells reflect a compressive strain on complete unloading, as shown in the dashed line of Fig. 6.2. When a cell is not well embedded in the concrete or when the bonding cement of the strain gages creeps the cells may indicate a locked-in-tension after unloading. The data from such cells are discarded in the analysis.

3. A typical plot of the output of a reliable level of cells below the surface of the ground is presented by the solid line of Fig. 6.3. The slope of the curve increases with the applied load until it becomes a constant when the soil above the level under consideration fails and offers a constant resistance to the downward movement of the shaft. A curvature decrease as shown in the dotted line of Fig. 6.3 indicates that the cells offer no resistance to the load and must, therefore, be moving into a void as would be the case of cells seated in mud pockets.
4. After unloading, compressive stresses are usually locked in a shaft that has been loaded to failure and particularly when a high tip resistance has been reached. Although theoretically possible, tensile stresses are very unlikely to be locked in, and cells recording tension after unloading (dashed-dotted line of Fig. 6.3) usually indicate a poor embedment of the cells or a creep in the bonding cement of the gages.
5. Cells indicating a significantly higher response than the rest of the cells are also discarded as they generally reflect the existence of a reduced section in the shaft or a poorly compacted concrete.

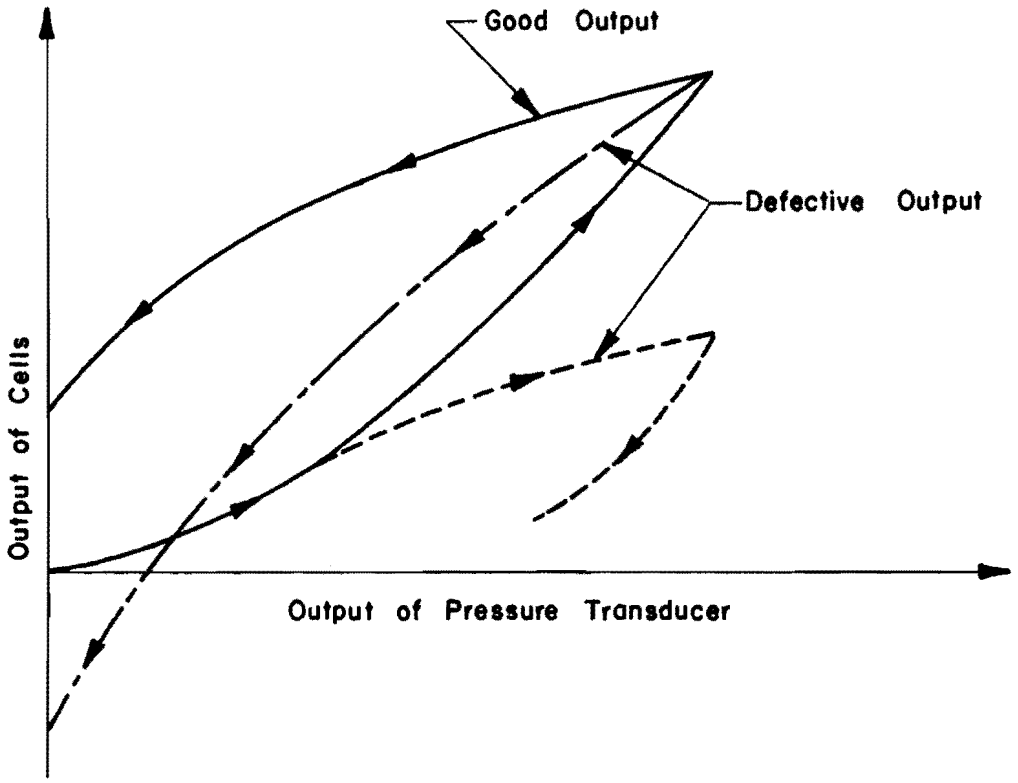

Fig. 6.3 Output of Cells below the Ground Surface as a Function of Load on Shaft

In the analyses, the data were also corrected to take care of changes in the cross section of the shaft wherever these changes were known. In Harris County the exact diameter of the extracted shafts was measured at the levels of the cells. In Live Oak County, the diameter of the shaft was arbitrarily taken as one inch larger than the diameter of the sonotube and, where the hole was observed to slough, the diameter of the shaft was estimated.

NON-LOADING PERFORMANCE OF THE INSTRUMENTATION

Monitoring of the instrumentation after the end of the construction revealed information on the temperature variation and the strains of the concrete during its curing. Immediately after casting, the temperature of the concrete rises due to the setting of the concrete. The temperature drops normally to the temperature of the ambient medium in about two days after the end of construction. The temperature of the concrete in the top ten feet of the shaft oscillates with the normal cycles of the air temperature while the temperature of the concrete at greater depths remains practically constant. This temperature was found to be about 72°F in shafts cast in saturated soil and about 80°F in shafts cast in dry soil.

Figure 6.1 shows a typical non-loading output of the Mustran cells. The cells generally indicated a compression strain which tracked the rise of the temperature of the concrete. The indicated strain of the cells after the dissipation of the setting heat varied with the locations of the cells and with the nature of the soil surrounding the shaft. In general, the cells of the test shafts at Live Oak County indicated a compressive strain while the cells of the test shafts at Harris County indicated a tensile strain.

The compression of the cells associated with the rise of temperature is believed to be due to a thermal incompatibility between the concrete and the cells. The observed behavior of the cells reflects a coefficient of expansion of the concrete smaller than that of the steel. This agrees with results reported by other investigators (York, et al., 1970) when subjecting concrete specimens instrumented with vibrating wire gages to a rise in temperature. The same explanation is offered for the tension indicated by the cells after the dissipation of the setting heat. The coefficient of thermal expansion of the concrete varies with the degree of curing and with the composition of the concrete, and, therefore, the real strains in the concrete cannot be determined from the output of the Mustran cells. In the following paragraphs an attempt is made to estimate the curing strains of the concrete.

The autogenous curing of concrete normally results in a shrinkage between 40 and 100 μ in/in (Troxell and Davis, 1956). Curing in a dry medium may further result in a shrinkage of the order of 1000 μ in/in (Neville, 1963). However, the existence of the reinforcing steel prevents the development of excessive shrinkage strains which are relieved by the cracks in the concrete. Concrete design codes require the design of structures to withstand a concrete shrinkage of about 200 μ in/in (AASHO, 1963). This value is believed to be a maximum for drilled shafts and can only be attained under very unfavorable conditions. On the other hand data reported by Neville (1971) indicate an expansion in concrete specimens cured under water in the order of 100 to 160 μ in/in. However, significant

expansion starts taking place only about three months after casting, and it is believed that during the period of testing, which extended about two months after the casting of the concrete, expansion could not have taken place.

The thermal strain of the concrete starts affecting the stresses on the sides of the shaft from the time the shear strength of the concrete exceeds that of the surrounding soil. The temperature at which the concrete starts shearing the soil is not known. This temperature is believed to be about 100°F for the shafts cast at 90°F. When the temperature finally stabilizes at about 75°F the concrete will have incurred a net drop in temperature of about 25°F. This variation in temperature is associated with strains of the order of 100 to 150 μ in/in.

In summary, it is believed that when the curing and temperature strains are combined at the time of testing of the shafts, a contraction strain in the order of 200 μ in/in may have taken place.

REDUCTION OF THE LOAD TEST DATA

A computer program was written to plot the raw data from the Mustran cells versus the hydraulic pressure in the loading system measured by the pressure transducer. These plots served to eliminate defective cells as discussed above. The data from reliable cells were then reduced using the computer program DARES prepared by Barker and Reese (1970), specifically for the purposes of reducing data from axial loads on instrumented drilled shafts. The program DARES performs mainly the following functions:

1. Obtains for the calibration levels of cells a best fit polynomial relating the load in the shaft to the average output of the cells.
2. Determines the load in the shaft at each level of cells from the output of these cells and the relation obtained in the previous step. A best fit polynomial is then obtained to describe the load distribution along the length of the shaft.
3. Computes the downward movement of specified points along the length of the shaft by subtracting the elastic compression of the shaft from the measured settlement at the ground surface. The elastic compression of the shaft is computed by integrating the load distribution polynomial and using the elastic properties of the concrete.
4. Evaluates the load transfer from the derivative of the load distribution polynomial at the same specified points.

The program has also the capacity of considering variations in the cross section of the shaft and variations in the sensitivity of the cells. The program was further supplemented with routines to plot the load-settlement, load distribution, and load transfer curves.

CALIBRATION CURVES

Each test shaft was equipped with more than one level of Mustran cells above the ground surface to insure a reliable calibration curve for each shaft. Invariably, and for reasons discussed before, many of the calibration levels in each shaft did not function properly and considerable

judgement was exercised in selecting a calibration curve for some of the test shafts. Figure 6.4 presents the calibration curves adopted for the test shafts of this study, and the calibration curve reported by O'Neill and Reese (1970) for similar cells. The difference in the slopes of the curves is mostly due to the difference in the modulus of elasticity of the concrete of the various test shafts. An exact relationship between the modulus of elasticity of the concrete and the output of the cells could not be obtained because of difficulties in obtaining a representative modulus for the concrete of each shaft. The general trend of behavior, however, conforms well with the expected behavior. The lower response of the Live Oak County cells results from the stiffer concrete used at these sites. The output of the calibration cells in the G2 shaft is higher than of the calibration cells of other shafts with concrete of similar stiffness, and no explanation can be offered for this deviation. All the calibration cells at the BB site showed evidence of entrapping mud and were, therefore, discarded. The calibration curve selected for this shaft was arbitrarily chosen as the dashed line shown in Fig. 6.4. It was reasoned that this calibration curve should be slightly steeper than that of the G1 shaft because the BB shaft had concrete of similar stiffness as G1 but was tested at an earlier age. This calibration curve was further found to yield load distribution curves that appeared to be reasonable.

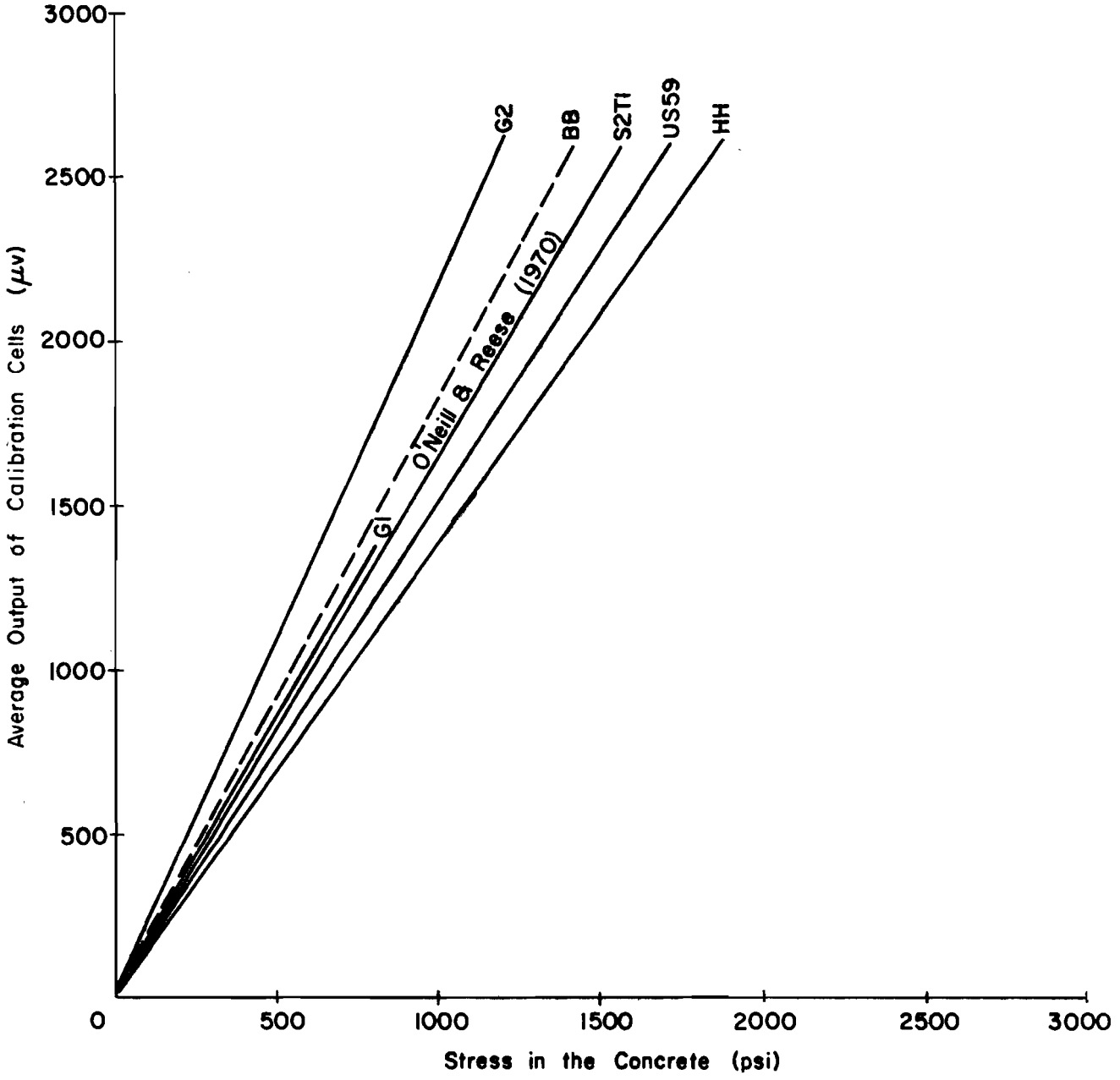

Fig. 6.4 Calibration Curves for the Test Shafts

RESULTS OF LOAD TESTS

The results of the first load test on each shaft are presented in Fig. 6.5 through Fig. 6.24 in the following order:

1. Load distribution curves are shown in Figs. 6.5, 6.9, 6.13, 6.17, and 6.21. The curves present, at selected butt loads, a plot of the load measured by the load cells and the corresponding best-fit curves. It was found in all tests that a polynomial of the fourth or fifth order provides a reasonable representation of the distribution of the load in the shaft. However, anomalies in the behavior of the curves at the top and the bottom of the shaft were observed. In these regions the curves were visually adjusted as shown by the dashed lines on the above mentioned figures. A brief discussion of these anomalies is offered in the following paragraphs.

   The best fit curve represents a statistical average of the load at various levels in the shaft, except at the ground surface, where the curve is forced through a point of known applied load. This imposed boundary condition results in an erroneous evaluation of the load transferred in the top of the shaft between the ground surface and the next level of cells.

   The level of cells at the tips of shafts HH, G1, and BB was destroyed during construction. The analytical best-fit polynomial was, therefore, extrapolated beyond the lowest reliable level of

(Text continued on page 181)

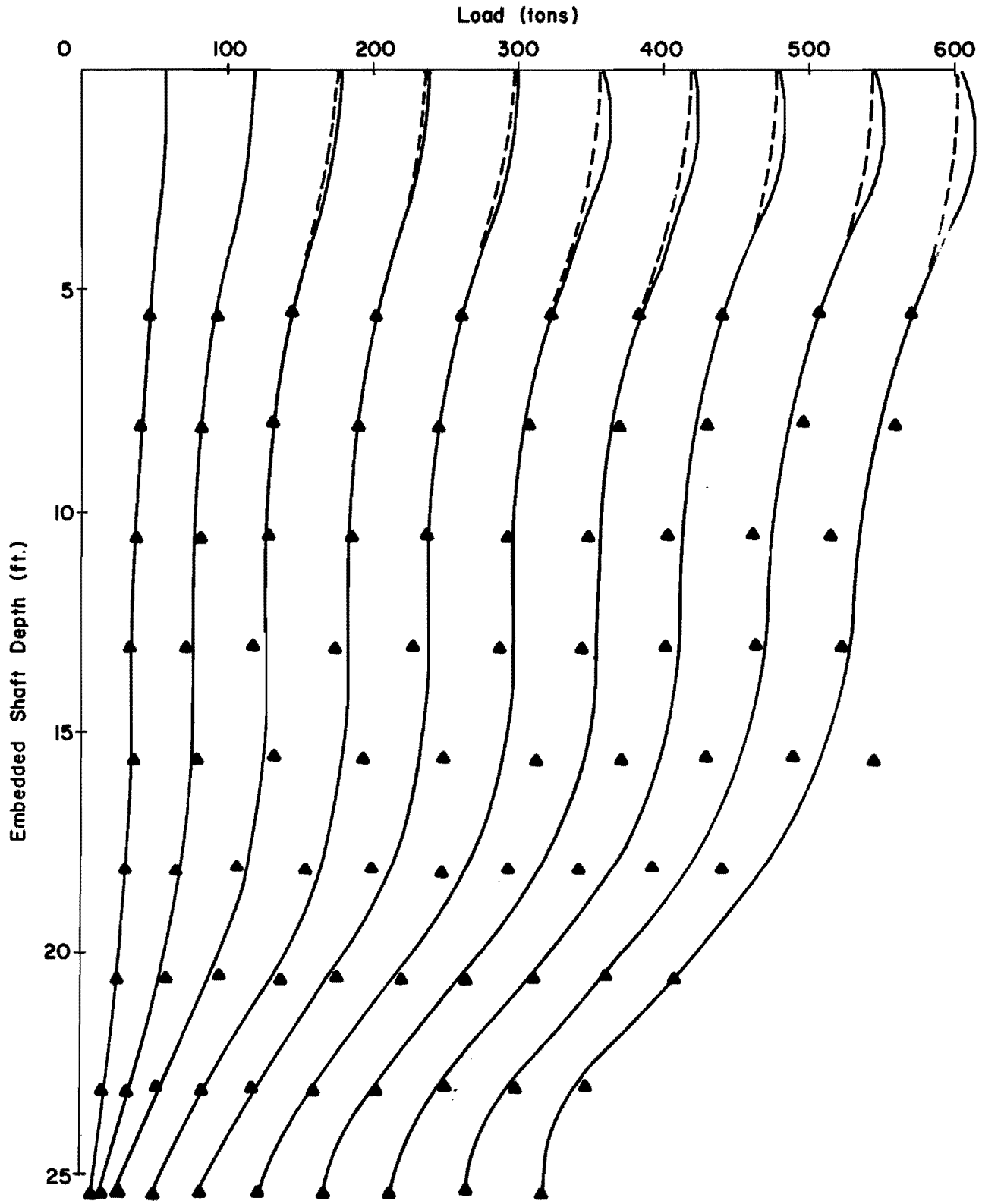

Fig. 6.5 Load Distribution Curves - US59, Test 1

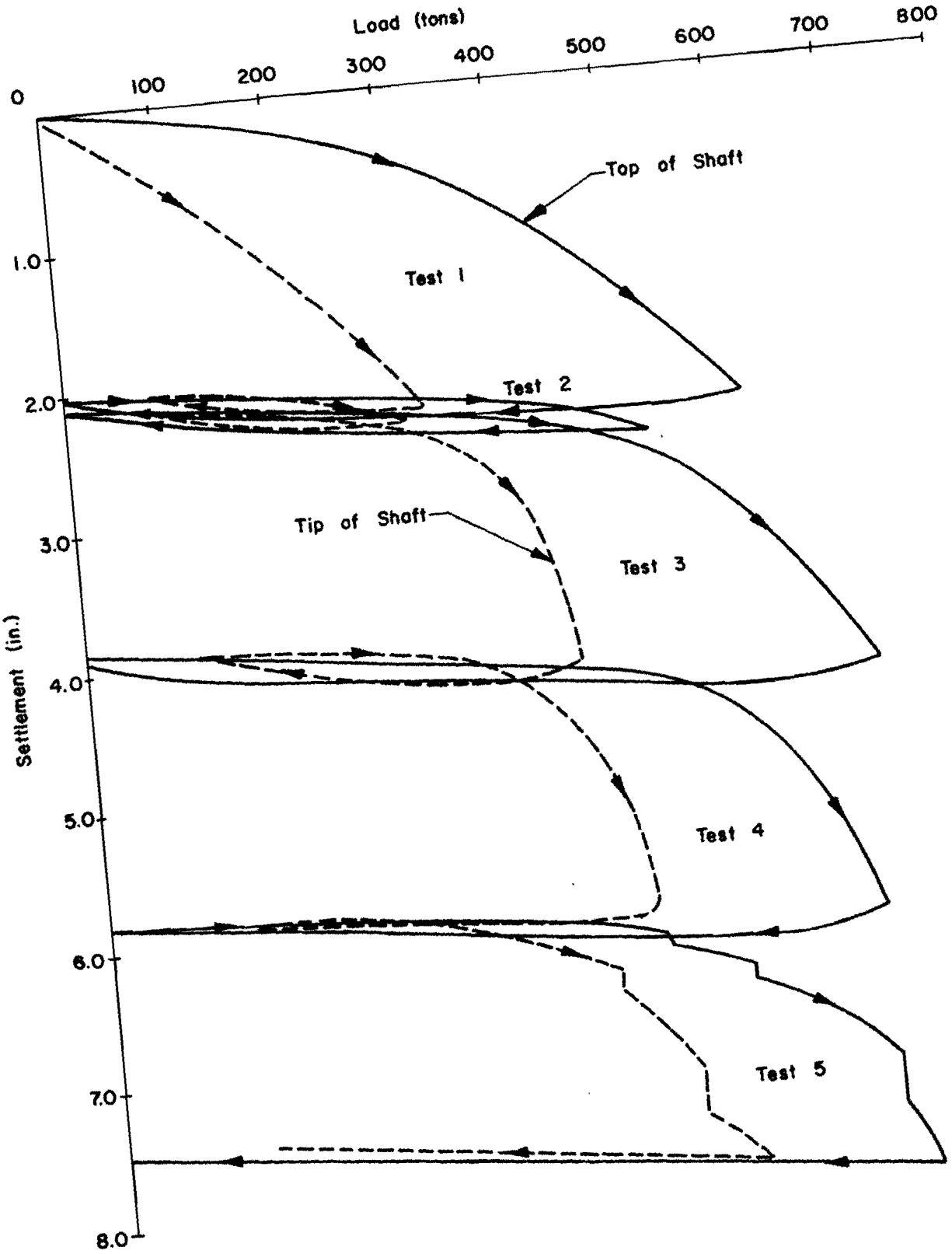

Fig. 6.6 Load-Settlement Curves - US59

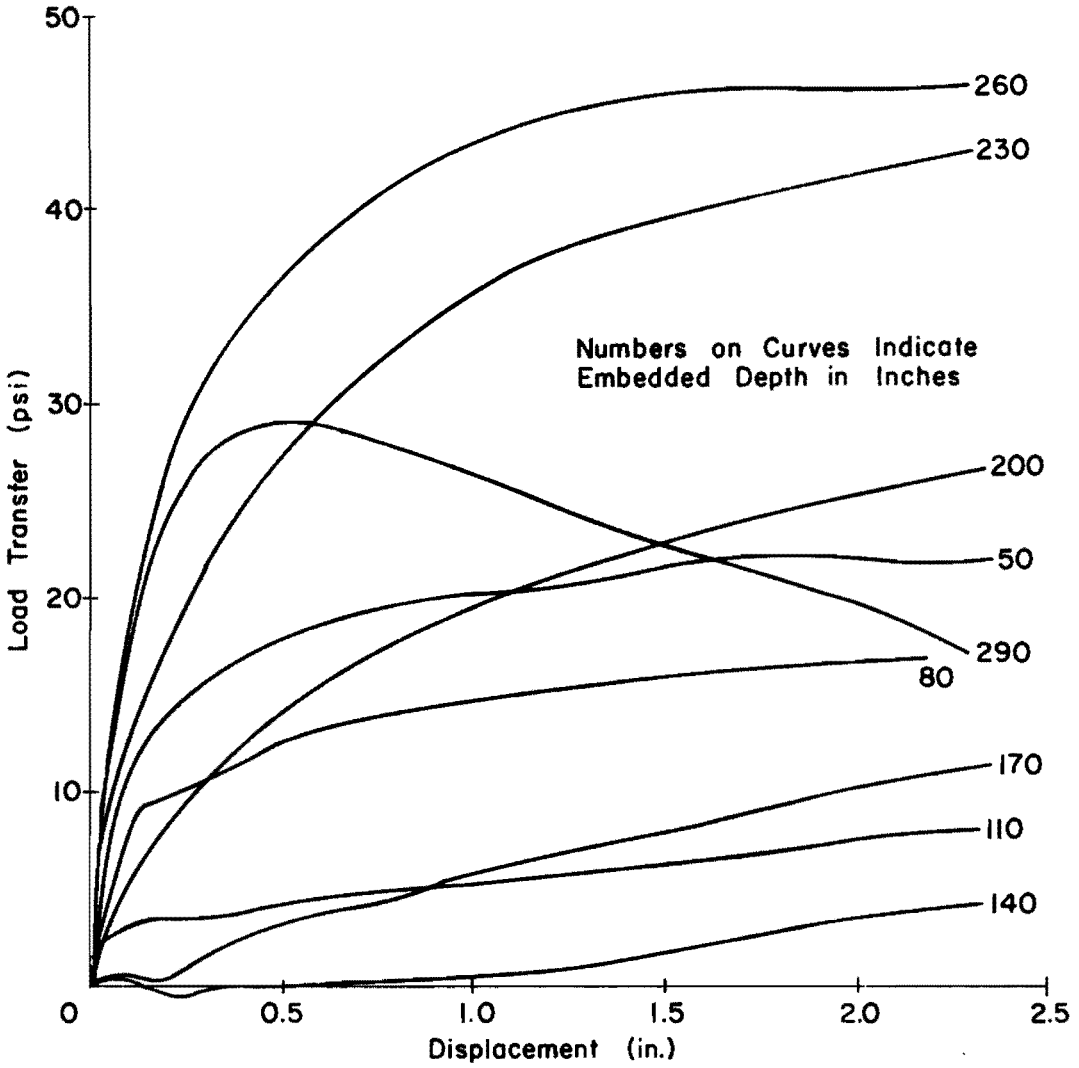

Fig. 6.7 Load Transfer Curves - US59, Test 1

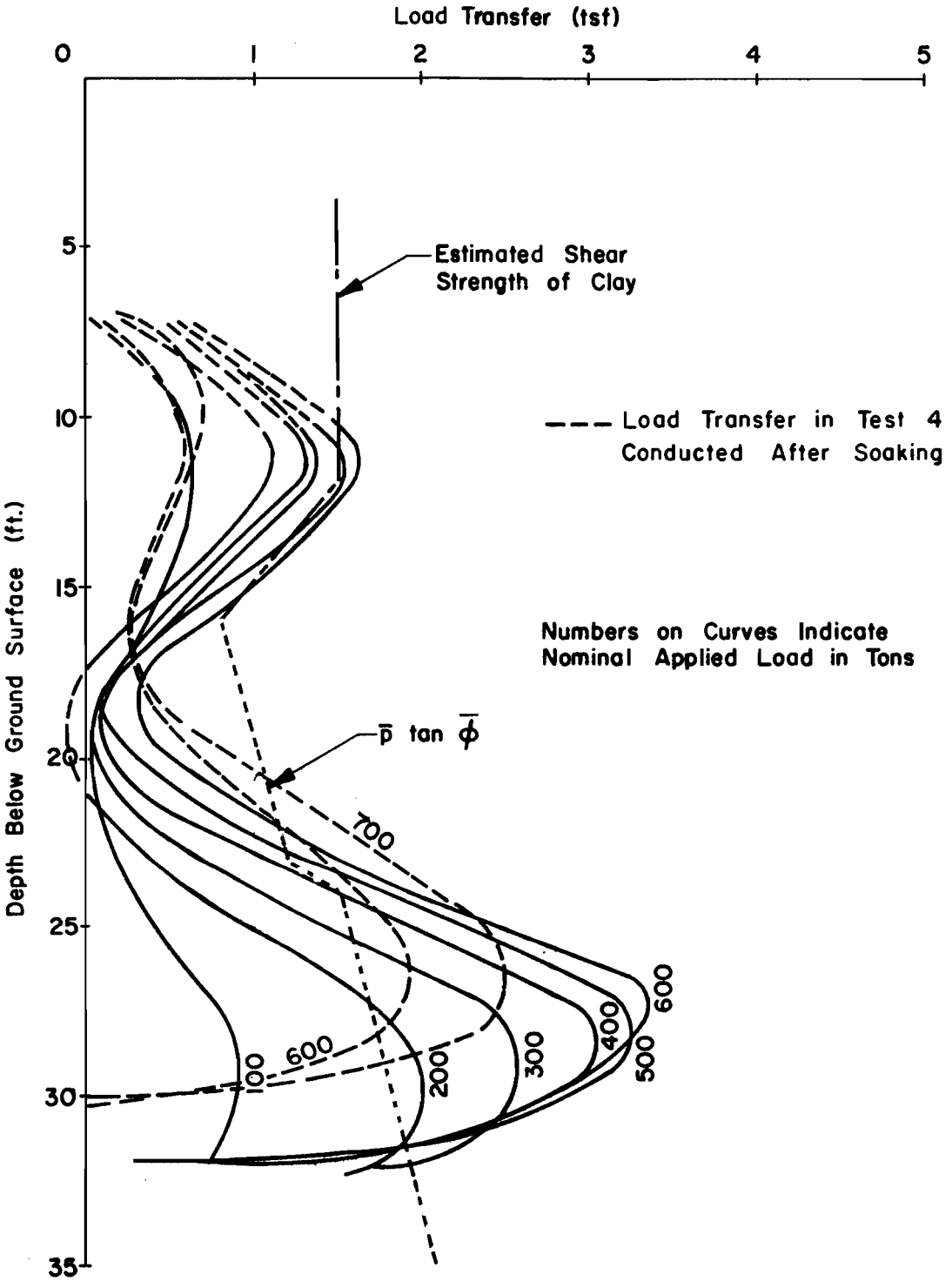

Fig. 6.8 Load Transfer Vs. Depth - US59, Test 1 and Test 4

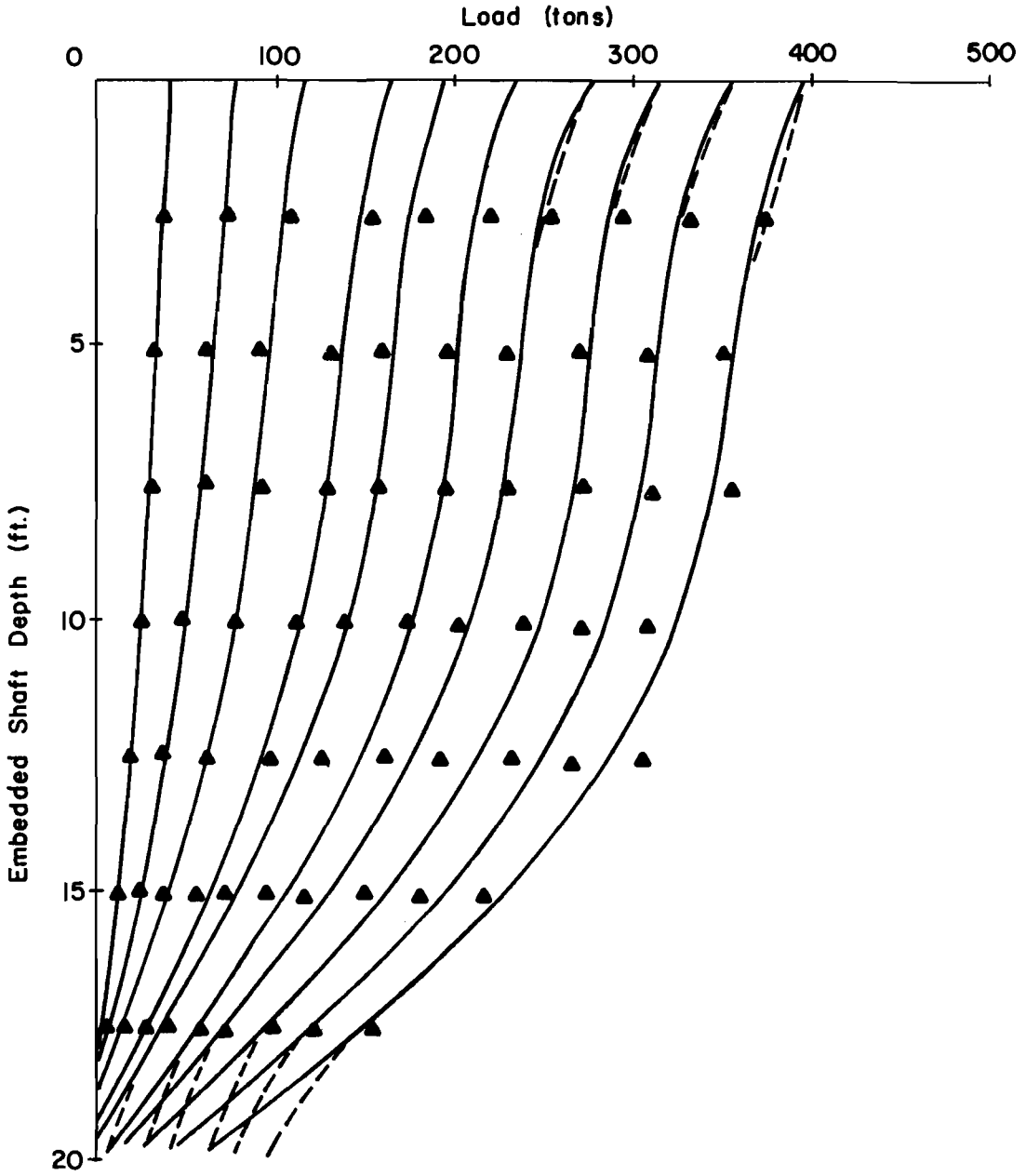

Fig. 6.9 Load Distribution Curves - HH, Test 1

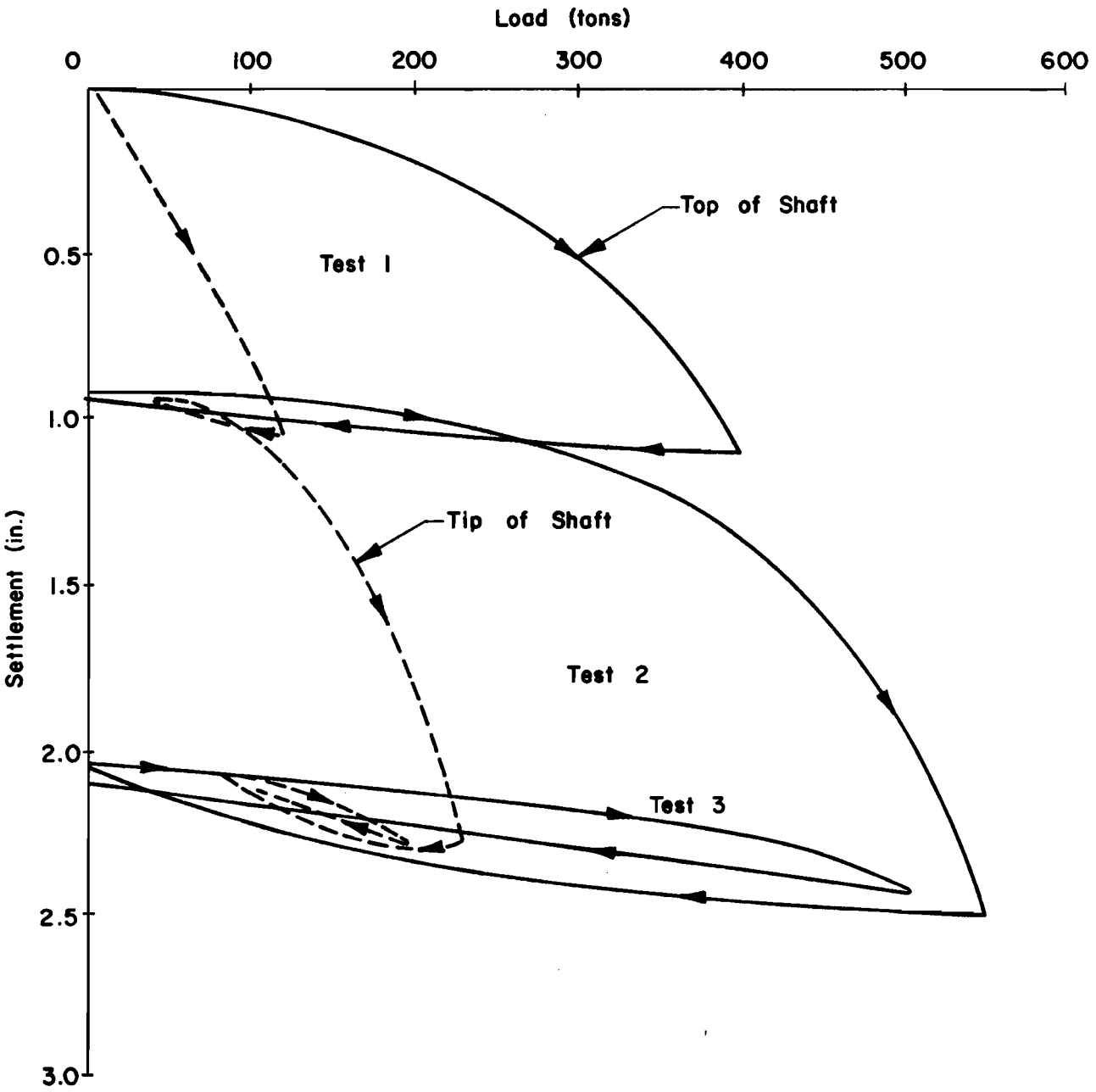

Fig. 6.10 Load-Settlement Curves - HH

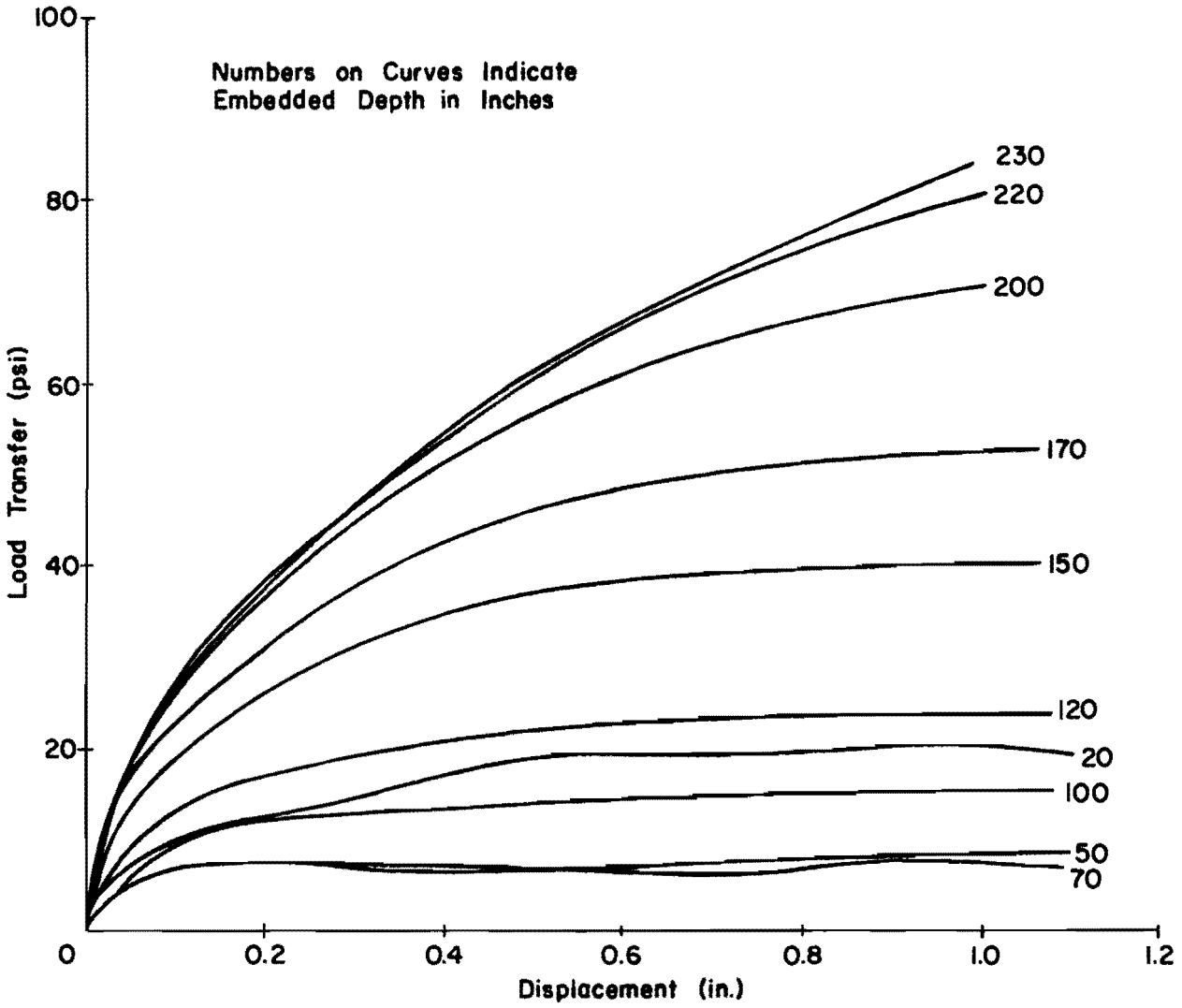

Fig. 6.11 Load Transfer Curves - HH, Test 1

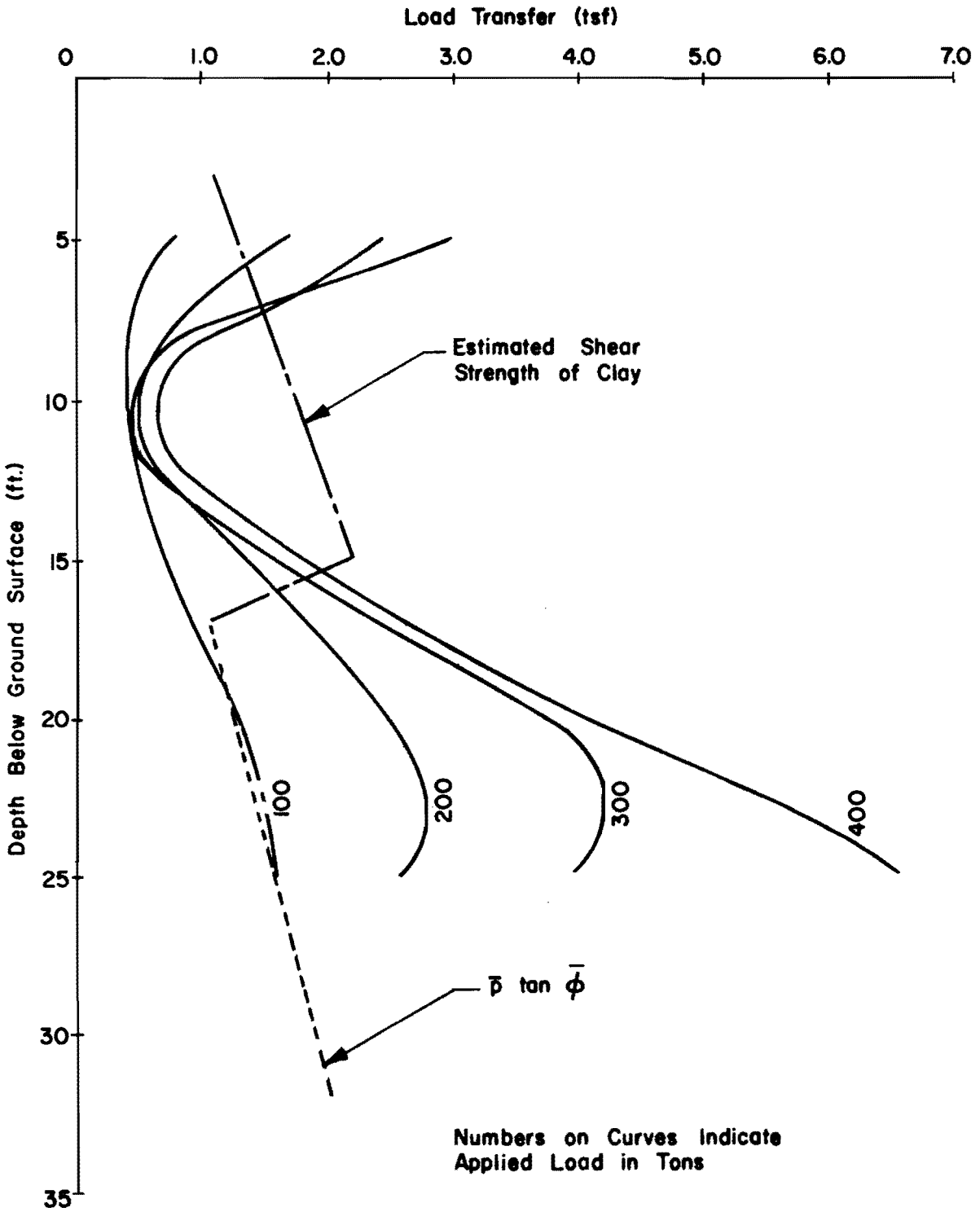

Fig. 6.12 Load Transfer Vs. Depth - HH, Test 1

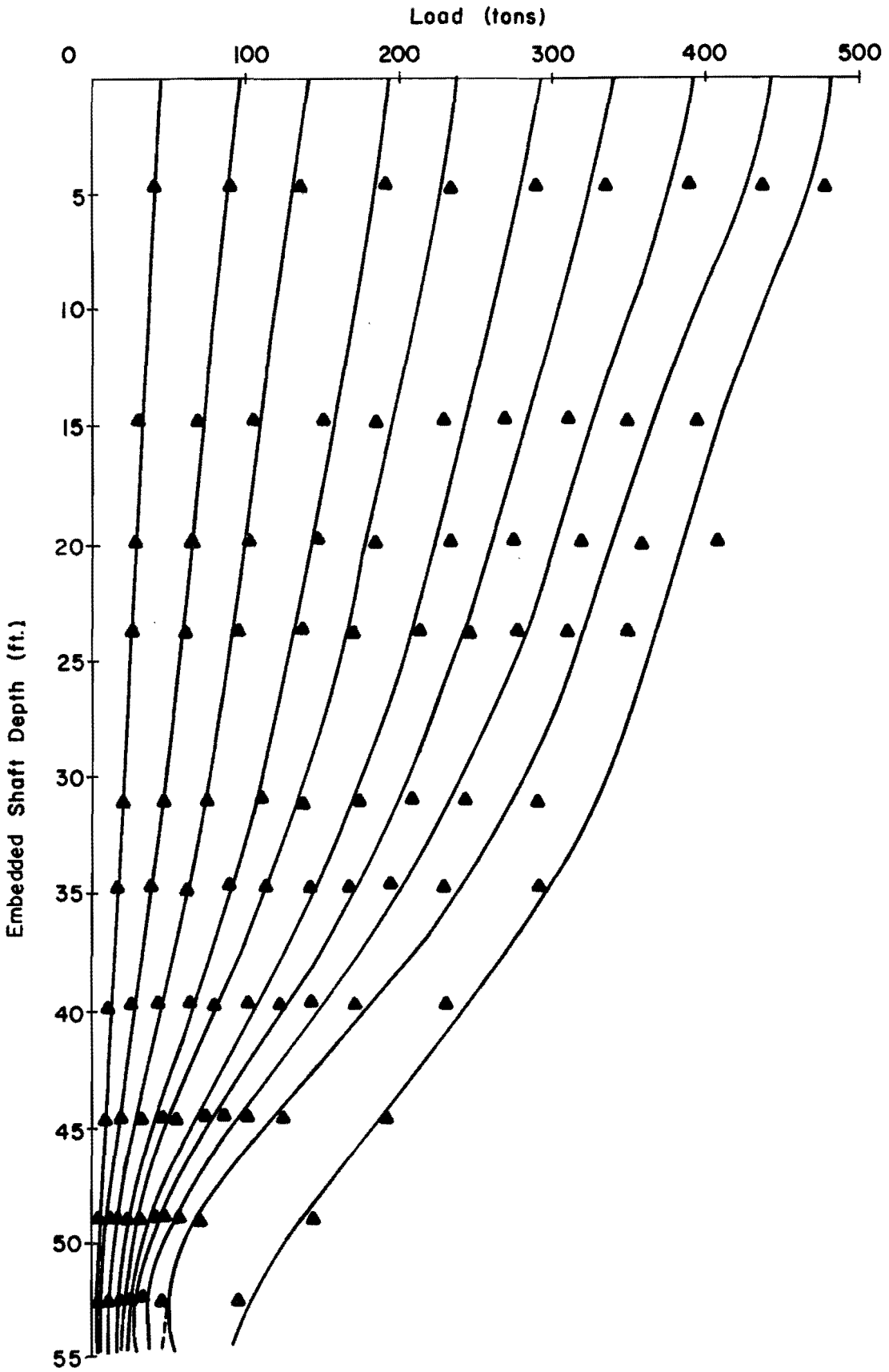

Fig. 6.13 Load Distribution Curves - G1, Test 1

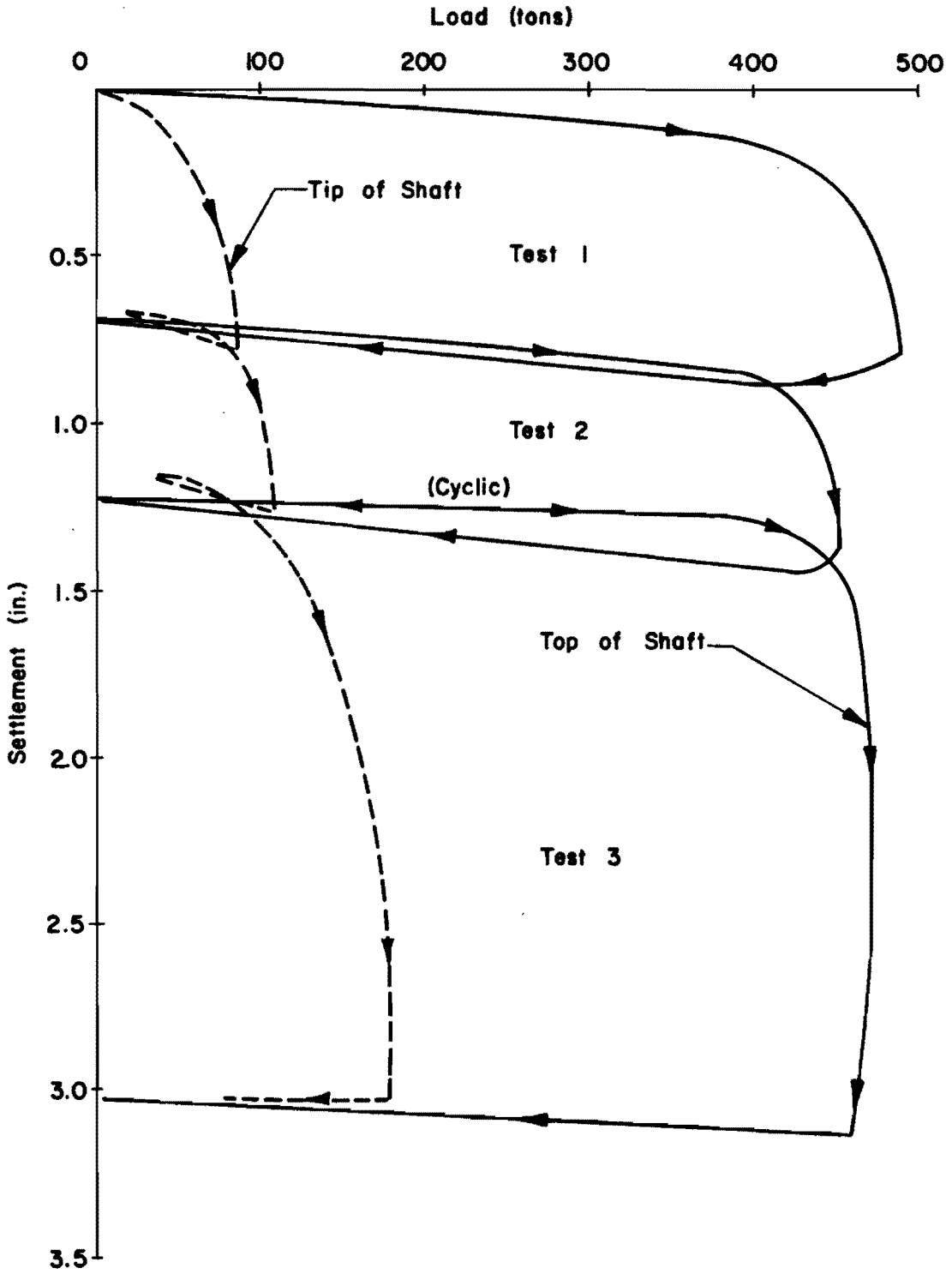

Fig. 6.14 Load-Settlement Curves - G1

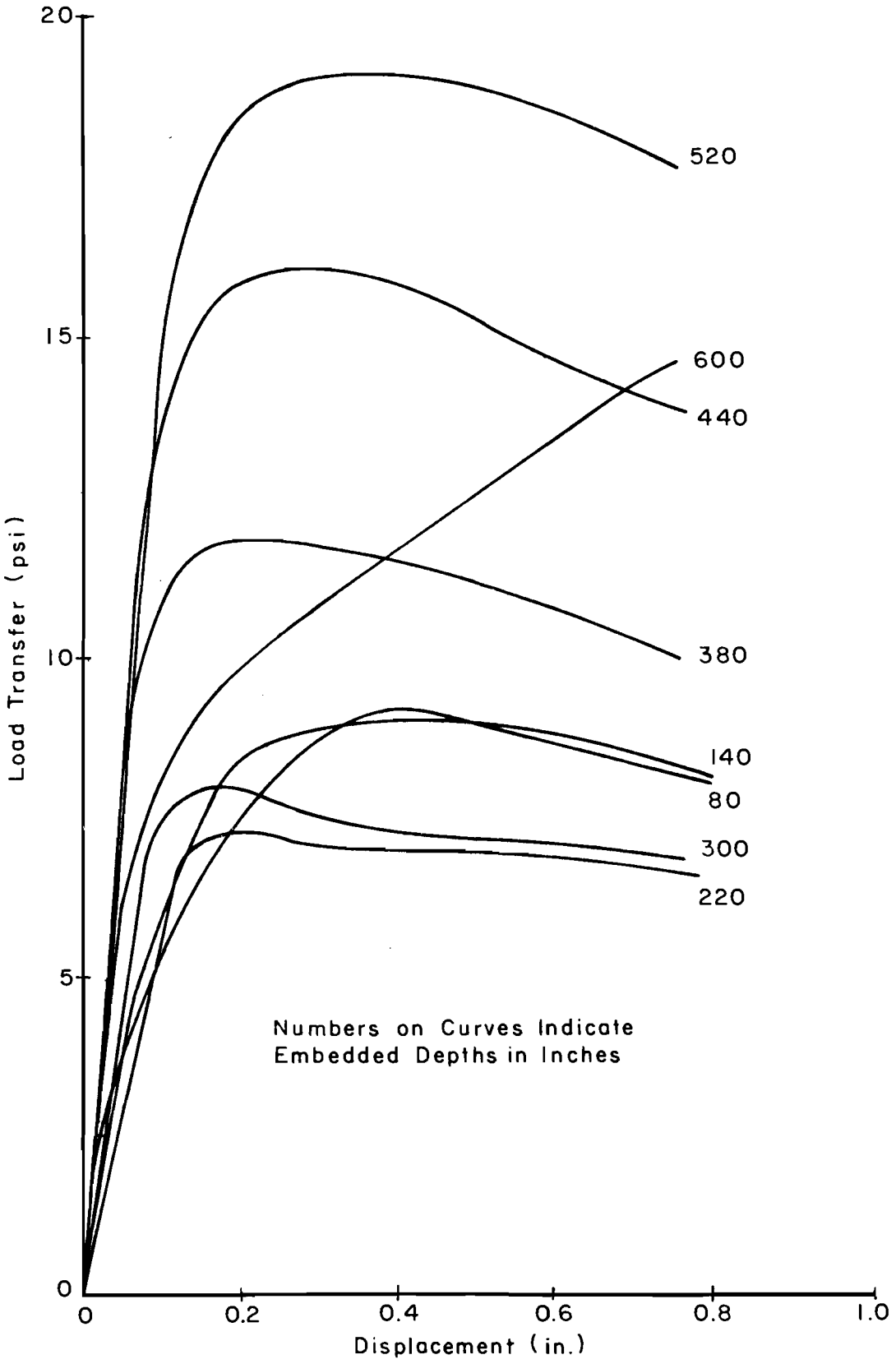

Fig. 6.15 Load Transfer Curves - G1, Test 1

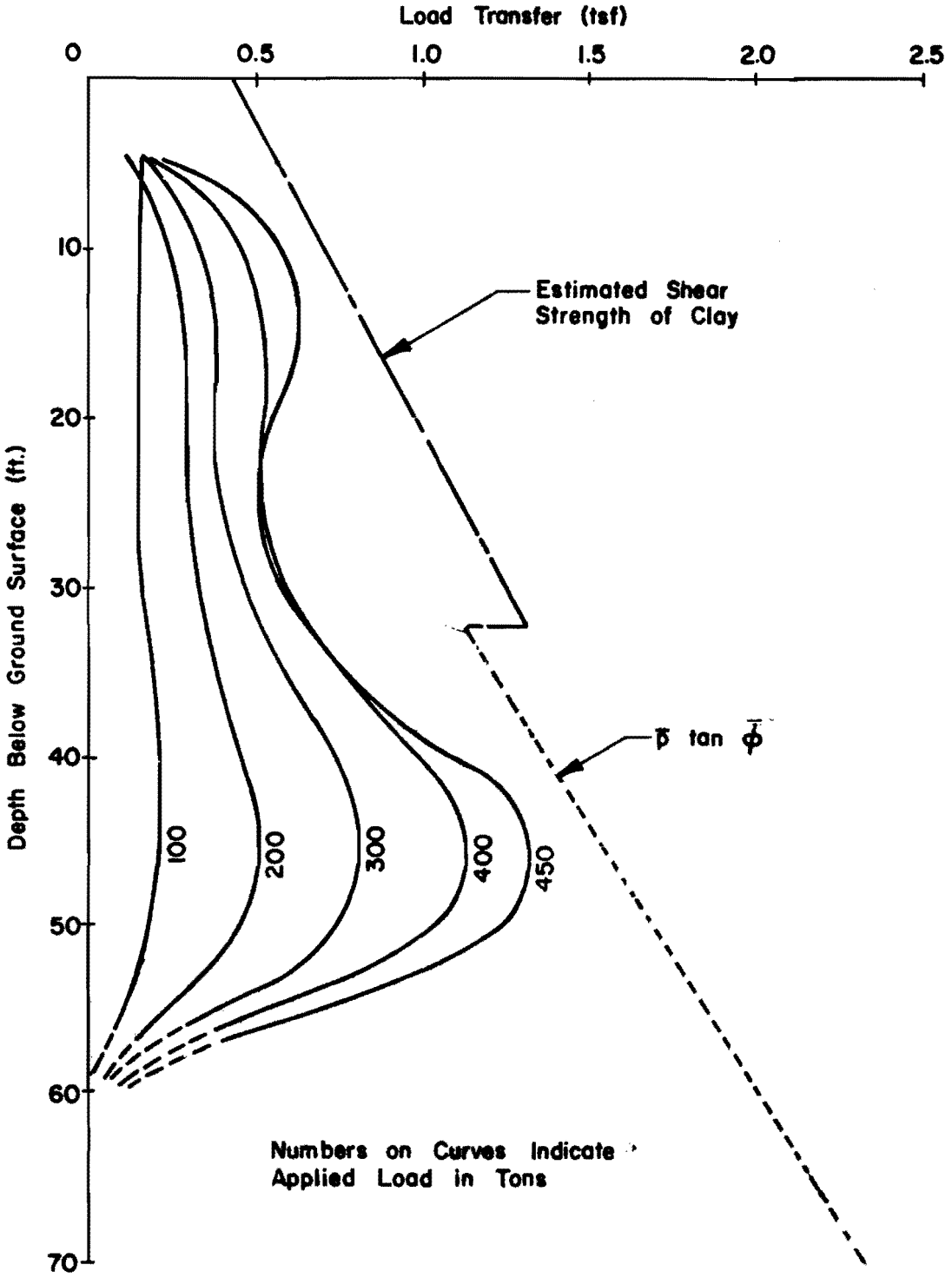

Fig. 6.16 Load Transfer Vs. Depth - G1, Test 1

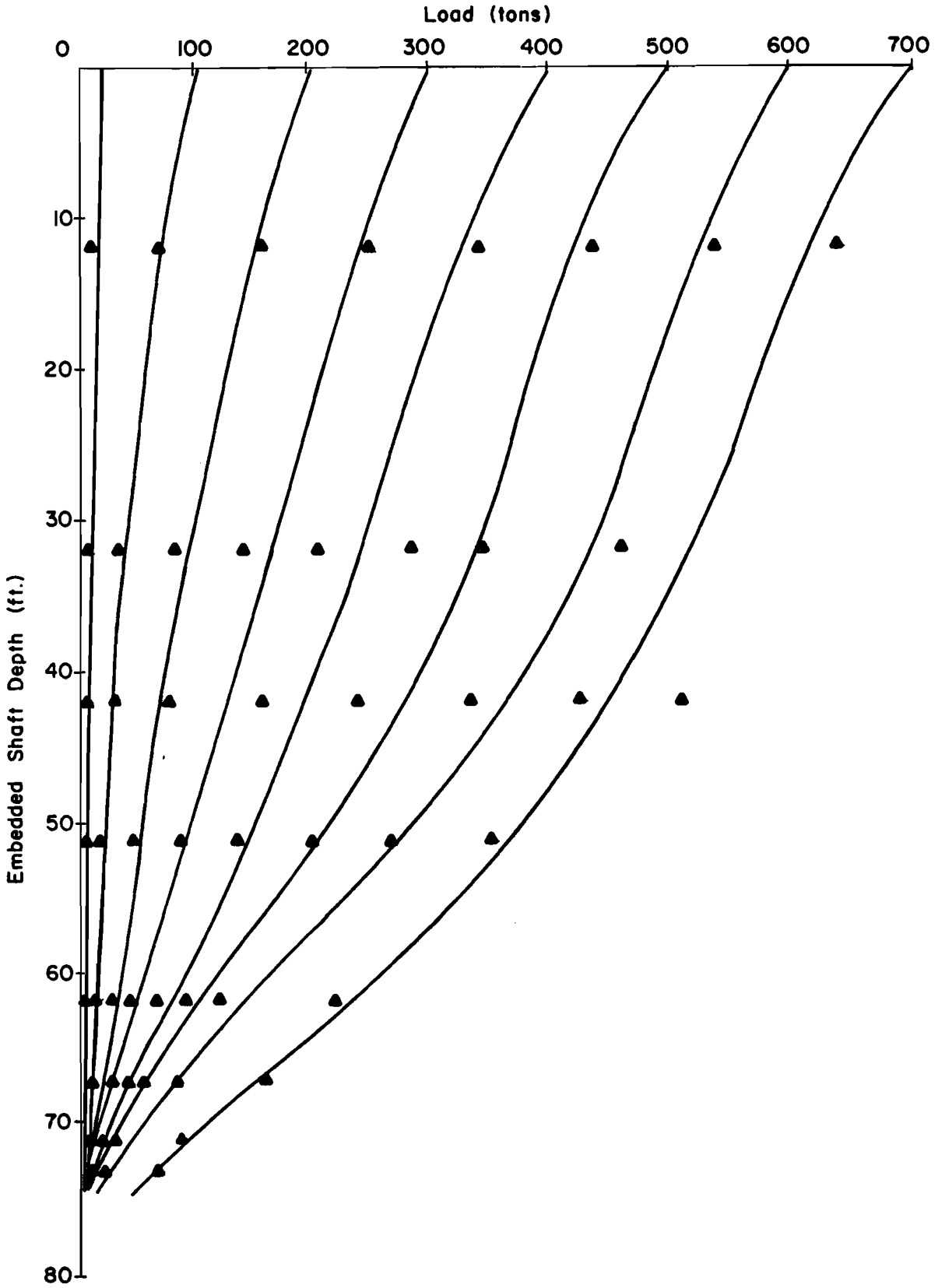

Fig. 6.17 Load Distribution Curves - G2, Test 1

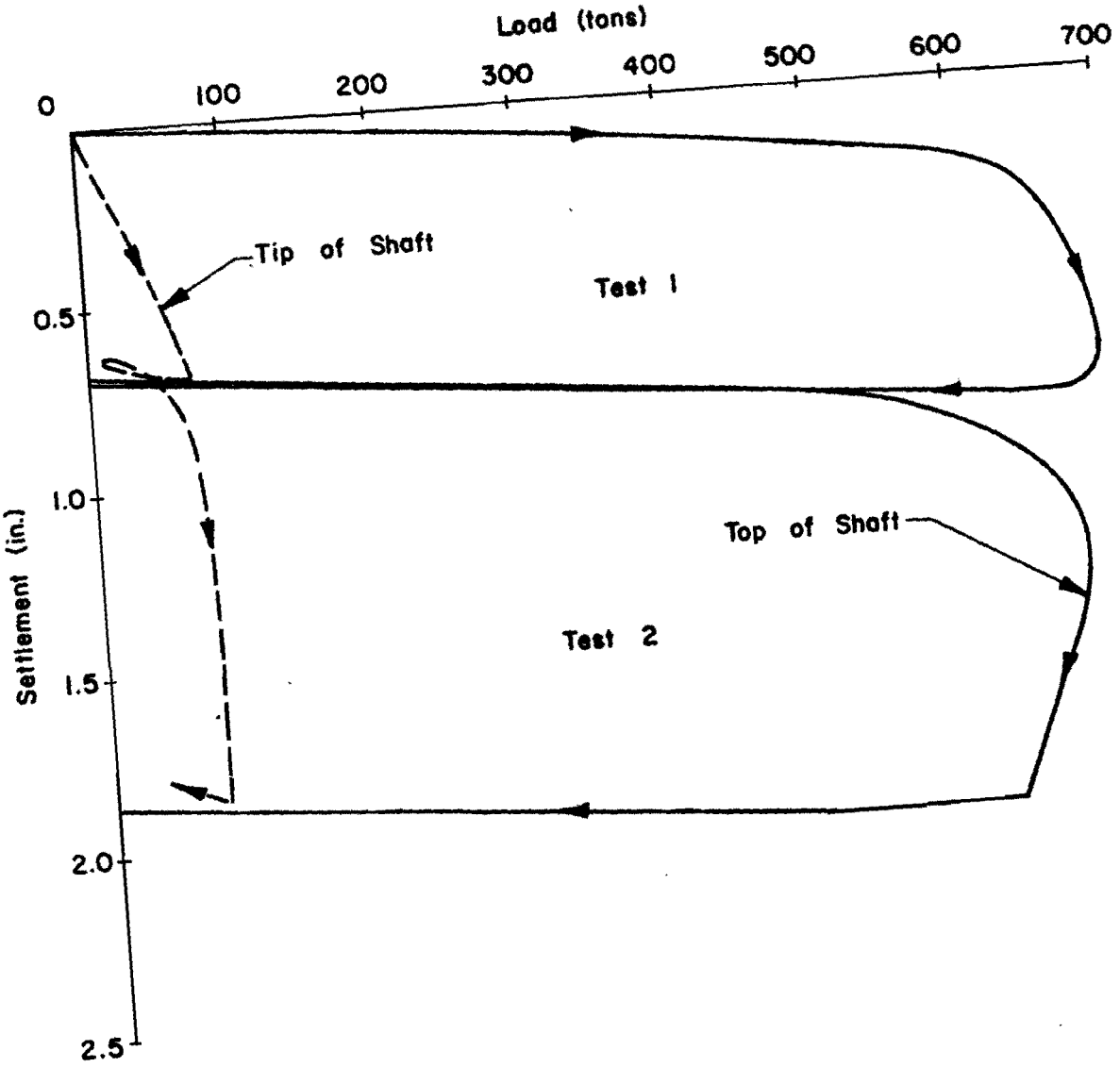

Fig. 6.18 Load-Settlement Curves - G2

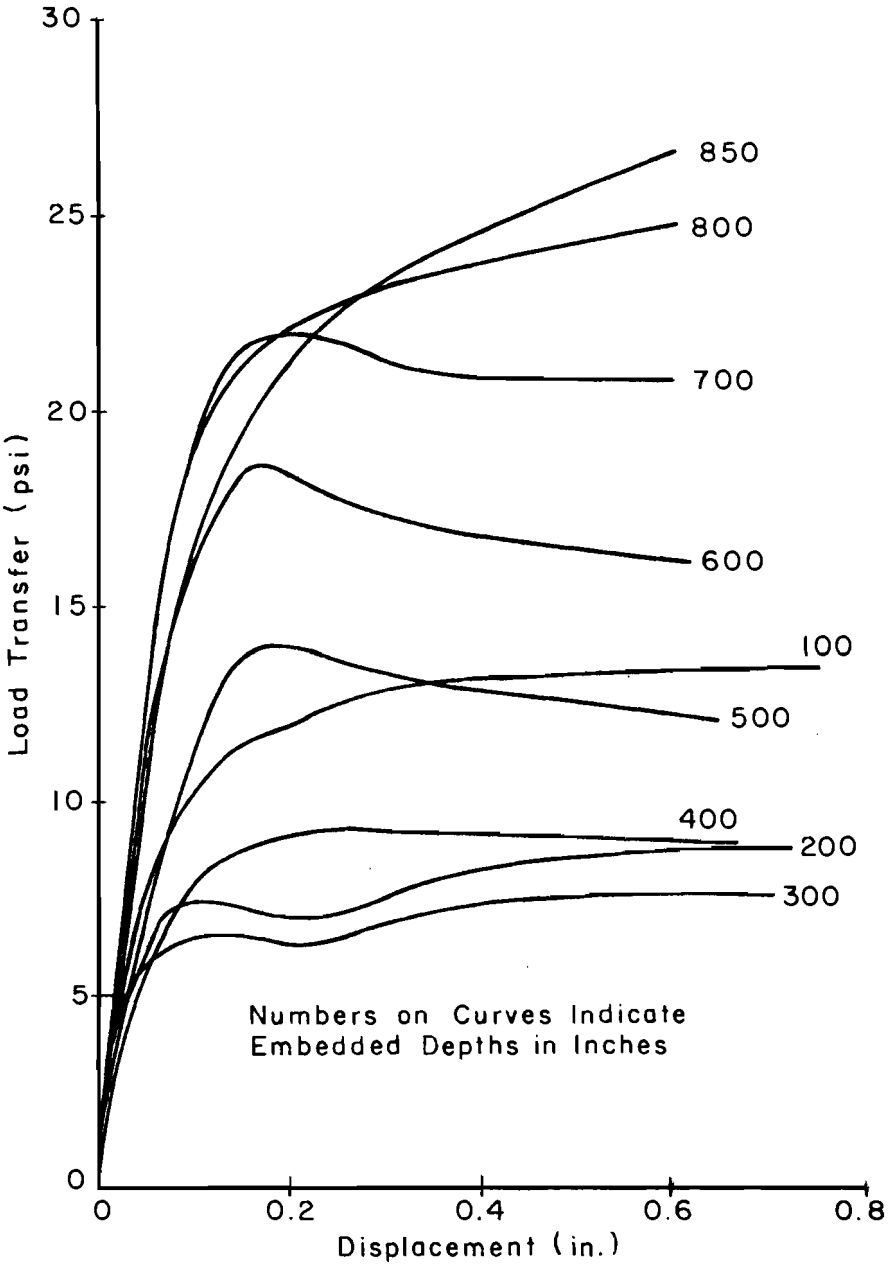

Fig. 6.19 Load Transfer Curves - G2, Test 1

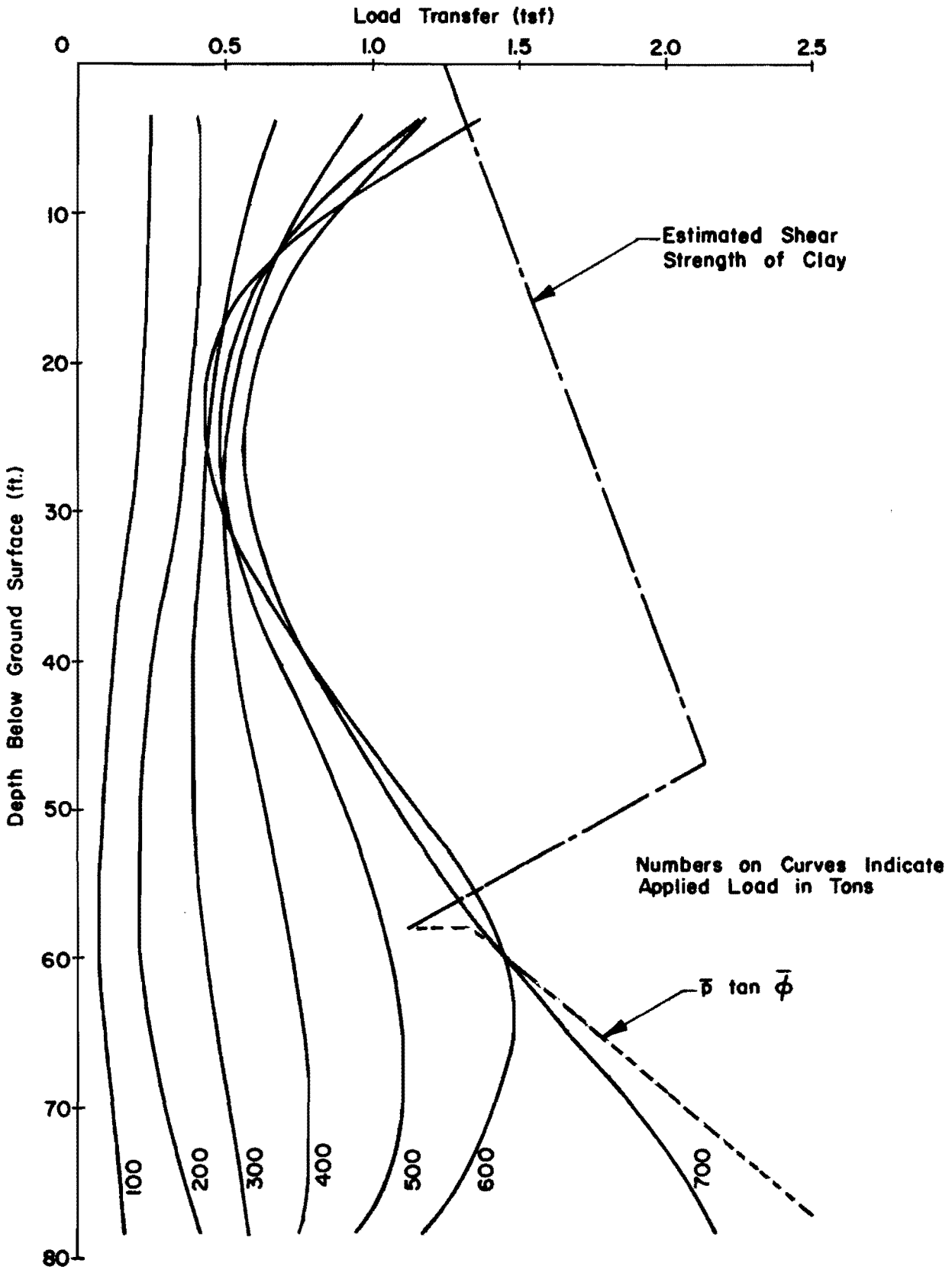

Fig. 6.20 Load Transfer Vs. Depth - G2, Test 1

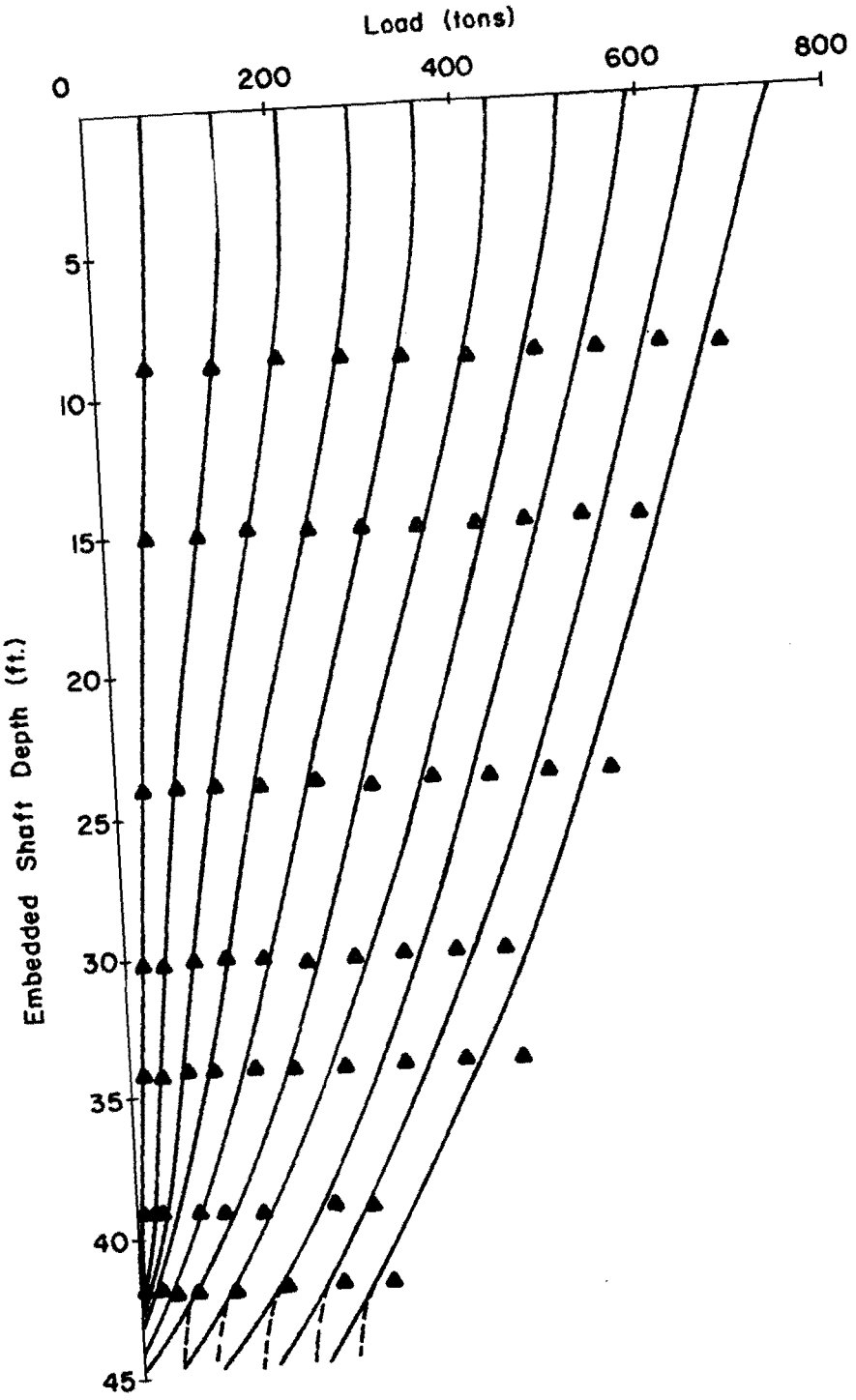

Fig. 6.21 Load Distribution Curves - BB, Test 1

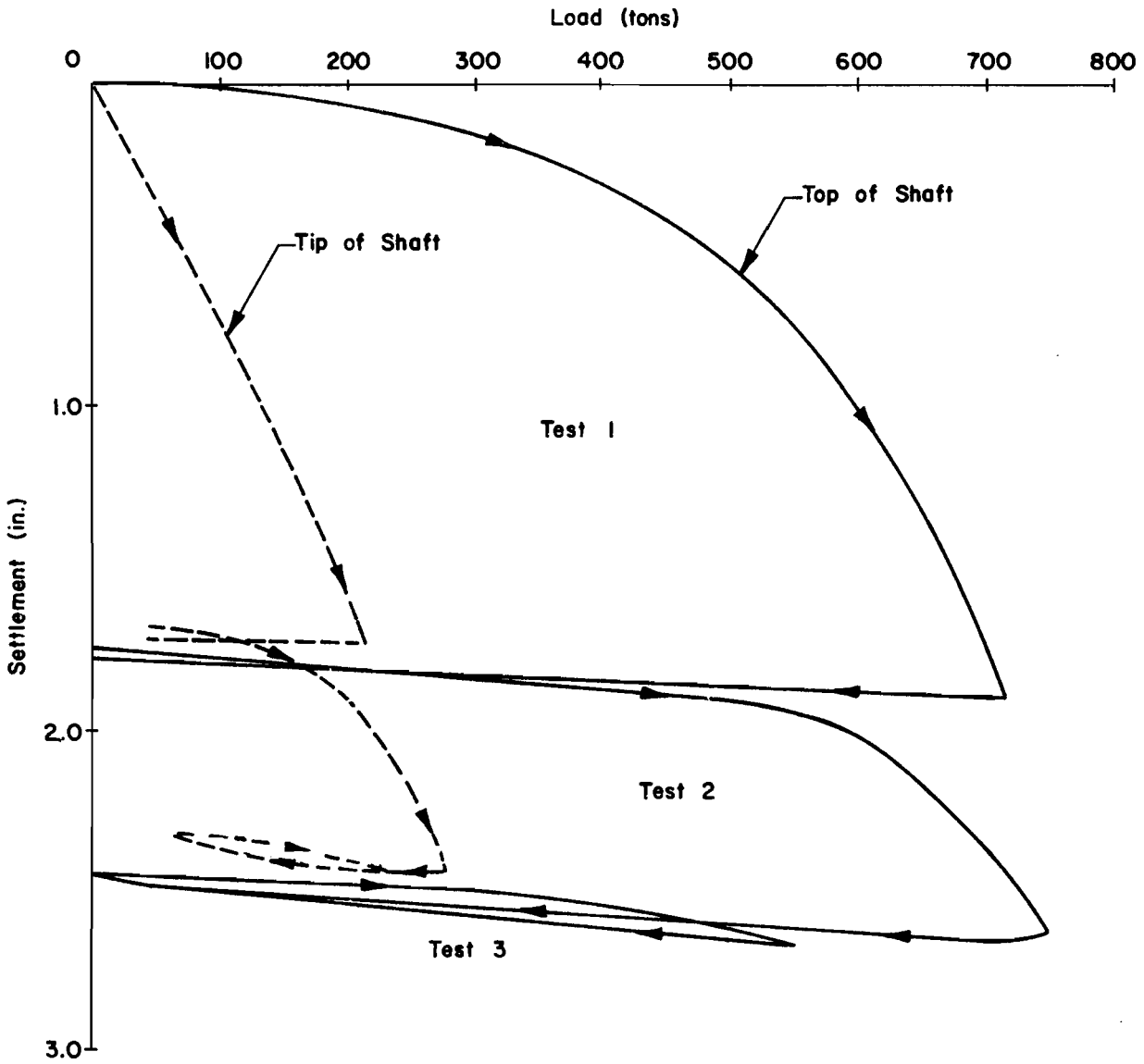

Fig. 6.22 Load-Settlement Curves - BB

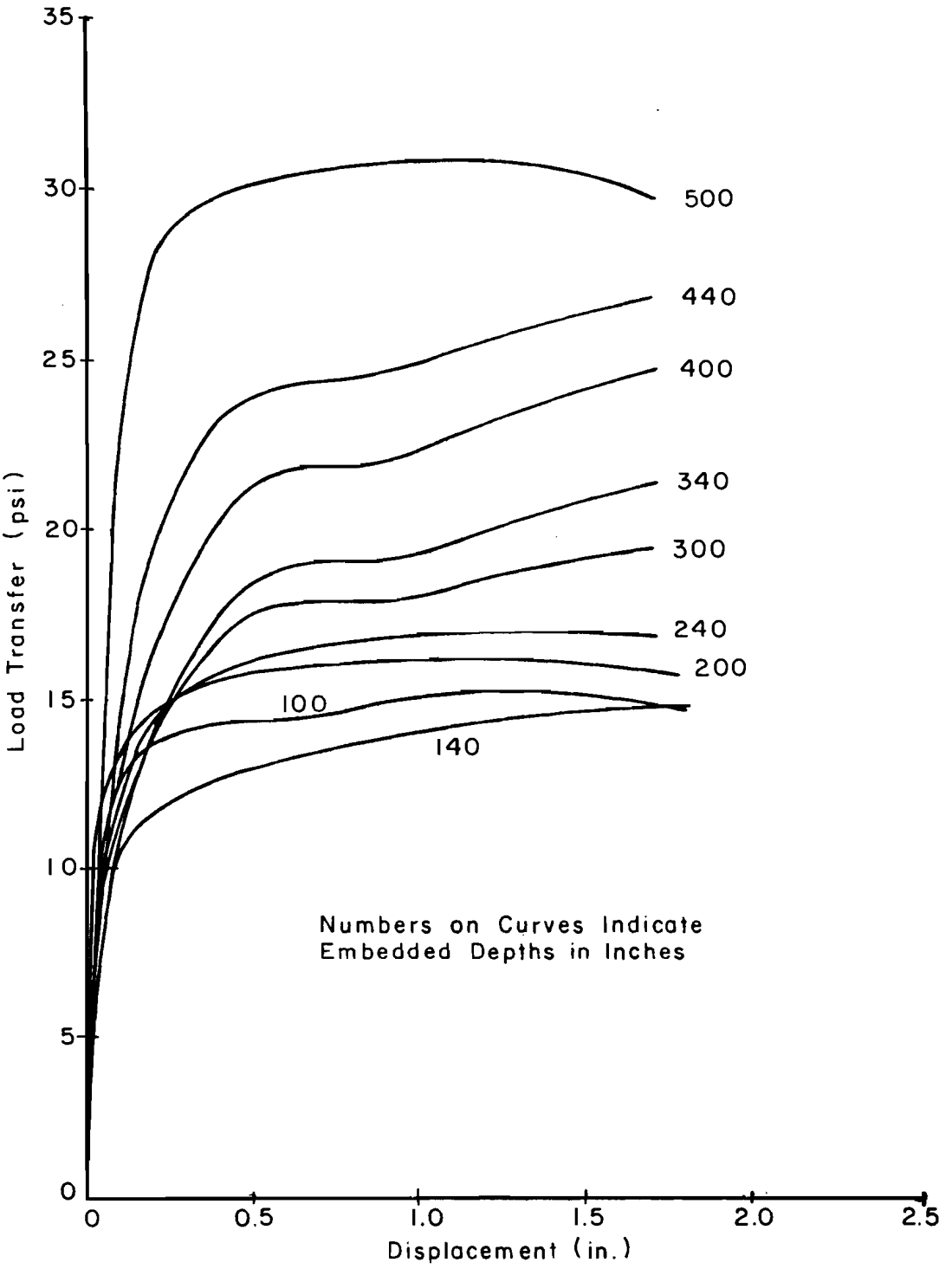

Fig. 6.23 Load Transfer Curves - BB

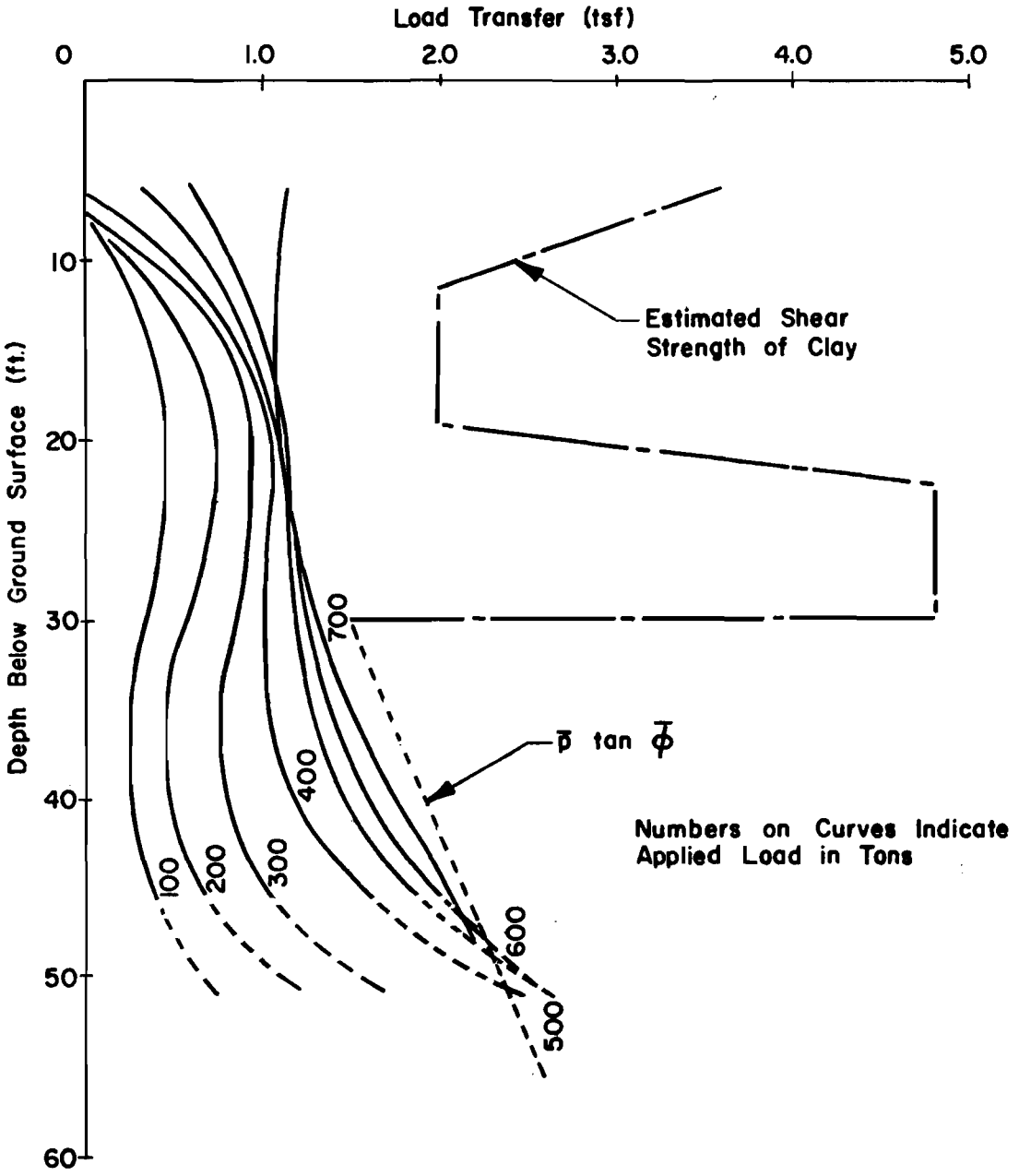

Fig. 6.24 Load Transfer Vs. Depth - BB, Test 1

cells to obtain the load at the tip of the shaft. However, this extrapolation did not reflect in most cases the known interaction between the tip and side resistances of the shaft that was evidenced by the tests on shaft US59 and was reported by Vesić (1970) and O'Neill and Reese (1970). The dashed line adjustments are believed to represent a more probable behavior of the curves near the tip.

2. Load settlement curves for the top and the tip of the shafts are presented in Figs. 6.6, 6.10, 6.14, 6.18, and 6.22. The load settlement curve of the top of the shaft was obtained by direct measurement. For the tip of the shaft, the load was obtained from the load distribution curves discussed above, and the settlement was computed by subtracting the computed elastic compression from the observed settlement of the top of the shaft.
3. Load transfer curves, Figs. 6.7, 6.11, 6.15, 6.19, and 6.23, were obtained at different depths in the shaft by plotting the shear stress developed at a point, obtained by a differentiation of the load distribution curves, versus the displacement of that particular point with respect to its original position. The displacement of a point is computed from knowledge of the butt settlement, the load distribution curve, and the elastic properties of the shaft.
4. Curves plotting the load transfer versus depth at various butt loads are presented in Figs. 6.8, 6.12, 6.16, 6.20, and 6.24. On the same charts are plotted the shear strength profile of the

clay layers as estimated from the soil tests, and the line representing the product $\bar{p}$ tan ϕ, where $\bar{p}$ is the effective overburden pressure.

CHAPTER VII. INTERPRETATION OF RESULTS

The problem of the bearing capacity of drilled shafts in sand depends on a large number of variables which were not separately controlled in this testing program. The results presented in the previous chapter reflect the interference of these different variables in their random occurrence. The approach followed in interpreting the data will consist first of identifying the common findings of all the tests followed by an explanation of the peculiar behavior of the different shafts.

TIP RESISTANCE

The instrumentation allowed a direct measurement of the tip resistance of shafts US59 and G2. On the other shafts, only a reasonable estimate of the tip resistance was possible. Figure 7.1 presents plots of the tip pressure for all the shafts versus the relative settlement of the tip, which is defined as the ratio of the settlement of the tip to the diameter of the shaft. Also plotted on Fig. 7.1 are the results of tests conducted on piles installed in cased boreholes and reported by Koizumi, et al. (1971).

As may be seen from the examination of Fig. 7.1, considerable displacement is required to mobilize a significant tip resistance of drilled shafts installed in sand.

On the average, the curves obtained for very dense sand tend to behave fairly linearly to a pressure of about 40 tsf. Beyond that pressure, the curves become nonlinear and diverge in an undefined manner.

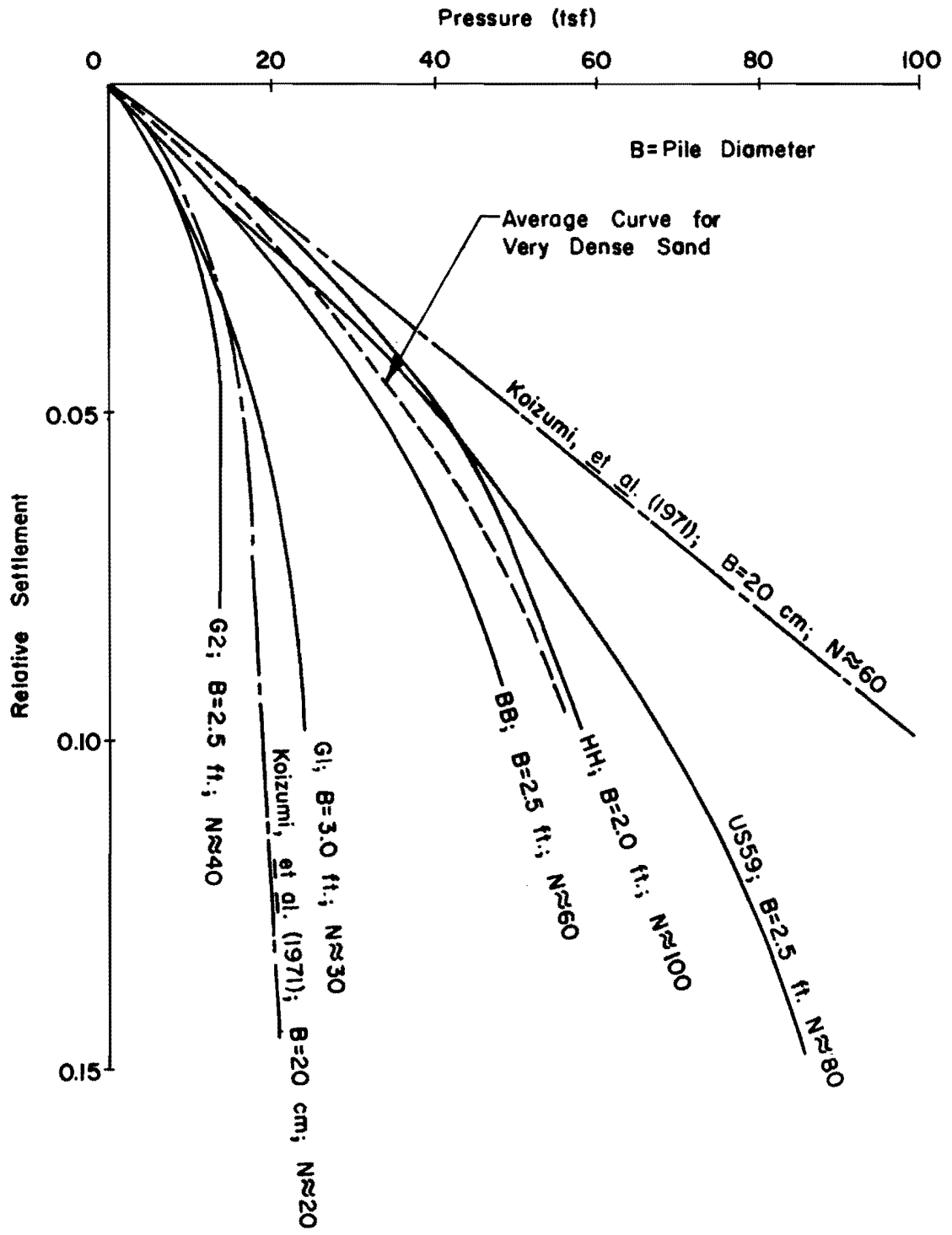

Fig. 7.1 Pressure Vs. Relative Settlement for the Tip of the Test Shafts

The nonlinearity of the curves is probably due to the excessive compression and crushing of the sand grains at high stresses. The divergence of the curves is believed to be due to the influence of the gradation of the sand on the stress-strain properties of sand at very high stresses. The sands tested in this study were of a relatively uniform gradation whereas the sand tested by Koizumi was a well graded sand. Well graded sands compress less than sands of uniform gradation and, therefore, can resist higher pressures.

The divergence may also have to do with the size of the shaft. There are indications that arching effects are more significant in large diameter drilled shafts.

Shaft G1 was presumably tipping in sand of medium density. Later, observations made on the extracted shaft revealed the existence of lumps of soft soil trapped at the tip of the shaft, which left doubts about the measurements of the tip resistance of that shaft. However, measurements made in medium dense sands by Koizumi, et al. (1971) indicate values in the same order as those measured in shaft G1. These curves are, therefore, believed to be an indication of the behavior of the tip resistance of drilled shafts in sand of medium density.

No measurements were made in loose sands. It is, however, believed that loose sands can offer only a very small tip resistance.

The failure load is not easily defined on curves such as those presented in Fig. 7.1. A rational approach consists of defining failure at the maximum settlement tolerated by the structure. This settlement depends on the nature and the stiffness of the structure envisaged. For

purposes of design, it is, therefore, desirable to define the load-settlement curve of the shaft for a wide range of settlement. The load tests in this study were carried only to a settlement of about 10% of the diameter of the shaft. The linear portion of tip pressure-settlement curves ends at a relative settlement of about 0.05, which for drilled shafts of a usual diameter of 30 in. corresponds to a settlement of 1.5 in. It is believed that this settlement is greater than most structures can tolerate and, therefore, a study of the behavior of the curve beyond this range is not of immediate importance.

There are very few field measurements reported in the literature on the tip resistance of bored piles. Vesić (1970) summarized the results of laboratory model tests on buried piles and the results of other tests reported in the literature. His summary indicates that the ultimate tip pressure of deep foundations may vary from over 100 tsf for very dense sands to about 5 to 10 tsf for sands of medium density. Measurements made in this study indicate smaller ultimate resistance for the very dense sands. There are indications from the results of this study that sands of medium density can resist slightly higher pressures than those indicated by Vesić.

SIDE RESISTANCE

The following sections discuss separately the side resistance developed in both the clay and the sand formations.

Side Resistance in Clay

The clay formations at the test sites were heterogeneous and were interbedded with many layers of silt. An evaluation of the load transfer in each independent layer was not possible. An average load transfer in the total thickness of the clay layers could, however, be computed fairly accurately.

The average load transfer in clay is conventionally expressed as a fraction, α_{avg}, of the average shear strength of the clay formation. Figure 7.2 presents plots of the values of α_{avg} versus the average displacement of the shaft. On these plots it is observed that the peak load transfer in clay occurs at displacements of the order of 0.25 inch and that for the stiff clays of sites US59, HH, and G1, as well as the stiff clay 1 of site G2, the peak α_{avg} assumes values between 0.5 and 0.6. These observations are in general agreement with the findings of previous research (Whitaker and Cook, 1966; O'Neill and Reese, 1970). A higher α_{avg} value is exhibited, however, by the slightly overconsolidated clay 2 layer at the G2 site which has an overconsolidation ratio of about two. It is believed that the effects of remolding and softening during the construction of drilled shafts are significantly reduced in slightly overconsolidated clays.

The peak α_{avg} value is much smaller for the hard clays of the BB site where failure is believed to have taken place at the interface between the concrete and the soil. It is thought that, when the slurry displacement method is used, the shear transfer in hard clays is limited

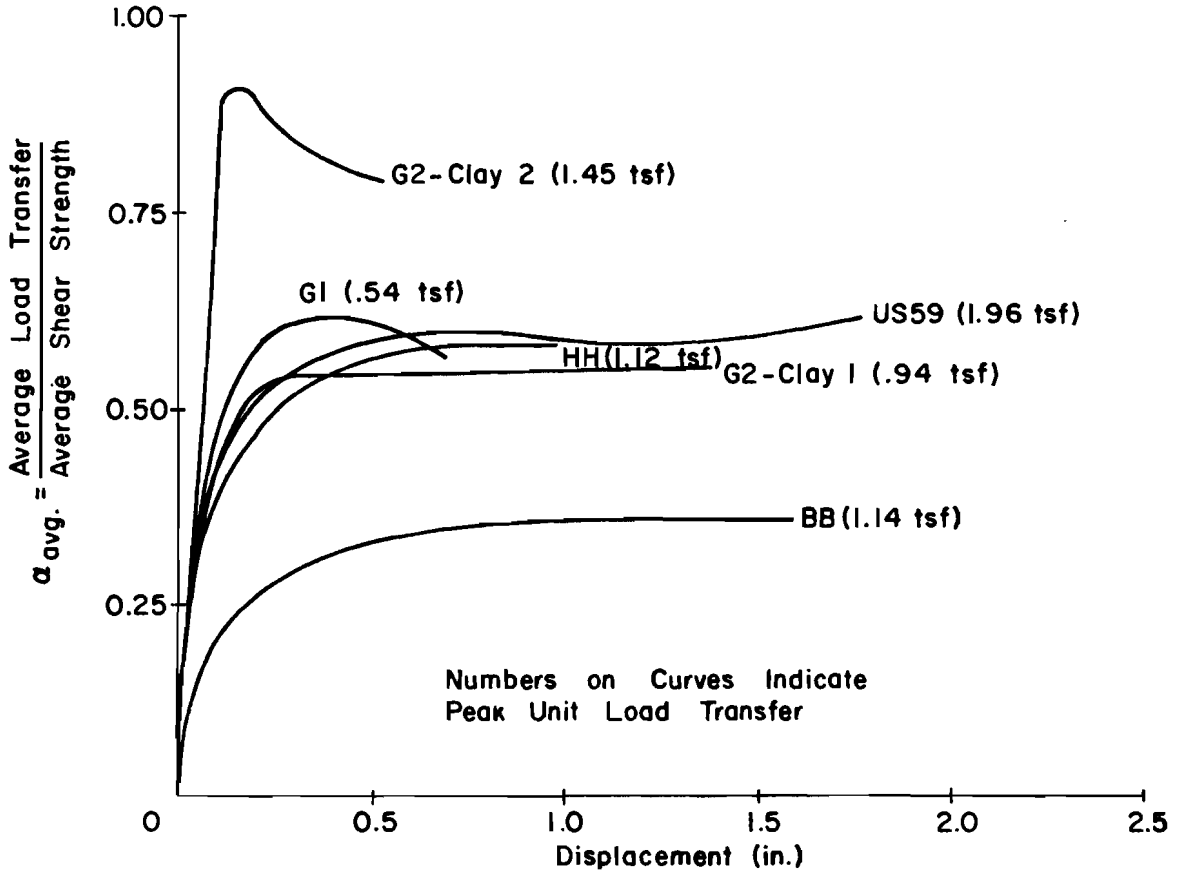

Fig. 7.2 Load Transfer in Clay

to the shear strength of the coating separating the soil and the concrete. In this case, the average shear transfer measured was about 1 tsf (Reese and Touma, 1972).

Side Resistance in Sand

The inconsistency of the results from the different test shafts reflects the influence of many variables on the measured load transfer in sand. Some of these variables, discussed in previous chapters, are related to the method of construction, the effect of load transfer, the interference of layered soil systems, the interaction with the tip, and the nature and relative density of the sand. A definite evaluation of the influence of each variable is not possible from the obtained results. The complexity of the problem challenges also the more sophisticated analytical tools. While a finite element analysis may evaluate the influence of the variables on the general behavior of the shaft, neither the constitutive properties of the natural deposits nor the initial state of stress is yet reasonably defined.

Figure 7.3 presents what is believed to be a typical behavior of the side shear transfer in a homogeneous sand medium. The nonlinear increase of the shear transfer with depth reflects the influence of the load transfer in the upper layers of the soil and the arching of the sand near the tip of the shaft. The significant reduction in shear transfer in the lower depth of the pile is associated with the flow of the sand near the tip as described previously. The extent of the zones of flow and arching is dependent on the settlement of the tip and on the relative

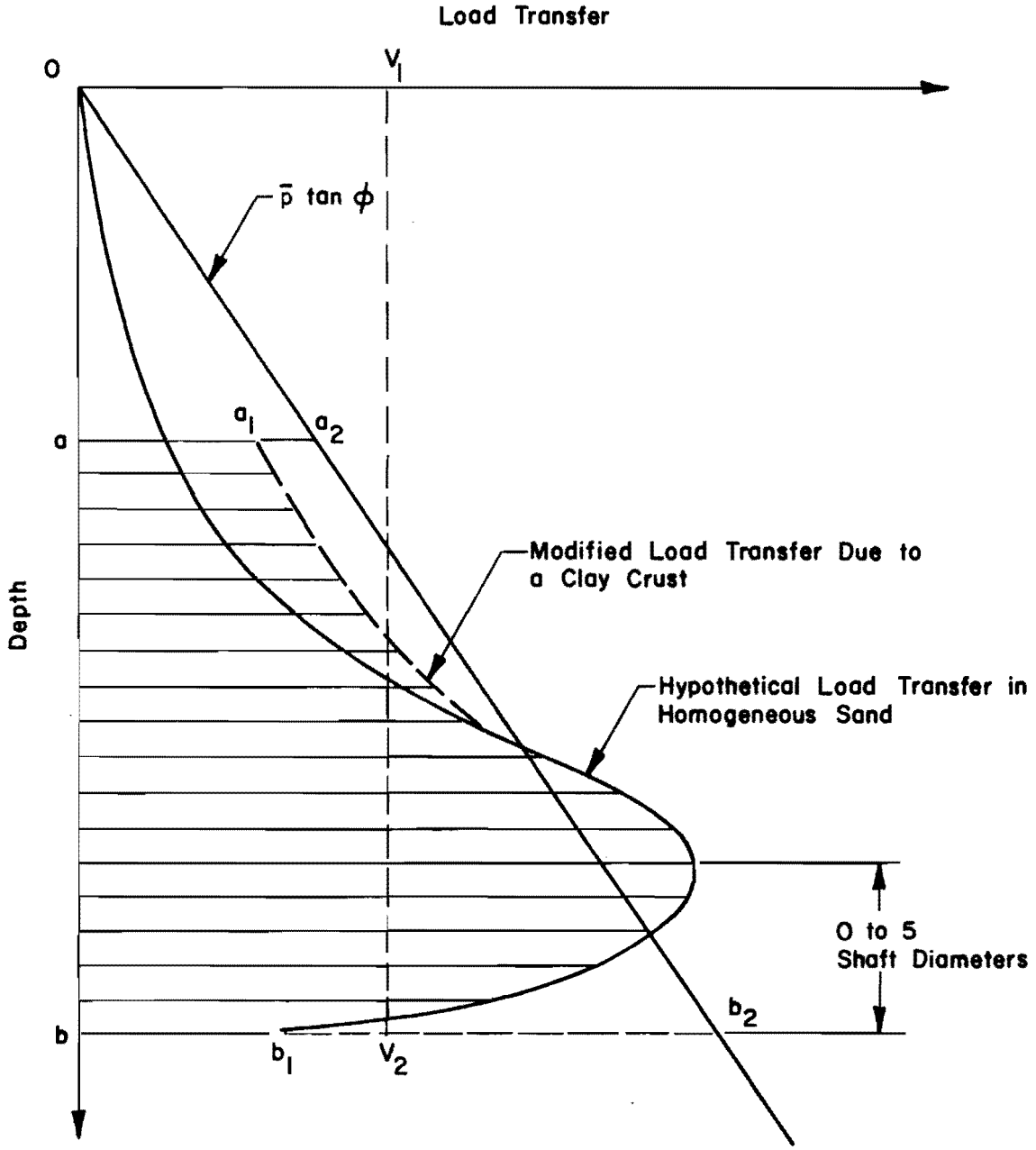

Fig. 7.3 Typical Behavior of Load Transfer in Sand

density of the sand. This hypothetical curve is similar to curves from experimental measurements on driven piles in sand deposits (Vesić, 1970) and is in general agreement with load transfer curves measured in this study.

At all test sites used in this study, the soil profile consisted of an upper clay layer overlaying sand deposits. Thus, it was not possible to study the shear transfer in sand at shallow depths. The influence of the clay layer on the shear transfer in sand cannot be accurately measured. The high load transfer in the top stiff clay increases the confinement of the sand and should increase the shear transfer in the sand, as shown by the dashed line in Fig. 7.3.

The total load transfer by side resistance is the product of the circumference of the shaft and the integral of the area under a load transfer curve, such as the curve shown in Fig. 7.3. For the drilled shafts tested in this study, correlations were obtained between the average load transfer in the sand and the average value of the product $\bar{p} \tan \bar{\phi}$. This is equivalent to saying that the hatched area aa_1b_1b under the load transfer curve of Fig. 7.3 is related to the area aa_2b_2b under the line representing the product $\bar{p} \tan \bar{\phi}$.

It is convenient to define a factor α_{avg} as the ratio of these areas. Figure 7.4 presents plots of α_{avg} versus the displacement of the shaft as obtained from the various tests. That α_{avg} for shaft HH is larger than for the other shafts is due to the existence of thin layers of sandstone and hard conglomerates in the sand formation and is not, therefore, representative

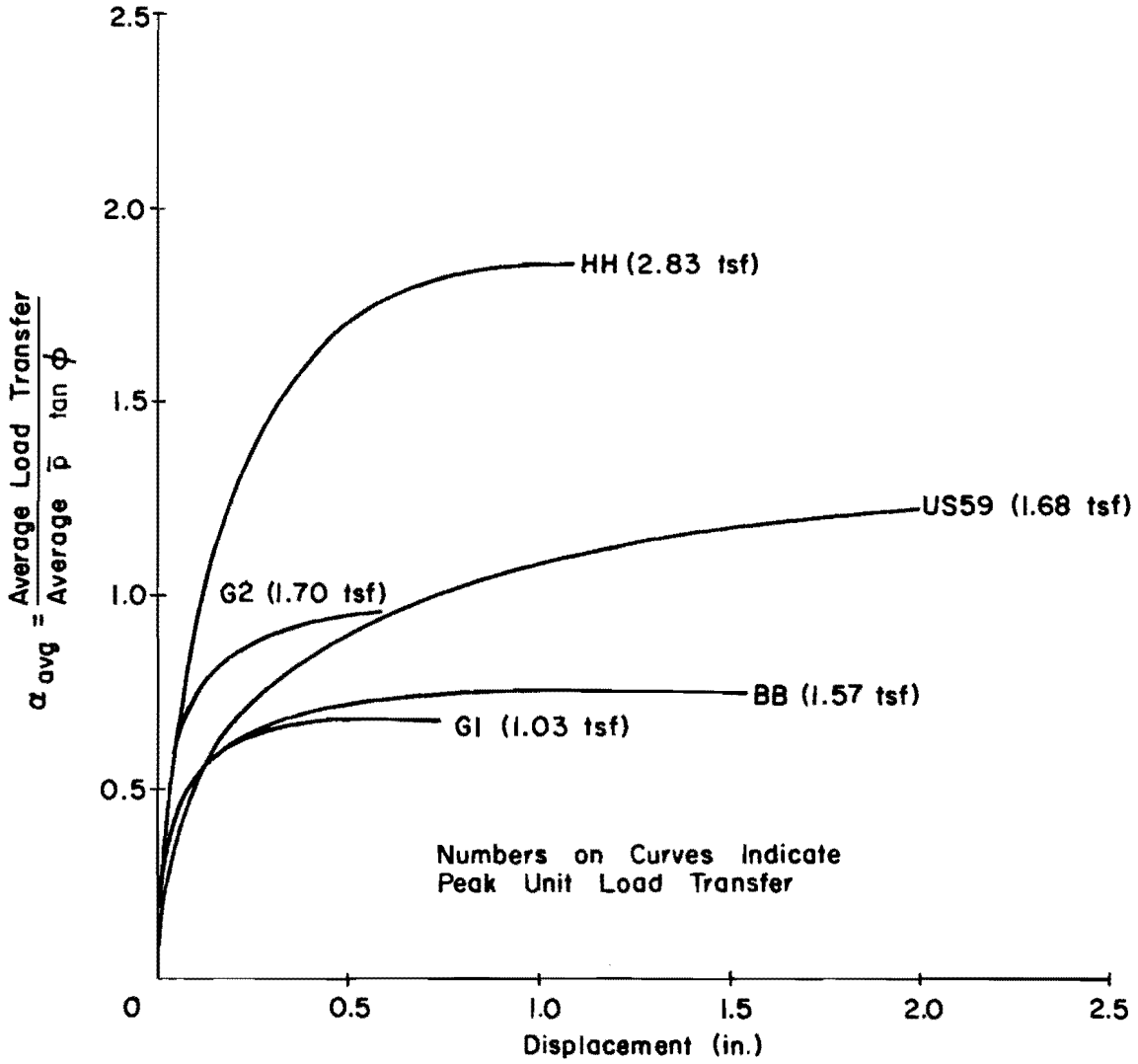

Fig. 7.4 Average Load Transfer in Sand

of shafts in sand. The slight carbonaceous cementation of the sand at the US59 test site partially explains the high load transfer measured at that site. The differences between the α_{avg} values of the G1, G2, and BB sites may be partially due to the varying influence of the load transfer in the upper clay layers.

It is of interest to note that shafts US59 and G2, which penetrated 10-15 ft. in sand, exhibited larger α_{avg} values than those of shafts G1 and BB, which penetrated 20-25 ft. in sand. This difference could be partially attributed to the varying influence of the interaction between the sides and the tip. The arching stresses from this interaction have a greater influence on shafts of smaller penetration in sand. This phenomenon suggests that shafts having a penetration in sand greater than 25 ft. may indicate smaller α_{avg} values than those measured in this study.

It is also observed from a study of Fig. 7.4 and the results presented in the previous chapter that the movement required to mobilize the side resistance of a sand element on the periphery of the shaft varies with the density of the sand and the relative position of the sand element. Outside the arching zone, shear failure takes place at a displacement of about 0.25 in. On the other hand, the continuous expansion with settlement of the arching zone results in larger displacements at failure of the sand elements in that zone. Larger displacements are observed, as a result, in the US59 and BB shafts where dense to very dense sands were tested, and where the shear transfer in the arching zone accounted for a large fraction of the total shear transfer.

PARTICULAR BEHAVIOR AND SPECIAL TESTS

The observations relative to the particular behavior of each of the test shafts are discussed in the following paragraphs.

Shaft US59

This test shaft provides the best data on the behavior of the tip resistance of drilled shafts installed in very dense sand because the shaft was well seated in the sand and the tip level of Mustran cells functioned properly. The results on load transfer indicated a behavior similar to that described in Fig. 7.3. A very small side resistance was measured in the medium dense sand layer, whereas a very large side resistance was measured in the lower very dense and slightly cemented sand layer. The cementation of the sand was evidenced by the fact that the construction was made in a free-standing hole. Although the cohesive component of the shear strength of the sand was not very significant, its presence may have allowed a larger extension of the arching zone.

After soaking, the total bearing capacity of the shaft was not changed although a redistribution of the load transfer was manifested between the different layers. The load transfer in the top clay layer was reduced as a result of an increase in the moisture content. On the other hand, the repeated testing resulted in the compaction of the medium dense sand layer and increased the load transferred in that layer. The load transfer in the lower sand layers was reduced by the continuous downward movement of the shaft while the tip resistance increased due to the compaction of the sand at the tip.

The time required for the stabilization of the downward movement under a constant load varied between 0 and 30 minutes depending on the load applied. Studies by Vesić (1968) showed that the consolidation of sand takes place in a comparable amount of time for stresses comparable to those applied at the tip of the shaft.

Shaft HH

This test shaft yielded valuable information on the tip resistance of drilled shafts in sand. However, the evaluation of the side resistance in sand was not meaningful, because of the existence of very hard layers in the sand deposits.

Shaft G1

The first test on this shaft yielded very valuable information on the side and tip resistance of shafts cast in sands of medium density. Results from the second and the third tests indicated a significant influence of repeated loading on the load transfer. Cyclic loading and large settlements of the shaft reduce significantly the load transfer in the clay layer, as was previously reported from research results (O'Neill and Reese, 1970). The influence of cyclic loading on the load transfer in sand was not well defined. While the average value of the side resistance in sand remained essentially the same, its distribution with depth varied in the different tests.

Shaft G2

The measured load distribution in the shaft during the first test indicated a considerable scatter which was attributed to variations in the

modulus of elasticity of the concrete. However, the average measured load transfer in the major soil layers is believed to be fairly representative.

Nonhomogeneous soil conditions existed below a depth of 55 feet, and there was uncertainty about the character of the soil at the tip of the shaft. Back calculations of the shear strength of the soil at the tip from the measured tip resistance indicate that the shaft may be tipping in a clay.

Shaft BB

The Mustran cells in the upper sections of the shaft were found to be unreliable, and only an average value of load transfer could be obtained in the upper clay formation. The destruction of the cells at the tip and the scatter of the data allowed only the measurement of an average value of the side shear transfer in the sand layer. The zones of flow and interaction could not be identified in this shaft.

DESIGN IMPLICATIONS

Previous discussions emphasized the long sweeping character of the load-settlement curve of drilled shafts in sand and the large settlements required to mobilize the ultimate resistance of the shafts. Figure 7.5 presents straight line approximations of the side, tip, and total load transfer in an average size shaft of 30 inches in diameter. It is observed on this figure that the failure of the sides of the shaft takes place at a downward movement of about 0.25 to 0.50 in. and that a large fraction of the tip resistance is mobilized at a tip movement of 1.50 in.

A, B, and C = Failure Loads at 1" Settlement

A', B', and C' = Ultimate Failure Loads

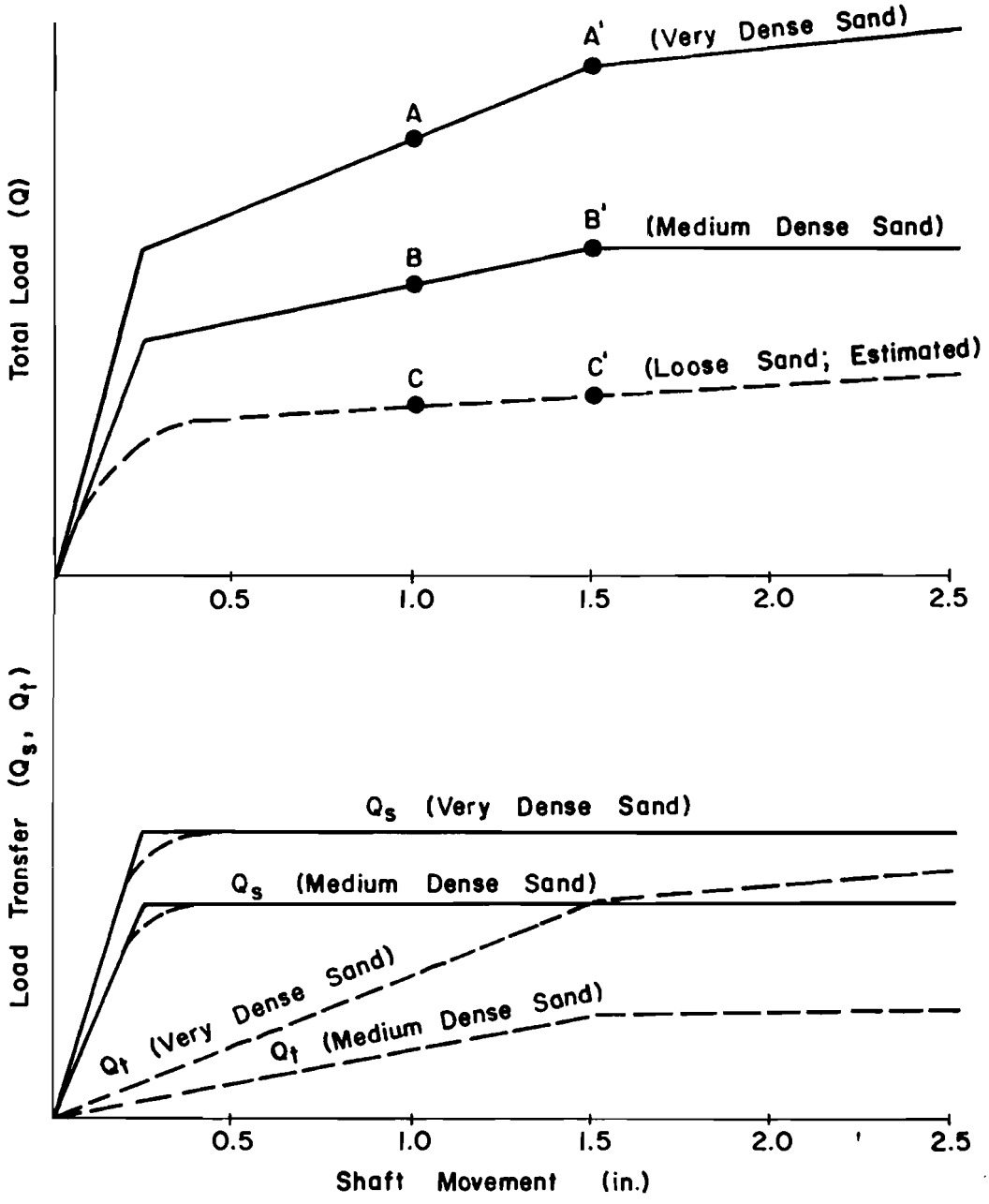

Fig. 7.5 Approximate Load Transfer and Load-Settlement Curves for a 30 in. Drilled Shaft

representing 5% of the tip diameter. Beyond this movement the tip resistance flattens progressively and its magnitude becomes uncertain. The design of drilled shafts, therefore, depends greatly on the settlement that can be tolerated by the supported structure. In bridge design, the allowable settlement depends on the stiffness of the bridge (continuous vs. simple span, and reinforced vs. prestressed concrete), on the desired rideability and on the cost of maintenance of the road.

The choice of design criteria from empirical results poses a philosophical question: what factor of safety must be applied? The factor of safety must reflect the confidence in the obtained results and in their application to the design of similar shafts. It must also take into consideration the existence of a multitude of variables in the analysis, design and construction of drilled shafts, and must consider the competence of the designing engineer.

For the purposes of design of bridge bents where the diameter of drilled shafts varies commonly between two and four feet, the failure load of a drilled shaft will be defined as the load corresponding to one inch of settlement of the shaft. The working design load is taken as one-half the failure load. It is believed that these criteria limit the differential settlements to satisfactory values for most bridges (less than 0.5 inch) and allow an economical design.

In the proposed criteria, the failure load includes the total side resistance and a fraction of the ultimate tip resistance, varying between 40 and 100%. The larger fraction of the ultimate tip resistance is

developed in smaller diameter shafts and looser sands; however, in both of these situations the tip resistance is only a small fraction of the total shaft resistance. The uncertainties of the construction methods, the variabilities of the measured results, and the large settlements associated with the tip resistance make the tip resistance the more uncertain quantity of the two components of the shaft resistance. A greater factor of safety against ultimate failure is, therefore, required where the tip resistance constitutes a larger fraction of the total shaft resistance. In the proposed criteria, a factor of safety of two against the failure load defined at one inch of settlement corresponds to a factor of safety of two against the ultimate failure of small diameter shafts in loose sand and to a larger factor of safety against ultimate failure of large diameter shafts in very dense sand.

The following procedure for design is, therefore, suggested:

1. Obtain from the dynamic penetrometer blow count estimates of the friction angle and the relative density of the sand. For the standard penetration test, the USBR charts presented in Fig. 4.5 can be used in conjunction with the curve relating the friction angle to the relative density of the sand given by Peck, Hanson, and Thornburn in Fig. 4.8. For the THD cone penetrometer the charts presented in Fig. 7.6 can be used. These charts were obtained from the USBR charts based on previous correlations that showed that the THD cone penetrometer blow count in sand is

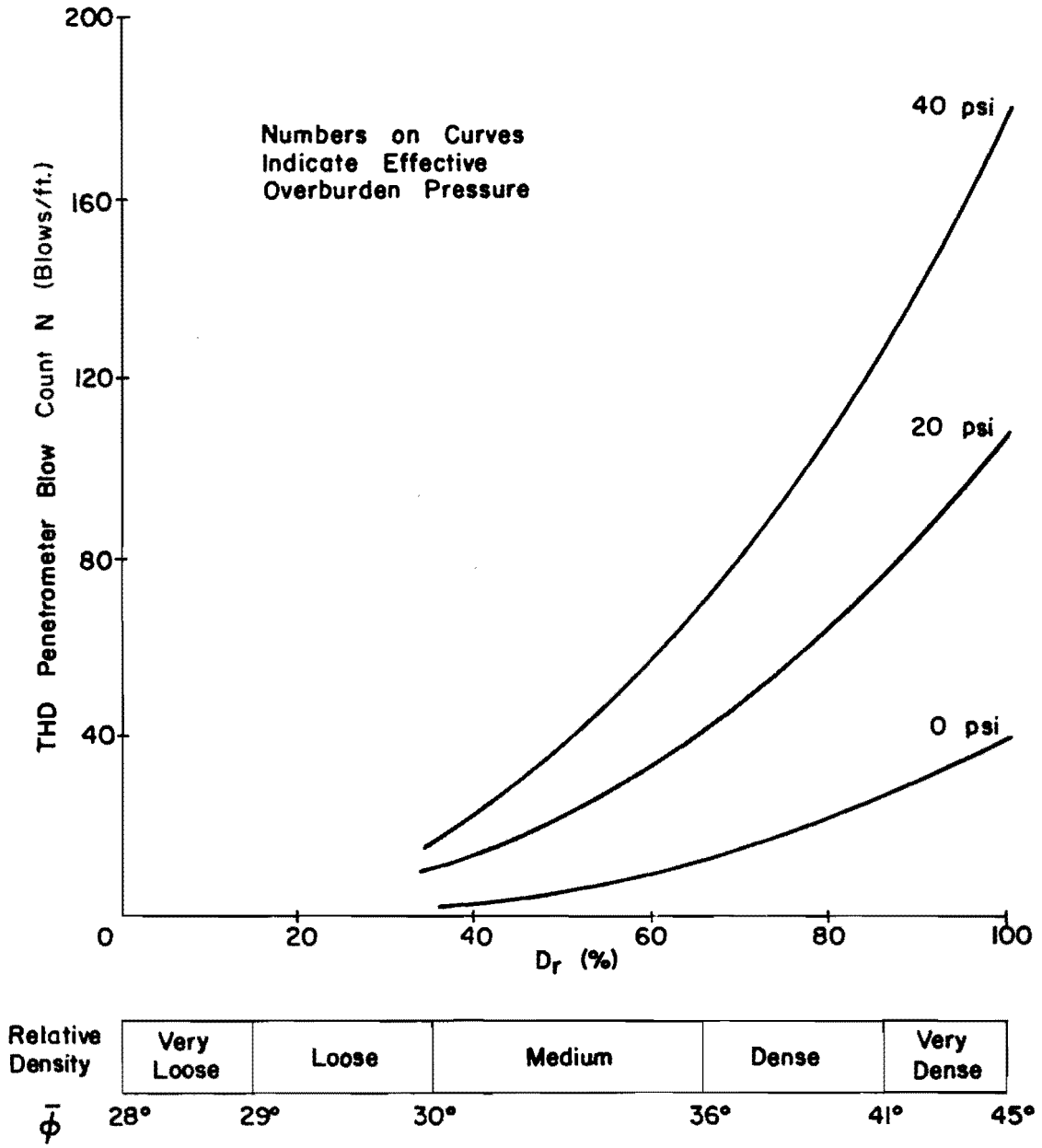

Fig. 7.6 Relation Between THD Penetrometer Blow Count and the Friction Angle

approximately equal to twice the SPT blow count. The relations in Fig. 7.6 can be further approximately expressed as

$$\bar{\phi} = \frac{8N(THD)}{20 + 0.01\,\bar{p}} + 29 \leq 45^\circ$$

where

$\bar{\phi}$ = effective friction angle, degrees,

N = THD blow count,

$\bar{p}$ = effective overburden pressure, psf.

2. Obtain the ultimate side resistance Q_s (lb) in sand as

$$Q_s = \alpha_{avg}\, C \int_0^H \bar{p} \tan \bar{\phi}\, dz$$

where

C = circumference of the shaft, ft,

H = total depth of embedment of the shaft in sand, ft,

dz = differential element of length, ft.

The results of the load tests indicated a minimum α_{avg} of about 0.7 which can safely be used for the design of shafts of a penetration in sand not exceeding 25 ft. There are indications that the value of α_{avg} may decrease with greater penetration in

sand and, therefore, smaller values must be used in the design of deeper shafts. Pending future research, it is suggested that for shafts penetrating more than 25 but less than 40 ft. in sand an α_{avg} value of 0.6 shall be used and that an α_{avg} value of 0.5 shall be used for shafts of greater penetration.

3. Obtain the failure tip resistance Q_t (lb) in sand at one inch of downward movement of the shaft as

$$Q_t = \frac{A}{0.6\ B}\ q_t$$

$$= \frac{\pi B}{2.4}\ q_t \ ;\ B \geq 2 \text{ ft.}$$

where

A = cross-sectional area of the shaft, ft^2,

B = diameter of the shaft, ft,

q_t = tip resistance at five percent movement. q_t is taken equal to 0, 32000 psf, and 80000 psf for loose, medium dense, and very dense sand respectively. For sands of intermediate densities linear interpolations can be used. (These values of the tip resistance are limited to shafts deeper than 10 shaft diameters).

4. Obtain the failure load Q (lb) at one inch downward movement of the shaft as

$$Q = Q_s + Q_t$$

5. Obtain the working resistance of the shaft by dividing the failure load Q by two.

Based on these criteria, back calculations were made to evaluate the failure load of the test shafts defined at one inch movement. The results of these calculations are presented in Table 7.1 and are compared to the measured values. In doing these calculations the measured load transfer in clay was added to the computed load transfer in sand. Table 7.2 shows similar calculations for the total measured and calculated load transfer in sand at the various test sites.

In these tables it is observed that the error in estimating the failure load is relatively small for all shafts except shaft HH. The existence of sandstone and conglomerate layers at this site resulted in very high load transfer that cannot be correlated to the load transfer in sand. Of interest in Table 7.1 are also the small values of settlements measured at the design loads and the factors of safety against the maximum loads applied on the shaft. The factors of safety are close to two for shafts depending greatly on the side resistance such as shaft G1, and G2, that were installed in medium dense sand and in clay. Larger factors of safety are shown for shafts US59 and BB that were installed in very dense sand. The factor of safety of shaft HH is not comparable to the others because of reasons mentioned earlier. It is also important to note that the larger factors of safety in shafts US59 and BB are associated with larger settlements.

Table 7.1 Comparison of Total Calculated and Measured Loads

	Shaft				
	US59	HH	G1	G2	BB
Calculated Load at One Inch Movement (T)	370	240	430	670	560
Measured Load at One Inch Movement (T)	410	430	450	670	590
Percent Difference*	-9.7	-44.2	-4.4	0	-5.1
Maximum Load Applied (T)	700	540	480	690	750
Displacement at Design Load (In.)	.36	.05	.07	.11	.10
Displacement at Max. Load (In.)	7.0	2.5	0.5	0.5	2.5
Factors of Safety w.r.t. Max. Load	3.78	4.50	2.14	2.00	2.68

* Percent Difference is equal to $\left(\frac{\text{Calculated load - Measured load}}{\text{Measured load}} \right) \text{X } 100$

Table 7.2 Comparison of Calculated and Measured Load Transfer in Sand

	Shaft				
	US59	HH	G1	G2	BB
Calculated Load	250	145	305	200	340
Measured Load	300	300	350	220	365
Percent Difference	-27.8	-51.2	-12.8	-9.1	-9.4

CHAPTER VIII. CONCLUSIONS

The solution of problems in soil mechanics and foundation engineering is limited mostly by the following major factors: the indeterminate three-dimensional stress-strain behavior of an element of soil, the heterogeneity of natural soil deposits, the complexity of the analysis of stresses in a nonlinear material, and the unknown influences of the different methods of construction. Practical, rigorous solutions to these problems cannot be developed before tangible progress is realized in laboratory techniques, field measurements, analytical procedures, and analysis of the methods of construction.

This study has been concerned with the design and construction of drilled shafts in sand. Five full-scale test shafts were constructed using the dry method and the slurry displacement method. These two construction methods were analyzed and evaluated in the light of field observations made during the construction of test shafts and using published information on similar construction techniques. With respect to the design, a rigorous solution evaluating the influence of the many variables controlling the behavior of drilled shafts in sand could not be obtained. However, measurements taken from full-scale load tests on five drilled shafts, and observations made during the construction and the extraction of the shafts, allowed the development of approximate solutions to the problem. In the following sections the main conclusions concerning the construction and the design of drilled shafts will be summarized.

CONSTRUCTION

The dry method and the slurry displacement method can both be successfully used in the construction of drilled shafts. The dry construction is preferable where feasible, and the rules for its good execution are well known. Research made in this study on the more recent slurry displacement technique resulted in the following findings:

1. The stability of a drilled hole is greatly influenced by the quality of the drilling mud. While a high density mud may be needed in holes with artesian pressures, a low density mud is more desirable in general and can stabilize a hole when the mud is maintained at a sufficient level above the ground water table. The flocculation, and the weight of mud, can be reduced by using fresh, soft, and uncontaminated water to mix the mud and by using the proper mud constituents when penetrating contaminating formations.

   Expansive clays are more troublesome than sands when exposed to the drilling mud. In general, a calcium drilling mud prevents the dispersion and erosion of the expansive clays.
2. The concreting must be executed with great care. Sediments deposited at the bottom of the hole may be washed out by the first charge of concrete if the proper seal of the tremie is used. It was found that a seal made of a wood block and a polyethylene sheet causes sediments to be trapped at the bottom of the hole. Possible improvements of the seal are described in Chapter II. Care must

be exercised to keep the tremie well embedded in concrete (about 5 ft.) during concreting to prevent the entrapment of mud in the concrete.

The development of a thin mud cake on the side of the hole and the existence of a thin coating of mud on deformed reinforcement steel do not reduce the capacity of the shaft. However, a heavy and flocculated mud may be entrapped in large lumps on the reinforcing steel and on the sides of the shaft. A light, dispersed mud and a high-slump concrete (6-7 in.) must be used to insure good concreting.

The flow of the concrete is a function of the size of the hole and the head of concrete applied. No criteria can be suggested at this time for establishing the necessary flow of the concrete; however, the construction by slurry displacement of shafts smaller than 24 in. is not recommended.

DESIGN

The following paragraphs summarize findings concerning the design of drilled shafts in sand.

1. With respect to the tip resistance, it was found that very large displacements are required to mobilize a significant reaction at the tip. In loose sand this resistance is a very small fraction of the side resistance. In medium and in very dense sand, curves

relating the pressure at the tip to the settlement of the pile have been recommended. In the general case, the designer's choice of an allowable tip resistance is a function of the nature of the proposed structure and the settlements it can tolerate. A method has been recommended for the design of drilled shafts in bridge bents. This method is based on defining the failure load at a downward movement of the top of the shaft of one inch.

2. With respect to the side resistance, it was found that several variables control the pattern of behavior of the shear resistance at the periphery of the shaft. The influence of each of these variables could not be evaluated separately. Instead, it was found empirically that the average side resistance developed on the periphery of the shaft is related to the overburden pressure and the friction angle of the sand. This relationship can be expressed as

$$Q_s = \alpha_{avg}\, C \int_0^H \bar{p} \tan \bar{\phi}$$

where

Q_s = total side resistance of the depth of the shaft embedded in sand,

α_{avg} = factor that can be taken equal to 0.7 for penetrations in sand not exceeding 25 ft. (Tentative values for greater

depths are suggested as 0.6 for shafts penetrating sand between 25 and 40 ft. and 0.5 for shafts of greater penetration.),

C = circumference of the shaft,

$\bar{p}$ = effective overburden pressure,

$\bar{\phi}$ = effective friction angle of the sand,

H = depth of embedment in sand.

These findings must be applied cautiously. The designer should keep in mind that the construction of these test shafts was completed under close supervision that may not be available on many construction sites. Although results did not allow a significant distinction of the effects of the dry and the slurry displacement methods of construction, the possible adverse effects of excessive entrapment of mud and sediments at the tip and at the sides of shafts cast by slurry displacement cannot be overemphasized, and every care must be exercised in using this technique.

RECOMMENDED RESEARCH

The large number of variables controlling the behavior of drilled shafts in sand and the small number of controlled tests left many questions for future investigations. Some of the recommended future research is discussed in the following paragraphs.

1. The distribution of the effective concrete pressure on the walls of the hole is a function of the size of the hole and the rate

of placement, the slump, the temperature, and the placing procedure of the concrete. These variables deserve serious attention from future investigators.

2. A finite element analysis, taking into consideration the proper constitutive properties of the sand, may allow a better understanding of the behavior of drilled shafts. Such a study could evaluate the relative influences of the volumetric concrete strains and the interaction of the stresses in the sand surrounding the shaft. This analysis could also evaluate the influence of the interaction, between the tip and the sides of the shaft, on the total load transfer by side shear. It must be noted, however, that our present knowledge of the constitutive properties of sand allows the use of the finite element analysis to give only a better understanding of the behavior of drilled shafts and of the influence of the controlling variables. The limitations of our present soil testing techniques in defining the in situ properties of sand deposits and the behavior of sand under generalized stress conditions prevent the use of the finite element analysis to define practical design parameters.

REFERENCES

AASHO (1963), Standard Specifications for Highway Bridges, 1963.

API, Subcommittee API Southern District L9696), "Principals of Drilling Fluid Control," 12th Edition, 1969.

Awoshika, K. and Reese, L.C. (1971), Analysis of Foundation with Widely Spaced Batter Piles, Research report 117-3, Center for Highway Research, The University of Texas at Austin, Austin, 1971.

Barbedette, R. and Beria, E. (1961), "Procedé d'execution de Tranchees et puits sans souténement," Proceedings of the Fifth International Conference on Soil Mechanics and Foundation Engineering, Vol. 2, Paris, 1961.

Barker, W.R. and Reese, L.C. (1969), Instrumentation for Measurement of Axial Load in Drilled Shafts, Research Report 89-6, Center for Highway Research, The University of Texas at Austin, Austin, November, 1969.

Barker, W.R. and Reese, L.C. (1970), Load-Carrying Characteristics of Drilled Shafts Constructed with the Aid of Drilling Fluids, Research Report 89-9, Center for Highway Research, The University of Texas at Austin, Austin, 1970.

Bazaraa, A.R.S.S. (1967), Use of the Standard Penetration Test for Estimating Settlements of Shallow Foundations on Sand, Thesis presented to the University of Illinois in partial fulfillment of the requirements for the degree of Doctor of Philosophy, Urbana, Illinois, 1967.

Berezantzev, V.G. and Yaroshenko, V.A. (1957), "The Bearing Capacity of Sands Under Deep Foundations," Proceedings of the Fourth International Conference on Soil Mechanics and Foundation Engineering, Vol. 1, London, 1957.

Berezantzev, V.G., Khristoforov, V.S., Golubkov, V.N. (1961), "Load Bearing Capacity and Deformation of Piles Foundations," Proceedings of the Fifth International Conference on Soil Mechanics and Foundation Engineering, Vol. 2, Paris, 1961.

Bishop, A.W. (1948), "A New Sampling Tool for Use in Cohesionless Sands Below Ground Water Level," Geotechnique, Vol. I, No. 2, London, 1948.

Burland, J.B. (1963), Discussion in Grouts and Drilling Muds in Engineering Practice, Butterworths, London, 1963, pp. 223-225.

Butler, H.D. (1972), Personal Communication, 1972.

Caquot, A. and Kérisel, J. (1949), Traité de Mecanique des sols, Gauthier-Villars, Paris, 1949.

Chadeisson, R. (1961), "Parois Continues Moulées dans le sol," Proceedings of the Fifth International Conference on Soil Mechanics and Foundation Engineering, Vol. 2, Paris, 1961.

Chadeisson, R. (1961), "Influence Du Mode De Perforation Sur Le Comportement Des Pieux Forés Et Moulés Dans Le Sol," Proceedings of the Fifth International Conference on Soil Mechanics and Foundation Engineering, Vol. 2, Paris, 1961.

Chuang, J.W. and Reese, L.C. (1969), Studies of Shearing Resistance Between Cement Mortar and Soil, Research Report 89-3, Center for Highway Research, The University of Texas at Austin, Austin, 1969.

Chellis, R.D. (1961), Pile Foundations, Second Edition, McGraw-Hill, New York, 1961.

Cole, R.W. (1963), Discussion in Grouts and Drilling Muds in Engineering Practice, Butterworths, London, 1963.

Coyle, H.M. and Reese, L.C. (1966), "Load Transfer for Axially Loaded Piles in Clay," Journal of the Soil Mechanics and Foundations Division, ASCE, Vol. 92, No. SM2, March, 1966.

Coyle, H.M. and Sulaiman, I.H. (1967), "Skin Friction for Steel Piles in Sand," Journal of the Soil Mechanics and Foundations Division, ASCE, Vol. 93, No. SM6, November, 1967.

DeBeer, E.E. (1963), "The Scale Effect in the Transportation of the Results of Deep-Sounding Tests on the Ultimate Bearing Capacity of Piles and Caisson Foundations," Geotechnique, Vol. 11, No. 1, March, 1963.

DeBeer, E.E. (1964), "Some Considerations Concerning the Point of Bearing Capacity of Bored Piles," Proceedings, Symposium on Bearing Capacity of Piles, Central Buliding Research Institute, Vol. 1, Roorkee, India, February 1964.

DeMello, V.F.B. (1969), "Foundations of Buildings in Clay," Proceedings of the Seventh International Conference on Soil Mechanics and Foundation Engineering, State-of-the-Art Volume, Mexico City, 1969.

DeMello, V.F.B. (1971), "The Standard Penetration Test," Fourth Panamerican Conference of Soil Mechanics and Foundation Engineering, Vol. 1, Puerto Rico, 1971.

Denisov, N.Y., Durante, V.A., and Kazanov, M.I. (1963), "Studies of Changes of Strength and Compressibility of Hydraulically Filled Sands in Time," Proceedings of the European Conference on Soil Mechanics and Foundation Engineering, Vol. 1, Weisbaden, 1963.

DuBose, L.A. (1955), "Small Scale Load Tests on Drilled and Cast-in-Place Concrete Piles," Proceedings, Highway Research Board, Vol. 34, Washington, D.C., 1955.

DuGuid, D.R., Forbes, D.J., Gordon, J.L., and Simmons, O.K. (1971), "The Slurry Trench Cut-Off for the Duncan Dam," Canadian Geotechnical Journal, 8,94, 1971.

Edison Group, S.A.D.E. Group, S.I.M.A. Company (1961), "Construction of Concrete Diaphragms (Cut-Off Walls) in Italy," Proceedings of the Fifth International Conference on Soil Mechanics and Foundation Engineering, Vol. 2, Paris, 1961.

Farmer, I.W., Buckley, P.J.C., and Sliwinsky, Z. (1970), "The Effect of Bentonite on the Skin Friction of Cast-in-Place Piles," Behavior of Piles, Proceedings of the Conference Organized by the Institution of Civil Engineers in London, September, 1970.

Fernandez-Renau, L. (1965), Discussion in Proceedings of the Sixth International Conference on Soil Mechanics and Foundation Engineering, Vol. 3, Montreal, Canada, 1965.

Florentin, J. (1969), "Cast-in-Situ Diaphragm Walls," Proceedings of the Seventh International Conference on Soil Mechanics and Foundation Engineering, Vol. 3, Mexico City, 1969.

Gibbs, H.J. and Holtz, W.C. (1957), "Research on Determining the Density of Sands by Spoon Penetration Testing," Proceedings of the Fourth International Conference on Soil Mechanics and Foundation Engineering, Vol. 1, London, 1957.

Glossop, R. and Greeves, I.S. (1946), "A New Form of Bored Pile," Concrete and Construction Engineering, London, December, 1946.

Greer, D.M. (1969), "Drilled Piers State of the Art, 1969," W.C.A. Geotechnical Bulletin, Vol. 3, No. 2, Woodward-Clyde & Associates, New York, September, 1969.

Hager, R.F. (1970), Cast-in-Drilled Hole-Piles in Adverse Soil Conditions Part I Wet Installations, Report Prepared in the Engineering Geology Section of the Bridge Department of the California Department of Public Works, July, 1970.

Hendron, A.J. (1963), The Behavior of Sand in One-Dimensional Compression, Thesis presented to the University of Illinois in partial fulfillment of the requirements for the degree of Doctor of Philosophy, Urbana, Illinois, 1963.

Henkel, D.J. (1970), Geotechnical Considerations of Lateral Stresses, ASCE 1970 Special Conference on Lateral Stresses in the Ground and Design of Earth-Retaining Structures, Cornell University, Ithaca, New York, June 1970.

Ireland, H.O. (1957), "Pulling Tests on Piles in Sand," Proceedings of the Fourth International Conference on Soil Mechanics and Foundation Engineering, Vol. 2, London, England, 1957.

Jones, G.K. (1963), Discussion in Grouts and Drilling Muds in Engineering Practice, Butterworths, London, 1963.

Jezequel, J. (1971), "Foundations Sur Pieux," Ecole National Des Ponts Et Chaussees, St. Quay-Portrieux, France 15-17, Juin, 1971.

Kérisel, J.L. (1957), "Contributions a la Determination Experimentale des Réactions d'un Milieux Pulvérulent sur une Foundation Profonde," Proceedings of the Fourth International Conference on Soil Mechanics and Foundation Engineering, Vol. 1, London, 1957.

Kérisel, J.L. (1961), "Fondations Profondes en Milieux Sableux: Variation de la Force Portante Limite en Fonction de la Densité, de la Profondeur du diametre et de la Vitesse d'enforcement," Proceedings of the Fifth International Conference on Soil Mechanics and Foundation Engineering, Vol. 2, Paris, 1961.

Kérisel, J.L. (1964), "Deep Foundations - Basic Experimental Facts," Proceedings, Conference on Deep Foundations, Mexican Society of Soil Mechanics, Vol. 1, Mexico City, 1964.

King, J.C. and Bush, E.G.W. (1961), "Grouting of Granular Materials," Symposium on Grouting, Journal of the Soil Mechanics and Foundations Division, ASCE, Vol. 87, No. SM2, April 1961.

Koizumi, Yasunori, et al., B.C.P. Committee (1971), "Field Tests on Piles in Sand," Soils and Foundations, Vol. 11, No. 2, Tokyo, June 1971.

Komornik, A., and Wiseman, G. (1967), "Experience with Large Diameter Cast-in-Situ Piling," Proceedings of the Third Asian Regional Conference on Soil Mechanics and Foundation Engineering, Jerusalem Academic Press, Jerusalem, 1967.

Ladanyi, B. (1961), Discussion in Proceedings of the Fifth International Conference on Soil Mechanics and Foundation Engineering, Paris, 1961.

Ladanyi, B. (1963), "Expansion of a Cavity in a Saturated Clay Medium," Journal of the Soil Mechanics and Foundation Division, ASCE, Vol. 89, No. SM4, July 1963.

Lambe, T.W. and Whitman, R.V. (1969), Soil Mechanics, Wiley, New York, 1969.

Mansur, C.I. and Hunter, A.A. (1970), "Pile Tests-Arkansas River Project," Journal of Soil Mechanics and Foundation Division, ASCE, Vol. 96, SM5, September, 1970.

Martins, J.B. (1963), "Pile Load Tests on the Banks of the River Pungué," Proceedings of the Third Regional Conference for Africa on Soil Mechanics and Foundation Engineering, The Rhodesian Institution of Engineers, Salisbury, 1963.

Mazurkiewicz, B.K. (1968), "Skin Friction on Model Piles in Sand," Bulletin No. 25, Danish Geotechnical Institute, Copenhagen, 1968.

Meyerhof, G.G. (1951), "The Ultimate Bearing Capacity of Foundations," Geotechnique, Vol. 2, No. 4, London, December, 1951.

Meyerhof, G.G. (1956), "Penetration Tests and Bearing Capacity of Cohesionless Soils," Journal of the Soil Mechanics and Foundation Division, ASCE, Vol. 82, No. SM1, January, 1956.

Meyerhof, G.G. and Murdock, L.J. (1953), "An Investigation of the Bearing Capacity of Some Bored and Driven Piles in London Clay," Geotechnique, Vol. 3, No. 7, London, September, 1953.

Mindlin, R.D. (1936), "Force at a Point in the Interior of a Semi-Infinite Solid," Physics, Vol. 7, May, 1936.

Morgenstern, N.R. (1963), Discussion in Grouts and Drilling Muds in Engineering Practice, Butterworths, London, 1963.

Morgenstern, N.R. and Amir-Tahmassib, I. (1965), "The Stability of a Slurry Trench in Cohesionless Soils," Geotechnique, Vol. 15, No. 4, 1965.

Nash, J.K.T. and Jones, G.K. (1963), "The Support of Trenches Using Fluid Mud," Grouts and Drilling Muds, Butterworths, London, 1963.

Neville, A.M. (1963), Properties of Concrete, Wiley, New York, 1963.

Neville, A.M. (1971), Hardened Concrete: Physical and Mechanical Aspects, American Concrete Institue, 1971.

O'Neill, M.W. and Reese, L.C. (1970), Behavior of Axially Loaded Drilled Shafts in Beaumont Clay, Research Report 89-8, Center for Highway Research, The University of Texas at Austin, Austin, 1970.

Palmer, D.J. and Holland, G.R. (1966), "The Construction of Large Diameter Bored Piles with Particular Reference to London Clay," Proceedings of the Symposium on Large Bored Piles, Institution of Civil Engineers, London, February, 1966.

Parker, F., Jr. and Reese, L.C. (1970), Experimental and Analytical Studies of Behavior of Single Piles in Sand Under Lateral and Axial Loading, Research Report 117-2, Center for Highway Research, The University of Texas at Austin, Austin, 1970.

Peck, R.B., Hanson, W.E., and Thornburn, T.H. (1953), Foundation Engineering, Wiley, New York, 1953.

Perdue, G.W. and Coyle, H.M. (1970), In-Situ Measurements of Friction and Bearing Correlated with Instrumented Pile Tests, Report No. 125-4, Texas Transportation Institute, Texas A & M University, College Station, Texas, 1970.

Peurifoy, R.L. (1965), "Lateral Pressure of Concrete on Formwork," Civil Engineering, ASCE, December, 1965.

Polivka, M., White, L.P., and Cinaedingoer, J.P. (1957), "Field Experience with Chemical Grouting," Journal of the Soil Mechanics and Foundation Division, ASCE, Vol. 83, No. SM2, April, 1957.

Potyondy, J.G. (1961), "Skin Friction Between Various Soils and Construction Materials," Geotechnique, Vol. 11, No. 4, London, December, 1961.

Reese, L.C. (1964), "Load Vs. Settlement for an Axially Loaded Pile," Proceedings, Symposium on Central Building Research Institute, Vol. 2, 1964, Roorkee, India, 1964.

Reese, L.C., Brown, J.C., and Dalrymple, H.H. (1968), Instrumentation for Measurements of Lateral Earth Pressure in Drilled Shafts, Research Report 89-2, Center for Highway Research, The University of Texas at Austin, Austin, September, 1968.

Reese, L.C., O'Neill, M.W., and Smith, R.E. (1970), "Generalized Analysis of Pile Foundations," Journal of the Soil Mechanics and Foundations Division, ASCE, Vol. 96, No. SM1, January, 1970.

Reese, L.C. and Seed, H.R. (1955), "Pressure Distribution Along Friction Piles," Proceedings, American Society for Testing and Materials, Vol. 55, 1955, pp. 1156-1182.

Reese, L.C. and Touma, F.T. (1972), Load Test of Instrumented Drilled Shafts Constructed by the Slurry Displacement Method, Research Report Interagency Contract 108, Center for Highway Research, The University of Texas at Austin, Austin, 1972.

Robinsky, E.I. and Morrison, C.F. (1964), "Sand Displacement and Compaction Around Model Friction Piles," Canadian Geotechnical Journal, Vol. 1, No. 2, March, 1964.

Sadlier, N.A. and Dominioni, G.C. (1963), "Underground Structured Concrete Walls," Grouts and Drilling Muds in Engineering Practice, Butterworths, London, 1963.

Sarota, S. and Jennings, R.A. (1957), "Undisturbed Sampling Techniques for Sands and Very Soft Clays," Proceedings of the Fourth International Conference on Soil Mechanics and Foundation Engineering, Vol. 1, London, 1957.

Schneebeli, G. (1971), Les Parois Moulées Dans Le Sol, Editions Eyrolles, Paris, 1971.

Schmertmann, J.H. (1967), "Static Cone Penetrometers for Soil Exploration," Civil Engineering, ASCE, 1967.

Schultze, E. and Meltzer, K.J. (1965), "The Determination of the Density and Modulus of Compressibility of Non-Cohesive Soils by Soundings," Proceedings of the Sixth International Conference on Soil Mechanics and Foundation Engineering, Vol. 1, Montreal, 1965.

Seed, H.B. and Lee, K.L. (1967), "Undrained Strength Characteristics of Cohesionless Soils," Journal of the Soil Mechanics and Foundations Division, ASCE, SM6, November, 1967.

Sherard, J.L., Decker, R.S., and Ryker, N.L. (1972), "Piping in Earth Dams of Dispersive Clay," Proceedings of the Specialty Conference on Performance of Earth and Earth Supported Structures, Purdue University, 1972.

Taylor, D.W. (1948), Fundamentals of Soil Mechanics, Wiley, New York, 1948.

Terzaghi, K.V. (1936), "Stress Distribution in Dry and in Saturated Sand above a Yielding Trap-Door," Proceedings of the International Conference on Soil Mechanics and Foundation Engineering, Vol. 1, No. 2-3, Harvard, 1936.

Terzaghi, K. (1943), Theoretical Soil Mechanics, Wiley, New York, 1943.

Terzaghi, K. and Peck, R.B. (1967), Soil Mechanics in Engineering Practice, Wiley, New York, 1967.

Troxell, G.E. and Davis, H. (1956), Composition and Properties of Concrete, McGraw-Hill, New York, 1956.

Veder, C. (1953), "Procedé de Construction de Diaphragm Impermeables a Grande Profondeur au Moyen de Boues Thixotropiques," Proceedings of the Third International Conference on Soil Mechanics and Foundation Engineering, Vol. 3, Zurich, 1953.

Veder, C. (1963), Discussion in Grouts and Drilling Muds in Engineering Practice, Butterworths, London, 1963.

Veder, C. and Kienberger, H. (1969), "Behavior of Concrete Poured Under Bentonite Suspensions," Proceedings of the Seventh International Conference on Soil Mechanics and Foundation Engineering, Mexico City, 1969.

Vesić, A. (1963), "Bearing Capacity of Deep Foundations in Sand," Highway Research Record No. 39, Highway Research Board, Washington, D.C., 1963.

Vesić, A. (1965), "Ultimate Loads and Settlements of Deep Foundations," Bearing Capacity and Settlement of Foundations, Proceedings of a Symposium held at Duke University, April 5-6, Durham, North Carolina, 1965.

Vesić, A. and Clough, W.G. (1968), "Behavior of Granular Materials Under High Stresses," Journal of Soil Mechanics and Foundation Engineering, ASCE, Vol. 94, No. SM3, May, 1968.

Vesić, A. (1970), "Tests on Instrumeted Piles, Ogeechee River Site," Journal of the Soil Mechanics and Foundations Division, ASCE, Vol. 96, No. SM2, March, 1970.

Vesić, A. (1972), "Expansion of Cavities in Infinite Soil Mass," Journal of the Soil Mechanics and Foundations Division, ASCE, Vol. 98, No. SM3, March, 1972.

Vijayvergiya, V.N., Hudson, W.R., and Reese, L.C. (1969), Load Distribution for a Drilled Shaft in Clay Shale, Research Report 89-5, Center for Highway Research, The University of Texas at Austin, Austin, March, 1969.

Welch, R. and Reese, L.C. (1972), Lateral Load Behavior of Drilled Shafts, Research Report 89-10, Center for Highway Research, The University of Texas at Austin, Austin, 1972.

Westergaard, H.M. (1940), "Plastic State of Stress Around a Deep Well," Journal of the Boston Society of Civil Engineers, Vol. 27, No. 1, Boston Society of Civil Engineers, Boston, 1940.

Whitaker, R. and Cooke, R.W. (1966), "An Investigation of the Shaft and Base Resistance of Large Bored Piles in London Clay," Proceedings of the Symposium on Large Bored Piles, Institution of Civil Engineers, London, February, 1966.

Wu, T.H. (1957), "Relative Density and Shear Strength of Sands," Journal of Soil Mechanics and Foundations Division, ASCE, Vol. 83, No. SM1, January, 1957.

York, Guy, P., Kennedy, Thomas, W., and Perry, Ervin, S. (1970), Experimental Investigation of Creep in Concrete Subjected to Multiaxial Compressive Stresses and Elevated Temperatures, Research Report 2864-2 to Oak Ridge National Laboratories, Department of Civil Engineering, The University of Texas at Austin, Austin, June, 1970.

This page replaces an intentionally blank page in the original.
-- CTR Library Digitization Team

APPENDIX

This page replaces an intentionally blank page in the original.
-- CTR Library Digitization Team

APPENDIX. SOIL TESTS

This appendix presents the soil data obtained at the test sites and a brief description of the various soil tests conducted.

THE TEXAS HIGHWAY DEPARTMENT CONE PENETROMETER (THDP)

The apparatus and the procedure used in this test are described in detail in the Texas Highway Department "Foundation Exploration and Design Manual." The test consists of driving a three-inch diameter, 60-degree cone with a 170-pound hammer dropped a distance of two feet. Though the specifications require the penetrometer cone to "be driven twelve blows in order to seat it in the soil or rock," this seating process is usually left to the "feel" of the driller. Driving then proceeds in increments of six inches. The reported blow count is usually the number of blows required to drive the cone a distance of one foot. When the number of blows required for one foot of penetration exceeds a hundred, driving ceases and the penetrated distance is reported. In such cases the blow count per foot is obtained by a linear extrapolation of the measured blow counts. In soils that require less than 100 blows/ft. the shear strength is obtained from Fig. A.1. The "Foundation Exploration and Design Manual" does not specify a procedure to be followed to evaluate the shear strength of soils indicating a resistance of more than 100 blows/ft. The procedure used in such cases by the Engineers of the Houston Urban Office consists of evaluating the ultimate "Point Bearing" P from Fig. A.2 and then evaluating the shear strength s as

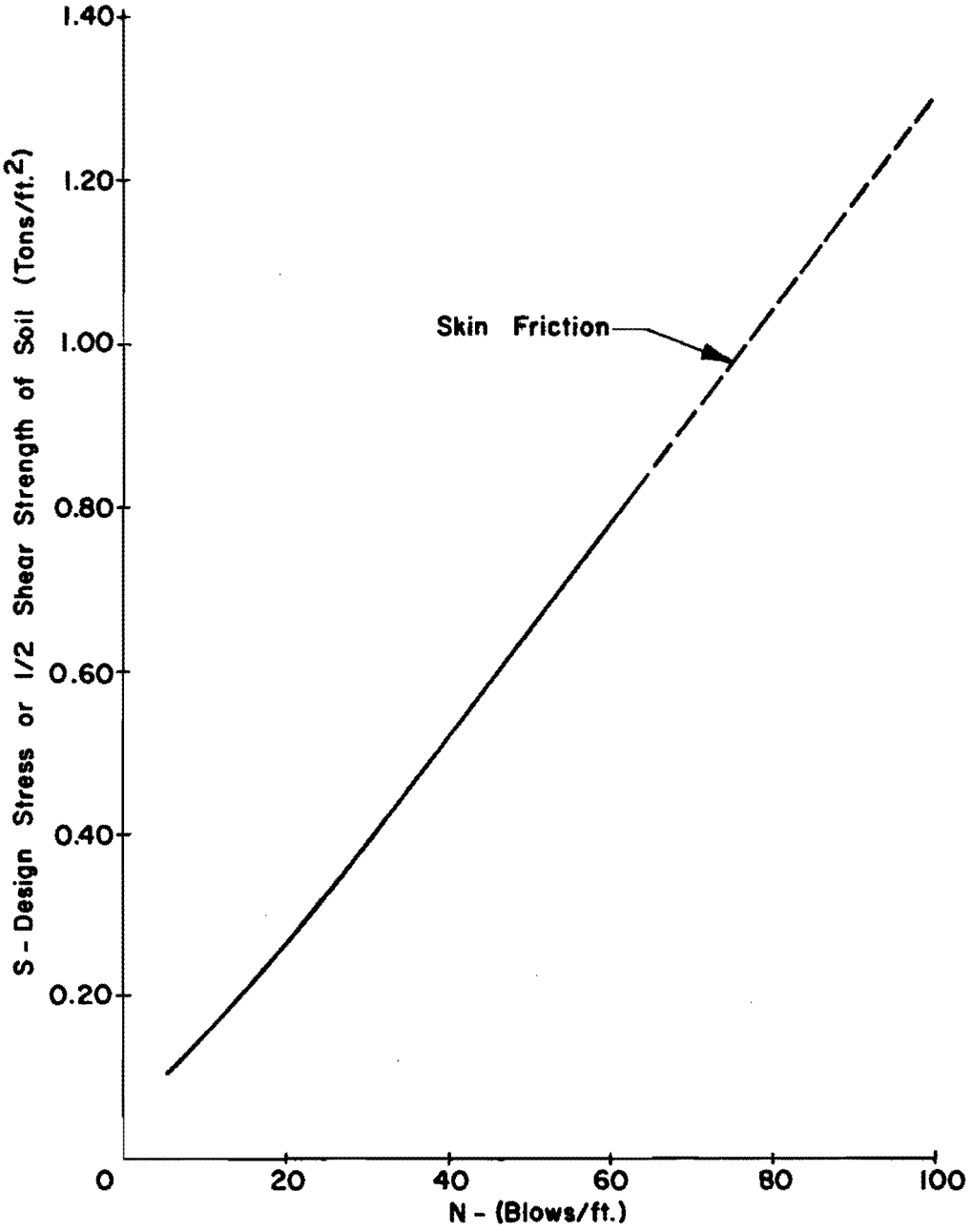

Fig. A1 THD Cone Penetrometer Correlation to Shear Strength (THD Foundation Manual, 1964)

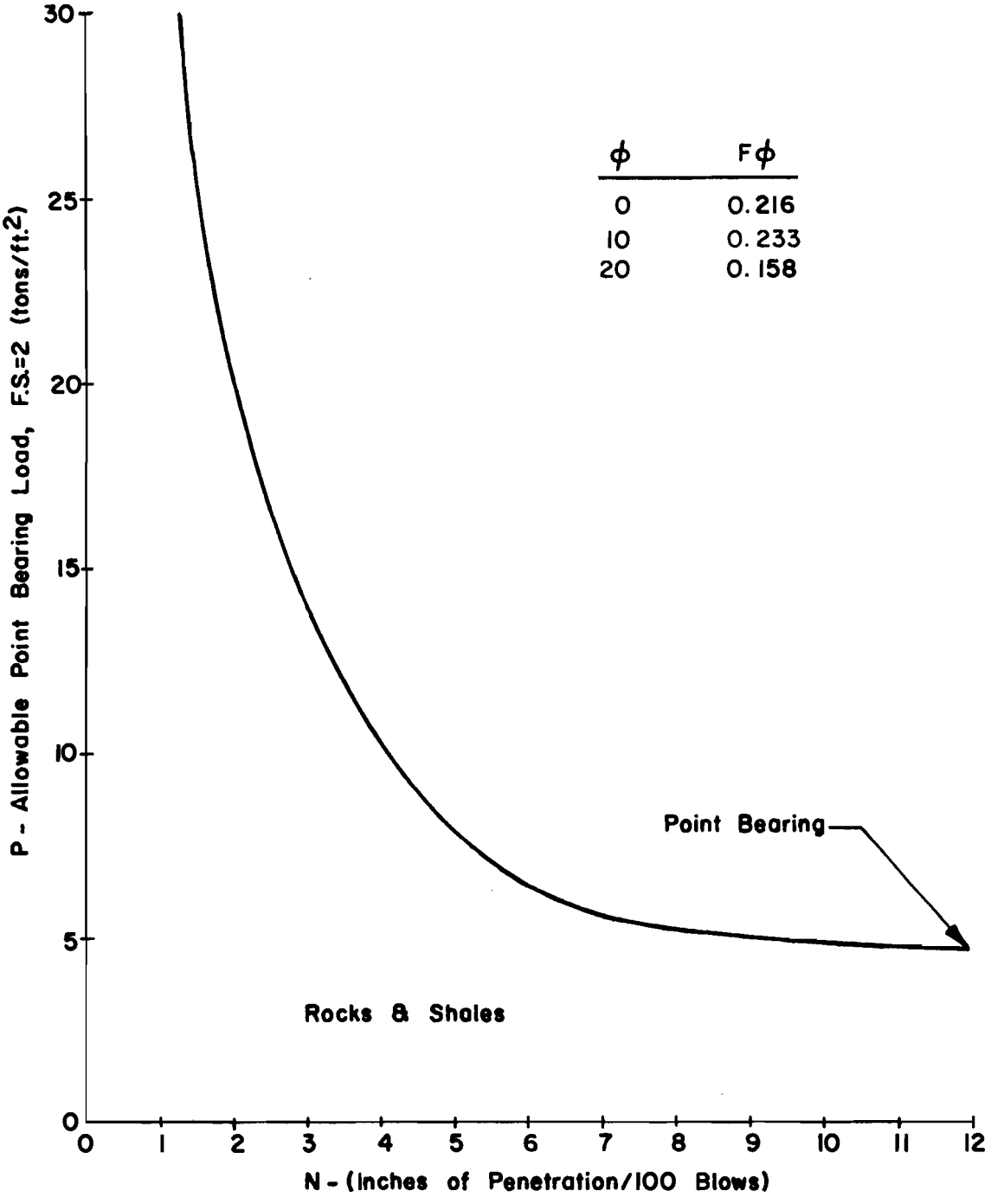

Fig. A2 Allowable Point Bearing Load Vs. THDP Penetration (THD Foundation Manual, 1964)

$$s = p \cdot F(\phi)$$

where

$F(\phi)$ = a function of ϕ as given in Fig. A.2.

THE STANDARD PENETRATION TEST (SPT)

The apparatus and the procedure to be used in this test are specified in ASTM Standards (D1586-67). In this study the Texas Highway Department rotary drilling rigs, namely those of the Corpus Christi and Houston districts, were used in conducting this test. The automatic tripping mechanism, the driving rod, and the steel anvil used in the THDP test were used in running the SPT. The drilling rod used is a three thread "N" rod (2 3/8" O.D.) with a wall thickness of 0.281 inches. A 140-pound hammer was machined from one of the 170-pound hammers used in the THDP. The split spoon was provided by The University of Texas laboratories. The original spoon, shown in Fig. A.3, had a standard cross section but had a length shorter than the standard one. Tests at US59 and HH sites were run with that spoon. For the tests on the Houston sites a ten-inch closed barrel section of the same cross section as the spoon was added to bring the sampler to a standard length.

The procedure used in running the test varied slightly between the different sites depending on the penetrometer used and the soils encountered.

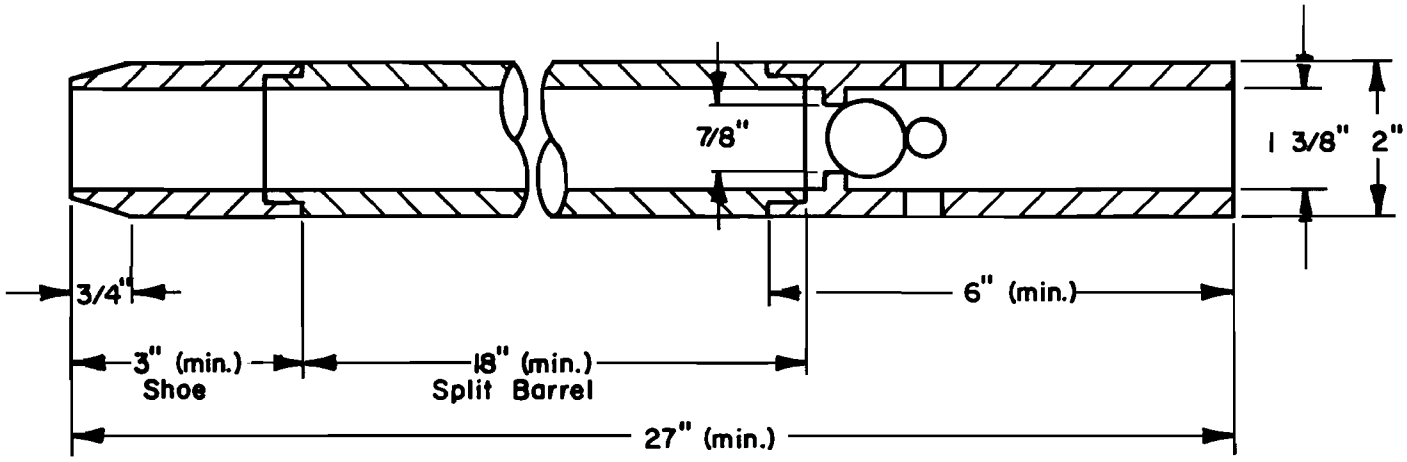

a. ASTM Spoon

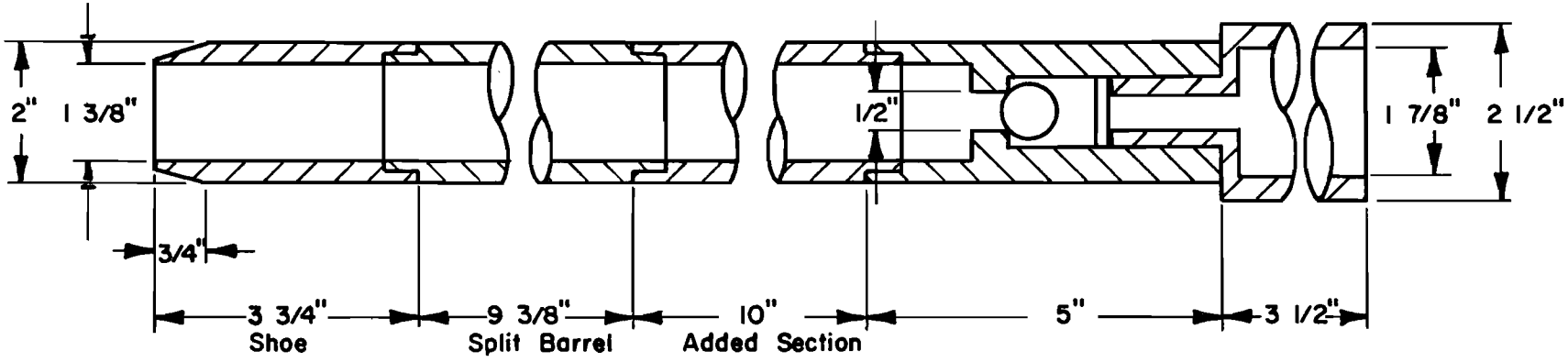

b. Spoon Used in this Study

Fig. A3 Spoons for Standard Penetration Test

Live Oak County

The tested soils at these sites were above the water table. A four-inch hole was first cored in the clay until the sand was encountered. Drilling mud was then introduced and drilling was continued with a coring barrel by a combined action of cutting and washing. It was in general possible to core about six inches of soil at the test elevation to obtain a relatively clean bottom.

The standard procedure requires that the spoon be driven in increments of six inches a total distance of eighteen inches, and the number of blows required for the last foot of penetration is reported as the penetration resistance. The split spoon used at these sites had only a barrel length of about fourteen inches and a total length of about eighteen inches. When the eighteen-inch penetration was reached, the short length of the barrel resulted in a driving of the "N" size drilling stem, and in a "jamming" of the soil in the barrel. To eliminate the driving of the drilling stem, the sampler was only seated four inches. However, jamming was still observed on some of the tests. In certain cases, this problem is clearly indicated by an excessive increase in the blow count needed for the last six inches of penetration. However, this problem was not significantly experienced in clay, and the blow count in sand was much larger than 50, so that the increase in blow count due to jamming could not significantly influence the interpretation of the data.

Harris County (Houston)

The depth of the water table in this area varied between fifteen and thirty feet, and drilling mud was used from the beginning in drilling all

the test holes. Careful consideration was given to the cleaning of the bottom of the hole by coring the soil at the bottom with a Shelby tube and then slowly extracting the drilling pipe. The sampler used on these sites had standard dimensions and was driven eighteen inches without any "jamming" problem.

The shear strength was obtained from the SPT as follows:

$$\text{in clays:} \quad s = \frac{\text{No. of blows/ft}}{15}$$

$$\text{in sand:} \quad s = \bar{p} \tan \bar{\phi}$$

where

s = shear strength (T/ft^2),

$\bar{p}$ = effective overburden pressure (T/ft^2),

$\bar{\phi}$ = effective angle of shear resistance obtained as explained in Chapter IV.

THE DUTCH CONE PENETROMETER

(Run only at US59 site)

This test consists of measuring the force required to push steadily in the ground a steel cone that has a cross-sectional area of ten square centimeters. The cone is mounted on the end of a solid steel rod protected by an outer steel casing. The role of the casing is to prevent the

buckling of the inner rod and to allow it to displace with a minimum of friction. The cone used in this investigation is equipped with a friction sleeve (Fig. A.4) to allow the measurement of the skin friction. The ratio of the unit sleeve friction to the unit point bearing is an indicator of the type of soil penetrated (Schmertmann, 1967). The cone penetrometer and the rods were provided by the laboratory of The University of Texas. The drilling rig of the Texas Highway Department was used to run the test because the standard equipment used to drive the cone was not available. The procedure followed consisted of opening a four-inch hole in the ground to a desired elevation, inserting the rods in the hole and using a ten-ton jack to force the cone and the rods at least two feet below the bottom of the hole. The reaction for jacking was provided by the drilling truck. The rods were restrained horizontally near the surface by a wooden block inserted in the collar of the mud reservoir, Fig. A.4. The force required to push the cone at the test elevation was measured with a calibrated load cell, connected to the jack. The displacement of the inner rod with respect to the outer casing was measured with a Linear Variable Differential Transformer. Measurements of the load and the displacement were recorded on an x-y plotter. When the truck reaction was insufficient, the hole was advanced further and testing continued. Penetration became impossible in the sand at twenty feet and the testing was discontinued. The measurements taken in the sand were not very meaningful and are not presented here.

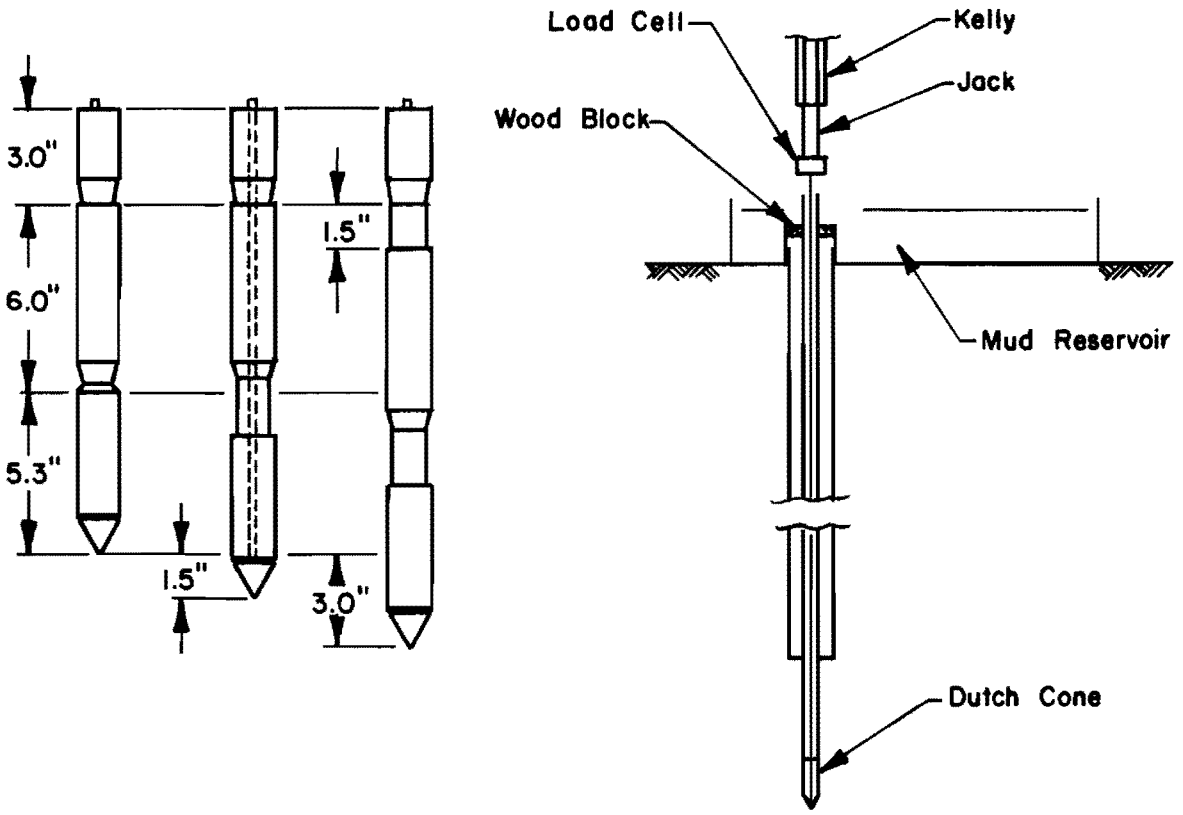

a. Dutch Cone Penetrometer

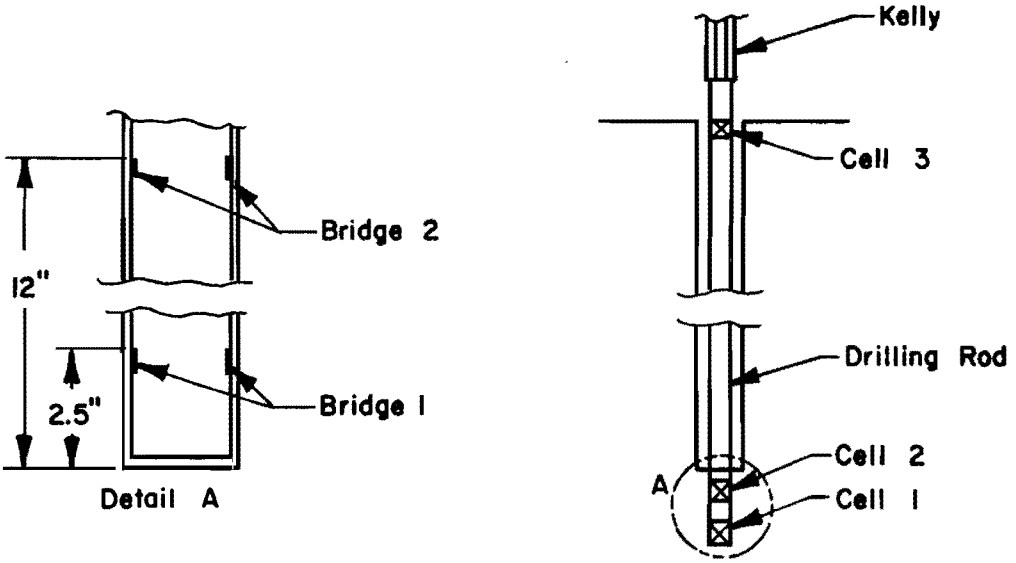

b. Texas A & M Penetrometer

Fig. A4 Static Penetrometers

THE TEXAS A & M PENETROMETER

(Run only at US59 site)

This test consists of steadily pushing in the ground an instrumented steel cylinder (Perdue and Coyle, 1970) which measures separately the tip and the side resistance. The penetrometer developed at Texas A & M University was slightly modified for the purposes of this study. The penetrometer consists (Fig. A.4) of a closed section of a drilling "N" rod, equipped with two full bridges of strain gages. One of the bridges was located near the tip of the penetrometer to enable measurements of the tip reaction, while the other bridge was located eleven inches above the first one and permitted the measurement of the load transferred by side friction in the distance between the gages. A third load cell, made also from a piece of drilling pipe, was used at the ground surface to monitor the total load applied. The test proceeded by drilling a four-inch hole to a certain desired depth. The penetrometer was placed in the hole and pushed for a distance of one foot below the bottom of the hole. The surface load cell, connected to an x-y plotter, was then monitored as penetration was further continued. When the applied load became relatively steady, the lower load cells were read with a Budd strain indicator. The penetrometer could not be pushed at all in the sand layers. The data obtained in the clay are not thought to be reliable and are not reported here.

LABORATORY TESTS

Triaxial tests were run on clay samples recovered with a thin-wall Shelby tube. The samples were extruded in the field, wrapped in aluminum foil and sealed with wax. The samples from the Houston sites were further preserved in cylindrical "ice cream" cans. All samples were stored in a 100 percent moisture room until they were tested. The triaxial test run at the laboratories of The University of Texas is described by O'Neill and Reese (1970). The test consisted of trimming the soil samples to a diameter of 1.4 inches and to a height of about three inches. Then the specimens were tested at a constant rate of strain in a triaxial testing machine. The confining pressure used in the test is equal to the total overburden pressure applied on the sample in the field. Samples from Live Oak County sites were quite sandy, and could not be conveniently trimmed. All those samples were, therefore, tested as extracted, with diameters of three or four inches.

A transmatic triaxial test, used by the Houston Urban office, has been conducted on the clay samples of the Houston sites. The test is described by O'Neill and Reese (1970), and the evaluation of the shear strength from this test is described by Reese and Touma (1972).

Routine laboratory tests, such as the measurements of moisture content, total density, and Atterberg limits, were further conducted on the soil samples. The moisture contents of the sandy soils of Live Oak County were measured on samples taken from the auger during the drilling of the test shafts. The samples preserved in moisture cans were weighed in the field and were later oven dried in the University laboratories.

Mechanical sieve analysis was run on all the sand samples from the split spoon barrel or from the drilling auger. The samples were carefully washed on the sieves to measure accurately the content of fines. A hydrometer analysis was run on the clayey silty sands of the Live Oak County sites to determine the relative percentages of each grain size.

DRILLING LOG REPORTS AND SOIL TEST RESULTS

Figure A.5 shows plans of the test sites and the locations of the test boreholes. The drilling log reports are not presented here because it is believed that the important information can be more explicitly presented in diagrammatic charts. Figures A.6 to A.27 represent the pertinent soil data.

(Last page of text)

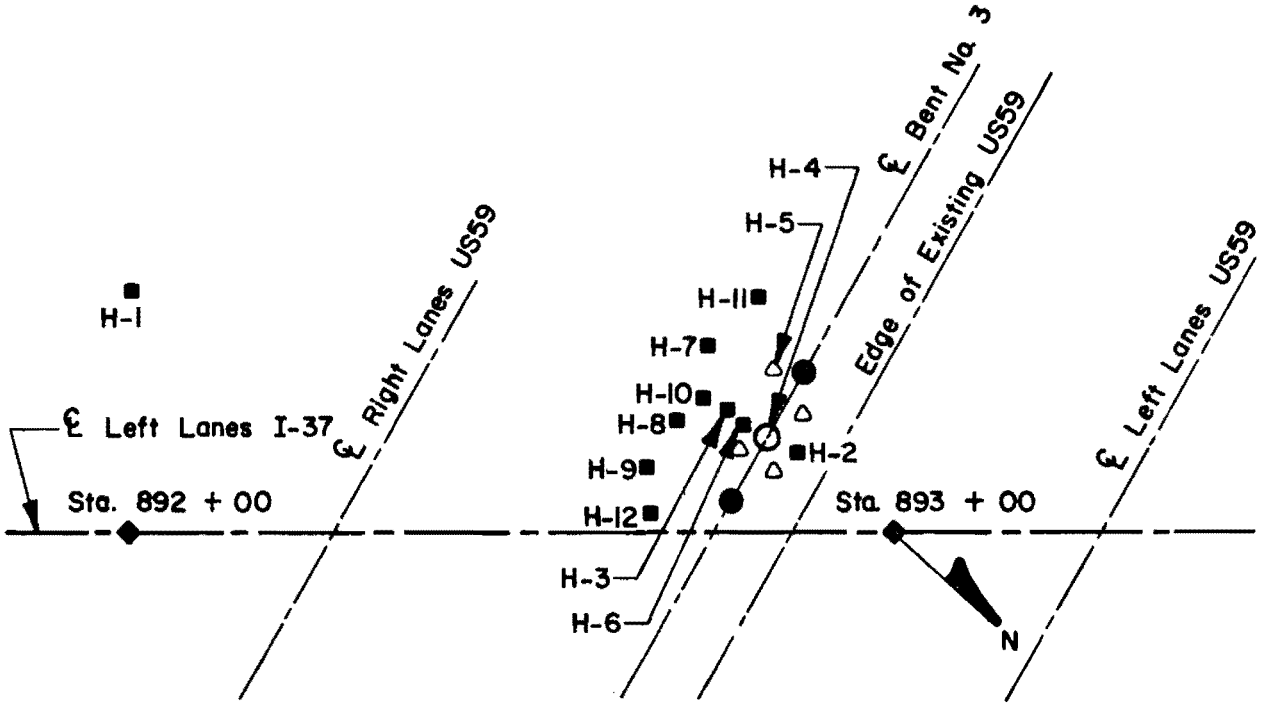

a. US59 Site

△ ■ = Borehole

● = Anchor Shaft

○ = Test Shaft

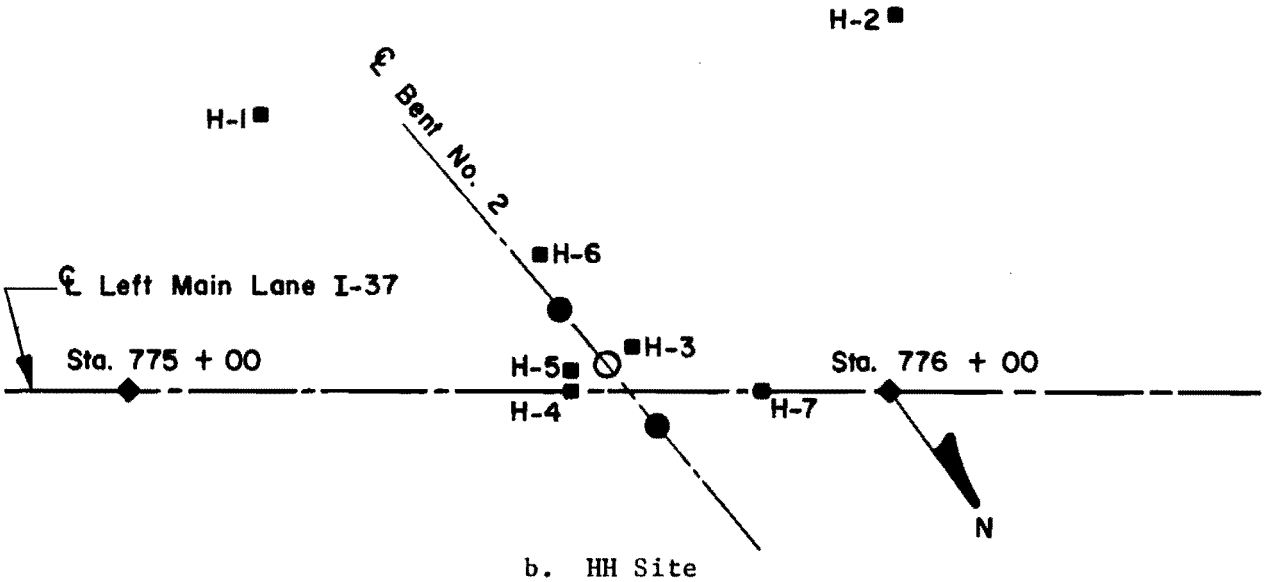

b. HH Site

Fig. A5 Location of Test Shafts and Boreholes

(Continued)

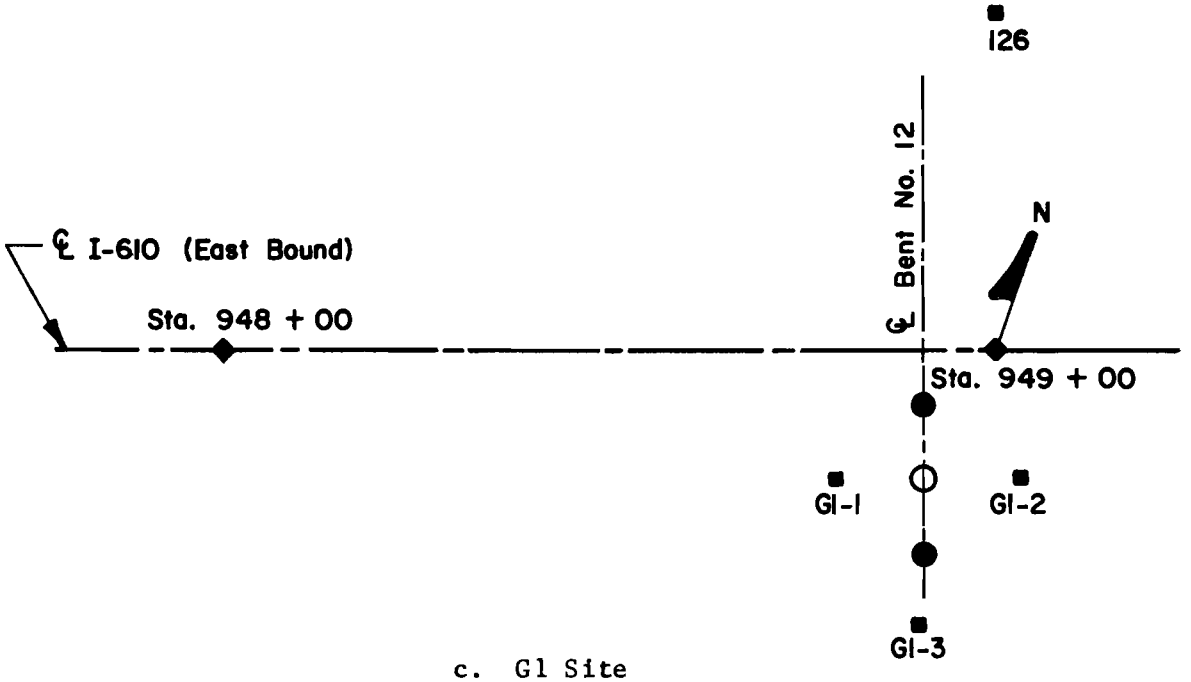

c. G1 Site

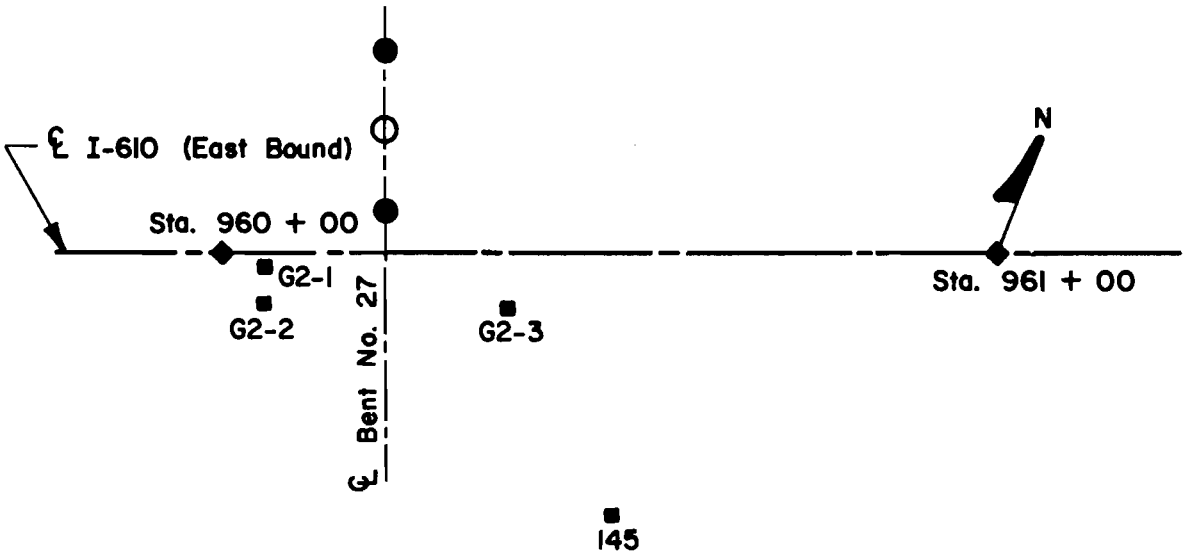

d. G2 Site

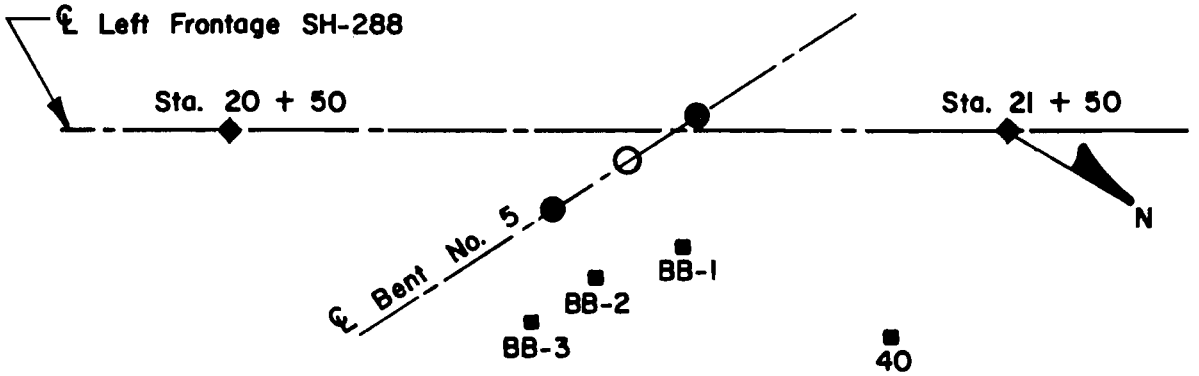

e. BB Site

Fig. A5 (Continued)

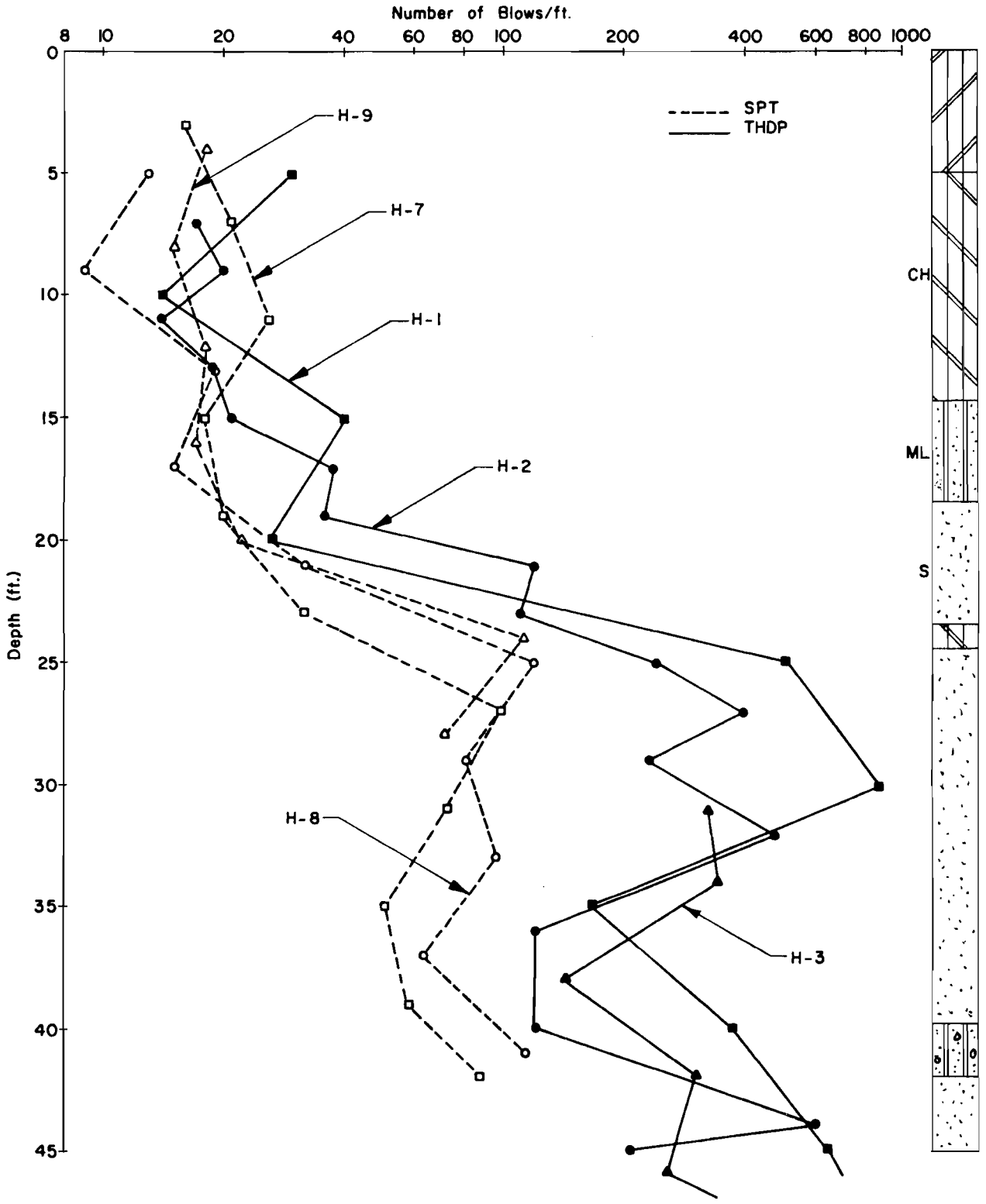

Fig. A6 Plot of Dynamic Penetration Tests at US59 Site

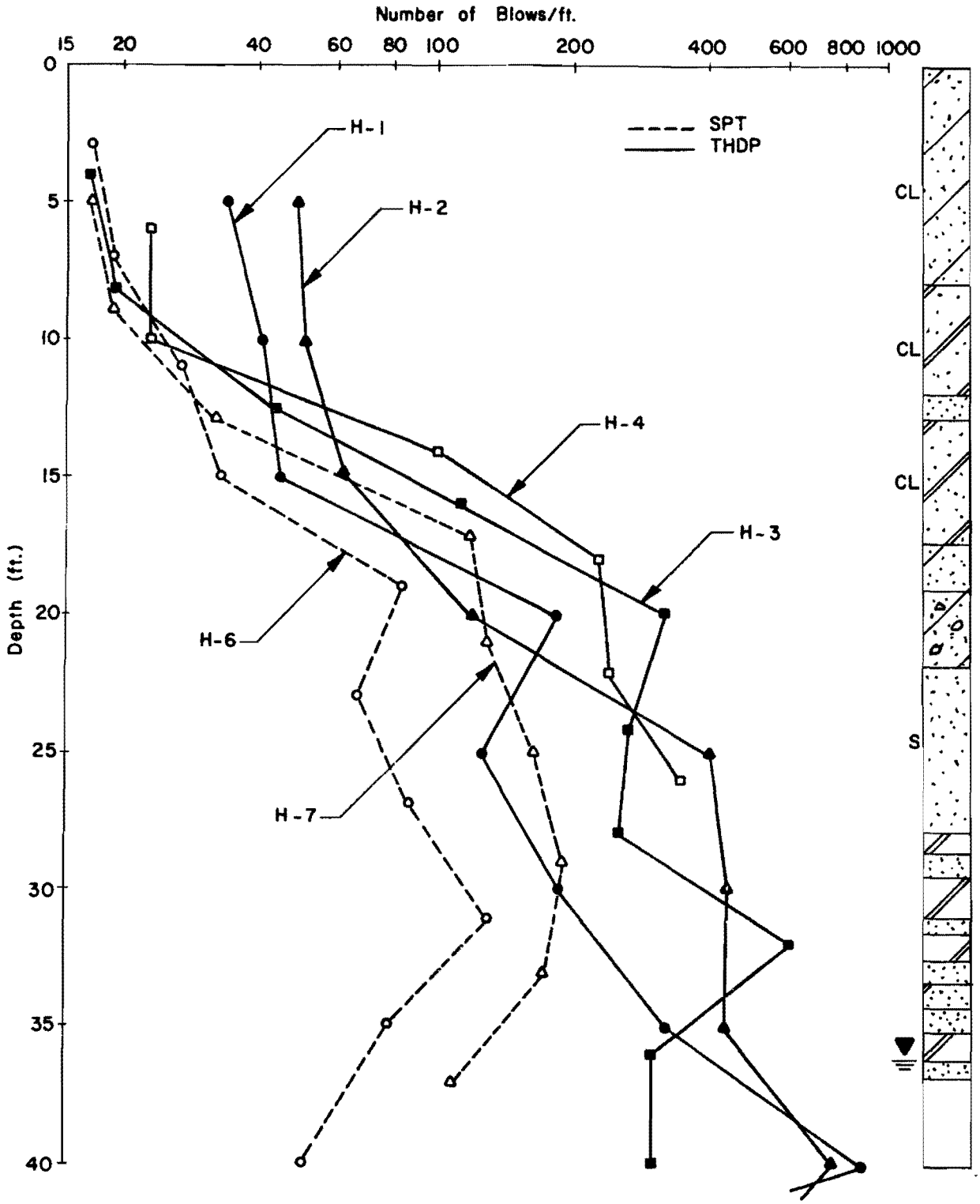

Fig. A7 Plot of Dynamic Penetration Tests at HH Site

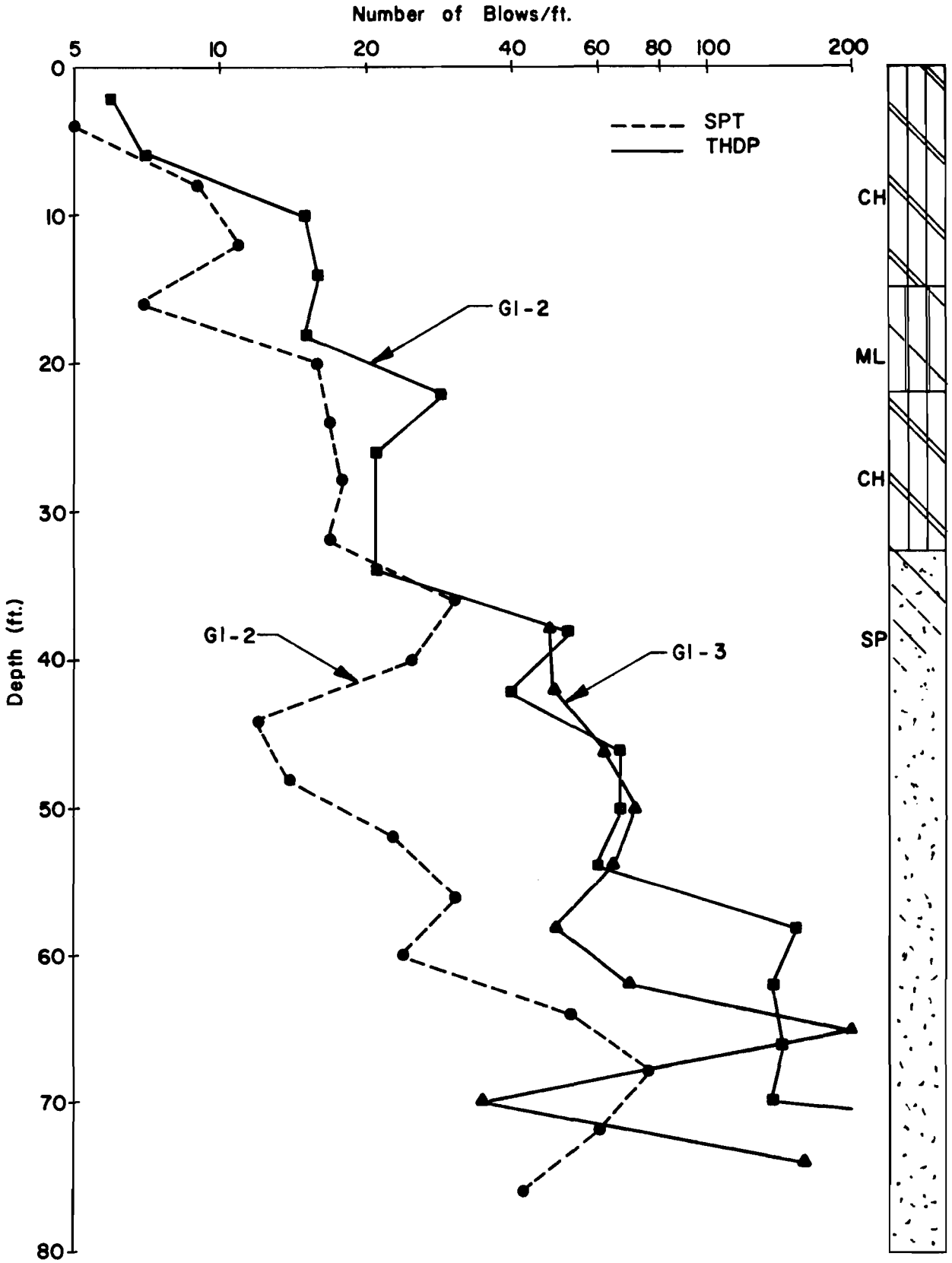

Fig. A8 Dynamic Penetration Tests - G1 Site

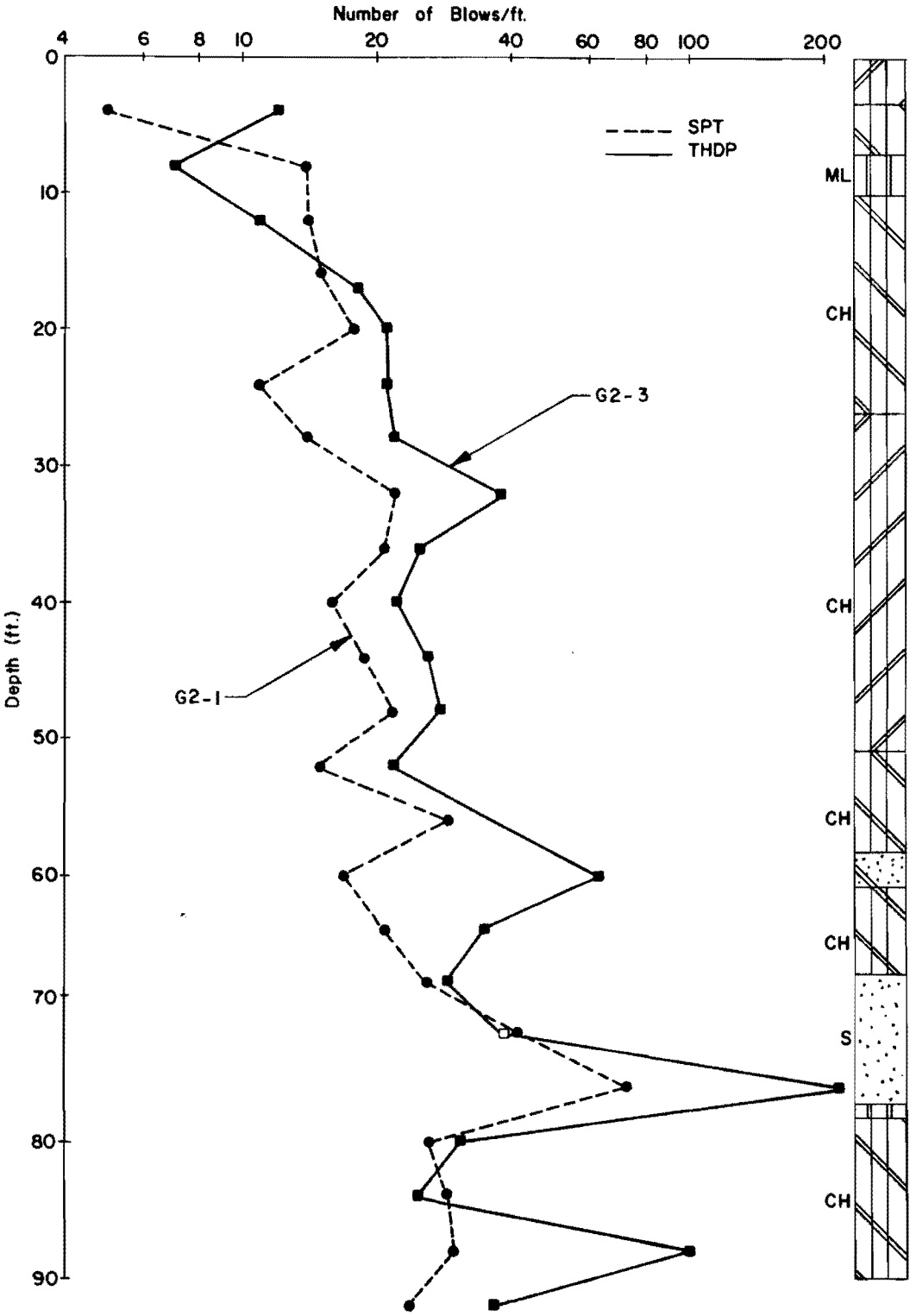

Fig. A9 Dynamic Penetration Tests - G2 Site

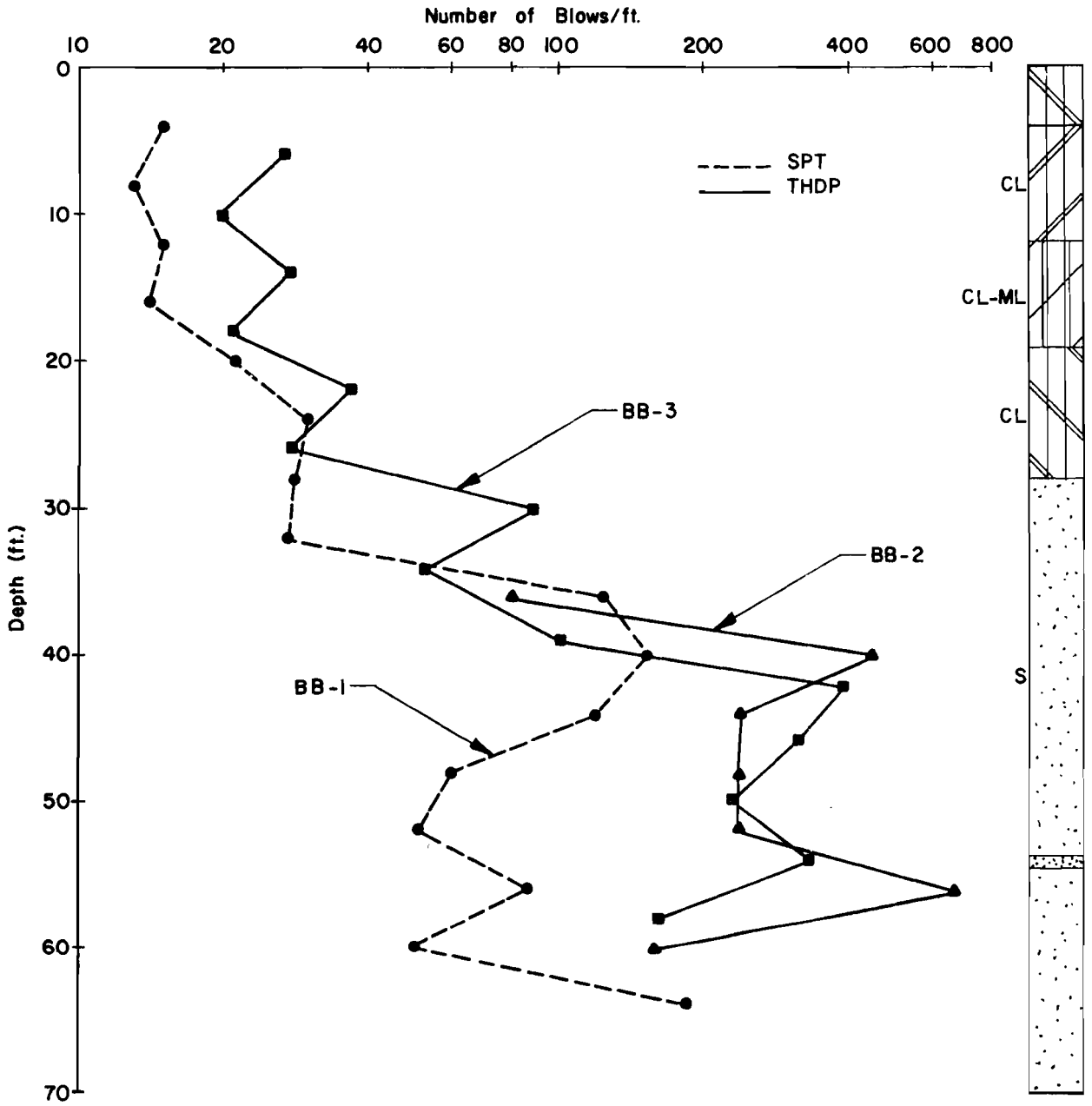

Fig. A10 Dynamic Penetration Tests - BB Site

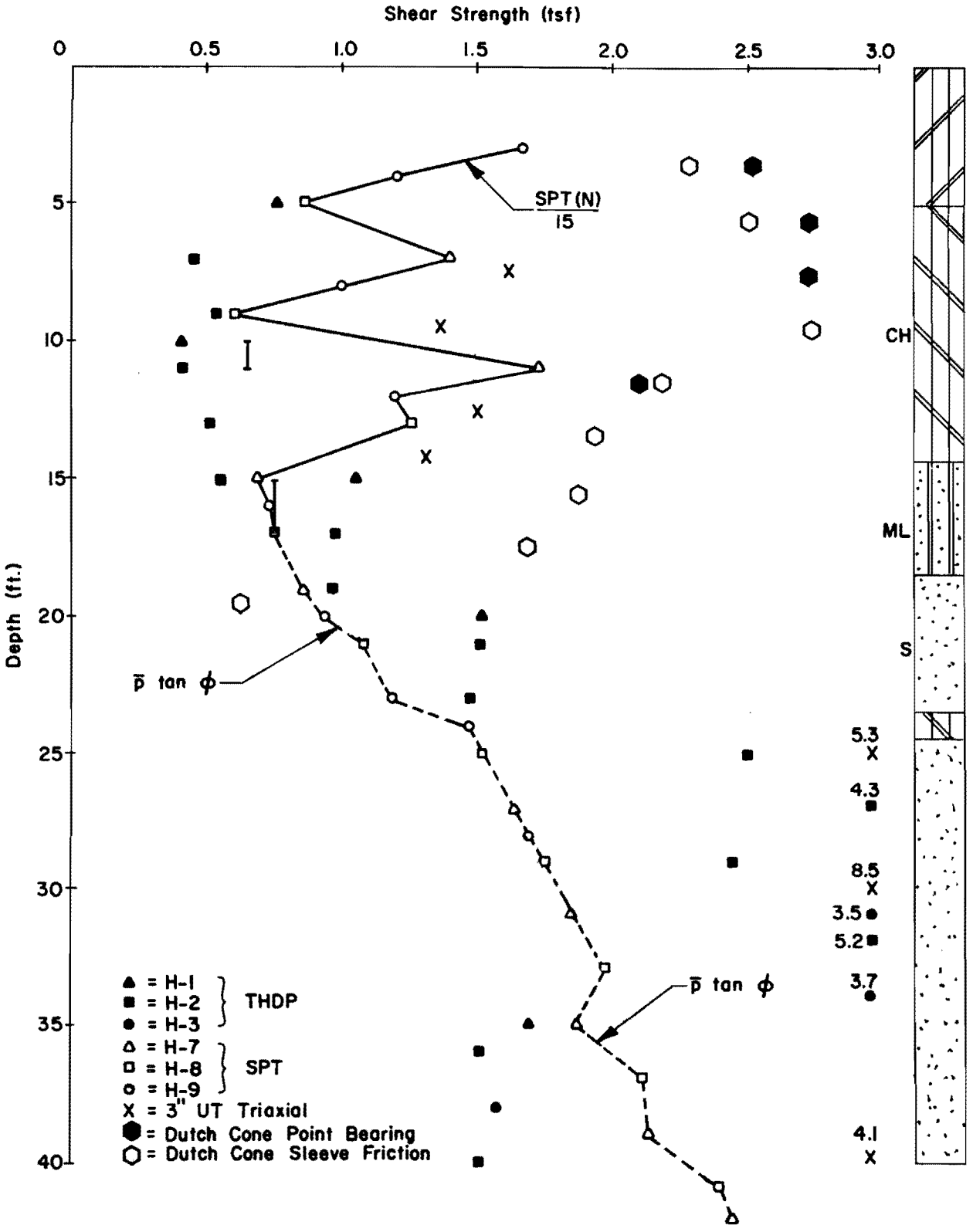

Fig. A11 US59 - Site: Shear Strength Profile

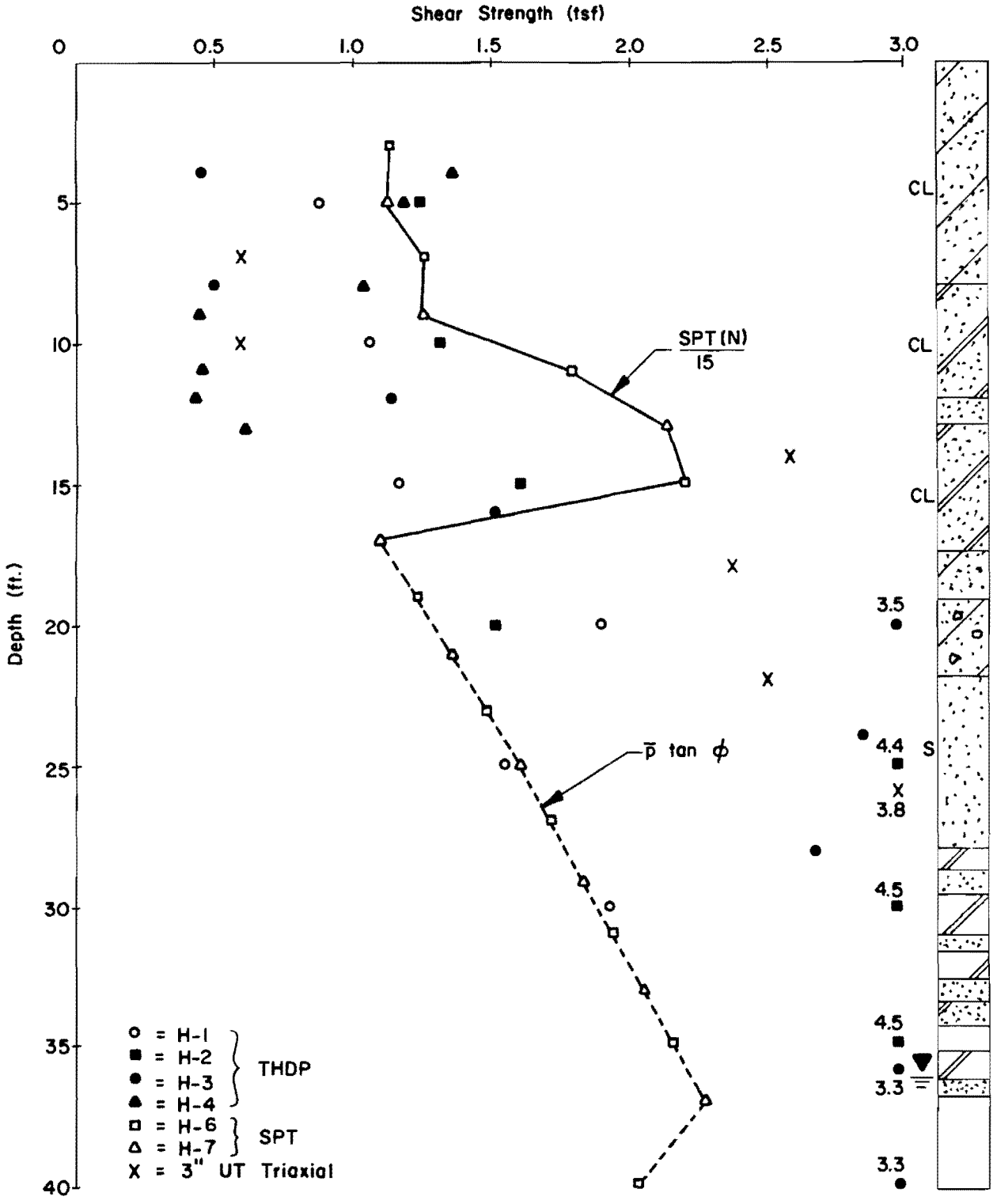

Fig. A12 HH - Site: Shear Strength Profile

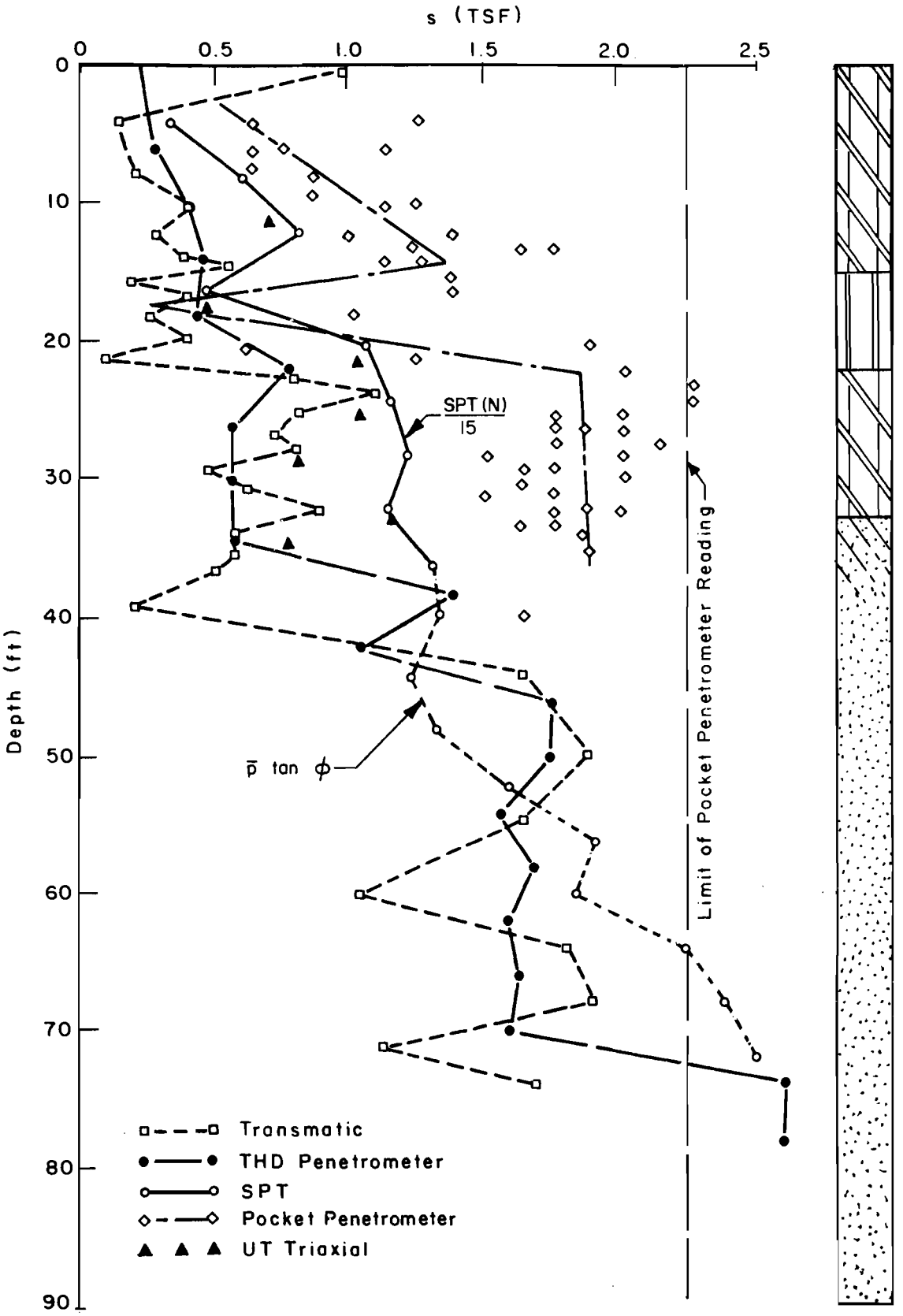

Fig. A13 G1 - Site: Shear Strength Profile

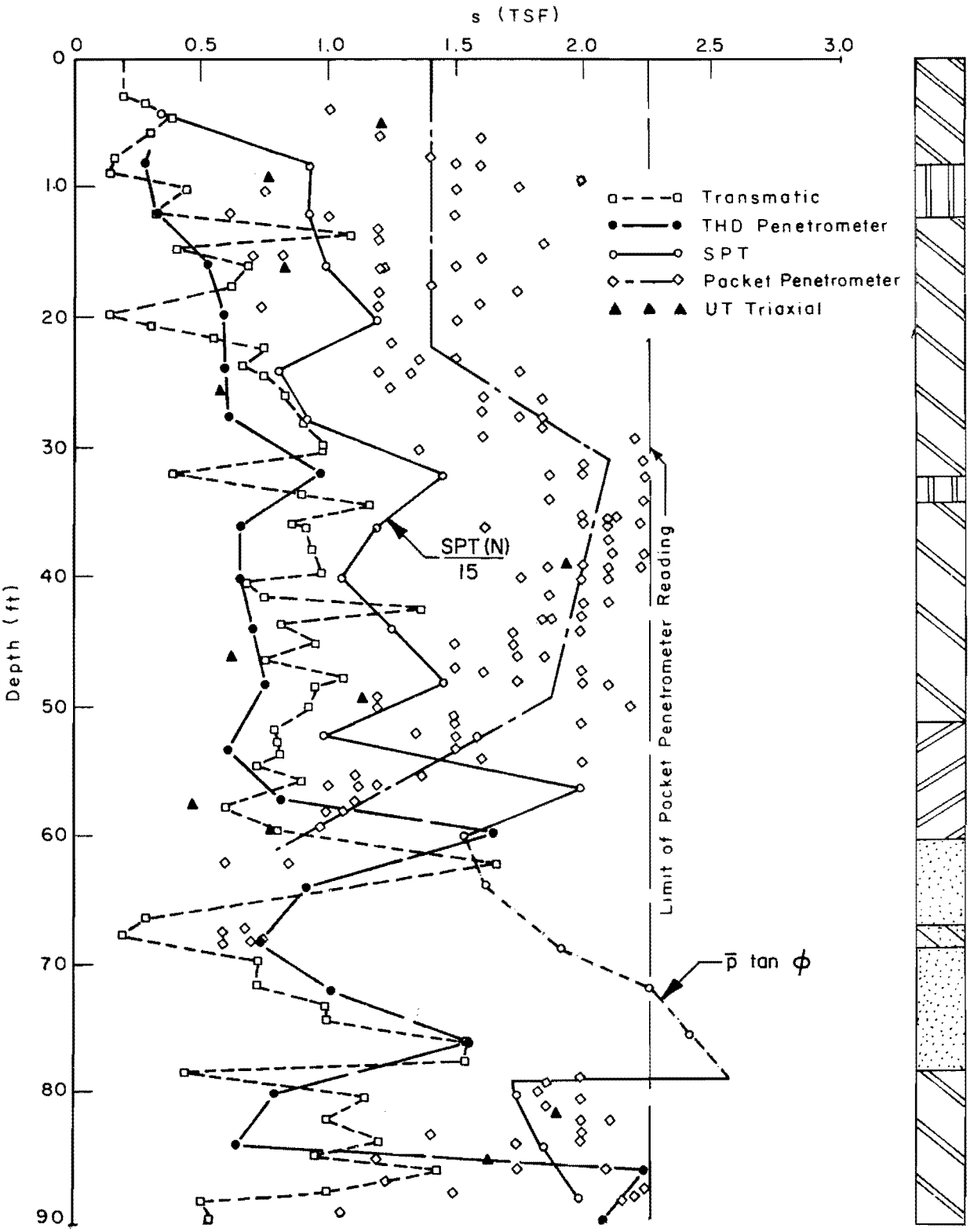

Fig. A14 G2 - Site: Shear Strength Profile

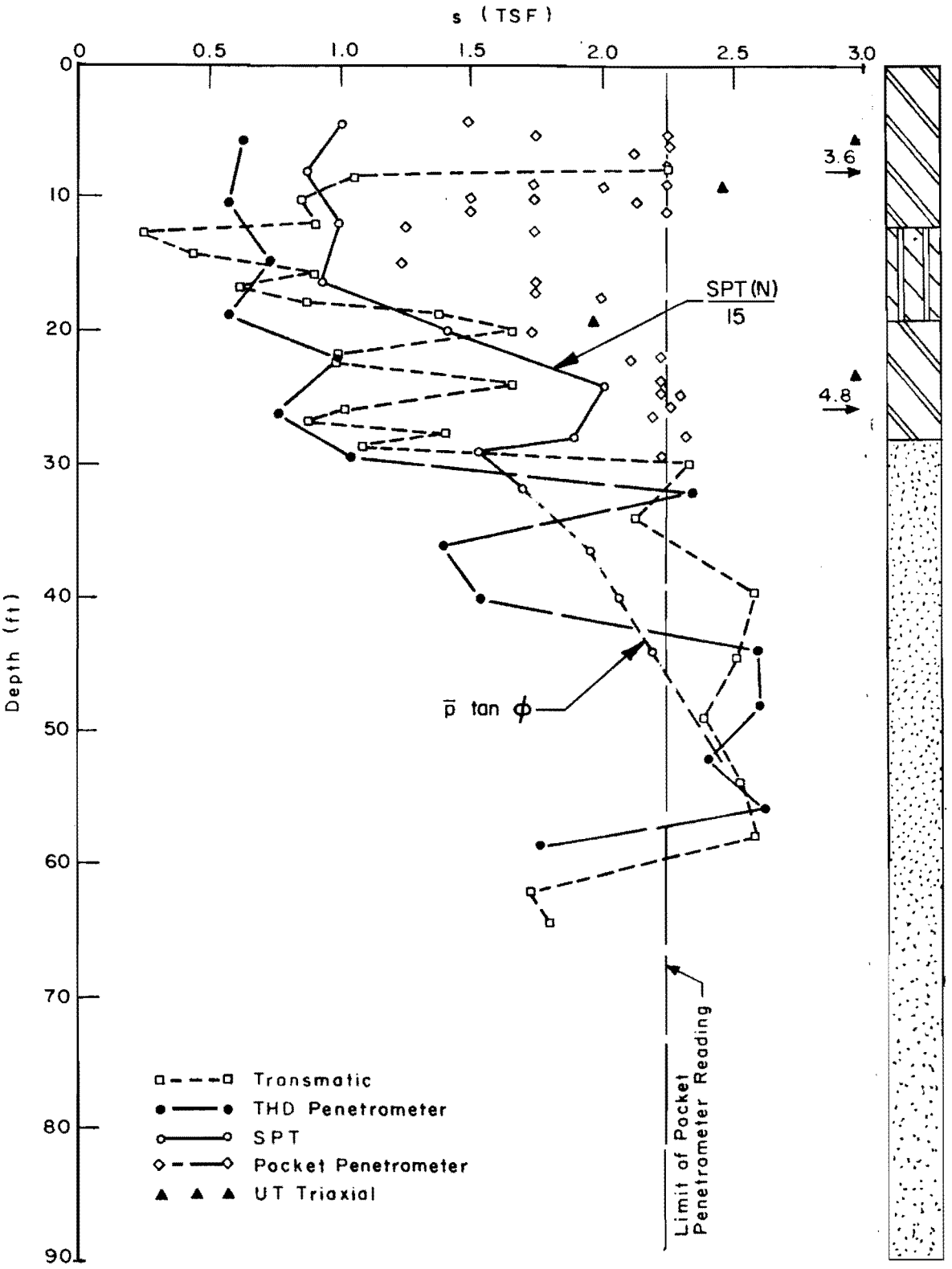

Fig. A15 BB - Site: Shear Strength Profile

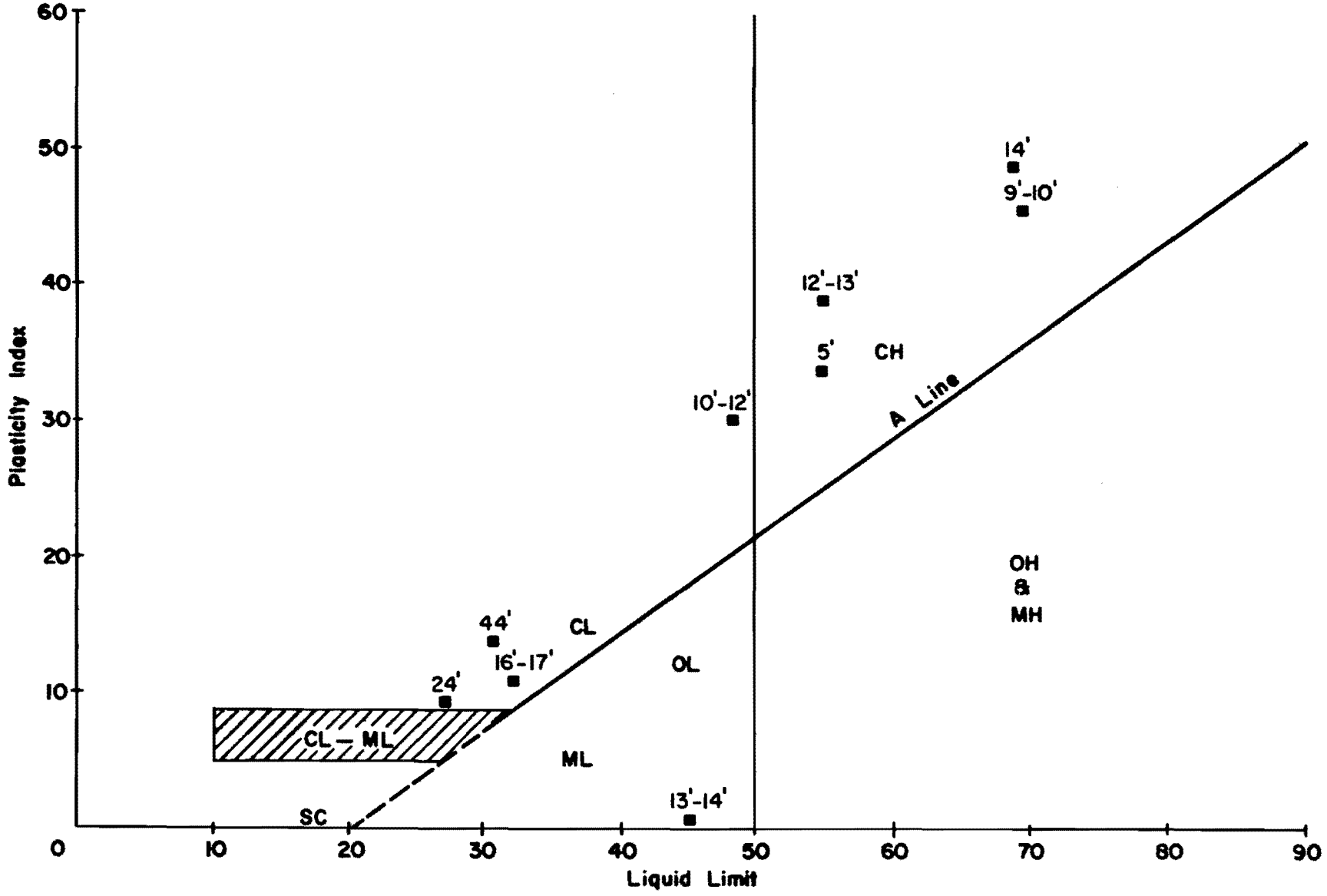

Fig. A16 Plot of Clays from US59 Site on the Plasticity Chart

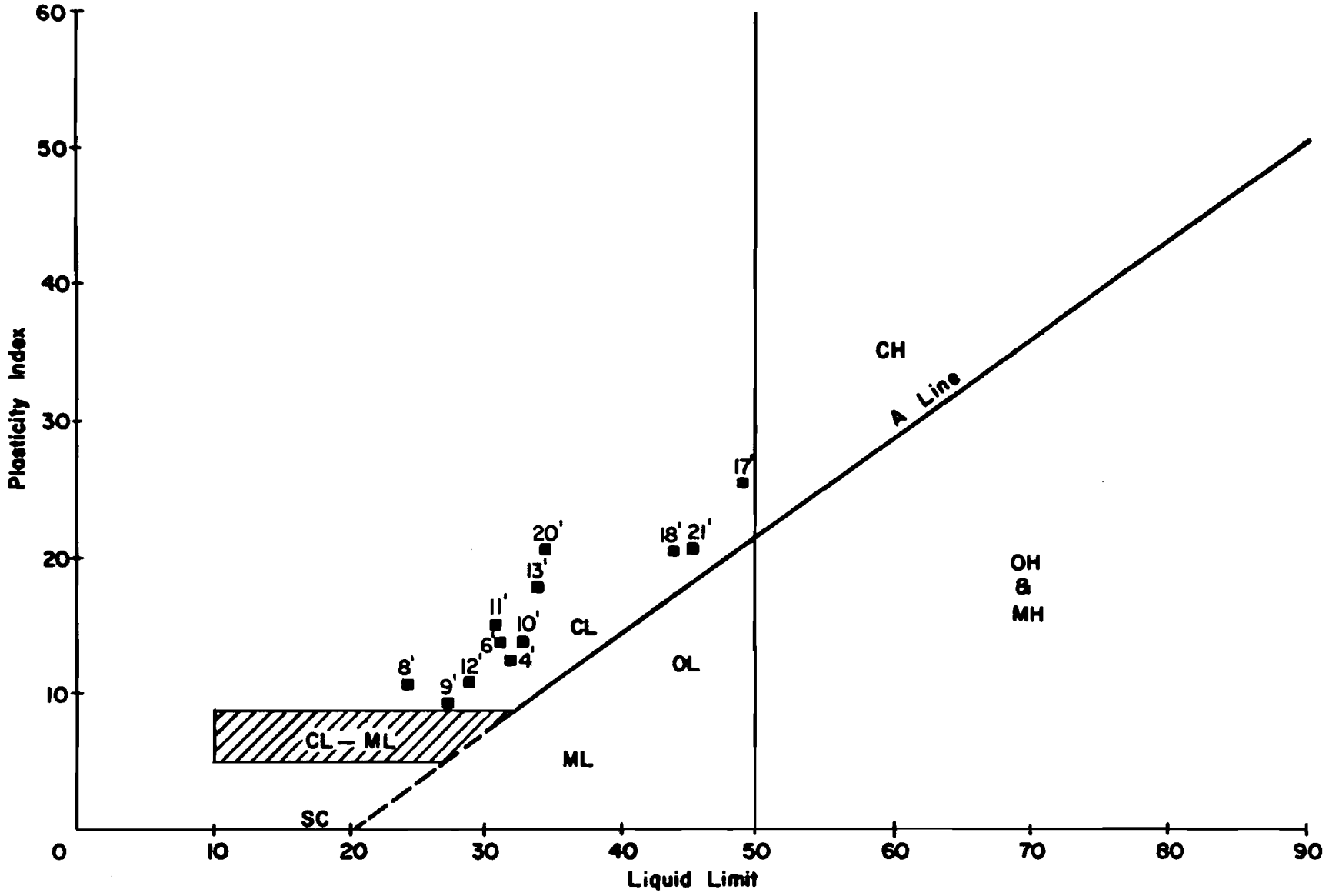

Fig. A17 Plot of Plastic Soils from HH Site on the Plasticity Chart

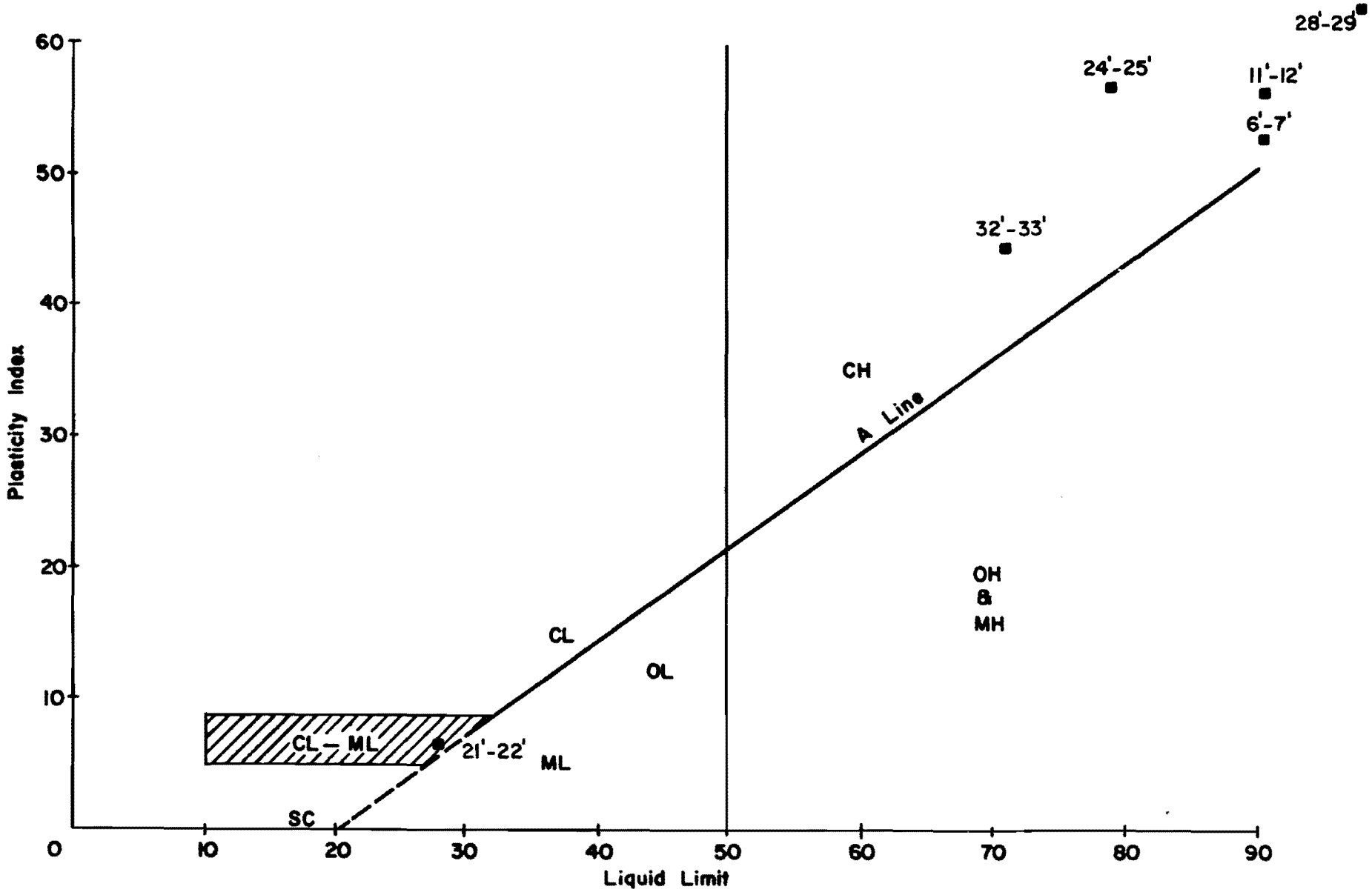

Fig. A18 Plot of Clays from G1 Site on Plasticity Chart

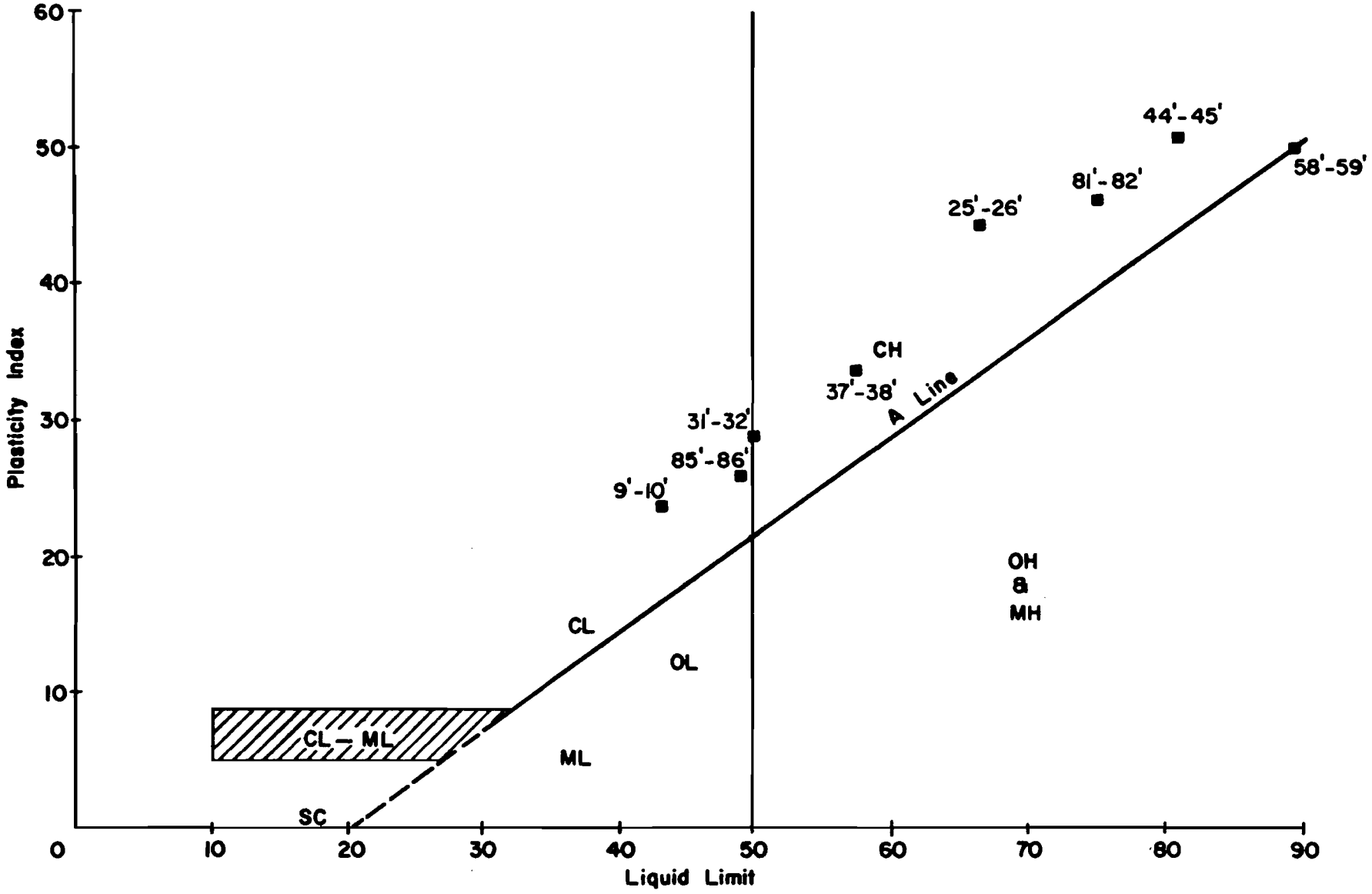

Fig. A19 Plot of Clays from G2 Site on Plasticity Chart

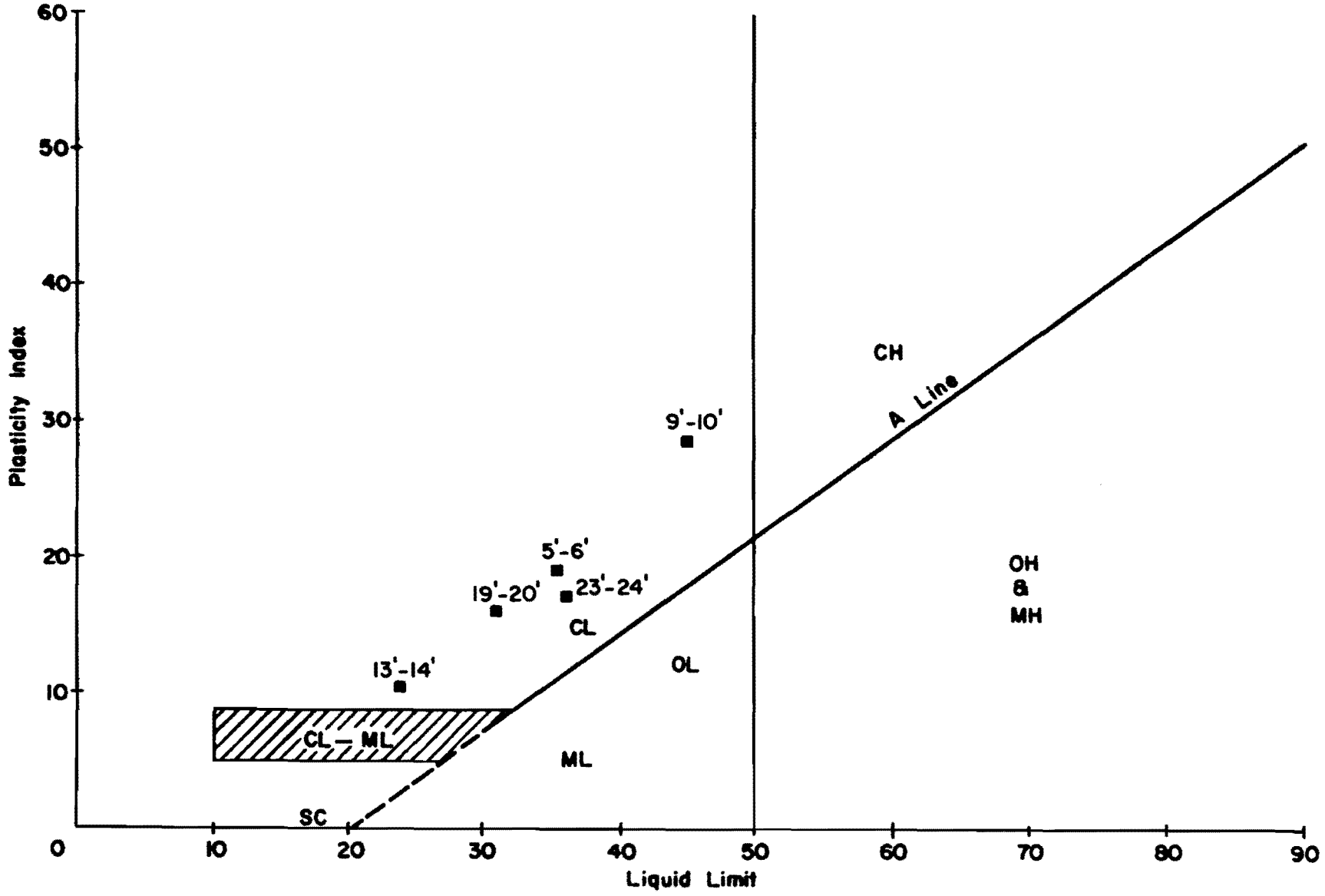

Fig. A20 Plot of Clays from BB Site on Plasticity Chart

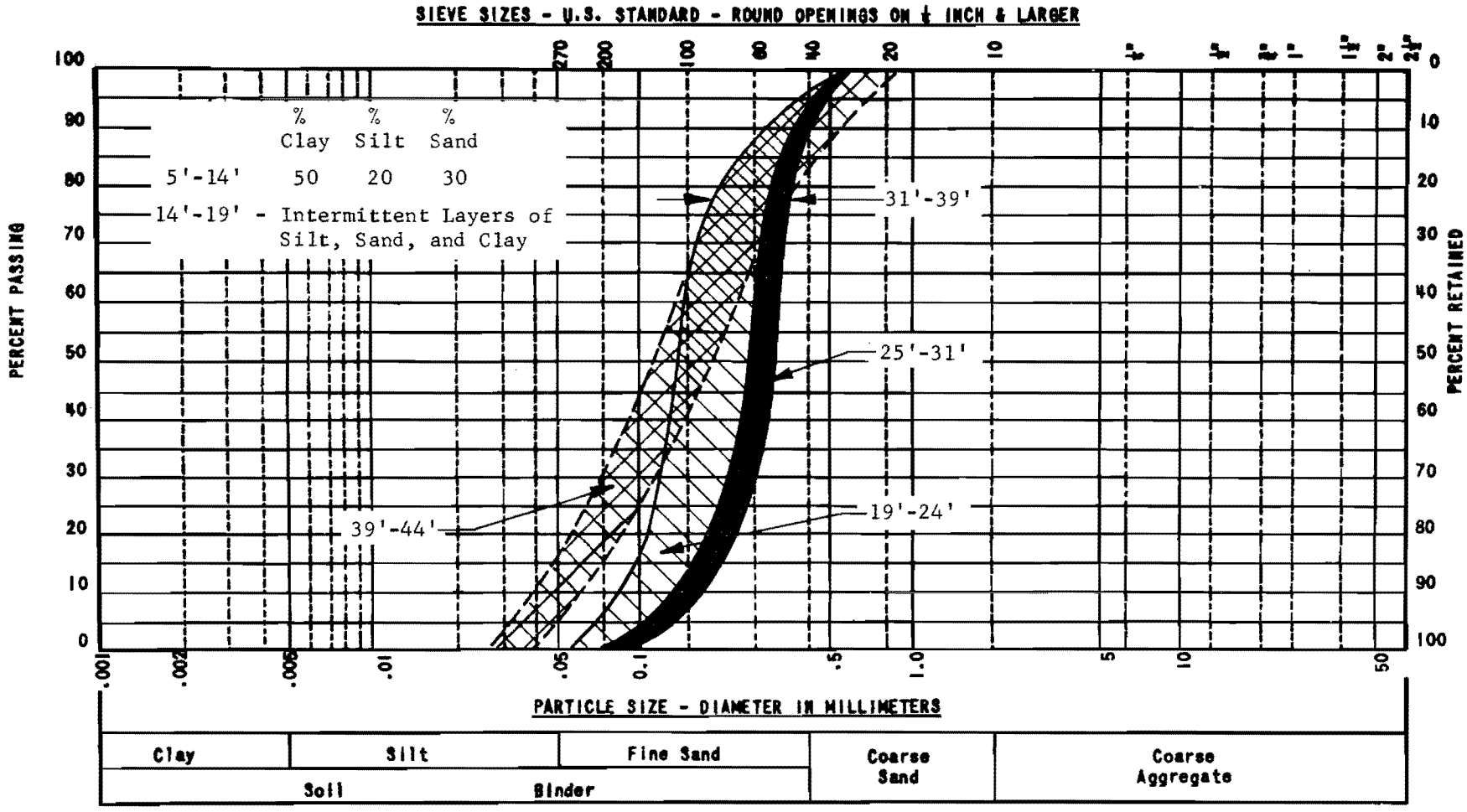

Fig. A21 Granulometry of Soil at US59 Site

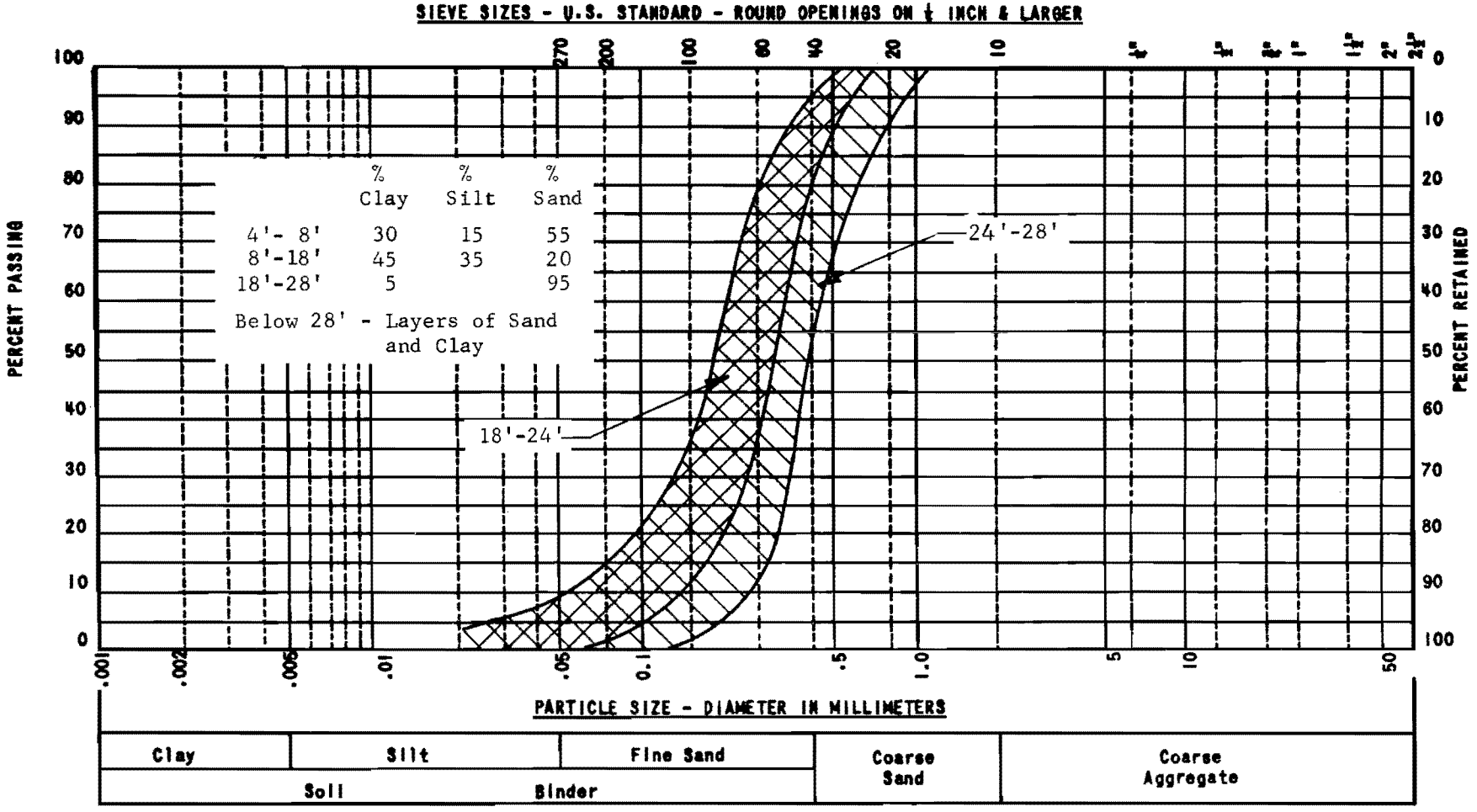

Fig. A22 Granulometry of Soil at HH Site

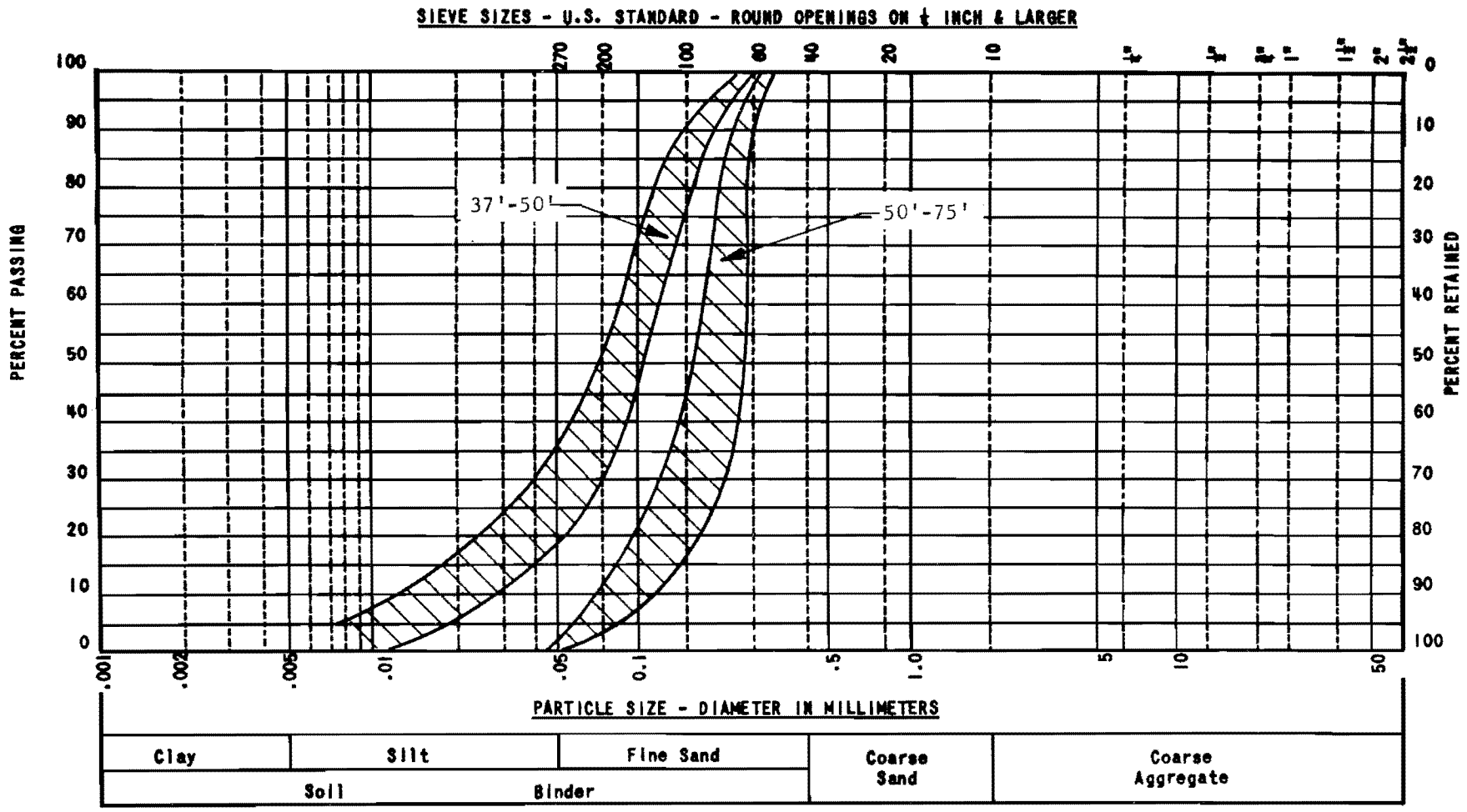

Fig. A23 Granulometry Analysis - G1 Site

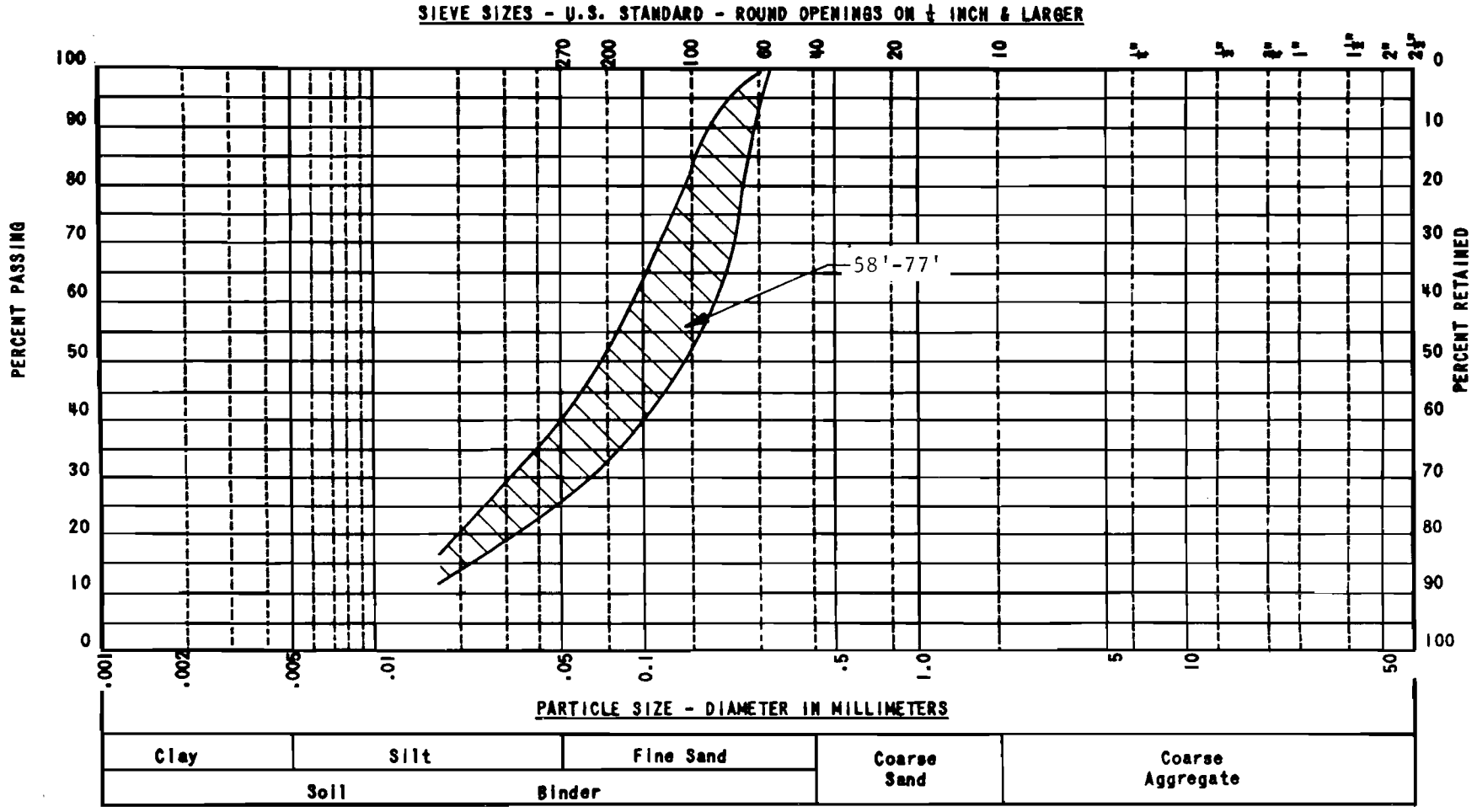

Fig. A24 Granulometry Analysis - G2 Site

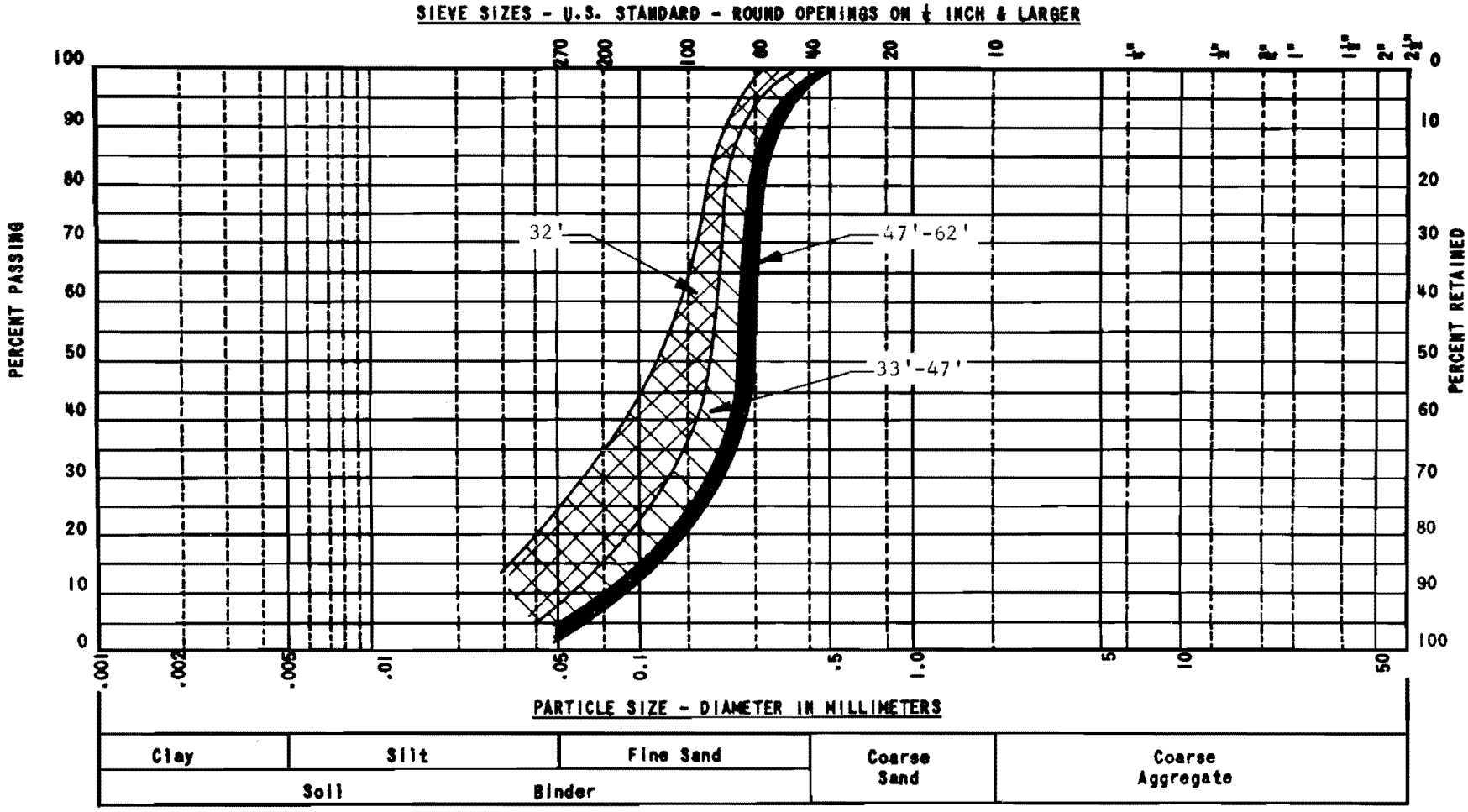

Fig. A25 Granulometry Analysis - BB Site

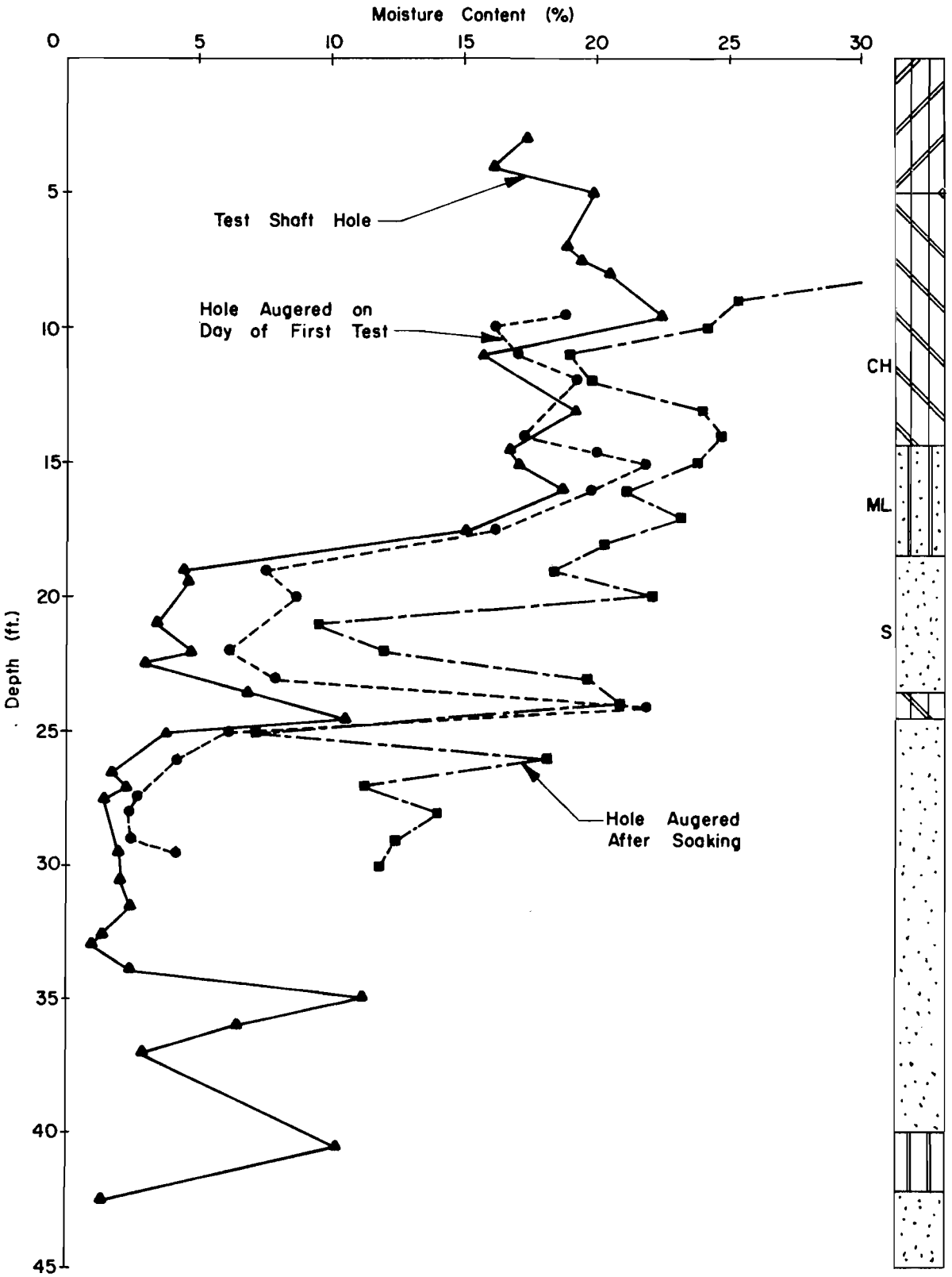

Fig. A26 Moisture Content at US59 Site

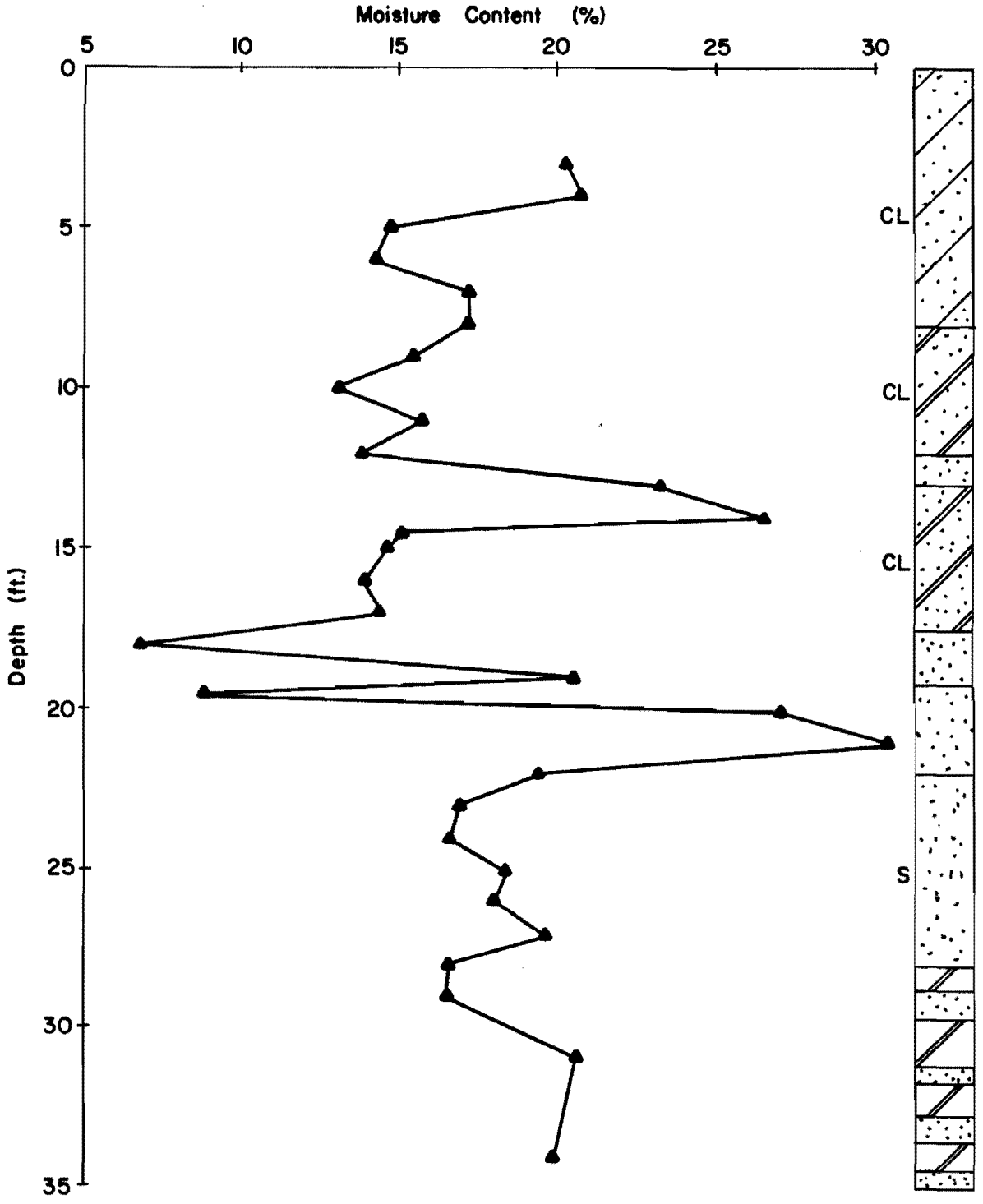

Fig. A27 Moisture Content at HH Site

THE AUTHORS

Fadlo T. Touma is an instructor in civil engineering at The University of Texas at Austin. His research interests include work on foundation problems and in particular the behavior of drilled shafts. He has worked for several years on a variety of civil engineering problems, with special emphasis on structural problems in building and bridge design. He is the coauthor of several papers and reports on the behavior of drilled shafts.

Lymon C. Reese is a Professor of Civil Engineering and Associate Dean of Engineering at The University of Texas at Austin. His specialization is in the area of soil mechanics and foundation engineering. He was the recipient of the Thomas A. Middlebrooks Award of the American Society of Civil Engineers in 1958. One of his primary interests has been in the design of offshore structures and pile foundations. In recent years, he has become well known for his research in the application of the finite-element method of analysis to problems in soil and rock mechanics. He holds memberships in numerous professional and learned societies and is a Registered Professional Engineer in Texas.